Population Pharmacokinetic models describing drug-drug interactions and variability in HIV infected South Africans on protease inhibitor-based antiretroviral regimens with and without tuberculosis

Chao Zhang

(Student number: CHXZHA001)

August 2012

Supervisor

Assoc Prof Helen McIlleron

Division of Clinical Pharmacology, Department of Medicine, Faculty of Health Science, University of Cape Town, South Africa

Co-supervisors

Dr Paolo Denti

Division of Clinical Pharmacology, Department of Medicine, Faculty of Health Science, University of Cape Town, South Africa

Prof Mats O Karlsson

Department of Pharmaceutical Biosciences, Uppsala University, Sweden.

Abstract

Chao Zhang. Population Pharmacokinetic models describing drug-drug interactions and variability in HIV infected South Africans on protease inhibitor-based antiretroviral regimens with and without tuberculosis. August 2012.

Lopinavir/ritonavir is an important component of the first-line and second-line antiretroviral treatment for young children and adults respectively in the current World Health Organization guidelines. Rifampicin, a key component of antituberculosis treatment, profoundly reduces lopinavir concentrations. Therefore, investigation of the optimal dosage regimens of lopinavir/ritonavir when co-administered with rifampicin-based antituberculosis treatment is needed urgently. Moreover, treatment adherence is associated with virological and clinical responses to antiretroviral treatment, and reduced adherence leads to the development of drug resistance. The projects in this thesis were designed to characterize the population pharmacokinetic parameters of lopinavir and ritonavir in HIV infected South Africans, to account for the drug-drug interactions between lopinavir, ritonavir and rifampicin, to investigate optimal dose regimens of lopinavir/ritonavir when administered with rifampicin, and to investigate new approach to evaluate adherence.

Population pharmacokinetic models were developed using a nonlinear mixed modeling approach. The models provided, in pediatric and adult populations, a thorough description of the pharmacokinetics and their variability of antiretroviral agents (lopinavir, ritonavir and lamivudine) with and without coadministration of rifampicin-based antituberculosis treatment. Antituberculosis treatment reduced bioavailability and increased oral clearance of lopinavir and ritonavir respectively. The dynamic influence of ritonavir concentration on lopinavir oral clearance was modeled as direct inhibition with an E_{max} model. Optimal dose regimens of lopinavir/ritonavir coadministration with rifampicin-based antituberculosis treatment were predicted for adults and young children, respectively. An integrated model was studied to investigate the pharmacokinetic differences of lopinavir and ritonavir with rifampicin-based antituberculosis treatment between adults and children. Compare to adults, a lower bioavailability and stronger induction effect of rifampicin in children was found. Furthermore, since lamivudine's concentrations following an observed dose are predicable and it is not prone to drug-drug interactions, in this project lamivudine concentration measurement in young children was used to propose the reference cutoff values for evaluation of adherence to prior doses.

In summary, the models we developed in this thesis are useful for the optimization of antiretroviral therapy regimens for tuberculosis patients with HIV infection in different populations, and for adherence evaluation, and therefore could be helpful for improvement of clinical outcome.

Keywords: Lopinavir; Ritonavir; Lamivudine; Rifampicin; Antiretroviral therapy; Drug-drug interaction; NONMEM; Population pharmacokinetics

Synopsis of this thesis

A key concern regarding coadministration of antiretroviral and antituberculosis agents is drug-drug interactions, which may lead to clinically important alterations in drug concentrations. Lopinavir/ritonavir is an important component of the first-line antiretroviral treatment for adults in the current World Health Organization guidelines. The preferred antiretroviral regimen for young children (< 2 years old) previously exposed to nonnucleoside reverse transcriptase inhibitors is lopinavir/ritonavir plus two nucleoside reverse transcriptase inhibitors. Children with drug susceptible tuberculosis require rifampicin-based antituberculosis treatment. With maturation of antiretroviral programmes in many high burden settings, increasing numbers of adults require a second-line protease inhibitor-based regimen, and many of these patients need cotreatment with first-line antituberculosis treatment. However, rifampicin, a key component of antituberculosis treatment, profoundly reduces lopinavir concentrations. Although rifabutin is recommended to replace rifampicin in such patients, this is not feasible for the majority of adults in high burden countries because of prohibitively high cost and it is not available for use in children due to lack of a suitable formulation. Therefore, investigation of the optimal dosage regimens of lopinavir/ritonavir when co-administered with rifampicin is needed urgently. Moreover, treatment adherence is associated with virological and clinical responses to antiretroviral treatment, and reduced adherence leads to the development of drug resistance. Lamivudine is commonly administered as part of antiretroviral treatment. Unlike protease inhibitors and nonnucleoside reverse transcriptase inhibitors, it's concentrations following an observed dose are predictaable and it is not prone to drug-drug interactions. Therefore, it can be used as a marker of recent adherence, to aid interpretation of protease inhibitor and nonnucleoside reverse transcriptase inhibitor concentrations which might be particulary variable during antituberculosis treatment. In this thesis, pharmacometric models were developed to describe the pharmacokinetics of lopinavir and ritonavir, to account for the drug-drug interactions

between lopinavir, ritonavir and rifampicin, and to investigate optimal dose regimens of lopinavir/ritonavir when administered with rifampicin. Moreover, we investigated the use of lamivudine concentration measurement in young children to propose the reference cutoff values for evaluation of adherence to prior doses.

Integrated population pharmacokinetic models of lopinavir and ritonavir were developed in young children and adults, respectively. For young children, a one-compartment model with first-order absorption and elimination best described the pharmacokinetics of lopinavir and a one-compartment model with transit absorption compartments described ritonavir pharmacokinetics. The dynamic influence of ritonavir concentration on lopinavir oral clearance was modeled as direct inhibition with an E_{max} model. Antituberculosis treatment reduced the oral bioavailability of lopinavir by 77% in children receiving twice usual lopinavir/ritonavir doses and increased ritonavir clearance by 50%. Simulations predicted that respective 27, 21, 20 and 18 mg/kg 8 hourly doses of lopinavir (in lopinavir/ritonavir, 4:1) maintains lopinavir concentrations >1 mg/L in at least 95% of children weighing 3-5.9, 6-9.9, 10-13.9 and 14-19.9 kg.

For adults, a one-compartment model with first-order absorption and elimination best described the pharmacokinetics of lopinavir and a two-compartment model with transit absorption compartments described ritonavir pharmacokinetics. Rifampicin reduced the oral bioavailability of lopinavir and ritonavir by 20% and 45% respectively, and it increased their clearance by 71% and 36% respectively. Similar to young children, with increasing concentrations of ritonavir, clearance of lopinavir decreased in an E_{max} relationship. Simulations predicted that 99.5% of patients receiving doubled doses of lopinavir/ritonavir achieve morning trough concentrations of lopinavir >1 mg/L during rifampicin co-administration, and 95% of those weighing less than 50 kg achieve this target already with 600/150 mg doses of lopinavir/ritonavir.

Doubling the standard doses of lopinavir/ritonavir can overcome the great reduction of lopinavir concentrations due to rifampicin induction to attain the target concentration in adults, but this approach failed in 59% of young children in our study. A comprehensive population pharmacokinetic model using the combined data from children and adults was developed simultaneously, to compare the pharmacokinetic differences of lopinavir and ritonavir between young children and adults, with and without rifampicin co-administration. The bioavailability of lopinavir was reduced by 24.7% in adults whereas children on antituberculosis treatment experienced a 58.7% reduction in the bioavailability of lopinavir, an effect that was moderated by the dose of ritonavir. Conversely, rifampicin increased the oral clearance of both lopinavir and ritonavir to a lesser extent in children than in adults. As adult studies cannot reliably predict their magnitude in children, drug-drug interactions should be evaluated in pediatric patient populations.

A population pharmacokinetic model of lamivudine was developed to describe the variability of lamivudine concentrations in young children, and to propose reference lamivudine concentrations for adherence investigation. A two-compartment model with transit absorption best described the lamivudine pharmacokinetics. Clearance was found to mature with age in a sigmoidal relationship: the clearance at full maturation is 12.1 L/h in a 10 kg child, and it reaches half of this value by 4 months after birth. Oral clearance of lamivudine was found to be 16.7% slower overnight. The variability of clearance was small so that simulations could accurately predict lamivudine concentrations. Most of the variability in lamivudine pharmacokinetics could be explained by body weight and age. Reference cutoff values for lamivudine concentrations that can be used to evaluate adherence to recent treatment doses were proposed.

Peer reviewed publications included in this thesis

The following papers describe the results arising from the body of work comprising this thesis:

Paper I: Zhang C, McIlleron H, Ren Y, van der Walt JS, Karlsson MO, Simonsson USH, Denti P. Population pharmacokinetics of lopinavir and ritonavir in combination with rifampicin-based antitubercular treatment in HIV-infected children. *Antiviral Therapy* 2012; 17(1):25-33.

Paper II: Zhang C, Denti P, Decloedt E, Maartens G, Karlsson MO, Simonsson USH, McIlleron H. Model-based approach to dose optimization of lopinavir/ritonavir when co-administered with rifampicin. *British Journal of Clinical Pharmacology* 2012; 73(5):758-67.

Paper III: Zhang C, Denti P, van der Walt JS, Ren Y, Smith P, Karlsson MO, McIlleron H. Population pharmacokinetic model for adherence evaluation using lamivudine concentration monitoring. *Therapeutic drug monitoring* 2012; 34(4):481-4.

Paper IV: Zhang C, Denti P, Decloedt E, Ren Y, Marrten G, Karlsson MO, McIlleron H. Model-based evaluation of the pharmacokinetic differences between adults and children administered lopinavir and ritonavir in combination with rifampicin. *Clinical Pharmacology and Therapeutics*. Submitted.

Table of Contents

Abbreviations

HIV	Human immunodeficiency virus
TB	Tuberculosis
WHO	World health organization
MTB	Mycobacterium tuberculosis
ATT	Antituberculosis treatment
PIs	Protease inhibitors
NRTIs	Nuclecoside reverse transcriptase inhibitors
HAART	Highly active antiretroviral therapy
NNRTIs	Nonnucleoside reverse transcriptase inhibitors
CYP 450	Cytochrome P450
EC_{50}	50% effective concentrations
LPV/r	Lopinavir/ritonavir as a ratio of 4:1
Pgp	P-glycoprotein
C_{max}	Maximum plasma concentrations
AUC	Area under the plasma concentration-time curve
HBV	Hepatitis B virus
Lamivudine	3TC
MDR	Multidrug resistant
XDR	Extensively drug resistant
FDCs	Fix dose combinations
PXR	Pregnane X receptor
CAR	Active/androstane receptor
FDA	Food and drug adminstration
NONMEM	Nonlinear mixture effect model
IIV	Interindividual variability

IOV	Interoccasion variability
RUV	Residual unexplained variability
OFV	Objective function value
FO	First-order method
FOCE	First-order conditional method
LAPLACE	Laplacian second-order approximation method
PRED	Population typical model prediction
IPRED	Individual model prediction
WRES	Weighted residuals
CWRES	Conditional weighted residuals
NPDE	Normalized prediction distribution error
VPC	Visual predictive check
CI	Confidence interval
BSA	Body surface area
ALT	Alanine transaminase
PsN	Perl speaks NONMEM
CV	Coefficient of variation
RSE	Relative standard error
SCM	Stepwise covariate modeling
GAM	Generalized additive models
CL/F	Apparent clearance
V/F	Apparent volume of distribution
ka	Absorption rate constant
ktr	Transit absorption rate constant
MTT	Mean transit time
LLOQ	Lower limit of quantification
BQL	Blow the quantification limit

Introduction and literature review

Human immunodeficiency virus (HIV) infection is a prevalent and big public health issue all over the world. According to estimates from the UNAIDS 2011 AIDS Epidemic Update [1], around 34 million adults and 3.4 million children were living with HIV at the end of 2010. There were 2.7 million new HIV infections in 2010. The number of people living with HIV increased dramatically for ten years before this trend began to decline in 2007 (Figure 1.1). The overwhelming majority of people with HIV live in low- and middle-income countries. Sub-Saharan Africa accounts for 68% of all infected people. South and South-East Asia have the second highest number of people living with HIV [2].

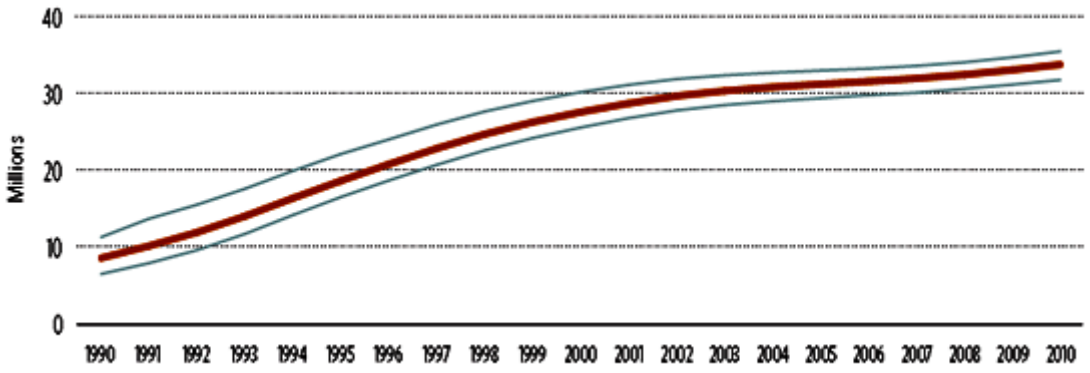

Figure 1.1. The trend of global number of people living with HIV during 1990-2010 (UNAIDS 2011 http://www.who.int/hiv/pub/progress_report2011/en/).

Tuberculosis (TB) is the most common opportunistic infection among people with HIV infection and is also associated with substantial morbidity and mortality. An estimated 1.1 million HIV-infected persons developed TB globally in 2010, the enormous majority in Africa (Figure 1.2) [3]. Up to 60% of TB patients have HIV co-infection in high burden countries, and in some locations more than 30% of

patients commencing antiretroviral therapy (ART) have TB [3]. Not only does HIV increase the risk of reactivating latent Mycobacterium tuberculosis (MTB) infection, it also increases the risk of rapid TB progression soon after infection and re-infection with MTB [4,5]. Compared with HIV uninfected TB patients, HIV infected TB patients experience greater morbidity and mortality, as well as an increased risk of rapid disease progression. Therefore, the development of effective HIV and TB control strategies, including collaborative antiretroviral and antituberculosis interventions, is one of the most important public health challenges facing sub-Saharan Africa today.

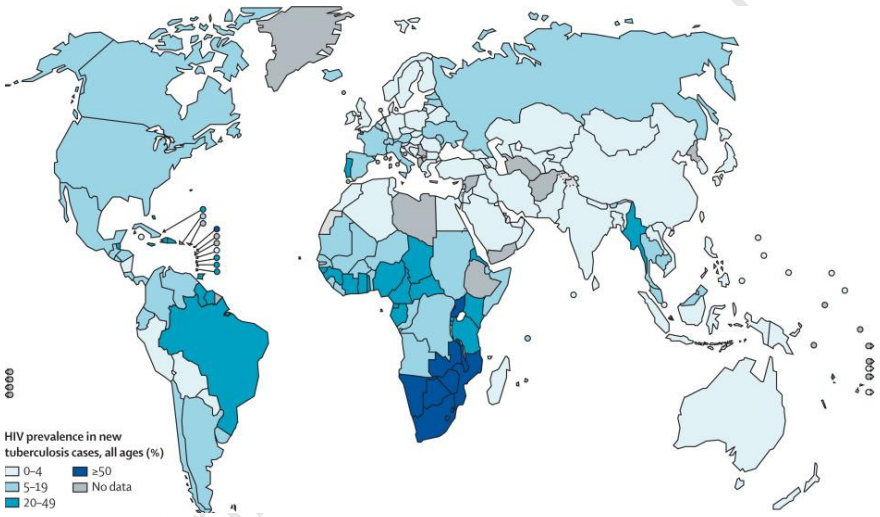

Figure 1.2 Estimate HIV positive TB prevalence, 2010 (WHO 2011 http://www.who.int/tb/publications/global_report/en/)

Despite the complexities of treating two infections requiring multidrug therapy at the same time, ART can be life-saving among patients with TB and advanced HIV disease[6]. Such patients should commence ART as soon as possible after starting antituberculosis treatment (ATT) [6]. However, concomitant use of treatment for TB and ART is often complicated by drug-drug interactions, adherence challenges due to polypharmacy, overlapping toxicity, an increasing cost burden and development

of the immune reconstitution inflammatory syndrome. Drug interactions between ART and ATT may lead to drug resistance and treatment failure or life-threatening side effects, which further challenge overburdened heath care systems. Some of the drug-drug interactions are extensive [7–11]. For example, rifampicin reduces the trough concentration of PIs>90% [12] and reduces exposure to NNRTIs, such as nevirapine, efavirenz, and abacavir, about 60-70% [13]. Subtherapeutic concentrations of ART related to these interactions might result in the development of resistance. Adherence and tolerability in patients also need to be evaluated as the increased pill burden is considerable and the risks of combined toxicity have not been adequately described, especially for second-line therapies, across patients with different levels of immune suppression, and a variety of other risk factors. There is a critical need to investigate optimal regimens and monitoring strategies for TB patients co-infected with HIV. The optimization of co-treatment strategies is important in the context of limited available ART regimens which need to be conserved at the population level and the individual level. Furthermore, HIV-infected children in high burden countries have very high rates of TB, often with severe, life-threatening manifestations, but there are very limited data about co-administration of antituberculosis and antiretroviral drugs among children. The pharmacokinetics of drugs behaves differently in adults and pediatric populations, the latter being particularly heterogeneous. Therefore there is an even greater need to investigate the optimal ART regimens in children co-administered ATT.

In this thesis, population models for antiretroviral drugs during co-administration with rifampicin-based ATT in adults and children are presented. The models investigated the pharmacokinetics and drug-drug interactions between lopinavir, ritonavir and ATT, thus providing a semi-mechanistic basis for the interactions, and explored the pharmacokinetic differences between children and adults. Moreover, the models could be used to predict optimal doses of antiretrovirals during rifampicin-based ATT. Lastly lamivudine concentrations were explored as a

potentially useful measure of adherence to recent doses to aid interpretation of protease inhibitor or nonnucleoside reverse transcriptase inhibitor concentration monitoring results.

1. Treatment of HIV in patients with tuberculosis

1.1. Antiretroviral therapy

There are different stages that the virus goes through after it has entered the human body and antiretroviral drugs use those different stages as target sites for their action. Some drugs interfere with the multiplication and release of the mature virus from the host cell while others interfere with the attachment and penetration of the host cell by the infecting virus. Figure 1.3 indicates the viral replication process and the site of action of antiviral treatment.

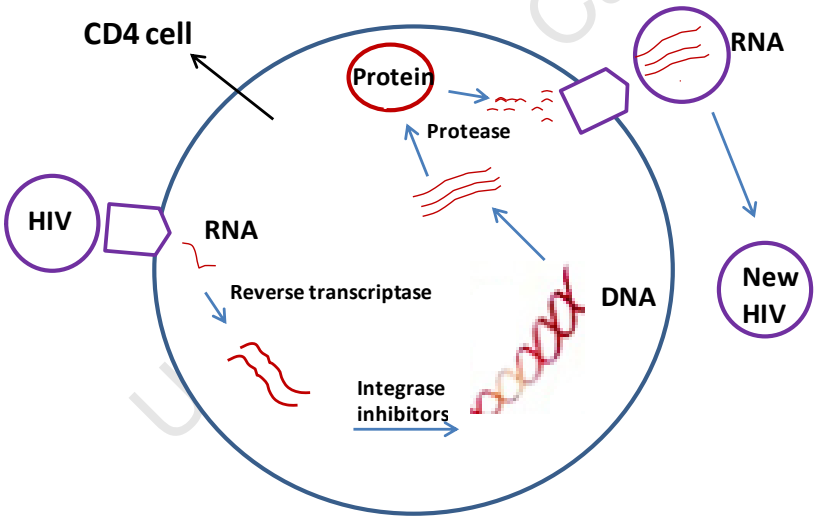

Figure 1.3 The viral replication process and the site of action of antiviral drugs. (HIV virus binds to and enter human immune cells first, then replicates through the reverse transcriptase and protease, and then exclude from the human cell to form a new HIV.)

Antiretroviral agents are classified under five unique drug classes: protease inhibitors (PI), nucleoside reverse transcriptase inhibitors (NRTI), nonnucleoside

reverse transcriptase inhibitors (NNRTI), integrase inhibitors and entry or fusion inhibitors. Each of these groups acts in a different way (summarized in Table 1.1). The last two classes are not widely used in clinics due to high prices and not being readily available in developing economies.

Table 1.1. Summary of different types of antiretroviral drugs

Antiretroviral drug class	**Action site**	**Represent drugs (abbreviation)**
Nucleoside/Nucleotide Reverse Transcriptase Inhibitors (NRTIs)	NRTIs interfere with the action of an HIV protein called reverse transcriptase, which the virus needs to make new copies of itself	Lamivudine (3TC); Abacavir (ABC); Zidovudine (AZT); Stavudine (d4T); Didanosine (ddI); zalcitabine (ddC); Tenofovir (TDF); Emtricitabine (FTC)
Non-Nucleoside Reverse Transcriptase Inhibitors (NNRTIs)	NNRTIs also stop HIV from replicating within cells by inhibiting the reverse transcriptase protein	Delavirdine (DLV); Efavirenz (EFV); Etrairine (ETR); Nevirapine (NVP)
Protease Inhibitors (PIs)	PIs inhibit protease, which is another protein involved in the HIV replication process	Amprenavir (APV); Atazanavir (ATV); Darunavir (DRV); Indinavir (IDV); lopinavir (LPV); Ritonavir (RTV); Nelfinavir (NFV); Saquinavir (SQV); Tipranavir (TPV)
Fusion or Entry Inhibitors	Fusion or entry inhibitors prevent HIV from binding to or entering human immune cells	Enfuvirtide (T-20); Maraviroc (MVC)
Integrase Inhibitors	Integrase inhibitors interfere with the integrase enzyme, which HIV needs to insert its genetic material into human cells	Raltegravir (RAL)

NRTIs are the structural analogues of the nucleotide, which block RNA and DNA.

NRTIs competitively block reverse transcriptase's enzymatic function and prevent completion of synthesis of the double-stranded viral DNA, thus effectively inhibit viral replication [14]. NRTIs are generally not metabolized by hepatic cytochrome P450 (CYP450) enzymes, instead, intracellular enzymes such as nucleoside kinases, 5'-nucleotidases, purine and pyrimidine nucleoside monophosphate kinases or similar enzymes are involved [15]. NRTIs are generally safe and well tolerated, but they are associated with important toxicities, for example, mitochondrial toxicity and lactic acidosis.

NNRTIs, like NRTIs, also target HIV reverse transcriptase, but the mechanism of action is different. NNRTIs block complementary DNA elongation through binding directly and noncompetitively to the enzyme, which stimulates irreversible alteration in protein at the active site and decreases affinity for nucleoside binding [14]. NNRTIs are metabolized to some degree by CYP450 enzymes and they can act as either inhibitors or inducers, therefore affecting the metabolism of other drugs.

PIs prevent gag-pol polyprotein cleavage through acting on the active site of viral protease thus new viral particles cannot mature. PI-based combination regimens can result in profound and sustained suppression of viral replication [16,17]. PIs are extensively metabolized by CYP3A4 present in the liver, while the isoenymes CYP2C19, CYP2C9 and CYP2D6 may also contribute to the metabolism of some PIs [18–22]. The combination of PIs with low dose of ritonavir is developed and widely used in ART regimens in order to minimize the risk of treatment failure and maximize the durability of treatment response [23–25]. This positive drug-drug interaction increases the exposure to the PIs, allowing administration of lower doses at reduced dosing frequencies with less dietary restrictions.

1.2. Rifampicin-based antituberculosis therapy

Contemporary treatment of drug-sensitive tuberculosis is divided into two phases:

intensive phase and continuation phase. In the intensive phase, covering the first two months of drug therapy, the bactericidal effect of the drugs administered is most prominent, with rapid bacteriological sputum conversion to culture negativity in the majority of adult patients. The continuation phase is usually four months and prolonged treatment may be given to some patients with initially poor response.

The first-line antituberculosis drugs include isoniazid, rifampicin, ethambutol, and pyrazinamide. The WHO guideline [26] recommends fixed-dose combinations (FDCs) of antituberculosis drugs with the purpose of preventing drug resistance due to monotherapy. Rifampicin is the key component of first-line antituberculosis treatment regimens. For new patients with TB, guidelines recommend a regimen: 2HRZE/4HR (rifampicin (R) and isoniazid (H) for 6 months with pyrazinamide (Z) and ethambutol (E) for the first 2 months) [26].

Among treated TB patients, death rates are higher in HIV-positive than in HIV-negative patients. The case-fatality rate is reduced in patients who receive concurrent ART [27]. The first priority for HIV-positive patients presenting with TB is to initiate TB treatment, followed by ART. Rifampicin is a potent inducer of multiple metabolizing enzymes and drug transporters including CYP3A4 and P-glycoprotein (Pgp) [28], while isoniazid has been shown to inhibit CYP3A4 [29] , and therefore strong pharmacokinetic interactions with other drugs should be anticipated. CYP2C19 and CYP3A were inhibited potently by isoniazid in a concentration-dependent way, but isoniazid did not show significant inhibition of CYP2C9, CYP1A2, and CYP2D6[29]. No data supports remarkable effects on any CYP activity by pyrazinamide and ethionamide.

1.3. Current recommended regimens

The current WHO guidelines [6] indicate that for the adults and adolescents,

first-line ART includes an NNRTI in combination with two NRTIs, with the preferred regimens comprising AZT or TDF + 3TC or FTC + EFV or NVP. Meanwhile, ritonavir-boosted PIs plus two NRTIs are recommended as the second-line ART for adults and adolescents and the preferred PIs are atazanavir/ritonavir or lopinavir/ritonavir (4:1, LPV/r) [6], which have comparable antiretroviral effect. As antiretroviral programs mature and patients move onto second-line regimens, a sharp increase in the use of PIs is expected. However, most PIs have low bioavailability and a relative short half-life [28], and the pharmacokinetic interactions with food and other medications are common [30]. Accordingly, the treatment regimens are complicated by these factors.

For children < 2 years of age, LPV/r plus two NRTI is recommended as the first-line ART regimen by WHO guidelines [31]. HIV infected infants exposed to single dose nevirapine, or maternal NNRTIs-containing ART or prevention regimens, PI-based ART should be used [31,32]. Infants should start ART as soon as possible regardless of level of immune suppression. LPV/r is the preferred regimen in <2 year-olds with ART exposure (maternal ART or a regimen for prevention of mother-to-child transmission). Recently released results of the P1060 study suggest that LPV/r might also be preferred to a NVP-based regimen in infants not exposed to ART [33].

As for the treatment of HIV infected patients presenting with TB, ATT is started first, followed by ART as soon as possible afterwards. The ATT regimen is the same as for patients who are not HIV-infected. Compared to adults, young children (especially those under 2 years) are at particularly high risk of developing TB in high burden settings and up to 25% of HIV infected children not on ART develop TB each year in South Africa [31]. All children presenting with TB regardless of age or CD4 count should be started on ATT immediately with continuous ART[13]. However, considering the potential for combined toxicities and drug-drug

interactions, the following ART regimen adjustments are recommended: EFV plus 2NRTIs is preferred for children > 3 years-old; a triple NRTIs regimen is recommended for children < 2 years and NVP plus 2NRTIs for children 2-3 years old; super-boosted LPV/r (adding ritonavir in a 1:1 ratio of lopinavir: ritonavir) is recommended for children already on a PI when they get TB or in children who have failed the first-line therapy. But adding extra ritonavir is technically difficult and cumbersome to implement since it is with a high risk of prescription and dosing errors. Moreover, ritonavir is poorly tolerated in high doses and ritonavir solution should be kept in refrigeration and has a short shelf life to maintenance of supply difficult in many settings. Therefore, more studies are needed to evaluate pharmacokinetics, safety and efficacy.

2. Drugs of interest in this thesis

2.1. Lopinavir/ritonavir

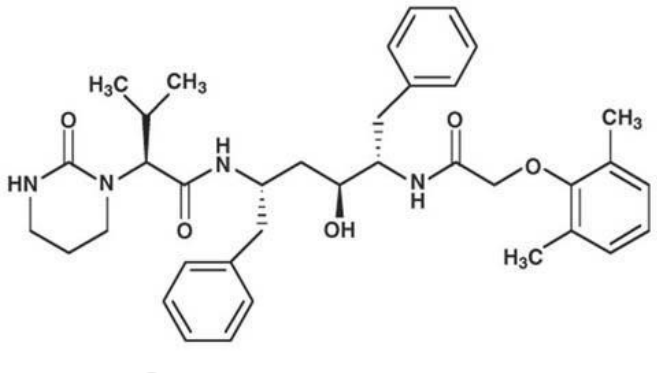

Figure 1.4 Structure of lopinavir

Lopinavir (Figure 1.4) is one of the most widely used PIs. It exerts a high intrinsic antiretroviral potency against viral strains coming from either ART-naive or -experienced patients [30,34]. From *in vitro* study, lopinavir is highly active against HIV-1 cultured in peripheral blood mononuclear cells, with a mean 50% effective concentration (EC_{50}) of 6.5 nmol/L [22]. The clrearance of lopinavir is 0.06-0.18 L/h.kg, volume is 0.56-2.16 L/kg, and half life is 6.2-8.4 h.[12] Lopinavir is 98.2% to

99.2% protein bound in both healthy volunteers and HIV-infected patients [35]. Protein binding is not concentration-dependent within the therapeutic range. Lopinavir is precluded the use as a single PI in ART regimens due to its poor oral bioavailability, and its extensive and rapid metabolism by the CYP 3A4 isoenzyme in the liver [22,34,36–38]. Therefore, lopinavir is always co-administered with low dose of ritonavir which inhibits intestinal and hepatic CYP3A4 and p-glycoprotein (Pgp). Lopinavir and ritonavir are co-formulated in a ratio of 4:1 (LPV/r). The antiretroviral activity of LPV/r combination is derived from lopinavir, but adverse effects are often due to ritonavir [39]. Compared with other PIs, this combination has demonstrated a favorable resistance profile and shown promising properties in suppression of HIV-RNA and recovery of CD4+ T cell counts [34].

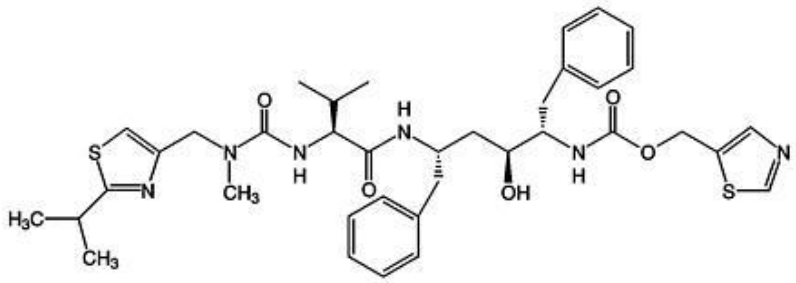

Figure 1.5 Structure of ritonavir

Ritonavir (Figure 1.5) is metabolized mainly by CYP3A4, and to a lesser but clinically relevant extent by CYP2D6 [40]. *In vitro*, the metabolism of lopinavir is inhibited by very low concentrations of ritonavir, with IC_{50} values of 0.026 mg/L and 0.053 mg/L in rat and human liver microsomes, respectively [28,40]. Ritonavir also has been shown to induce its own metabolism [35]. Ritonavir boosts lopinavir concentrations via two possible mechanisms [30,40–42]. Firstly, it may improve the oral bioavailability of lopinavir by inhibiting intestinal CYP3A4 and Pgp. Secondly, ritonavir may also decrease the rate of elimination of lopinavir by inhibition of CYP3A4 and Pgp in the liver. The mean steady-state lopinavir plasma concentrations in HIV infected patients administered LPV/r 400/100 mg

twice daily are 15- to 20-fold higher than those of ritonavir. *In vitro*, compared to ritonavir, the antiviral EC_{50} of lopinavir is approximately 10-fold lower [22]. LPV/r therapy also was found to result in moderate induction of CYP1A2 and CYP2C9 and potent induction of CYP2C19 activity [43]. It may be necessary to increase doses of concomitant medications metabolized by these enzymes. The median trough concentration was reported 5.2 ug/mL with 400/100 mg LPV/r by Crommentuyn et al [44], which is at least 51-fold above the protein binding-adjusted EC_{50} of lopinavir (0.07 ug/mL) [45]. The clrearance of ritonavir is 0.16-1.40 L/h.kg, volume is 0.56-1.39 L/kg, and half life is 2.3-3.2 h.[12]

The currently available formulations of LPV/r are tablet (Aluvia®, Abbott Laboratories), soft gelatin capsule (Kaletra®, Abbott) and oral liquid (Kaletra Oral Solution®, Abbott). Two tablet formulations are available: 200 mg lopinavir + 50 mg ritonavir or 100 mg lopinavir + 25 mg ritonavir (the latter is for pediatric dosing). The liquid formulation contains 80 mg lopinavir + 20 mg ritonavir per mL. The liquid formulation is 42% ethanol by volume and is the first and only co-formulated ritonavir-boosted PI approved for use in children.

The recommended dosage of LPV/r in ART-naive and -experienced adults and adolescents is 400/100 mg twice daily while for children it is dosed according to body surface area or body weight according to mg/kg and weight band dosing[31,46]. Studies conducted in ART-experienced and –naive patients indicated that the pharmacokinetics of lopinavir was similar [44,47]. The bioavailability of lopinavir is increased after administration of the LPV/r co-formulation with food, which effect is less prominent with the tablet. The mechanism is not clear, but it may be related with food prompting high-protein binding drugs. Compared with fasting, administration of a single dose of LPV/r 400/100 mg with a moderate to high fat-content meal increased lopinavir maximum plasma concentration (C_{max}) and area under the plasma concentration-time curve (AUC) by up to 56% and up to

130% with the capsule and liquid co-formulations respectively, and by up to 17% and up to 27% with the tablet co-formulation [48,49]. LPV/r is generally clinically well tolerated and the most common adverse events are gastrointestinal reactions, including diarrhea, nausea and vomiting, and hypertriglyceridaemia and hypercholesterolaemia. Hepatic or metabolic dysfunction has been also reported [50].

2.2. **Lamivudine**

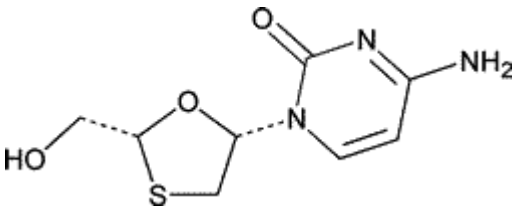

Figure 1.6. Structure of lamivudine

Lamivudine (3TC), the negative enantiomer of 2′-deoxy-3′-thiacytidine (Figure 1.6), is a dideoxynucleoside analogue widely used in combination with other agents in ART regimens and as monotherapy in the treatment of hepatitis B virus (HBV) infection[51,52]. As a NRTI, lamivudine is commonly included in first-line ART regimens [31,46]. Lamivudine is rapidly absorbed orally and has a wide distribution because of its high lipid solubility as well as tissue binding and low plasma protein binding (<36%). Lamivudine is primarily renally eliminated and about 5 to 10% is metabolized to the pharmacologically inactive trans-sulfoxide metabolite, the majority of which is also excreted in the urine within 12 hour after a single oral dose [53–55]. Since most of an oral dose is eliminated renally as unchanged drug, the dose needs to be reduced in patients with renal insufficiency [56]. Hepatic impairment does not affect the pharmacokinetics of lamivudine. The likelihood of metabolic interactions of lamivudine with other medicinal products is low due to its small extent of hepatic metabolism (5-10%) and low plasma protein binding. Systemic clearance after single intravenous doses averages 20 to 25 L/h

(about 0.3 L/h/kg) and the dominant elimination half-life of lamivudine is approximately 5 to 7 hours.

Lamivudine exhibits linear pharmacokinetics over the therapeutic dose range. The bioavailability of lamivudine in adults and adolescents is between 80 to 85%. The mean time to peak serum concentration (T_{max}) is approximately one hour [57–60]. Food reduces the peak serum concentration (C_{max}) and delays the time to T_{max}, however, no significant difference in overall bioavailability is observed; therefore, no dose adjustment is needed when co-administered with food [56]. A higher dose is recommended for pediatric patients (8 mg/kg/day) because the bioavailability in children is reduced to approximately 65% and clearance increased by 0.52 L/kg/h[58,59,61].

Lamivudine is well tolerated. Severe adverse effects such as liver and metabolic disorders are rare. Pancreatitis has been reported in patients receiving lamivudine, particularly in HIV-infected pediatric patients with prior nucleoside exposure [62–64].

2.3. Rifampicin

Rifampicin is the most important agent for the treatment of TB and is lipid soluble and readily absorbed from the gastrointestinal tract. Rifampicin is about 80% protein bound and widely distributed throughout the body. Rifampicin is rapidly eliminated in the bile, and an enterohepatic circulation occurs. Up to 30% of a dose is excreted in the urine, with about half of this being unchanged drug [65].

Rifampicin activates the pregnane X receptor (PXR), which is a nuclear receptor regulating transcription of multiple drug metabolizing enzymes including phase I enzymes such as CYP2A6, 2B6, 2C9, 2C19, 2C8, 3A5, 3A4 and 3A7, phase II enzymes such as the glutathione-S-transferases, UDP glucuronosyltransferases and sulphotransferases and transporters such as Pgp, multidrug resistance protein 2,

multidrug resistance-associated protein 2 and the organic anion transporter polypeptide 2 [66]. Hence rifampicin reduces the concentrations of many concomitantly administered drugs that are metabolized by CYP3A4 and/or are transported by Pgp. Rifampicin is regarded to be amongst the most potent inducers of CYP3A4 known. The induction by rifampicin at clinical doses of 600 mg is near maximal [67].

Rifampicin concentrations vary widely between patients and study populations. Low concentrations have been observed in children and reductions in the bioavailability of rifampicin of 30-50% have been found in HIV infected patients [68,69] and might be due to malabsorption because of HIV-associated enteropathy and increased susceptibility to enteric infections [70]. It is unknown how induction of enzyme expression associated with rifampicin may be affected with changing exposure [71] [19].Therefore, a higher dose of rifampicin should be considered for HIV infected patients, but related high incidence of adverse effects may become another concern. Significant CYP3A4 induction was detected 8 hours after a single rifampicin dose [72]. The activity of CYP3A4 during rifampicin administration reached steady state after one week and returned to baseline about 2 weeks after termination of rifampicin administration [73].

3. Variability in pharmacokinetics of antiretroviral and antituberculosis drugs

3.1. Pharmacokinetic variability

Large interindividual variability in the pharmacokinetics of the drugs could result in a given drug being effective for some patients but ineffective for others. Potential sources of pharmacokinetic variability include physiological factors such as age, sex, weight, height, hemoglobin, pathological states such as hepatic or renal impairment, cardiac failure, severity of HIV, co-administration of ATT

regimens, genetic factors, environmental factors and drug-drug interactions [19].

It is reported that NNRTIs display less interindividual and intraindividual pharmacokinetic variability than PIs [74]. In total of 457 PI and 172 NNRTI plasma concentrations, intraindividual variability was consistently lower than interindividual variability [74]. Genetic diversity could explain variability, for example, zidovudine clearance was shown 48% higher in glucuronidation and 33% higher in UGT2B7*1c carriers versus non-carriers [75]; and a wide range of efavirenz concentrations can be explained by genetic polymorphism encoding CYP2B6 [76–79]. Moreover, ATT tend to increase interindividual variability in efavirenz concentrations [80,81].

Body weight is an obvious source of pharmacokinetic variability, and bigger doses are often prescribed for heavier individuals (e.g. when mg/kg dosing schemes are used). Nevertheless, this normalization is not sufficient and it is common knowledge for example that many drug doses have to be modified in the elderly and children. Moreover, the drug elimination does not have a linear relationship with body weight. Therefore doses are increased less rapidly than predicted directly from body weight, and in most instances heavier individuals require lower dose per kg to achieve the same exposure. Children, especially infants and young children have extremely different pharmacokinetics compared to adults in many situations.

3.2. Pharmacokinetics in children

Physiological differences between adults and children can be expected to produce significant differences in the way they respond to drugs. For this reason, US Food and Drug Administration (FDA) has required trials of new drugs to be done in pediatric populations for the use of a product in pediatric patients prior to approval for use in adults. Numerous approaches for determining pediatric drug doses have

been recommended. Some of these approaches use discrete age points, and others use allometric principles that generally assume predictable relationship between children and adults [82]. However, as age-associated changes in body composition and organ function are dynamic and tend to be inconsistent especially during the first age of life, simplified dosing approaches are not adequate for individualizing drug dosages across the span of childhood.

Pharmacokinetics can be expected to differ between children and adults, especially for very young children. The oral formulations used for children have to be easy to swallow, such as liquid or powder and such formulations may have different absorption profile compared to tablets because of diverse solubility, permeability and excipients. When paediatric formulations are not available, tablets for adults are often crushed, before administration to children, a process which in itself might affect absorption. Furthermore, the relative amount of drug available for absorption will be influenced by age-dependent changes in luminal pH, which affects degree of ionization and drug stability. The solubility and subsequently absorb lipophilic drugs can be altered by age-dependent changes in biliary function [83]. There are also varying rates in absorption due to differences in gastric emptying and intestinal motility between children and adults. Developmental differences in the activity of intestinal drug metabolizing enzyme and efflux transporters are also likely to markedly alter drug bioavailability in children and adults.

Age-dependent changes in body composition alter the physiologic spaces into which a drug may distribute. Large extracellular and total body water in neonates and young infants who have higher water/lipid ratios than in adults, result in lower plasma concentrations for drugs which distribute into the respective compartments. The composition and amount of circulating plasma protein (eg. albumin, α 1 acid-glycoprotein) are changed by age and therefore influence the distribution of

highly bound drugs, such as lopinavir and ritonavir [83,84]. Other differences between children and adults, such as regional blood flow, organ perfusion, permeability of cell membranes, acid-base balance can also affect drug binding or distribution.

Development of expression of CYP450 enzymes is profoundly affected by age. Hattis et al summarized the geometric mean ratios of children/adults elimination half-lives from 135 data groups for 41 drugs and found that the metabolism enzyme displayed different in the duration from premature neonates to 12-18 years old [84]. Distinct patterns of development of isoform-specific CYP expression have been found after birth. CYP3A7 is the predominant CYP isoform enzyme expressed in fetal hepatocytes and its expression attains a peak shortly after birth and then diminishes rapidly to levels that are undetectable in most adults. The clearance of carbamzaepine, which is largely dependent on CYP3A4, is greater in children than in adults [84]. Phenytoin metabolism is not attatining saturation until approximately 10 days of postnatal age, demonstrating the developmental attainment of CYP2C9 activity. For renal elimination, the maturation of renal function is a dynamic process that starts early during fetal organogenesis and is complete by early childhood [83].

Key considerations for drug exposures in HIV-infected pediatric patients include factors such as etiological, physiological, psychological and social differences between children and adults. This is further complicated for children during co-administration of ART and ATT regimens since the drug induction or inhibition may display differently between children and adults. Therefore, given the growing number of TB children with HIV-infection who have access to treatment, a better understanding and comparison of pharmacokinetics of ART drugs between adult and pediatric populations, as well as drug-drug interactions associated with antiretroviral and antituberculosis agents, is important.

3.3. Therapeutic drug monitoring of antiretroviral drugs

Since high variability is observed during ART, which may be accentuated when co-administered antituberculosis agents, therapeutic drug monitoring of antiretroviral drugs is quite necessary with the purpose of improvement of efficacy and reduction of toxicity. During therapeutic drug monitoring of ART, trough concentrations are usually applied for virological efficacy and peak samples for toxicity management. Guidelines provide therapeutic concentration ranges for PIs and NNRTIs based on current available clinical data [6,31]. A target lopinavir trough concentration greater than 1 mg/L is recommended for PI-naïve patients. For PI-experienced patients the minimum recommended trough concentration is based on the phenotypic or genotypic viral resistance patterns, therefore related to different mutations, ranging from 3.6 to 6.2 mg/L [85,86]. Although altered lipid profiles and elevated liver enzymes have been associated with increased concentrations of lopinavir, the available data does not support an upper limit for the therapeutic range [86]. Moreover, the presence of ATT, especially rifampicin, and possibly the sequence of treatment introduction with antituberculosis drugs and LPV/r, respectively, alters the risk of toxicity.

4. Pharmacokinetic drug-drug interactions

Drug-drug interactions occur when one therapeutic agent either alters the concentration (pharmacokinetic interactions) or the biological effect of another agent (pharmacodynamic interactions). Pharmacokinetic drug-drug interactions may include alterations in the pharmacokinetics of one drug by other drugs in the absorption, distribution, metabolism and excretion (ADME), leading to alterations in plasma or blood concentrations of the drug and subsequently at the site of action. Pharmacodynamic interactions are a result of the influence of combined treatment at a site of biological activity and produce altered pharmacological actions. Synergistic or antagonistic pharmacologic effects arise when pharmacodynamic drug interactions occur. Either type of drug interaction may lead to adverse effects in patients.

Pharmacokinetic drug-drug interactions that result in alteration of drug absorption can affect the rate or extent of absorption. The mechanisms include an alteration in blood flow to the intestine; increased or decreased drug metabolism by the intestine; change in intestinal motility; an alteration of pH in stomach or a change in the bacteria that reside in the intestine [87]. For example, magnesium, aluminium and iron cations have an affinity for fluoroquinolones, resulting in reduced absorption [88]. Hence, administration of buffered didanosine and antacids should be separated by several hours from administration of fluoroquinolones. Protein binding changes by drug-drug interaction can also influence the absorption, as well as drug distribution. The unbound concentrations of drug at steady state for most drugs will not be affected except high extraction drugs or drugs that are given in doses achieving near saturation of protein binding. Drug-drug interactions affecting the renal excretion of drugs can be caused by alterations in the transporters involved in the efflux of drug molecules into the urine by secretion. Alteration of pH in urine or flow of urine can also result in drug-drug interactions.

The most clinically vital drug-drug interaction result from alteration of drug metabolism. Drug metabolism occurs mainly in the liver, although other sites such as the gastrointestinal tract, kidneys, skin and lungs can be involved. The possible drug-drug interactions can be predicted by identifying the CYP enzymes that are modified through induction or inhibition by a particular drug. In addition to enzyme-based interactions, drug transporters play crucial roles in determining the pharmacokinetic profiles of drugs and are prone to induction and inhibition interactions.

4.1. Drug-drug interactions mediated by CYP enzyme

Drug metabolism by means of the CYP 450 system has been known as being of crucial importance for drug-drug interactions [24,89,90]. Enzyme induction or

inhibition results in enhanced or reduced drug metabolism, which results in higher or lower drug concentrations. CYP 3A4 isozyme is the most predominant hepatic and intestinal phase I enzyme and is responsible for the biotransformation of about 50% of all marketed drugs [91]. The substrates of CYP3A4 to a large extent overlap with those of Pgp, and the synergy effect is usually observed on the functions of Pgp and CYP3A4 [92], such as lopinavir and clarithromycin. The inhibition or induction of CYP3A4 by drugs often causes unpleasant and long-lasting drug-drug interactions, that may even result in fatal toxicity, depending on many factors associated with the enzyme, the drugs involved, or the patients [28,93–95].

4.1.1. Enzyme kinetics

The simple conversion of substrate (A) into product (P) catalyzed by the enzyme (E) is described Equation 1.1. Substrate binding first and the catalytic step is followed.

$$E + A \underset{k_{-1}}{\overset{k_1}{\rightleftharpoons}} EA \xrightarrow{k_{cat}} E + P \qquad (1.1)$$

where k_1 is the synthesis rate, k_{-1} is the degradation rate of enzyme-substrate complex , EA is the enzyme-substrate complex and k_{cat} is the catalytic rate constant.

During a very brief initial period, the enzyme–substrate complex is formed and reaches a concentration at which its consumption is matched by its formation. The [EA] then attains near constant as the steady state, and the Michaelis–Menten equation is used to describe (Equation 1.2). Finally, substrate diminishes in which the [EA] gradually falls.

Michaelis-Menten kinetics of enzyme metabolism is described as follows:

$$v = \frac{V_{max} \cdot C}{K_m + C} \qquad (1.2)$$

where *v* is the rate of metabolism of enzyme; *C* is the concentration of substrate. K_m is the Michaelis–Menten constant; The V_{max} is the maximum velocity that an enzyme could achieve and $V_{max} = k_{cat} \cdot$ [total amount of enzyme].

Therefore, clearance can be described as:

$$\mathrm{CL} = \frac{\mathrm{V}_{max}}{K_\mathrm{m} + \mathrm{C}} \quad (1.3)$$

and intrinsic clearance is

$$\mathrm{CL}_{int} = \frac{\mathrm{V}_{max}}{K_\mathrm{m}} \quad (1.4)$$

The K_m indicates the binding strength of that enzyme to its substrate. Assuming a stable pH, temperature, and redox state, this parameter is constant for a given enzyme. Michaelis–Menten kinetics assumes that k_{cat} is very low when compared to k_1 and k_{-1}. Therefore, a high K_m indicates the enzyme binds the substrate weakly. Conversely, a low K_m indicates a higher affinity for the substrate.

4.1.2. Enzyme induction

Enzyme induction can enhance synthesis of enzymes through either binding inducers to a nuclear receptor or stabilization of enzyme, such as the case of CYP2E1 [96]. Enzyme induction is a time-dependent process and may take from a few hours to several weeks to occur because it results from gene transcription and the following protein synthesis [97]. The steady-state levels of an enzyme depend on the balance between its rate of synthesis and degradation. Therefore, reaching a new steady-state level of induction or after withdrawal of the inducer will take time, no matter of whether the induction was due to synthesis of new enzymes or to enzyme stabilization. The time to reach a new steady state is determined by the enzyme half-life. The extent of CYP induction is related to the baseline levels of CYP enzymes, genetic polymorphism in the CYP enzymes, and environmental

factors such as smoking and alcohol consumption [98].

Enzyme induction enhances drug metabolism, and therefore may decrease its plasma concentration, which may be followed by a reduction in drug efficacy, depending on its therapeutic index. Induction effect will increase CL_{int} through complex binding to DNA and activating RNA polymerase or elevating level of protein [99,91,100]. Enzyme induction may increase plasma concentrations of metabolite. If the metabolite is toxic, enzyme induction results in aggravated toxicity, but alternatively it results in an enhanced effect for prodrugs.

4.1.3. Enzyme inhibition

Drug-drug interaction due to inhibition can be competitive, noncompetitive or uncompetitive [21,101,102]. The typical reactions in complex reality often involve mixed mechanisms of these three components. Competitive inhibition depends on the affinities of the substrate and inhibitor to the enzyme, since the inhibitor would be removed from the enzyme, and therefore increasing the concentration of the substrate can lead to recovery from inhibition. The presence of an inhibitor reduces the ability of the enzyme bind to its substrate. The half-life of the inhibitor decides on the recovery from competitive inhibition. An increase in the concentration of a competitive inhibitor will increase the apparent K_m of the enzyme, but there is no effect on V_{max} [101,103]. A noncompetitive inhibitor does not bind to the catalytic site but binds to a second site on the enzyme and acts by reducing the turnover rate of the reaction [28,104]. The binding of the inhibitor and substrate is completely independent, and binding of the inhibitor produces total inhibition of the catalytic step. Noncompetitive inhibitors will not alter the K_m but will reduce the apparent k_{cat} as inhibitor concentration increases. For uncompetitive inhibition, the enzyme can no longer metabolize the substrate because enzyme is inactivated by the inhibitor [28,101]. Inactivation of the enzyme usually lasts longer with uncompetitive compared to competitive inhibition, and recovery from uncompetitive inhibition is dependent on the half-life of the enzyme

if the half life of the inhibitor is comparatively negligible [28,90,105].

Enzyme inhibition decreases drug metabolism and increases plasma drug concentrations, which may lead to elevated pharmacological activity and, if the drug has a narrow therapeutic index, to adverse effects. For prodrugs, inhibiting drug metabolism would reduce the anticipated pharmacological effect. However, the metabolism pathway of a drug may shift to alternative minor pathways when the enzyme that is primarily involved in the metabolism has been inhibited.

4.2. Drug-drug interactions mediated by drug transporters

Uptake and efflux transporters, located in intestine, kidney, liver and other tissues, affect the pharmacokinetic profile of a drug substrate [106–108]. Efflux transporters expressed in the intestine and liver include Pgp or ABCB1, bile salt export pump (BSEP, ABCB11), multidrug resistance protein (MRP1-6, ABCC1-6), breast cancer resistance protein (BCRP, ABCG2), and all members of the ATP-binding cassette (ABC) superfamily [106,109,110]. Absorption transporters control drug transfer into the systemic circulation and secretary transporters mediate the excretion of substrates from the circulation into bile, urine, or intestinal lumen. Transporters also play important roles in oral drug disposition. Therefore, alteration of the functions of transporters may potentially change the disposition of drugs, as well as influencing drug-drug interactions.

The Pgp is an important efflux transporter which is expressed in many tissues and located on the apical side of intestine, liver, and kidney epithelia [111]. Drug-drug interactions can arise from induction or inhibition of Pgp by up-regulating the MDR1 gene, which encodes Pgp [28,112,113]. Induction or inhibition of intestinal Pgp results in alterations of the rate and extent of absorption of Pgp substrates. Drug metabolism is decreased by Pgp inhibition in the small intestine but enhanced in the liver. Moreover, alteration in Pgp activity can affect drug secretion in the urine

as well as distribution to different organs, such as the brain and placenta [111,113].

Intestinal transporters will exclusively affect bioavailability, thus clearance will not change in response to induction or inhibition of intestinal transporters, but the rate constant of absorption may be influenced [66,114–116]. Transporters in the liver and kidney can affect the clearance of orally administered drug that escapes the first-pass effect. Inhibiting uptake transporters prevents drug from being exposed to metabolizing enzymes within hepatocytes, decreasing the clearance of drugs that are substrates for these enzymes. For drugs that are not metabolized but are eliminated by biliary excretion, clearance may also decrease, since drug is prevented from getting into the bile through the hepatocytes [109]. Moreover, transporters may influence volume of distribution by mediating their transport into and out of a variety of tissue and organs [117]. If a tissue's uptake transporters are inhibited, more drug remains in the plasma and less drug is eliminated by the liver, which leads to decreased volume of distribution. Induction may increase the amount of drug remaining in the liver, decrease the concentration in plasma, and increase volume of distribution in action tissues. While the effect of altering function of hepatic efflux transporters on volume of distribution may behave in the opposite way, this effect is not always predictable.

4.3. Potential drug-drug interactions between lopinavir/ritonavir-based ART and ATT

Concomitant use of ATT and ART is complicated by drug-drug interactions. The result of interactions can be either a decrease or increase in drug exposure, which in turn can reduce efficacy or increase toxicity. Since PIs are extensively metabolized by the CYP450 system, there is considerable potential for pharmacokinetic interactions when these drugs are administered concomitantly with ATT drugs metabolized via the same pathway.

Rifampicin is a substrate of Pgp, and OATP1B1, as well as having a potent PXR-mediated action on CYP2B6, 2B9, 2C8, 2C9, 3A4, 3A7, GSTs, UGTs, SULTs, Pgp, MDR2, OATP2, MRP2, hence leads to a reduction in the concentrations of four classes of ART drugs: NNRTIs, PIs, CCR5-receptor antagonists, and integrase inhibitors. Rifampicin induction is mediated by the activation of PXR, which is highly expressed in the liver and intestine, and when a PXR ligand binds to PXR, it activates transcription of CYP 3A4 and Pgp [118]. CAR is another receptor is involved in CYP3A4 transcriptional regulation and it can trans-activate CYP3A4 gene expression both in vitro and in vivo [119]. The CAR response elements are also bound by PXR, which interacts in CYP3A4 expression. Rifampicin reduces trough concentrations of ritonavir-boosted PIs >90% and reduces exposure to NNRTIs (delavirdine > nevirapine > efavirenz), abacavir, zidovudine, maraviroc (60 – 70%), raltegravir (40%), linezolid (32%), moxifloxacin (30%) and rifampicin itself [11].

Though rifabutin is recommended instead of rifampicin to avoid drug-drug interaction[13], it is not a feasible option because rifabutin is currently prohibitively expensive and, in high burden countries, there is a tendency to rely on standard treatment regimens, often administered in FDCs. The use of rifabutin is further complicated by a lack of suitable formulations: a once daily dose that could be incorporated in a FDC would be easier to implement in tuberculosis control programs, and formulations suitable for children are not available. Moreover, ritonavir-boosted PIs significantly increase exposure to rifabutin and cause even greater increases in plasma concentrations of the active metabolite. Therefore, a reduced rifabutin dose is needed. However, there is not sufficient evidence for efficacy and safety of reduced rifabutin doses in HIV infected patients on PIs. It was reported that rifabutin three times weekly in combination with LPV/r- based ART may be feasible to achieve sufficient rifabutin concentrations [120], but it is difficult to implement in the clinic where daily administration of other

antituberculosis drugs is used. Therefore, rifampicin is still a key component in concurrent ATT and ART regimens.

Considering lopinavir being the substrate of both CYP3A4 and Pgp, it was reported that the concomitant administration of rifampicin with standard dose of LPV/r reduces the bioavailability and minimum concentration of lopinavir by approximately 75% and 99% respectively [12]. Rifampicin 300 mg or 600 mg once daily for 10 days decreased the AUC of ritonavir by about 35% [67]. Ritonavir is a potent inhibitor of CYP3A ,CYP2D6 and Pgp, and therefore a high dose of ritonavir can counteract the induction effect of rifampicin to be used to maintain concentrations of PIs', such as saquinavir and lopinavir during rifampicin therapy [121–123]. It has been demonstrated that ritonavir inhibition involves both reversible and irreversible mechanisms [21]. Meanwhile, ritonavir also has induction effects on other hepatic enzyme systems. The main drug-drug interactions between lopinavir, ritonavir and rifampicin related in this thesis are described in Figure 1.7. Moreover, isoniazid is often involved in the ATT regimens co-administered with lopinavir and ritonavir. It inhibits CYP1A2, 2C9, 2D6, 2C19, 3A4 and monoamine oxidase [29,69,96], and therefore affect the ritonavir metabolism. Co-trimoxazole is frequently used in young children on ART and rifampicin could reduce the AUC of trimethoprim [111]. Also, potential pharmacokinetic interactions between lopinavir, ritonavir and rifampicin have not been thoroughly evaluated and hence unanticipated interactions might arise. But all these effects are of secondary to those described in the Figure 1.7.

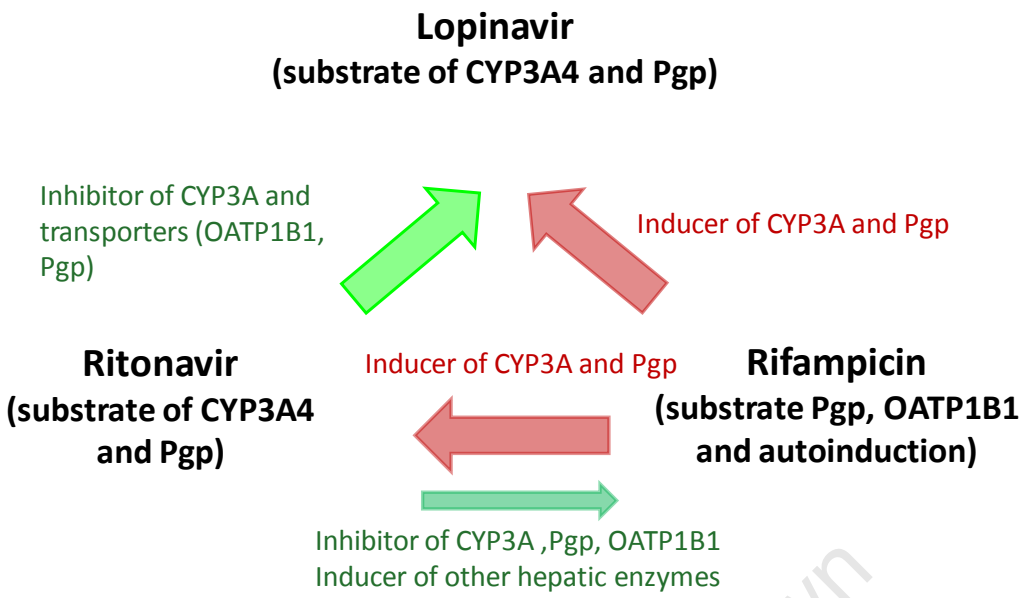

Figure 1.7. Drug-drug interaction between lopinavir, ritonavir and rifampicin.

In order to overcome the great induction effect from rifampicin, there is some evidence from a small study in adult volunteers to support the strategies of adding extra ritonavir to LPV/r, or increasing the dose of both lopinavir and ritonavir components, when rifampicin is given concomitantly [12]. The first approach is to add extra ritonavir to match the lopinavir dose (super-boosted) while on rifampicin-based TB treatment. However, in young children using the oral solutions, the approach of adding additional ritonavir to LPV/r is technically difficult, and cumbersome to implement with a high risk of prescription and dosing errors. Moreover, ritonavir oral solution is poorly tolerated in high doses and has a short shelf life hence clinics frequently run out of stock. The second approach is doubling the standard dose of LPV/r when it is given with rifampicin. As shown by la Porte et al. [12] and Decloedt et al [124], double dose of LPV/r can balance the rifampicin induction effect in adults. Another study by Nijland et al. [125] also evaluated the pharmacokinetics of adjusted dose LPV/r with rifampicin. However, the study which was conducted in healthy volunteers was discontinued prematurely due to very high rates of hepatotoxicity. Side effects such as nausea,

vomiting and elevated transaminases occur commonly when adjusted doses of LPV/r and rifampicin are co-administered [126, 12, 124 9]. Although altered lipid profiles and elevated liver enzymes have been associated with increased concentrations of lopinavir, the available data does not support an upper limit for the therapeutic range [86], and the presence of rifampicin, and possibly the sequence of treatment introduction with rifampicin and LPV/r, respectively, alters the risk of toxicity. The use of adjusted dose PIs with rifampicin might be better tolerated in patients than healthy volunteers. Moreover, patients with TB may have altered absorption of antiretroviral drugs. The loss of fat and lean body mass, and associated metabolic and endocrine abnormalities have the potential to influence the volume of distribution and total body clearance of antiretroviral drugs, particularly of lipophilic drugs, such as PIs. Also, it is more likely to cause hepatotoxicity in patients than healthy volunteers. Therefore, these approaches need to be evaluated in an adequately designed study amongst the relevant populations. There is also limited data for children about the outcomes associated with these approaches. Frohoff et al. reported that good short-term virologic outcomes have been achieved in children co-treated for TB and HIV who received super-boosted LPV/r and that treatment limiting toxicity was rare [9]. Super-boosted LPV/r was found to overcome rifampicin-related induction in young children by Ren et al. [127] Also, intracellular lopinavir could be specifically important for potential sanctuary sites of the virus and this concentration might be influenced by transporters, including rifampicin, which accordingly affect the drug efficacy. Furthermore, factors, such as diet, environment and genetics, influence the activity of transporters, metabolizing enzymes and their transcriptional regulators [66]. Therefore, more studies are needed to investigate the pharmacokinetic interactions, safety, efficacy and alternative dosage regimens to establish PI-based regimens for patients with HIV-associated tuberculosis in high-burden settings for adults and children respectively.

A more sophisticated analysis of the dynamic interactions between lopinavir, ritonavir and rifampicin-based ATT with adjustment for the relevant patients and treatment factors may allow the prediction of more suitable dosing approaches in patients with TB/HIV. Dosage modifications based on target concentrations require accurate knowledge of pharmacokinetic parameters governing drug absorption, distribution and elimination, and their variability among different individuals and occasions. Individual characteristics as well as simulation of drug concentrations are also useful in deciding the dosage regimen in clinics. A more thorough understanding of these interactions is required to optimize the dosing strategies in order to avoid toxicity and the emergence of drug resistance.

5. Adherence evaluation

Adherence is directly related to the clinical and virological outcomes of ART. It has been demonstrated in adult patients that higher levels of drug adherence are associated with improved virological and clinical responses, and that rates exceeding 95% are desirable with improved viral suppression of ART [31,46]. Adherence to ART has also been shown to help preventing drug resistance [128]. A full and sustained benefit can only be derived from high levels of adherence to ART regimens. Moreover, either in high-income or resource-limited settings, low adherence has been associated with higher hospitalization rates, productivity loss, disease progression and death [129]. Therefore, it is critical to ensure optimal adherence in order to maximize the benefit of ART, minimize the emergence of drug resistance and delay disease progression.

Adherence is complicated by internal and external factors, including the patient, the health system, the community and medication barriers. Patient factors could be psychosocial (e.g. depression, stigma, alcohol abuse), socioeconomic (e.g. income, education, cost of transport), demographics (e.g. gender, age) and clinical (e.g. current medical co-morbidity) in nature. Medication factors include pill burden,

dose frequency, dietary restrictions and side effects. Although most current first-line regimens are one to two pills once or twice daily, second-line regimens are more complex. Side effects related to ART are another important issue affecting adherence and studies have shown that when patients experience side effects, they tend to stop treatment or take medication irregularly [129].

Maintaining adherence may be even more challenging in young children, especially over long periods, because of factors relating to children, caregivers, medications, and the interaction of these factors. The limited number of pediatric formulations, poor palatability, high pill burden or liquid volume, frequent dosing requirement, dietary restrictions and side effects may hamper the regular intake of required medications. Successful adherence to treatment for a child requires the commitment and involvement of a responsible caregiver.

Accurate measurement of adherence is challenging. Many approaches, such as patient self-reports, pill counts, or pharmacy refill records, can be used to evaluate adherence though no standard method exists. Biological markers, including viral load and CD4 cell count, can be surrogates for suboptimal adherence. But this approach to large extent is influenced by viral resistance, prior treatment failure, or poor absorption of the drug. Studies have shown discordance between viral suppression and adherence in those contexts [130]. No approach can produce a completely valid and reliable measurement of adherence; hence, a new feasible and reliable method would be of utility.

Compared to other antiviral drugs, lamivudine can be used to investigate adherence because the concentrations of lamivudine are relatively predictable (interindividual variability of clearance is small) [131] and it is not affected by concurrent rifampicin-based ATT. The drug undergoes relatively rapid absorption and peak concentrations are reached in less than 1 h after the dose.

Pharmacokinetic studies have demonstrated that lamivudine is well absorbed from the gastrointestinal tract with high oral bioavailability of approximately 86% [131]. Based on data derived from a study in healthy volunteers, the mean AUC (CV) over a dosing interval of 12 hours is 8.9 µg.h/L (18%) [132]. Concentrations in 51 Zambian children aged 1.7 to 18 years, ranged from 0.82-2.28 mg/L at 1 h after the dose, while at 12 h the concentrations ranged from 0.06 to 0.11 mg/L [133]. The extent (based on the AUC) of lamivudine absorbed is not influenced by food. The likelihood of metabolic interactions of lamivudine with other medicinal products is low due to the small extent of hepatic metabolism (5-10%) and low plasma protein binding. Also, lamivudine metabolism does not involve CYP3A, making interactions with drugs metabolized by this system (e.g. PIs and rifampicin) unlikely. Thus the drug has ideal pharmacokinetic properties on which to base predictions of the probability of adherence to the previous dose. Therefore, it can be used as a marker of recent adherence, to aid interpretation of PI and NNRTI concentrations which might be particulary variable during ATT. Patients with concentrations below the lower limit of the reference ranges are likely to have skipped the previous doses. As part of the results reported in this thesis, we predict a normal concentration range for given time points after the dose of lamivudine in young children based on a population pharmacokinetic model, which can then be used to investigate adherence to ART and to aid interpretation of the therapeutic drug monitoring of PIs and NNRTIs.

6. Pharmacometrics

Pharmacometrics has been described as "the science of developing and applying mathematical and statistical methods to characterize, understand, and predict a drug's pharmacokinetic and pharmacodynamic behavior; and quantify uncertainty of information about that behavior; and rationalize data-driven decision making in the drug development process and pharmacotherapy." [134] Pharmacometrics belongs to the field of pharmacokinetic research and includes a large variety of

applications. Pharmacokinetics is referred to as "what the body does to the drugs" and pharmacodynamics is "what the drug does to the body". [135] Pharmacometrics was initially developed in order to facilitate more efficient development and use of pharmaceuticals through implementing mathematical and statistical models. The most commonly used pharmacometric approach is based on mixed-effect models, which are especially useful in application to heterogeneous biological data by its ability to characterize many sources and levels of variability. The model based approach can be used to integrate prior knowledge and pool data across studies [136]; to predict and compare doses and dosage regimens; to extrapolate to other target populations; to improve study design by application of optimal design theory and clinical trial simulations [137,138]; and to investigate optimal dosage for population and individual treatments [139].

6.1. Nonlinear mixed effect modeling

Traditional pharmacokinetic analysis was performed in two steps (two-stage method) [140–144]. In the first step, individual estimation was performed and in the second step the mean and standard deviation of parameters in the population were calculated. One weakness of this analysis method is that sufficient observations from each individual are required in order to identify the pharmacokinetic characteristics. Another weakness of traditional analysis is that it does not capture variability well between and within subjects. Furthermore, noncompartmental methods cannot be used to simulate alternative dosage regimens which can be applied to other situations or populations.

Nonlinear mixed effect modeling (NONMEM) is an alternative to the two-stage method. It involves simultaneous estimation of the typical and variance parameters based on data from all individuals [145] and allows sparse and unbalanced data to be used because individuals can utilize information contained in the entire population [146]. The term "mixed" is used because both fixed and random effects are estimated

in the model. Fixed effects relate to the typical parameter estimates and the random effect is the estimation of variability, including interindividual variability (IIV); interoccasion variability (IOV) [147], and intraindividual variability (residual error). The general structure of a mixed effects model is expressed as follows:

$$y_{ijk} = f(x_{ijk}, P_{ik}) \quad (1.5)$$

where y_{ijk} is the j^{th} observed dependent variable at occasion k in individual i. y_{ijk} is described by a vector of individual parameters P_{ik} and a vector of independent variables x_{ijk} (usually time and dose).

Compared to the traditional way of analyzing the data, population modeling is a powerful tool to summarize large amounts of data and quantify potential interactions. The model functions as a repository of knowledge and information about the biological system, disease and drug properties are integrated to achieve a collated picture. New information can be integrated into the model and thus confirm previous knowledge as well as refine the model and new knowledge may be obtained.

The individual parameter is a function of the typical value for the population and an individual random effect. For parameters that only can take on positive values the individual parameters are commonly described using a log-normal distribution as follows:

$$P_{ik} = \theta_p \cdot e^{\eta i + ki} \quad (1.6)$$

where P_{ik} is the individual parameter value at the k^{th} occasion, θ_p is the typical parameter estimate, and η_i and k_i are the random effects that describe IIV and IOV, respectively. The variables η_i and k_i are assumed to be normally distributed with a mean of zero and a variance of ω^2 and π^2. Many biological parameters are assumed to be log-normally distributed and IIV and IOV are therefore described exponentially.

Covariates, such as gender, weight, age, liver or kidney function, etc, can often explain a part of the variability between individuals. In such a case the typical parameter value will be a function of the individual covariate value, thereby explaining a part of the IIV.

The residual variability describes the difference between the individual prediction and the observed value. The residual variability may be due to assay error or measurement error, model misspecification or incorrect dosing or sampling history record. Residual error can be investigated using additive or proportional models. The j^{th} observation of individual *i* can be described using the general expression in equation 1.7.

$$y_{ijk} = f(x_{ijk}, P_{ik}) + \varepsilon_{ijk} \quad (1.7)$$

where y_{ijk} is the j^{th} observed dependent variable at occasion *k* in individual *i*. $f(...)$ is the individual prediction which is described by independent variables x_{ijk} (e.g. dose, time) and the individual parameters of the model P_{ik}, ε_{ijk} is the residual error term describing the difference between the observed value and the individual prediction. The ε values are assumed to be normally distributed with a mean of zero and a variance of δ^2.

6.2. Model estimation

NONMEM [148], which was used for analysis throughout this thesis, uses a parametric maximum likelihood method for parameter estimation, in which the parameters of a model are estimated by maximization of the probability of the data under the model. This is performed by minimization of the extended least squared objective function. The objective function value (OFV) is approximately proportional to -2 times the logarithm of the likelihood of the data and the difference in OFV between two nested models is approximately χ^2 distributed

under the assumption that the model is correct and that the errors are normally distributed. The likelihood ratio test can be used to compare nested models and a difference in OFV of 3.84 corresponds to a significance level of $p<0.05$ [149–151].

The likelihood function in most cases cannot be calculated exactly because of the non-linearity of the models [148]. In NONMEM, several alternative methods are available including the first-order method (FO), the first-order conditional method (FOCE) and Laplacian second-order approximation method (LAPLACE). These methods use different types of linearization of the non-linear models which results in closed solutions for the likelihood.

6.3. Model validation

Validation methods are always used throughout the model building process to evaluate the adequacy, accuracy and robustness of the model. Graphic and statistic diagnostics are most extensively used and enhance the understanding of the data and lead to an efficient analysis of the data. Graphic diagnostics are intuitive and powerful approaches to interpret the model [152]. A lot of available graphic diagnostic approaches, some of which rely on simulation, evaluate different aspects of model adequateness. Each diagnostic approach has its assumptions, strengths and weaknesses [153].

The plots of population typical model predictions (PRED) and individual model predictions (IPRED) versus observations are routinely used as goodness of fit plots (GOFs) for diagnostics. These plots interpret how well the observations are centered along the line of identity. Residual based diagnostic plots are commonly involved in GOFs, including individual weighted residuals (IWRES = observations – IPRED) versus IPRED, and conditional weighted residuals (CWRES) versus time. It has been demonstrated that CWRES, which are based on the FOCE linearization, have better properties compared to WRES. Another new

approach based on NONMEM 7 is normalized prediction distribution errors (NPDE) [154–156]. NPDE are not true residuals but based on the rank order of the observations in relation to multiple model simulation of the original dataset. The general interpretation of residuals-based plots is that they should be normally distributed with a mean of 0 across any independent variable.

The most powerful approach is visual predictive check (VPC). VPC is based on model simulation to graphically assess whether simulations from a model are able to reproduce both the median and certain variability in the observed data. The model usually is assessed by comparing the observations to simulations for a particular prediction interval, which is a robust approach for model validation.

Bootstrap re-sampling is another approach common used in model validation [157]. A large number of datasets is generated by re-sampling from the original dataset, and parameter estimates for each are obtained by estimation with the final model. Means, standard errors and 95% confidence intervals (CIs) are compared with the estimates calculated from the original dataset. The bootstrap approach provides measures of the stability of the final parameter estimates and the robustness of the final model.

Aims

The primary aim of this thesis was to investigate pharmacokinetics of PI-based antiretrovirals, including the complicated drug-drug interactions with rifampicin and to compare pharmacokinetic differences between children and adults, using population pharmacokinetic models. The secondary aim was to optimize the dose regimens of PI-based antiretrovirals in combination with rifampicin, and to investigate reference drug concentrations for adherence evaluation.

The specific aims of this thesis were to:

- To explore the pharmacokinetics of lopinavir and ritonavir, including effect of drug intake, bioavailability and mechanisms of metabolic inhibition and induction between lopinavir, ritonavir and rifampicin based on developed integrated population models in specific patient populations.
- To evaluate the effect of patient and treatment factors (including age, body surface area (BSA), weight, sex, haemoglobin, albumin, alanine transaminase (ALT), doses, maturation) on lopinavir and ritonavir pharmacokinetics in the respective study populations.
- To optimize the dose regimen for lopinavir/ritonavir co-administration with rifampicin-based ATT for young children and adults to achieve effective clinical targets.
- To investigate the pharmacokinetic difference of lopinavir and ritonavir, as well as drug-drug interactions with rifampicin between children and adults based on a combined adult-children population pharmacokinetic model.
- To describe pharmacokinetics of lamivudine in HIV/TB infected young children and predict lamivudine reference concentrations for adherence evaluation based on developed population pharmacokinetic model.
- To confirm model-based approach as a powerful tool for characterization of the underlying mechanisms and evaluation of potential drug effects

Material and Methods

1. Data

The data from three studies (Study I-III) were included in this thesis. Study I, Study II, and Study III are named as "children pilot study", "children double dose study" and "adult double dose study", respectively. Paper I and Paper IV were conducted based on pooled data of Study I and Study II; Paper II was conducted based on data of Study II; Paper III was conducted based on data of Study I-III (described in Figure 2.1). The patient characteristics of three studies are summarized in Table 2.1.

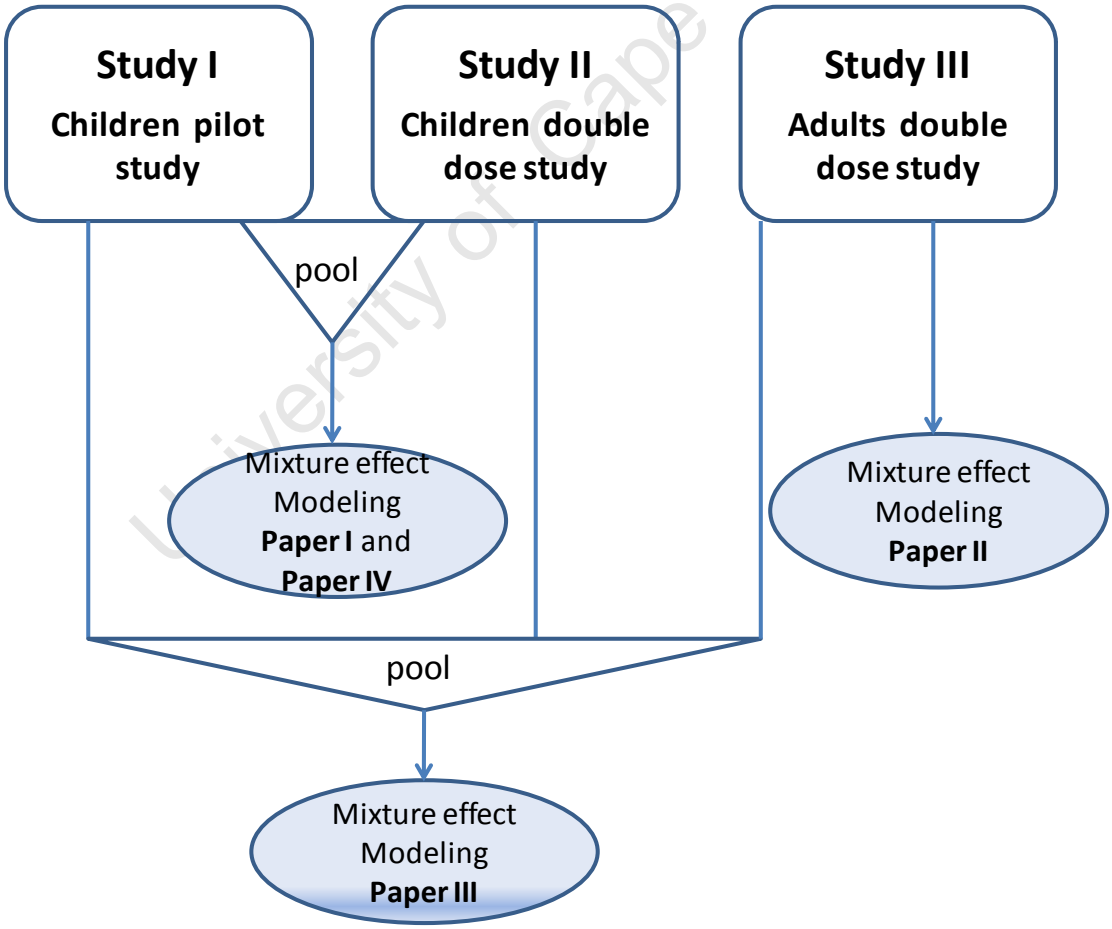

Figure 2.1 Data components of this thesis.

Table 2.1 Summary of subjects characteristics involved in the thesis

	Subgroup	Patient	Lopinavir :ritonavir ratio	Number of subject	Sampling approach
Children pilot study (Study I)	Control group	HIV	4:1	15	intensive
	Superboosted group (during TB treatment)	HIV/TB	1:1	15	
Children double dose study (Study II)	Control group	HIV	4:1	24	Intensive and sparse
	Double dose group (during TB treatment)	HIV/TB	8:2	20	
	After TB treatment	HIV/TB	4:1	11	
Adults double dose study (Study III)	Standard dose, no rifampicin	HIV	4:1	21	intensive
	Sequential increase dose (during rifampicin)	HIV	4:1; 6:1.5; 8:2	21	

TB treatment: standard first-line regimen including rifampicin dosed at approximately 10 mg/kg.

2. Study design

2.1. Children pilot study (Study I)

This was an open-label, cross-sectional comparative study conducted at multiple centers in South Africa. Steady state pharmacokinetic profiles of lopinavir and ritonavir were determined in two groups in children: treatment and control groups. Patients were recruited at 3 sites: the HIV Clinic at the Red Cross Children's Hospital, Cape Town; the Harriet Shezi Children's Clinic, Chris Hani Baragwanath Hospital, Soweto; and Brooklyn Chest Hospital, Cape Town. Ethical approved of this study was sought from the Research Ethics Committees of the University of Cape Town and the University of Stellenbosch. No subject was enrolled in the

study before they (if old enough) and their legal guardian has been fully informed about the study and by means of a subject information document, and had provided written informed consent to participate in the study.

Thirty children (aged 6 months to 4.5 years) were enrolled into two groups: 15 TB-HIV co-infected children receiving lopinavir/ritonavir (ratio of 4:1, LPV/r) with additional ritonavir (such that the total ratio of LPV:ritonavir=1:1) as part of ART and concomitant rifampicin-based ATT for at least 4 weeks (treatment group) and 15 HIV-infected children without TB receiving LPV/r-based ART for at least 4 weeks (control group).

In the control group, lopinavir at a dose of 230 mg/m^2 plus ritonavir at a dose of 57.5 mg/m^2 (LPV/r, liquid formulation, Kaletra®) were given twice a day in combination with twice-daily dual NRTIs to children. In the treatment group, besides dose regimens given in the control group, an additional ritonavir at a dose of 172.5 mg/m^2 twice daily (LPV:ritonavir ratio of 1:1) was given to children receiving rifampicin-based ATT. The maximum doses were 400 mg lopinavir/100 mg ritonavir twice daily (not with rifampicin-based ATT) or 400 mg lopinavir/400 mg ritonavir twice daily (with rifampicin-based ATT). Rifampicin-based ATT regimens were administered based on target doses of 10 mg/kg of rifampicin, 5 mg/kg of isoniazid in fixed dose combinations, as well as pyrazinamide and ethambutol, in accordance with the National Tuberculosis Treatment Program. Alcohol, caffeine, grapefruit juice, garlic and pepper were avoided during the whole study.

Lamivudine was given as a part of ART concurrently with LPV/r during this study. The dose of lamivudine was 4 mg/kg twice daily for each patient. The formulation used in this study was a suspension.

An intensive sampling approach was used in this study. Eight blood samples were collected for each patient and the exact time of the morning dose of LPV/r, which was administered by the study staff, was recorded. From each patient, 1.2 mL blood was taken at 0 (pre-dose), 2, 3, 4, 5, 6, 8, and 12 h after drug intake. The samples were centrifuged (3000 rpm for 5 minutes) within 30 minutes after sampling, and the plasma was stored immediately at -80℃ while awaiting quantification of lopinavir, ritonavir and lamivudine concentrations. The following potential covariates of pharmacokinetics were measured on the pharmacokinetic sampling days: height, weight, haemoglobin, ALT and serum albumin.

2.2. Children double dose study (Study II)

This was an open-label, cross-sectional comparative study conducted at three centers in South Africa. Steady state pharmacokinetic profiles of lopinavir and ritonavir were determined on two groups in children: treatment and control group. Children were recruited at: the HIV Clinic at the Red Cross Children's Hospital, Cape Town; the Harriet Shezi Children's Clinic, Chris Hani Baragwanath Hospital, Soweto; and HIV Clinic at Tygerberg Hospital, Cape Town. Ethics approval of the study was sought from the Medicines Control Council of South Africa, and the Research Ethics Committees of the University of Cape Town, Stellenbosch University, and the University of the Witwatersrand. No subject was enrolled in the study before they (if old enough) and their legal guardian has been fully informed about the study and by means of a subject information document, and had provided written informed consent to participate in the study.

In total Forty-four children (aged 6 months to 4.5 years) were studied: 20 TB-HIV co-infected children receiving double dose of LPV/r as part of ART and concomitant rifampicin-based ATT for at least 4 weeks (treatment group) and 24 HIV-infected children without TB receiving LPV/r-based ART for at least 4 weeks (control group). The data safety and monitoring board conducted an interim

analysis after pharmacokinetic sampling and terminated this study prematurely since most of the subjects could not achieve the effective concentrations.

In the control group, HIV-infected children received a standard dose of Kaletra® (lopinavir 230 mg/m^2+ ritonavir 57.5 mg/m^2, liquid formulation) and 2 NRTIs according to the recommended dosing strategy. In the treatment group, patients established on rifampicin-based ATT were commenced on an ART regimen comprising double the recommended dose of Kaletra® (lopinavir 460 mg/m^2+ ritonavir 115 mg/m^2) and 2 NRTIs. Eleven children underwent pharmacokinetic evaluation, again, at least 4 weeks after completion of ATT, and on standard LPV/r doses. These patients were looked as another occasion during modeling building. Rifampicin-based ATT regimens were administered based on target doses of 10 mg/kg of rifampicin, 5 mg/kg of isoniazid in fixed dose combinations, as well as pyrazinamide and ethambutol, in accordance with the National Tuberculosis Treatment Program. The child received food and beverages according to the hospital routine. Alcohol, caffeine, grapefruit juice, garlic and pepper were avoided during the whole study.

Lamivudine was given concurrently with LPV/r as a part of ART. The dose of lamivudine was 4 mg/kg twice daily for each patient. The formulation of lamivudine used in this study was suspension.

Intensive and sparse sampling approaches were used in this study. Intensive samples were collected at 0 (pre-dose), 2, 3, 4, 5, 6, 8 and 12 hours after drug intake. Sparse samples were collected at 0 (pre-dose), 2, 4 and 8 hours after drug intake. The samples were centrifuged (3000 rpm for 5 minutes) within 30 minutes after sampling, and the plasma was stored immediately at -80℃ while awaiting quantification of lopinavir and ritonavir concentrations. The following potential covariates of pharmacokinetics were measured on the pharmacokinetic sampling

days: height, weight, haemoglobin, ALT and serum albumin.

2.3. Adult double dose study (Study III)

The study was an open-label, sequential, four-period, multiple-dose trial in HIV-infected adults who were virologically suppressed (viral loads <400 copies/mL) on LPV/r together with two NRTIs according to the recommended dosing strategy. Patients were randomly recruited at antiretroviral clinics in the Western Cape and admitted to the pharmacokinetic facility at the Division of Clinical Pharmacology, University of Cape Town and Groote Schuur Hospital for pharmacokinetic assessment. Ethics approval of the study was obtained from the Human Research Ethics Committee of University of Cape Town. No patient was enrolled in the study prior to being fully informed about the study and by means of a subject information document, and all subjects signed consent had been obtained on the study specific consent form.

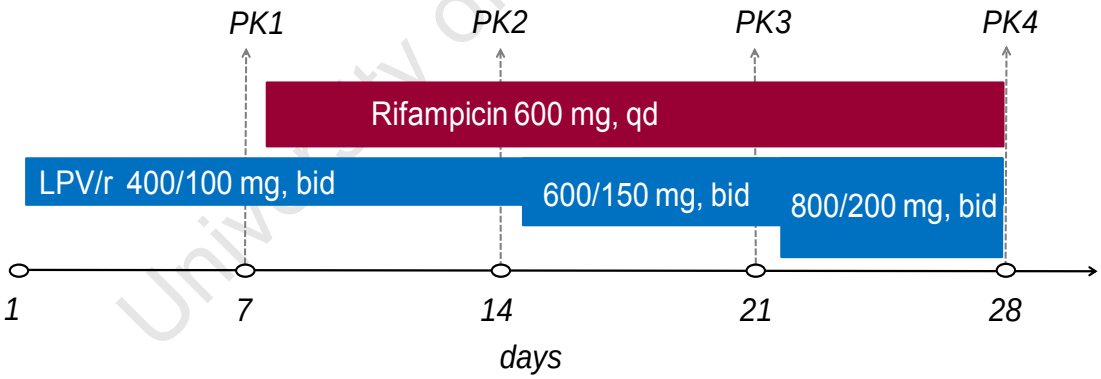

Figure 2.2 Description of study design.

The study design is shown in Figure 2.2. The steady state pharmacokinetics of lopinavir and ritonavir were evaluated in 21 South African HIV infected volunteers under four sequential treatment conditions: LPV/r in standard doses (400 /100 mg) 12 hourly together with two NRTIs, which is the standard 2nd-line

ART regimen in South Africa, without rifampicin (day 1 to day 7); LPV/r in standard doses 12 hourly together with two NRTIs and rifampicin 600 mg daily (day 8 to day 14); 1.5 times of the standard dose of LPV/r (600/150 mg) 12 hourly together with two NRTIs and rifampicin 600 mg daily (day 15 to day 21); and 2 times of the standard dose of LPV/r (800/200 mg) 12 hourly together with two NRTIs and rifampicin 600 mg daily (day 22 to day 28). The different treatment conditions were looked as four different occasions during model building. The formulations used in this study were: LPV/r (film-coated tablet): lopinavir 200 mg co-formulated with ritonavir 50 mg (Aluvia, Abbott); Rifampicin (tablet formulation): rifampicin 600 mg (Rimactane®, Sandoz). Alcohol, caffeine, grapefruit juice, garlic and pepper were avoided during the whole study.

Intensive pharmacokinetic sampling was performed one week after each dose adjustment (DAY 7, DAY 14, DAY 21 and DAY 28). 4 ml of blood were collected in heparinized tubes at 0 (pre-dose), 1.5, 2, 2.5, 3, 4, 5, 6, 8 and 12 h after drug administration, centrifuged within one hour from collection to separate the plasma (10 minutes at 3000 rpm), and then stored at -80 ℃ in the laboratory (Department of Clinical Pharmacology, University of Cape Town) until drug concentrations were determined. The following potential covariates of pharmacokinetics were measured on the pharmacokinetic sampling days: height, weight, haemoglobin, ALT and serum albumin.

2.4. Summary of study design

The general summary of study design of studies in this thesis is shown in Table 2.2.

Table 2.2. The summary of study design of studies in this thesis.

	Study design	ATT treatment	Food intake
Children (Study I, II)	Control and treatment groups	Rifampicin-based ATT	not very clear
Adults (Study III)	Sequential dosing	Rifampicin	Fast in the morning dose, but took food in the evening dose

3. Laboratory analyses

Lopinavir and ritonavir plasma concentrations were assayed at the laboratory of department of clinical pharmacology of University of Cape Town using validated liquid chromatography-tandem mass spectrometry methods [127]. The lower limits of quantification (LLOQ) were 0.05 mg/L for lopinavir and 0.025 mg/L for ritonavir. The concentratin of standard curve ranged from 0.12 mg/L to 16 mg/L for lopinavir and from 0.075 mg/L to 7 mg/L for ritonavir. Accuracy ranged from 94.3% to 103.0 for lopinavir and from 93.6% to 105.3% for ritonavir. The intra-day and inter-day precisions of both drugs ranged from 0.14% to 4.72% and from 1.61% to 4.22%, respectively.

Lamivudine plasma concentrations were assayed in the above mentioned laboratory using a validated liquid chromatography-tandem mass spectrometry method [158]. The calibration curve was linear over the range from 20 to 2000 ng/mL. Any sample whose lamivudine results were higher than 2000 ng/mL was diluted with drug-free plasma and reanalyzed. The LLOQ was 20 ng/mL and accuracy ranged from 98.35% to 104.32%. The intra-day and inter-day precisions of lamivudine ranged from 4.59% to 6.61% and from 4.23% to 6.62%, respectively.

Routine tests to monitor safety and efficacy of treatment were conducted

according to the National Treatment Guidelines which state that patients should have monthly monitoring of ALT if antiretroviral and ATT are given concurrently and that all patients receiving Kaletra® in conjunction with 2NRTIs should have baseline and 6 monthly monitoring of viral load (NASBA EasyQ, Biomerieux, Boxtel, The Netherlands), ALT, full blood count, serum cholesterol, glucose, and triglycerides as well as CD4+ cell counts at staging and 6 monthly.

4. Model development

4.1. Software

The data estimation and simulation were performed using nonlinear mixed effects modeling implemented initially in NONMEM 6 (Paper I) and NONMEM 7 (Paper II-IV) (GloboMax, Hanover, MD, USA) [148]. The first order conditional estimation method (FOCE) with eta-epsilon INTERACTION was used for the estimation of pharmacokinetic parameters. Perl speaks NONMEM (PsN) (updated version from from 3.2.4 to 3.4.8) [159] was used for executing estimations, covariate modeling building, bootstrap procedures, simulations as well as calculations of the VPC. Graphical diagnostics of the model fit was performed using Xpose (version 4.1.0) implemented in R [160]. The graphical diagnositics include GOFs, individual plots, scatterplots, boxplots, and VPC plots. GOFs and VPC plots have been explained in the introduction. GOFs include observed concentrations versus population predicted concentration (PRED), observed concentrations versus individual predicted concentration (IPRED), IWRES versus IPRED, and conditional weighted residuals (CWRES) versus time. The regression lines in these plots respresent equal predicted concentrations to observed ones. Therefore, these plots could indicate how close the predicted concentrations are close to the observed ones; the even and close distribution along the regression line would be a good evidence for model predicted profiles. VPC is an approach to diagnose model adequacy. The purpose of these plots is to compare if the 5^{th}, 50^{th}, 95^{th} percentile of observed data (solid and dotted lines) are agreement with the 95% confidence

interval of each percentile of simulated data (grey shaded areas) based on our model. This approach is based on simulation and is a more robust approach for model validation. A lot of sctterplots were used for diagonosis during model development, for example scatterplots of different candidate covariates versus pharmacokinetic parameters could provide strong evidence that which covariate would be a significant one. The scatterplots between parameters could indicate potential correlations. Boxplots were another useful tool for diagnosis, such as the boxplots of demographic characteristics, the individual parameters distribution in different subgroups or occasions, the variability distributions, etc.

4.2. Structure and statistic model building

Different model structures and features were evaluated: one- and two-compartment disposition [38,161–163]; zero- and first-order absorption; an absorption with lag time and a series of transit compartments as proposed by Savic et al [164]. The model scheme of transit absorption is shown as Figure 2.3. Mean transit time (MTT) was used to describe the drug absorption delay. The transit absorption rate (k_{tr}) was used to describe the transit absorption rate between different transit compartments. The calculation of k_{tr} is indicated as follows:

$$k_{tr} = \frac{n + 1}{MTT} \quad (2.1)$$

where n is the number of transit compartments.

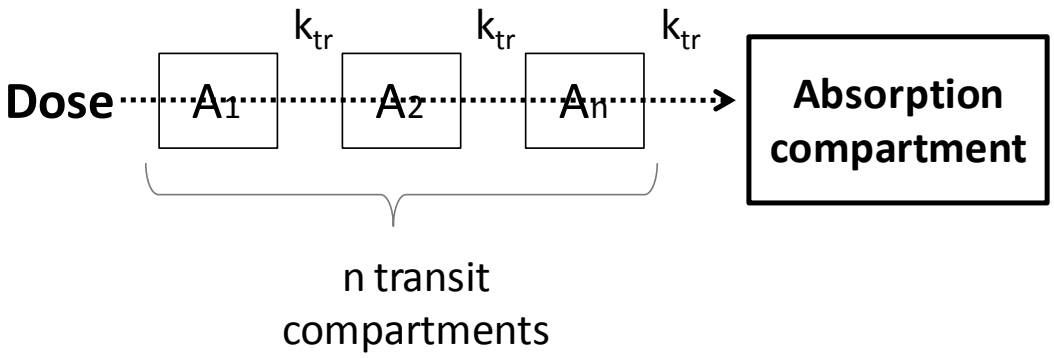

Figure 2.3. The model scheme of transit absorption model.

The IIV and IOV of the pharmacokinetic parameters of lopinavir and ritonavir were modeled using an exponential error model:

$$P_{ij} = P_{tvj} \cdot e^{\eta ij} \quad (2.2)$$

where P_{ij} is the *jth* pharmacokinetic parameter for the *ith* individual; P_{tvj} is the typical value of the *jth* population parameter, and η_{ij} represents a random variable for the *ith* individual in the *jth* parameter distributed with a mean of zero and variance of ω_{ij}. Using a first-order approximation, the variability of the lognormal distributions is reported as % coefficient of variation (CV).

Several different error structures were tested for the description of the residual unexplained variability (RUV): additive, proportional, combined error models. A combined proportional and additive error model (the difference between the observed and predicted concentrations) was described as follows:

$$C_{ij} = C_{ij}^{'} \cdot (1+\varepsilon_1) + \varepsilon_2 \quad (2.3)$$

where C_{ij} and $C_{ij}^{'}$ are the *jth* observed and predicted blood concentrations for the *ith* individual, respectively. ε_1 and ε_2 are random variables distributed with a mean of zero and variances of σ_1 and σ_2, respectively.

Model development was guided by the OFV, precision in parameter estimates (relative standard error, RSE%) obtained by NONMEM output or the bootstrap procedure, graphical analysis and scientific plausibility. The difference in OFV between two nested models is assumed to be χ^2-distrubutions. A decrease in the OFV of 3.84, 6.63 or 10.83 was required for addition of one parameter to the model to be considered significant, which corresponds to $p<0.05$, $p<0.01$ and $p<0.001$, respectively.

4.3. Covariate model building

Once the basic model (structure and statistic model) was developed, a covariate

analysis was performed following a forward inclusion and backward elimination stepwise approach similar to Wählby et al [165]. Firstly, scatter plots of pharmacokinetic parameters against each covariate were used to examine the effect and regression of covariates. Secondly, each potential covariate was incorporated into the basic model to develop the full model. A decrease of 3.84 of OFV was considered statistically significant (p=0.05). Covariate selections were also guided by a decrease in standard error of the parameters, reduction in IIV, IOV and RUV, and goodness-of-fit plots. Available continuous covariates in this thesis included age, body weight, height, body surface area, hemoglobin, ALT. The categorical covariate includes gender, which was evaluated by stepwise inclusion of scaling factor: gender =0 for males and gender =1 for females. Finally, a backward elimination process was employed to identify the significant covariates for the final model by fixing the significance level α=0.01, $\chi^2_{0.01}$ =6.63. If removal of a covariate resulted in an increase of 6.63 in the OFV, the covariate was retained in the final model. The covariate building was conducted manually or through programs, such as PSN stepwise covariate modeling (SCM) [166] or generalized additive models (GAM) [165]. The case deletions diagnostics (CDD) algorithm [159] was used during model building in order to confirm that there was no significant impact from specific individual patient on the overall estimation. This approach is a tool primarily used to identify influential components of the dataset, usually individuals. Moreover, the difference of OFV by individuals was evaluated during covariate building to assess the impact of individual patients.

Remaining physiologically plausible covariate candidates for each parameter were tested in NONMEM, using equations similar to those illustrated in Equation 2.4 (linear relationship) or Equation 2.5 (exponential relationship) for continuous covariates and Equation 2.6 for categorical covariates.

$$\left(\frac{CL}{F}\right)_{typ} = \left(\frac{CL}{F}\right)'_{\text{typ}} + \theta_{WT} \cdot (WT_i - WT_{med}) \quad (2.4)$$

$$\left(\frac{CL}{F}\right)_{typ} = \left(\frac{CL}{F}\right)'_{\text{typ}} \cdot (WT_i/WT_{med})^{\theta_{WT}} \quad (2.5)$$

$$\left(\frac{CL}{F}\right)_{typ} = \left(\frac{CL}{F}\right)'_{\text{typ}} \cdot (1 + \theta_{SEX} \cdot SEX) \quad (2.6)$$

Equation 2.4 and Equation 2.5 are examples describing the influence of body weight, a continuous covariate, on oral clearance. $(CL/F)_{typ}$ is the typical apparent oral clearance where F is bioavailability, WT_{med} is the population median body weight (kg), and WT_i is the body weight of individual *i* (kg). θ_{WT} is the change in *CL/F* per kg change in body weight. $(CL/F)'_{typ}$ is the value of oral clearance when body weight is equal to the population median body weight.

In Equation 2.6, the effect of the categorical covariate sex (SEX, 0 for males and 1 for females) is estimated on oral clearance, $(CL/F)_{typ}$ is the typical apparent oral clearance, where F is bioavailability, $(CL/F)'_{typ}$ is the typical value of *CL/F* in male patients, while the typical difference in this value seen in female subjects is represented by θ_{SEX}.

4.4. Modeling procedure

4.4.1. Modeling procedure (Paper I and II)

Modeling procedures are described in Figure 2.4. Firstly, the separate model of lopinavir and ritonavir, including basic structure and covariates model, were built respectively. Secondly, an integrated model was built involving drug-drug interaction as the final model. The covariates tested were body weight, height, body surface area, hemoglobin, ALT, gender, and effects of rifampicin administration. Since the morning pre-dose concentrations (C_0) were on average higher than the evening trough concentrations (C_{12}), differences in bioavailability

and CL/F after the evening and morning doses were tested in our model to capture the diurnal variation. The oral bioavailability of the standard dose of LPV/r without rifampicin co-administration was assumed as the reference (100%) to which the other conditions were compared.

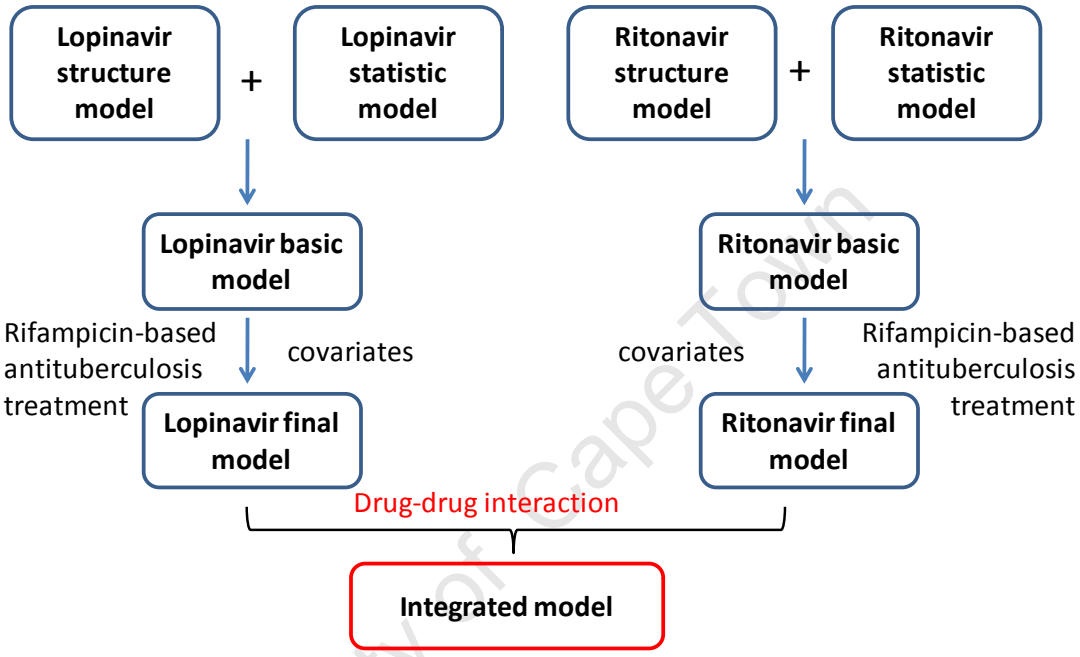

Figure 2.4. Model procedures of Paper I and Paper II.

4.4.1.1. Lopinavir and ritonavir separate model

The separate lopinavir and ritonavir models were built following basic model first and then covariate model. Model building was guided by OFV, precision of parameter estimates, variability (IIV, IOV and RUV) change and graphic diagnostics, which was described in the model development. Candidate covariates were evaluated by stepwise approach mentioned before. Rifampicin-based ATT was investigated as a covariate on the bioavailability and oral clearance. Ritonavir dose effect on the bioavailability of lopinavir and ritonavir was also investigated. Diurnal variation was tested to decrease the clearance or/and increase

bioavailability during model building.

4.4.1.2. Lopinavir-ritonavir integrated model

An integrate lopinavir-ritonavir model was built as the final model. Different enzyme inhibition models were tested to describe the drug interaction between lopinavir and ritonavir. The drug inhibition models could be chosen as follows:

(1) Empirical on-off model

Inhibitor is treated as a covariate and does not involve time [167].

(2) Time-dependent model

This model includes linear or nonlinear forms to describe time-dependent inhibition effects. Considering that the concentration of inhibitor would change with time, the clearance of substrate changes with time as well. The models can be described as follows:

Linear inhibition [162]:

$$CL = CL_{base} - SLP \cdot C_{inhibitor} \quad (2.7)$$

Nonlinear inhibition [162]:

$$CL = CL_{base} \cdot \left(1 - \frac{E_{max} \cdot C_{inhibitor}}{EC_{50} + C_{inhibitior}}\right) \quad (2.8)$$

where CL is the clearance of substrate, CL_{base} is the baseline clearance, $C_{inhibitor}$ is the concentration of inhibitor, SLP is the slope of the linear relationship between clearance of substrate and concentration of inhibitor, E_{max} is the maximum inhibition effect of inhibitor and EC_{50} is concentration of inhibitor required to reach half of E_{max},

(3) Enzyme turnover model

Inhibition effect can decrease R_{in} (production rate) or stimulate k_{out} (elimination rate[168]. The model describing the inhibitor concentrations decrease R_{in} is shown as follows:

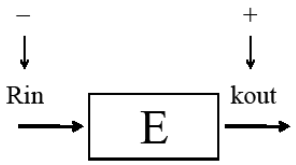

$$\frac{dE}{\mathrm{dt}} = R_{in} \cdot (1 - S\big(C(t)\big) - k_{out} \cdot E \qquad (2.9)$$

This model describes the time course of the inhibition. Time to steady state is determined by k_{out} and can be predicted by this model, as well as the enzyme turnover half life. The amount of enzyme at steady state (E_{ss}) depends on R_{in} and k_{out} ($E_{ss} = \frac{R_{in}}{k_{out}}$).

A sequential approach, in which the ritonavir parameters were fixed in population and individual levels, was applied first. Then a simultaneous model was built to estimate all parameters simultaneously as the final model.

4.4.2. Modeling procedure (Paper III)

The modeling procedures are described in Figure 2.5. Firstly, the separate model using combined dataset for lopinavir and ritonavir was built respectively. Secondly, integrated lopinavir-ritonavir model was developed to estimate all parameters for children and adults simultaneously.

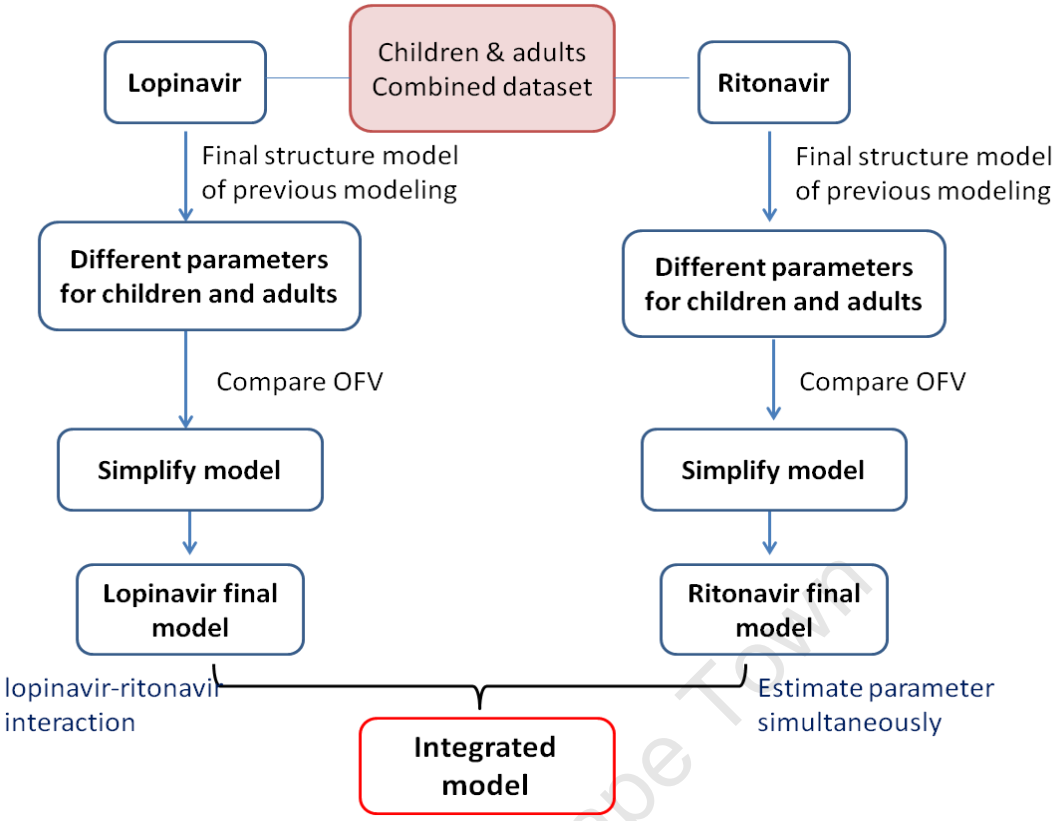

Figure 2.5. Modeling procedures of Paper III.

The separate model using combined dataset for lopinavir and ritonavir were built respectively. The same structure and covariates model was kept to fit combined children and adults dataset. Firstly, different parameters were estimated for children and adults respectively to build the initial model. Secondly, the model was simplified guided by OFV, precision of parameter estimates, variability (IIV, IOV and RUV). Finally, the final lopinavir and ritonavir model was obtained according to model development methods.

Once the final lopinavir and ritonavir separate model were built, integrated model was developed involving drug interactions between lopinavir and ritonavir. Correlations between lopinavir and ritonavir were also tested. Rifampicin-based ATT effects were tested on children and adults respectively and then compare

whether this kind of effect is same for children and adults. All parameters were estimated simultaneously.

4.4.3. Modeling procedure (Paper IV)

The modeling procedure is described in Figure 2.6. Structure and statistic model building procedures were similar to previous chapters. A one- and a two-compartment disposition were tested, as well as different absorption models: zero- and first-order absorption, absorption with lag time and a series of transit compartments. The correlations between different parameters were also evaluated. Covariate model development was guided by stepwise approach mentioned before and the candidate covariates included age, body weight, sex, height, and ALT. Rifampicin-based ATT was evaluated as a covariate to investigate whether it would influence lamivudine pharmacokinetic parameter. Since the predose concentrations were higher than 12 hourly concentrations, diurnal variation was also investigated on both clearance and bioavailability in our model.

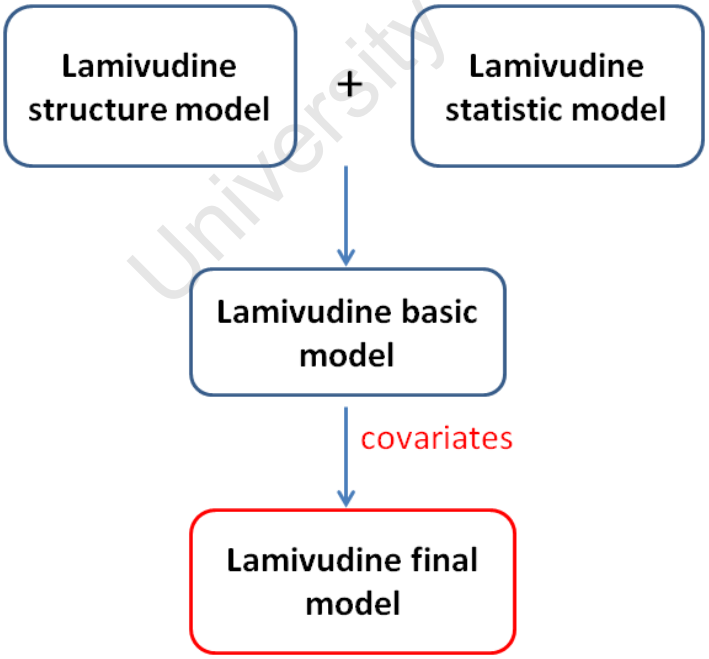

Figure 2.6 Modeling procedures of Paper IV.

4.5. Model validation

VPC was used to evaluate the robustness and properties of simulation of the model. VPC was based on 1000 datasets simulated with the obtained final parameter estimates and the same data structure as the original dataset. Statistics were calculated in the same manner for the observed and simulated datasets. For each dataset, the median, 5^{th} and 95^{th} percentiles of dependent variable (DV) value was calculated in each bin of independent variable (usually time or time after dose).

The nonparametric bootstrap re-sampling method, as implemented in PsN, was used to obtain standard errors to evaluate the accuracy and stability of our final model parameters. Briefly, from the original data set of N individuals, a fix number of bootstrap datasets of N individuals are re-sampled. For each bootstrap sample, the population pharmacokinetic parameters are estimated, and then parameter statistics are obtained from the whole bootstrap datasets. The 95% confidence intervals around the mean of each estimated parameter were assessed as their 5th and 95th percentiles and then used to assess precision and robustness of the final model parameters. The acceptability of the width of the confidence interval depends on the expectation for the particular parameter. This method is extremely demanding on time and computer resources.

5. Simulation

5.1. Simulation for dose optimization (Paper I)

The final integrated model was used to perform simulations using different dosing strategies for patients with different weight bands recommended by the WHO for dosing of antiretrovirals in children [31]. Simulations were performed with model variability but without residual error. Simulations using 1000 subjects in each weight band (3.0-5.9, 6.0-9.9, 10.0-13.9, and 14.0-19.9 kg) were performed. Trough concentrations were predicted using lopinavir/ritonavir ratios of 4:1 and 1:1 in different mg/kg doses. The target dose in each weight band was expected to

achieve lopinavir trough concentrations >1 mg/L in at least 95% of children during rifampicin-based ATT.

5.2. Simulation for dose optimization (Paper II)

The final model was used to simulate concentrations in 2000 in silico subjects (with covariates values matching the study population) to evaluate dose regimens achieving lopinavir trough concentrations >1 mg/L in patients during rifampicin co-treatment. Simulations were performed with model variability but without residual error. To explore the possibility that lower doses of LPV/r may be sufficient to achieve target concentrations in smaller patients, additional simulations using 2000 subjects were performed to predict the proportion of subjects with body weight 35-49 kg achieving lopinavir C_0>1 mg/L on a 600/150 mg dose of LPV/r. Simulations were also conducted to evaluate the adequacy of doubled doses (800/200 mg twice daily) of LPV/r in patients with weights 111-130 kg. The body weight used in simulations for each range was distributed evenly. The cutoff value of 10^{th} percentile of body weight in our study population was 50 kg and the highest value in the study population was110 kg.

5.3. Simulation for adherence investigation (Paper IV)

The final model was used to simulate reference concentrations for adherence evaluation in children with different ages. Simulations were performed with model variability but without residual error. Simulations using 2000 subjects in 6 months, 1 year, 2 years and 5 years age were performed. Cutoff concentration reference values for the 5^{th}, 2.5^{th} and 1^{st} percentiles at 4 h and 12 h after the morning dose were calculated. Different non-adherence scenarios were then studied in 2000 patients: missed last dose; missed last two doses; and missed second last dose. The proportions of patients whose concentrations fell below the cutoff reference values for the different non-adherence scenarios were estimated using further simulations of 2000 patients.

Results

1. Results (Paper I)

1.1. Patients and data description

The demographic characteristics of study patients are summarized in Table 3.1.1. There were no statistically significant differences (t test, $p>0.05$) in demography between the patients included in the 'super-boosted' and 'double dose' group. A total of 216, 120 and 96 concentrations of lopinavir and ritonavir were available from children on standard doses of LPV/r without concurrent rifampicin-based ATT, children receiving 'super-boosted' doses, and children given doubled doses of LPV/r, respectively. The data of this study are summarized in Table 3.1.2. Figure 3.1.1 illustrates the distribution of relvant demographic and clinical variables, in different treatment groups: control group, super-boosted group, and double dose group. Plots of concentration of lopinavir and ritonavir against time after dose in patients are in Figure 3.1.2 and Figure 3.1.3. The age and body weight distribution stratified by gender are shown in Figure 3.1.4.

Table 3.1.1. Demographic characteristics of study patients.

Characteristic	Median	Range
Age	21 month	6 months - 4.5 years
Body weight (kg)	10.2	5-17
Gender (M/F)	34/40	
Height (cm)	79	58-103
BSA (m^2)	0.48	0.28-0.69
Haemoglobin (g/L)	10.7	5.7-29.7
Albumin (g/L)	38	29-47

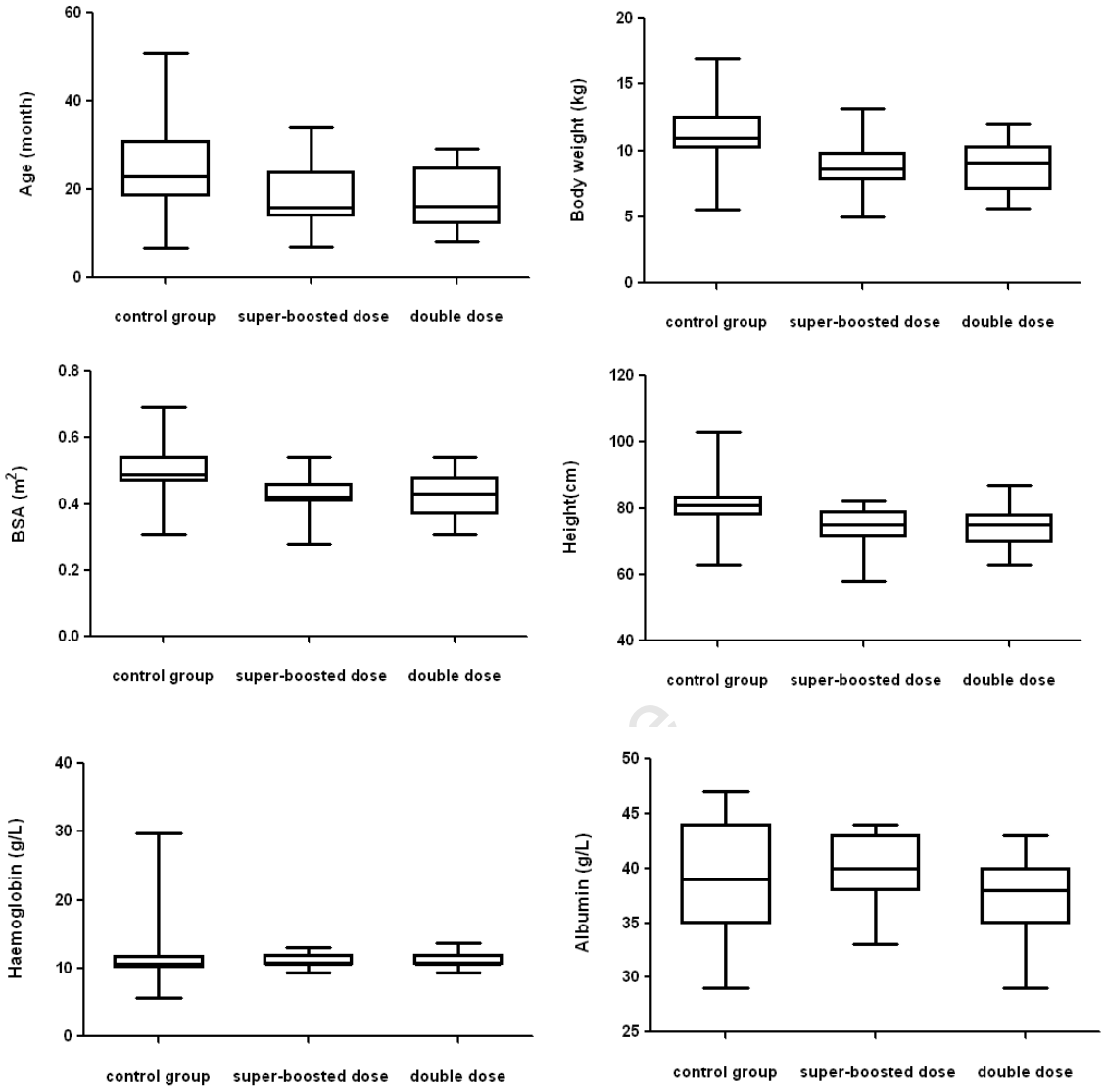

Figure 3.1.1 Demographic characteristics of study population in control, super-boosted, and double dose group.

Table 3.1.2. Data descriptions of Paper I.

	Control group	**Super-boosted group**	**Double dose group**
Patients status	HIV	HIV/TB	HIV/TB
Number of patients	39	15	15
Number of samples	216	120	90
Lopinavir median dose (mg/kg)	11.6	14.0	23.0
Ritonavir median dose (mg/kg)	2.9	3.5	5.8

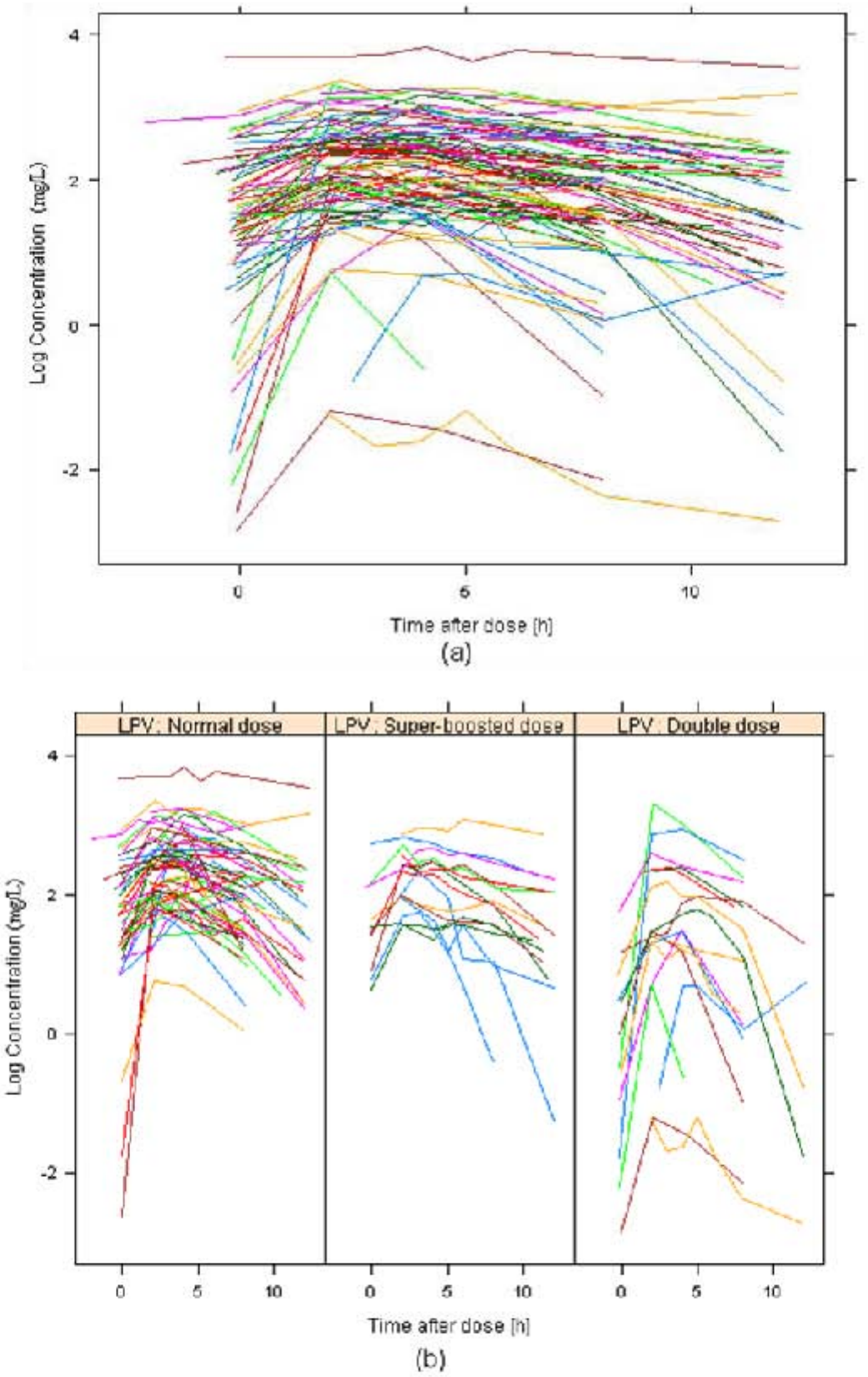

Figure 3.1.2. Plots of lopinavir concentration vs. time after dose in pooled patients (a) and different groups (b).

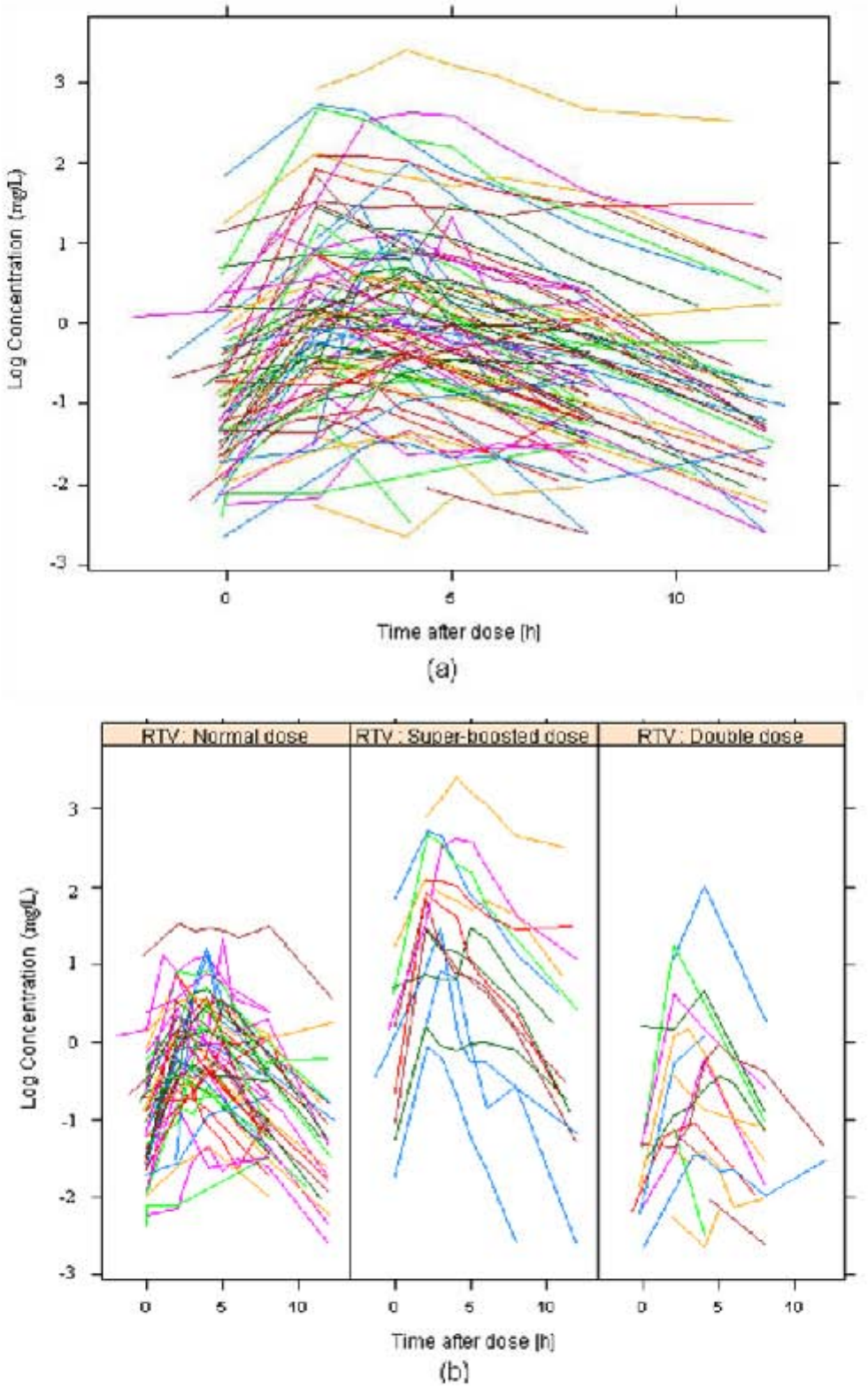

Figure 3.1.3. Pots of ritonavir concentration vs. time after dose in pooled patients (a) and different groups (b).

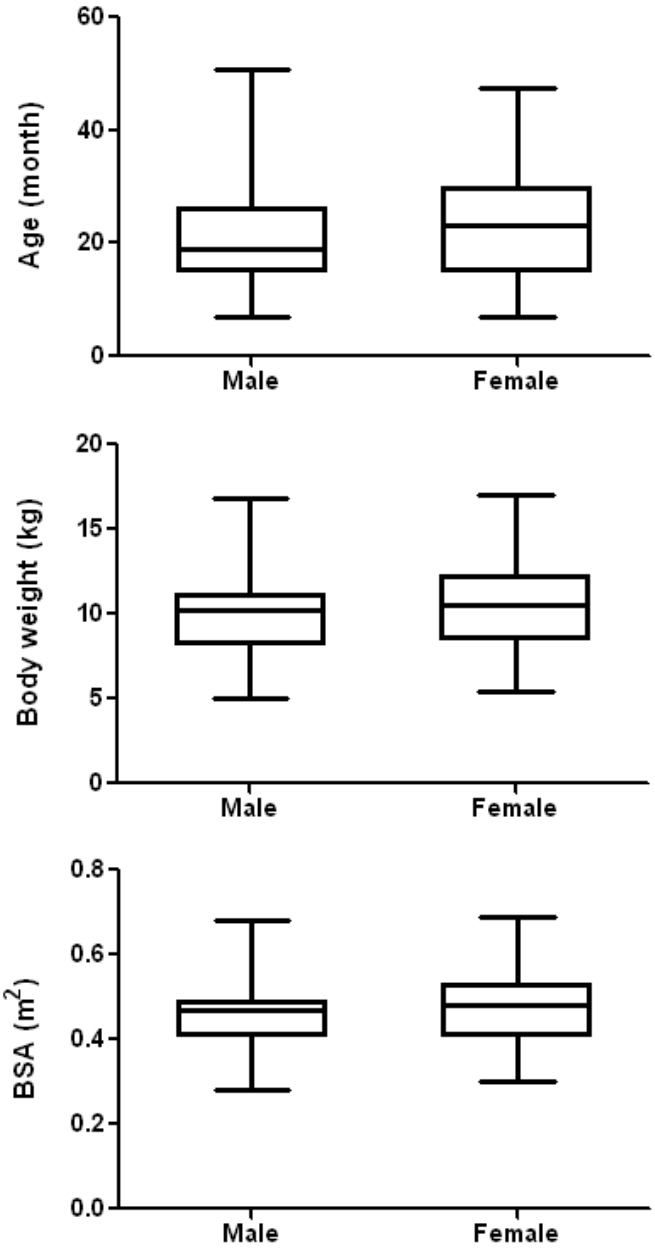

Figure 3.1.4. Covariates: age, body weight, and BSA distribution stratified by gender for all data in this study.

1.2. Model description

1.2.1. Lopinavir separate model

A one-compartment model with first-order absorption and elimination best described the pharmacokinetics of lopinavir. Models with two-compartment disposition did not adequately improve the model fit, nor did zero-order absorption

and the absorption with lag time. The absorption with transit compartments model was also tested for lopinavir, but it did not improve the model fit. The variability (IIV and IOV) in oral clearance, volume of distribution, and absorption rate constant (k_a) were tested in the model according to model development described in method. FOCE approach was chosen in the model building. Logarithm transforming data were used during the model building, and therefore the residual error is implemented as proportional to the observed value.

Rifampicin-based ATT was tested on the bioavailability and oral clearance of lopinavir as an on/off relationship since the rifampicin induction was assumed to achieve steady state. The additional effect of ATT on lopinavir clearance was not significant and was not included in the model. Compared to dosing without ATT (assuming 100% as a reference), the relative bioavailability of lopinavir with rifampicin was estimated for the different lopinavir/ritonavir dose strategies: 64.2% for super-boosted and 16.7% for double dose.

Different covariates, including body weight, age, haemoglobin, gender, BSA, and albumin, were analyzed one by one according to model covariates development steps as a continuous or discrete factor. Body weight was found to have a significant influence on the oral clearance and volume of lopinavir with an allometric scaling relationship in the final model. The OFV dropped about 20 points when this allometric scaling was added. The following formulas were used:

$$CL/F = CL/F_{STD} \cdot \left(\frac{WT_i}{10}\right)^{0.75} \quad (3.1.1)$$

$$V/F = V/F_{STD} \cdot \left(\frac{WT_i}{10}\right)^{1} \quad (3.1.2)$$

where the *CL/F* is the apparent oral clearance, CL/F_{STD} is the apparent oral clearance of standard patients (with mean body weight), WT_i is each patient's body weight and 10 kg is the median body weight in our population.

The oral clearance and volume of distribution were 1.23 L/h and 12.1 L, respectively. The IIV of oral clearance and volume were 48.5% and 29.5%, respectively. The IOV of relative bioavailability was 53.7%. The proportional residual error was 24.7%. The parameter estimates of lopinavir final model are shown in Table 3.1.3. The goodness-fit-plots are shown in Figure 3.1.5. VPC of lopinavir separate model is shown in Figure 3.1.6.

Table 3.1.3. Population pharmacokinetic parameter estimates of lopinavir model.

Parameter		Estimate (η shrinkage%)	RSE (%)
CL/F (L/h)		1.23	10.2
V/F (L)		12.1	12.2
Relative bioavailability	Super-boosted dose	64.2%	17.3
	Double dose	16.7%	18.3
ka (h^{-1})		0.55	13.4
Proportional residual error (%)		24.7	7.98
IIV on CL/F (%CV)		48.5 (28.9)	26
IIV on V/F (%CV)		29.5 (34.4)	58.2
IOV on F (%CV)		53.7 (30.8)	23.1
IIV on RUV (%CV)		57 (32.1)	22.2

CL: oral clearance; V: volume of distribution; F: bioavailability; RUV: residual unexplained variability; ka: oral absorption rate; IIV: interindividual variability; IOV: interoccasional variability.

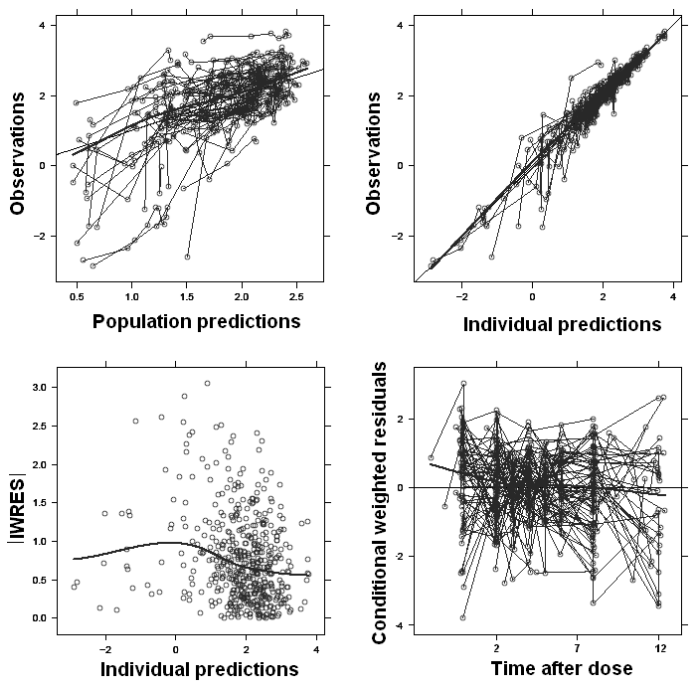

Figure 3.1.5. Goodness-fit-plots of final separate model for lopinavir.

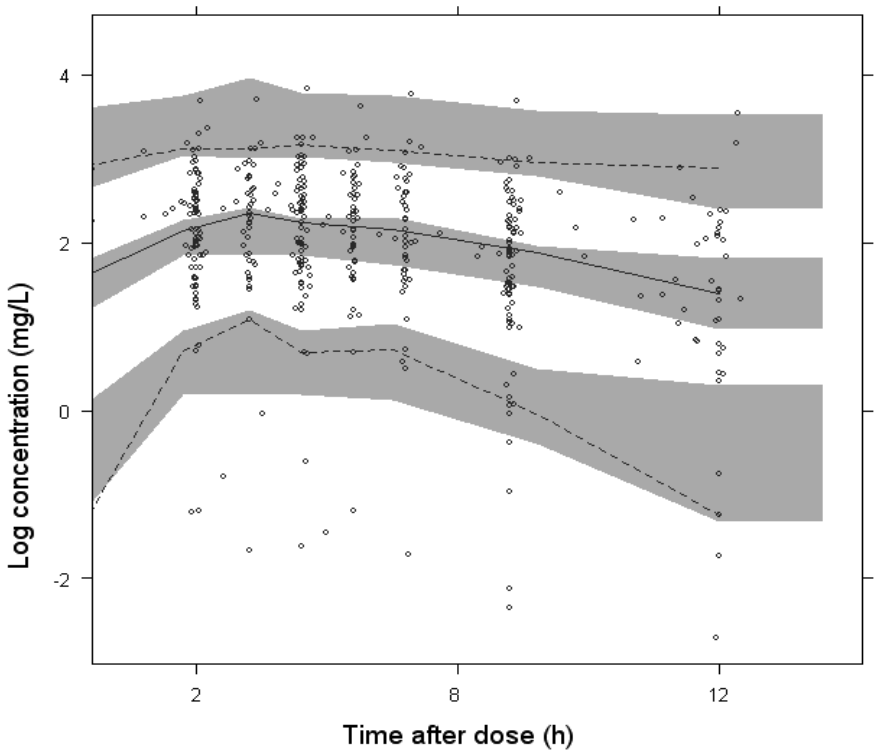

Figure 3.1.6. Visual predictive check (VPC) of the final separate model for lopinavir. The solid line is the median of the observed data and the dotted lines are the 5th and 95th percentiles of the observed data. The shaded areas are the 95% confidence intervals for the median, 5th percentile and the 95th percentiles of the simulated data (n=1000). Observed concentrations are displayed as circles

1.2.2. Ritonavir separate model

A one compartment model with first-order elimination and a transit compartment absorption best described the pharmacokinetics of ritonavir (Figure 3.1.7). Models with two compartments disposition and with zero-order absorption did not adequately fit the data. Transit compartment model was used to represent a more physiological delay in absorption onset and a gradual increase in absorption rate. The number of transit compartment was estimated 10.1 for the absorption model of ritonavir. Mean transit time (MTT) was used to describe the absorption delay of ritonavir. Drug transferred from the final transit compartment to the central compartment occurred through an absorption compartment with first-order absorption rate ka. The transit absorption rate (k_{tr}) was used to describe the transit absorption rate between different transit compartments. The calculation of k_{tr} is indicated as follows:

$$k_{tr} = \frac{n + 1}{MTT} \quad (3.1.3)$$

where n is the number of transit compartments.

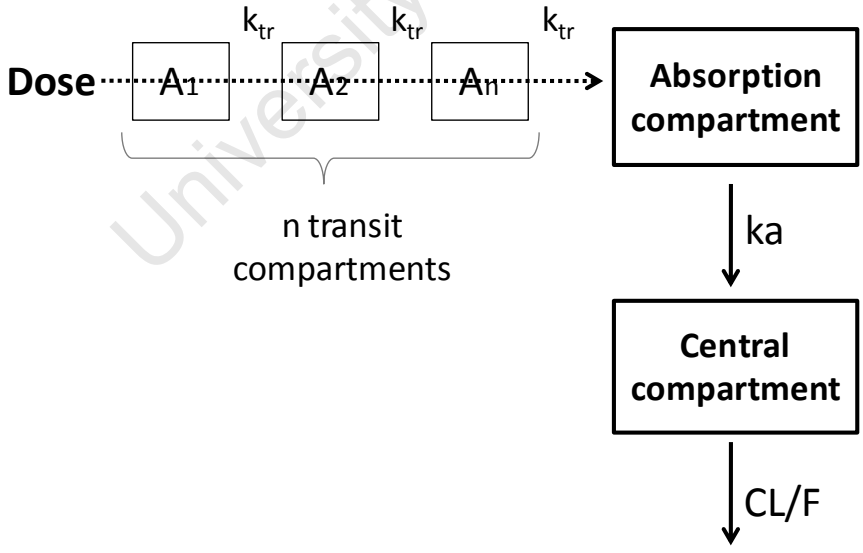

Figure 3.1.7 Structure of ritonavir model.

Similar to lopinavir, the variability (IIV and IOV) in oral clearance, volume of

distribution, and absorption rate constant was tested according to model development described in method. FOCE approach was chosen during the model building. Logarithm transforming data were used in the model, and therefore the residual error is implemented as proportional to the observed values. Rifampicin-based ATT was tested on the bioavailability and oral clearance of ritonavir as an on/off relationship. The additional effect of ATT on ritonavir bioavailability was not significant and was not included in the model. Rifampicin-based ATT induced the ritonavir clearance by about 50%.

Different covariates, as tested for lopinavir before, including body weight, age, haemoglobin, gender, BSA, and albumin, were analyzed one by one according to model covariates development steps as a continuous or discrete factor. The stepwise covariate model (SCM) building tool implemented in PsN was also used. Similar to lopinavir, body weight was found having significant influence on the oral clearance and volume of ritonavir with an allometric scaling relationship in the final model (Equation 3.1.1 and Equation 3.1.2). The OFV was dropped by about 15 points when allometric scaling was applied in the model.

The clearance of ritonavir without rifampicin effect was 12.8 L/h, whereas was 19.1 L/h with rifampicin. The volume was 110 L and MTT was 1.30 h. The IIV of oral clearance and volume of distribution were 72% and 81.6%, respectively and a strong correlation was found between IIV of clearance and volume (r=0.9). The IOV of clearance and MTT were 40.5% and 45.8%, respectively. The proportional residual error was 33.9%. The parameter estimates of ritonavir final model are shown in Table 3.1.4. The goodness-fit-plots are shown in Figure 3.1.8. VPC of ritonavir model is shown in Figure 3.1.9.

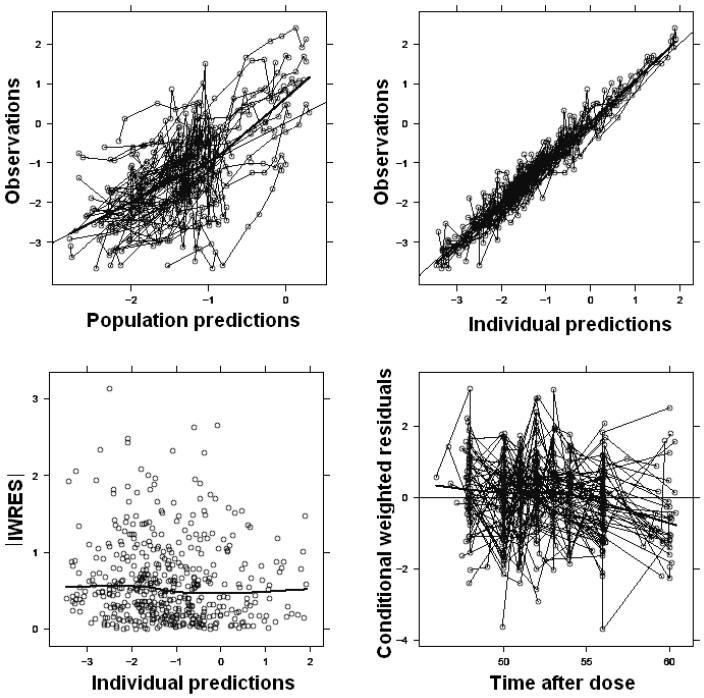

Figure 3.1.8. Goodness-fit-plots of final separate model for ritonavir.

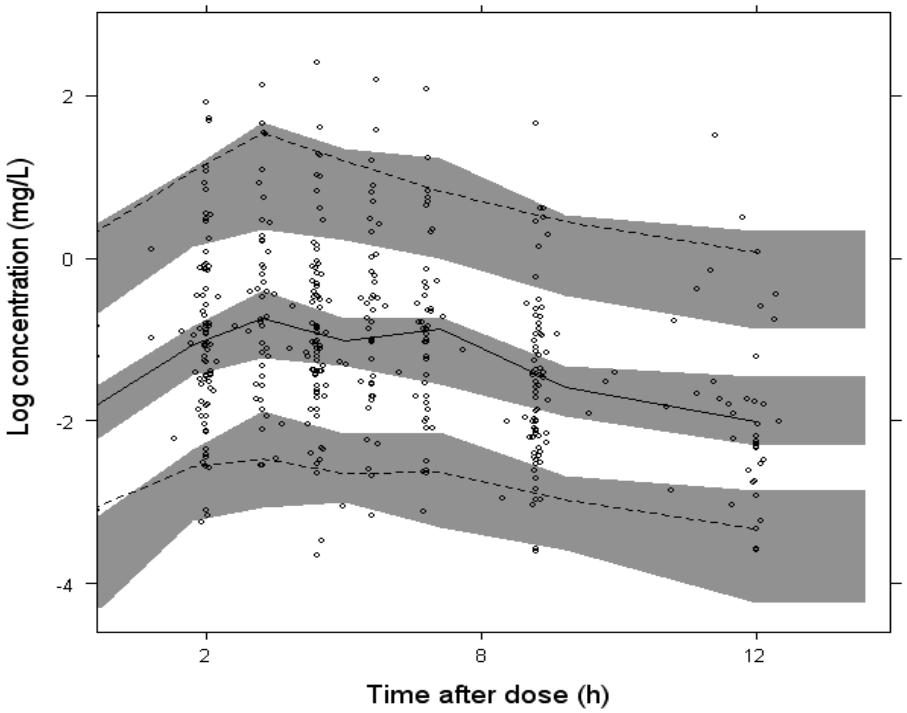

Figure 3.1.9. Visual predictive check (VPC) of the final separate model for ritonavir. The solid line is the median of the observed data and the dotted lines are the 5th and 95th percentiles of the observed data. The shaded areas are the 95% confidence intervals for the median, 5th percentile and the 95th percentiles of the simulated data (n=1000). Observed concentrations are displayed as circles.

Table 3.1.4. Population pharmacokinetic parameter estimates of ritonavir model.

Parameter		Estimate (η shrinkage%)	RSE (%)
CL/F (L/h)	without/after TB treatment	12.8	6.73
	with TB treatment	19.1%	11.6
V/F (L)		110	10.2
ka (h^{-1})		3.72	13.8
NN		10.1	24.5
MTT (h)		1.30	9.63
Proportional error (%)		33.9	6.21
IIV on CL/F (%CV)		72 (26.4)	22
IIV on V/F (%CV)		81.6 (31.2)	12.3
IOV on CL/F (%CV)		40.5 (25.3)	37
IOV on MTT (%CV)		45.8 (19.5)	37.6

CL: oral clearance; V: volume of distribution; F: bioavailability; RUV: residual unexplained variability; ka: oral absorption rate; NN: number of transit compartment; MTT: mean transit time; IIV: interindividual variability; IOV: interoccasional variability.

1.2.3. Integrated lopinavir-ritonavir model

After the separate lopinavir and ritonavir model being built, an integrated model need to be developed to describe drug-drug interactions between lopinavir and ritonavir. Covariates were also tested in order to obtain the final model which process described in the methodology. The structure of the final combined model is illustrated in Figure 3.1.10. The structural model for lopinavir and ritonavir are same as described in the built separate models. A one-compartment model with first-order absorption and elimination best described the pharmacokinetics of lopinavir. A similar model was used for ritonavir, but the absorption phase displayed more complex pharmacokinetics which was described best by a series of

10 transit compartments. Since a strong correlation was found between the absorption rate constant of lopinavir and ritonavir (r=0.9), the two parameters were estimated as proportional to one another. A similar solution was used for IIV in oral clearance and volume of distribution of ritonavir. Significant covariate relationships were found between body weight and oral clearance and volume of distribution of both lopinavir and ritonavir. The OFV dropped more than 50 points when allometric scaling was added to the model.

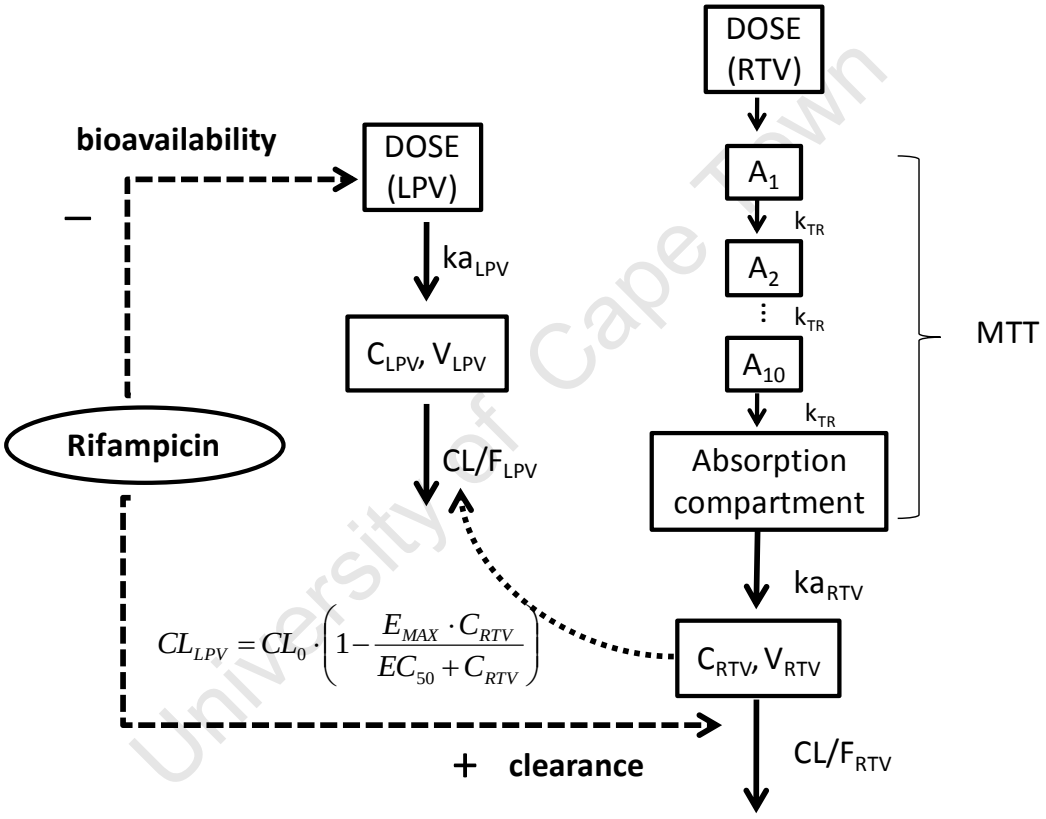

Figure 3.1.10 Structure of the final integrated lopinavir-ritonavir pharmacokinetic model. (LPV: lopinavir; RTV: ritonavir; MTT: mean transit time; CL/F: apparent oral clearance; V/F: apparent volume of distribution; k_a: absorption rate constant; k_{TR}: transit absorption rate constant; E_{max}: the maximum inhibition effect on lopinavir oral clearance by ritonavir; EC_{50}: the ritonavir concentration needed to reach half of E_{max}; C_{RTV}: concentration of ritonavir).

Antituberculosis treatment significantly reduced lopinavir bioavailability by 60%

and 77% when the 'super-boosted' and 'double dose' approaches were used, respectively. The additional effect of ATT on lopinavir clearance was not significant and was not included in the model. For ritonavir, the effect of ATT was significant on oral clearance, then therefore different typical values of clearance were estimated for the subjects with and without ATT. The individual parameters distribution of clearance of lopinavir and ritonavir were shown in Figure 3.1.11 and Figure 3.1.12, respectively.

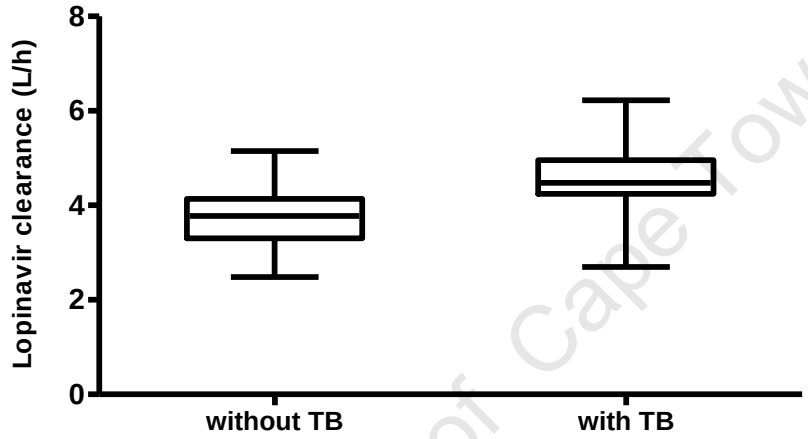

Figure 3.1.11. Individual relative oral clearance of lopinavir distribution by antituberculosis treatment (TB: rifampicin-based antituberculosis treatment).

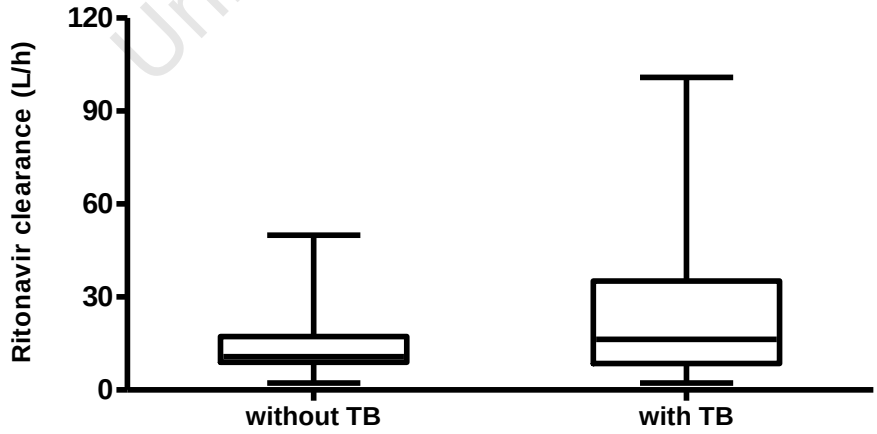

Figure 3.1.12. Individual relative oral clearance of ritonavir distribution by antituberculosis treatment (TB: rifampicin-based ATT).

In addition to ATT, the effect of ritonavir dose on the lopinavir bioavailability was investigated. In order to investigate both the effect of rifampicin-based ATT and the effect of different doses of ritonavir on lopinavir bioavailability (F_{LPV}), the following model was used:

$$F_{LPV} = 1 + SLP \cdot (Dose_{RTV} - Dose_{RTV-STD}) - RIF \qquad (3.1.4)$$

where $Dose_{RTV}$ and $Dose_{RTV\text{-}STD}$ denote the individual dose of ritonavir (mg/kg) and the median ritonavir dose given in the arm without rifampicin co-administration (3 mg/kg), respectively. The linear relation between F_{LPV} and ritonavir dose is described by the parameter *SLP*. *RIF* is the reduction of lopinavir bioavailability during ATT compared with reference (no rifampicin, median ritonavir dose).

In order to capture the inhibition effect of ritonavir on the lopinavir clearance, a lot of models were tested. Concentrations and exposures of ritonavir were tested respectively to investigate this kind of inhibition interaction effect and concentration was found better. Various enzyme models were tested, including direct inhibition and enzyme turnover models, to describe the relationship between ritonavir concentrations and lopinavir clearance. The direct inhibition model of ritonavir concentrations on the clearance of lopinavir was chosen and the sigmoid relationship used in the final model (see Equation 3.1.5). When this effect was introduced, the model fitness was significantly improved (ΔOFV=-95.46) compared to without this dynamic effect.

$$CL_{LPV} = CL_0 \cdot \left(1 - \frac{E_{max} \cdot C_{RTV}}{EC_{50} + C_{RTV}}\right) \qquad (3.1.5)$$

where CL_{LPV} is the oral clearance of lopinavir, CL_0 is the oral clearance of lopinavir when no ritonavir is present, E_{max} is the maximum inhibition effect of ritonavir, EC_{50} is the ritonavir concentration to reach half of E_{max}, and C_{RTV} is the concentration of ritonavir.

Addition of a maturation model was test on the clearance of lopinavir and ritonavir promoted by Anderson and Holford [169], but this model was not supported by the data. The model we used as follows:

$$CL/F = TVCL/F \cdot \frac{PMA_i{}^{Hill}}{PMA_i{}^{Hill} + PMA50^{Hill}} \quad (3.1.6)$$

where *CL/F* is the apparent oral clearance, *TVCL/F* is the typical value, PMA_i is postmenstrual age of each patient, *PMA50* is the PMA at which half of the maturation is reached, and *Hill* is a shape parameter that controls steepness of the sigmoidal maturation function.

Blow the quantification limit (BQL) data were few in the dataset, 2% of total data for both lopinavir and ritonavir, and these data were excluded during model building. In order to evaluate the accuracy of predictions for BQL data, the bias between predicted and LLOQ values were calculated, in which LLOQ values 0.05 mg/L for lopinavir and 0.025 mg/L for ritonavir were used. The following equation was applied to evaluate the prediction accuracy of BQL data:

$$BQLA\ (\%) = \frac{\mathrm{BQLE} - \mathrm{LLOQ}}{\mathrm{LLOQ}} \quad (3.1.7)$$

where BQLA is the accuracy of prediction for BQL data, BQLE is the individual estimate of BQL data by the final model, and LLOQ is the lowest limit of quantization. Figure 3.1.8 describes the accuracy of prediction for BQL data of lopinavir and ritonavir. The low BQLA indicates prediction of BQL data by our model are close to LLOQ value, which further proves the minor bias related to exclusion BQL data during modeling building.

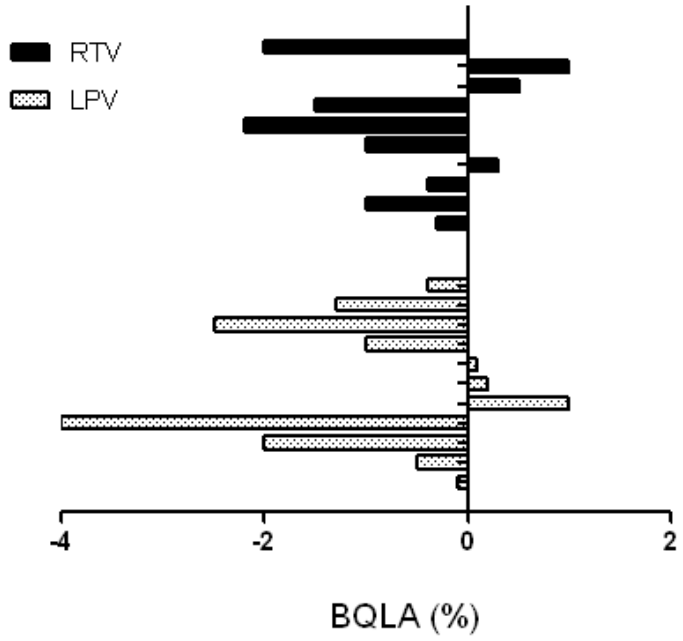

Figure 3.1.13 The accuracy of prediction for BQL data of lopinavir and ritonavir by the final model.

The typical volume of distribution of lopinavir was 11.6 L. While the typical oral clearance of lopinavir without ritonavir was 4.18 L/h, it should be kept in mind that this value is an extrapolation, since lopinavir was never given without ritonavir. The number of transit compartments of ritonavir was estimated to be 10.1 and fixed to 10 in the integrated model. The typical bioavailability of lopinavir was 40.5% when 'super-boosted' lopinavir was given and 22.6% when the dose of LPV/r was doubled during rifampicin-based ATT compared to without rifampicin-based ATT. Antituberculosis treatment increased the oral clearance of ritonavir by about 50%, from 12.7 L/h to 19 L/h. Figure 3.1.14 shows the distribution of lopinavir bioavailability in different dose strategy groups. Due to the complexity of the model, numerical instability was experienced when we attempted to estimate all of the parameters simultaneously. Consequently the maximum effect (E_{max}) was fixed to 0.9. This value was estimated when ritonavir parameters were fixed and only lopinavir parameters estimated. The EC_{50} was estimated 0.0519 mg/L. The population pharmacokinetic parameter estimates for

the final combined model are shown in Table 3.1.5. All the parameters were estimated simultaneously. The representative individual plots of lopinavir and ritonavir are presented in Figure 3.1.15 and Figure 3.1.16.

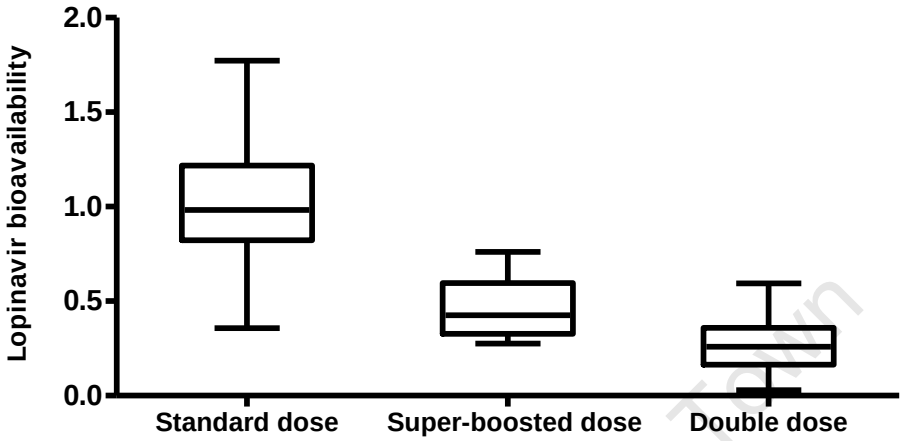

Figure 3.1.14. Individual bioavailability of lopinavir distribution in different doses groups.

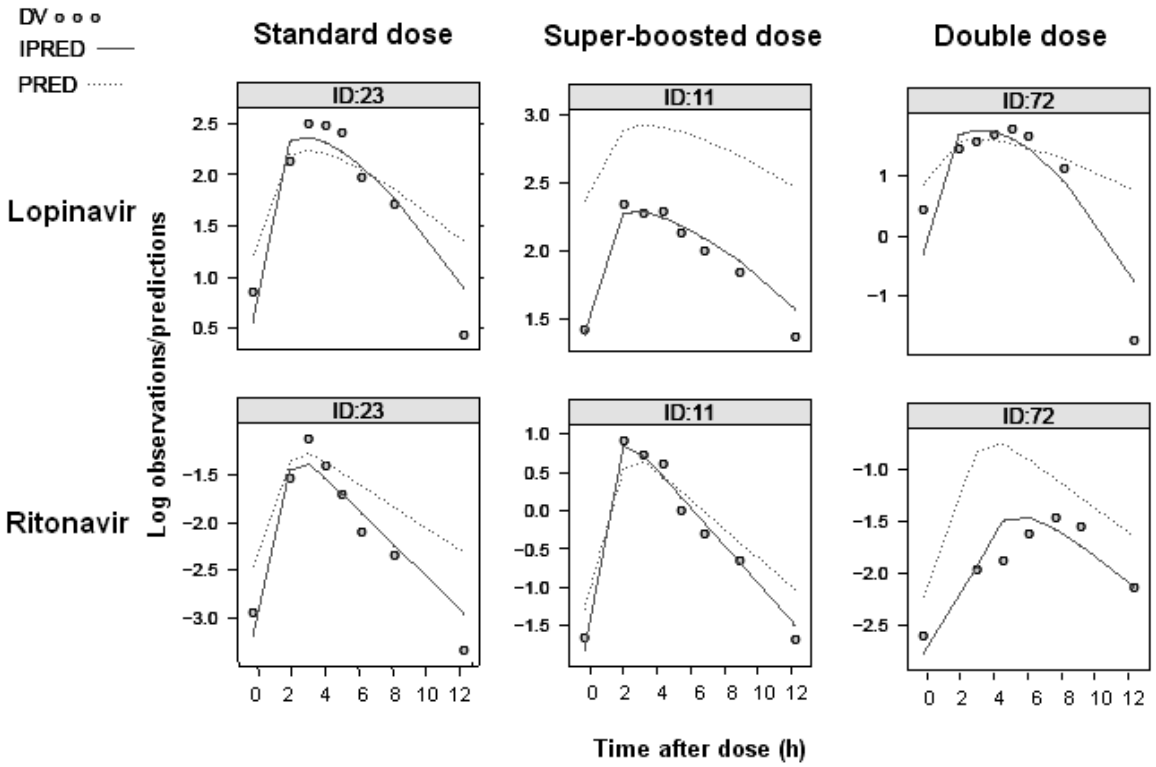

Figure 3.1.15. Representative individual plots of lopinavir and ritonavir in different regimen groups using intensive sampling approach (the solid line is the individual predictive data and the dotted line is the population predictive data and observed concentrations are displayed as circles).

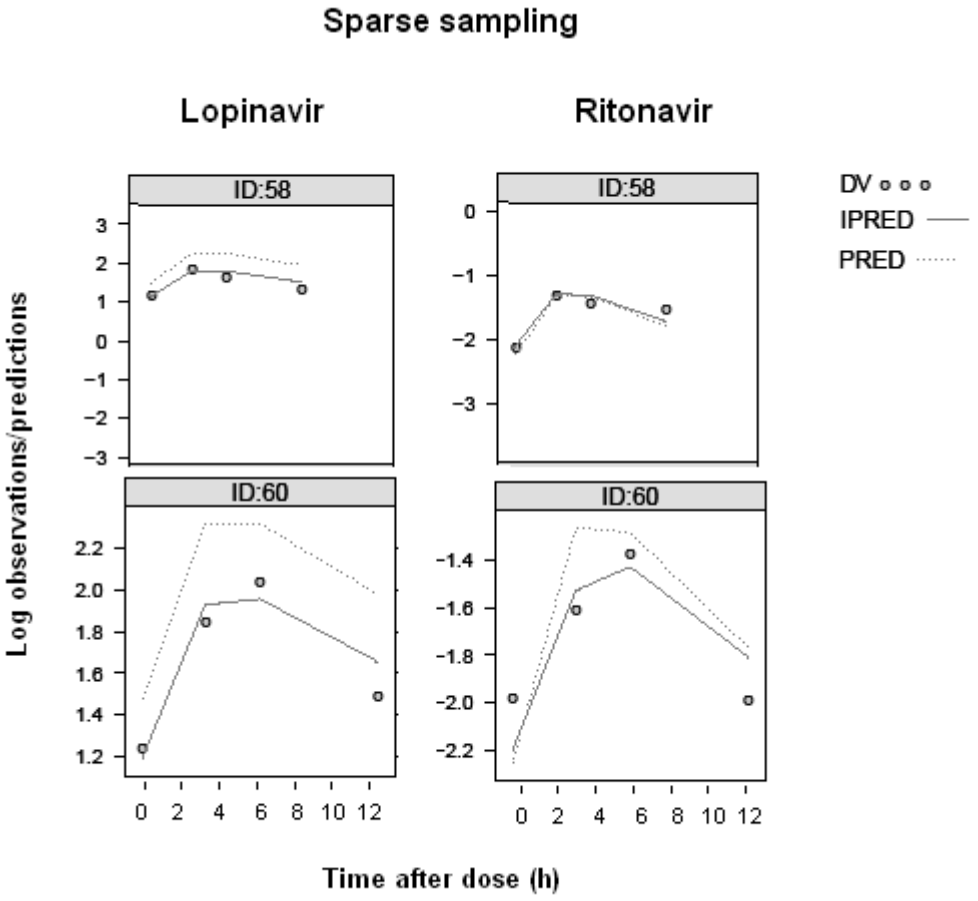

Figure 3.1.16. Representative individual plots of lopinavir and ritonavir using sparse sampling approach (the solid line is the individual predictive data and the dotted line is the population predictive data and observed concentrations are displayed as circles).

Table 3.1.5. Population pharmacokinetic parameter estimates for both lopinavir and ritonavir in final integrated model.

Parameters	**Final model**	**Bootstrap**	
	Estimates (ɳ shrinkage%)	**Mean**	**95% CI***
Lopinavir			
CL/F (L/h)[5]	4.18	4.42	3.41-5.42
V/F (L)[6]	11.6	11.8	9.20-14.49
k_a (h^{-1})	0.74	0.771	0.432-1.108
Slope[1]	0.021		
RIF on F[2]	0.832		
F[3] super-boosted dose	40.5%	45.9%	36.3%-55.5%
F[3] double dose	22.6%	22.5%	14.1%-30.9%
IIV V (% CV)	56.6 (28.3)	54.5	32.1-70.2
IOV k_a (% CV)	76.2 (31.2)	78.7	37.5-100.7
IOV F (% CV)	51.8 (30.6)	50.8	30.9-64.8
RUV	0.304	0.311	0.252-0.349
Ritonavir			
CL/F (L/h)[5] no TB and after TB	12.8	13.0	10.5-15.5
CL/F (L/h)[5] with TB treatment	19.1	18.5	13.9-23.1
V/F (L)[6]	105	105	80.7-129.5
k_a (h^{-1})	2.31	2.55	0.54-4.57
MTT (h)	1.28	1.21	0.80-1.62
IIV CL (%CV)	72.8 (25.7)	72.7	61.2-81.6
IOV CL (%CV)	41.6 (24.3)	40.0	21.2-52.6
IIV V (%CV)	43.3 (31.1)	42.4	30.3-56.2
IOV MTT (%CV)	31.1 (18.6)	46.9	23.6-65.8
IOV k_a (%CV)	98.1 (41.6)	104.3	78.5-120.3
RUV	0.339	0.342	0.291-0.372
Lopinavir-Ritonavir interaction[4]			
E_{max}	0.9 (fix)		
EC_{50} (mg/L)	0.0519	0.0492	0.0270-0.0715

CL: oral clearance; V: volume of distribution; F: bioavailability; RUV: residual unexplained variability; MTT: mean transit time; ka: oral absorption rate; IIV: interindividual variability; IOV: interoccasional variability;*CI: confidence interval from 250 bootstraps; [1]slope between ritonavir dose (mg/kg) and bioavailability of lopinavir; [2]the reduction of bioavailability of lopinavir caused by rifampicin $\left(F_{LPV} = 1 + SLP \cdot (Dose_{RTV} - Dose_{RTV-STD}) - RIF\right)$; [3]median of relative

bioavailability of lopinavir; [4] $CL_{LPV} = CL_0 \cdot \left(1 - \frac{E_{max} \cdot C_{RTV}}{EC_{50} + C_{RTV}}\right)$; [5] $CL/F_i = CL/F_{STD} \cdot \left(\frac{WT_i}{10}\right)^{0.75}$; [6] $V/F_i = V/F_{STD} \cdot \left(\frac{WT_i}{10}\right)^{1}$

1.3. Final model evaluation

Goodness fit plots of final integrated model for lopinavir and ritonavir are shown in Figure 3.1.17. Goodness fit plots of final integrated model for lopinavir and ritonavir stratified by age are shown in Figure 3.1.18. and Figure 3.1.19. Figure 3.1.20 shows VPC plots stratified by different lopinavir and ritonavir dose strategies. Figure 3.1.21 shows VPC plots stratified by age. The results of 1000 simulations from the final model demonstrated the adequacy of the model and indicated that the model had good properties to investigate alternative dosing strategies using simulation. The bootstrap results (Table 3.1.5) confirmed the robustness of the final model.

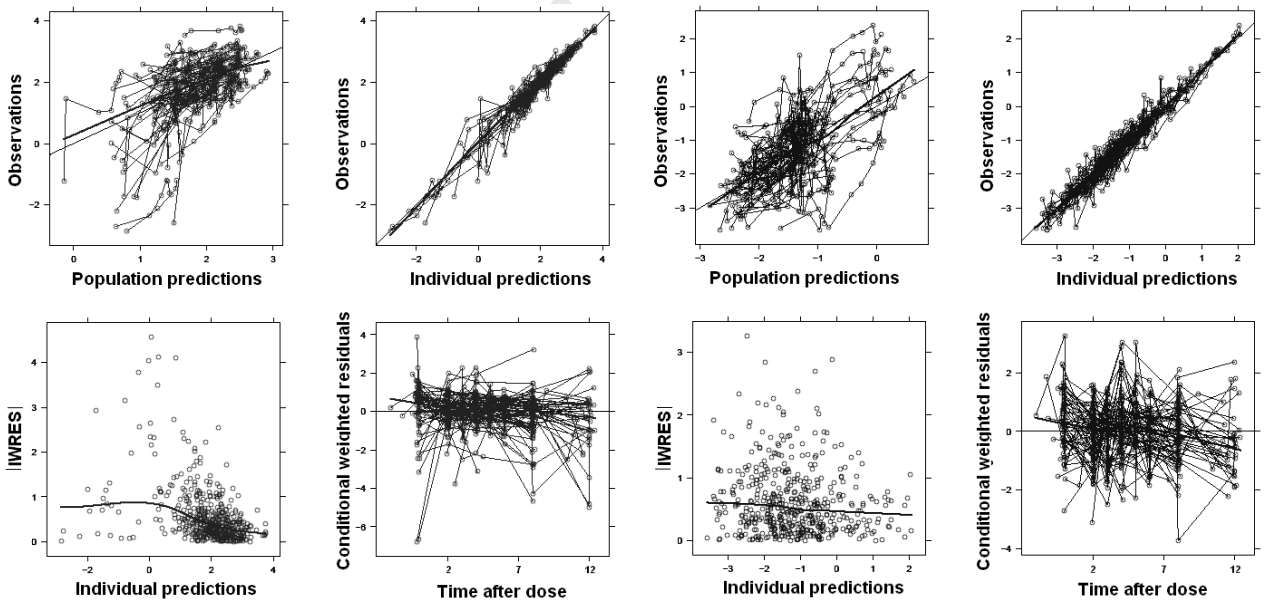

Figure 3.1.17. Goodness fit plots of final integrated model for lopinavir (a) and ritonavir (b).

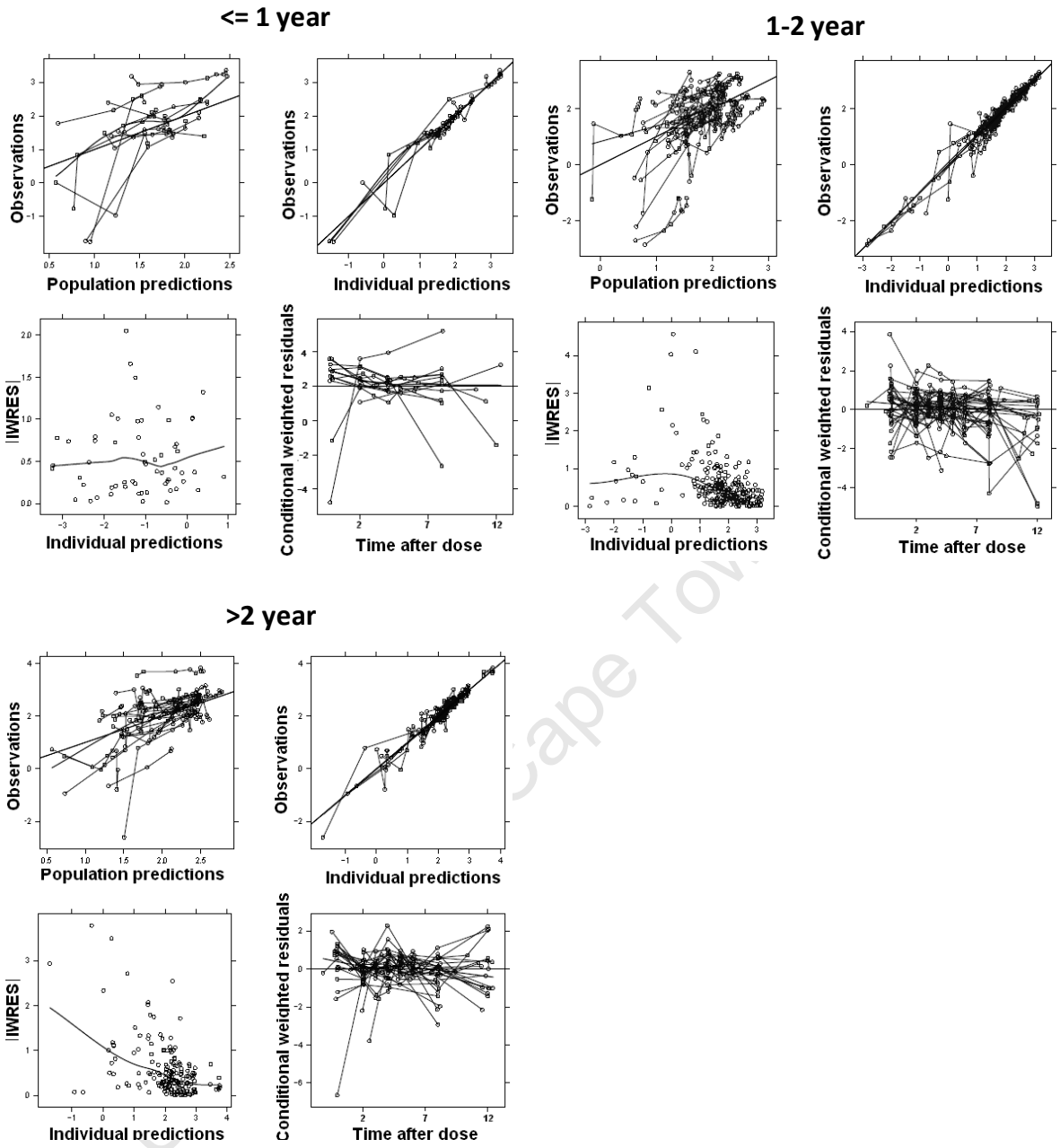

Figure 3.1.18. Goodness fit plots of final integrated model for lopinavir stratified by age

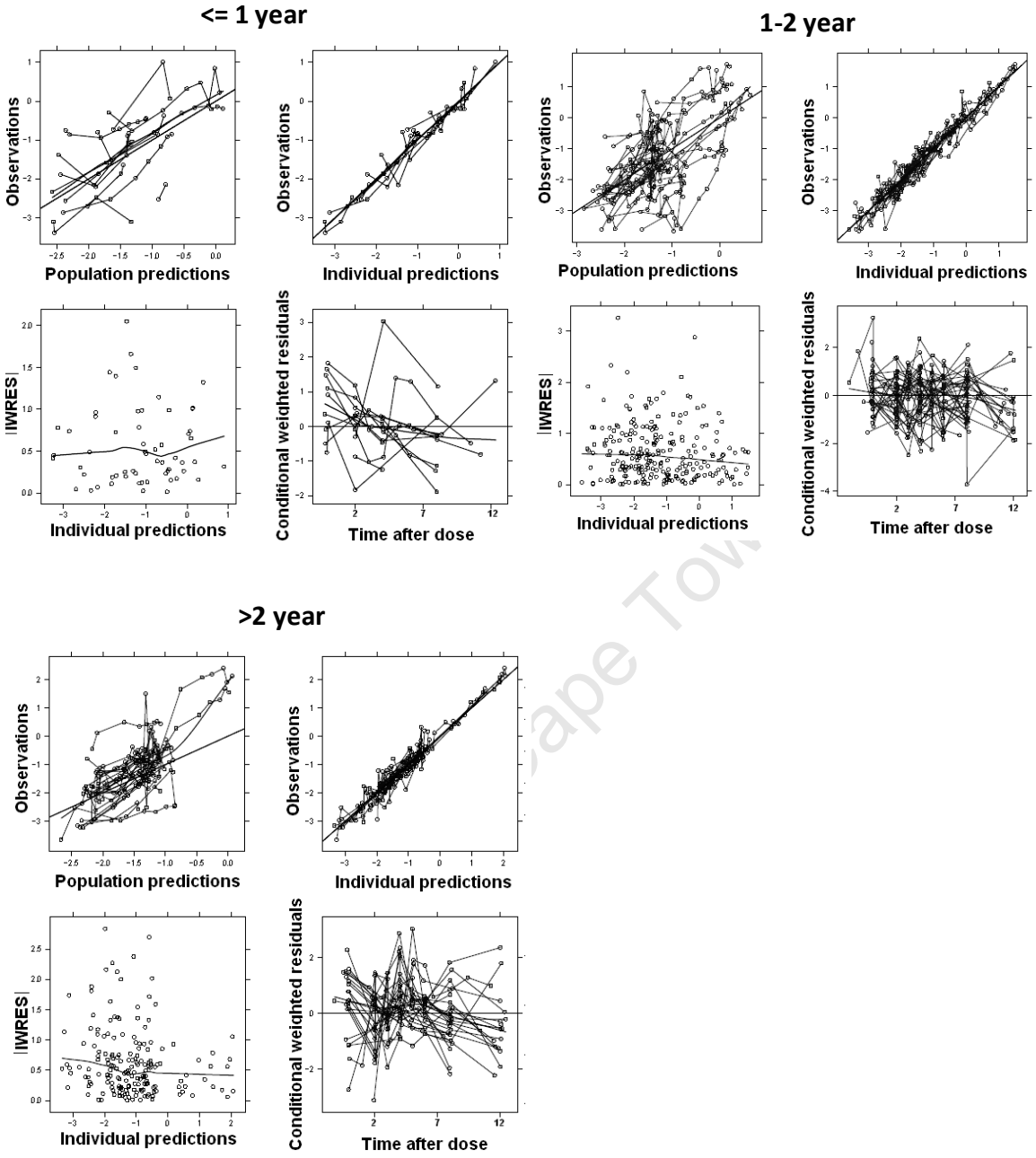

Figure 3.1.19. Goodness fit plots of final integrated model for ritonavir stratified by age

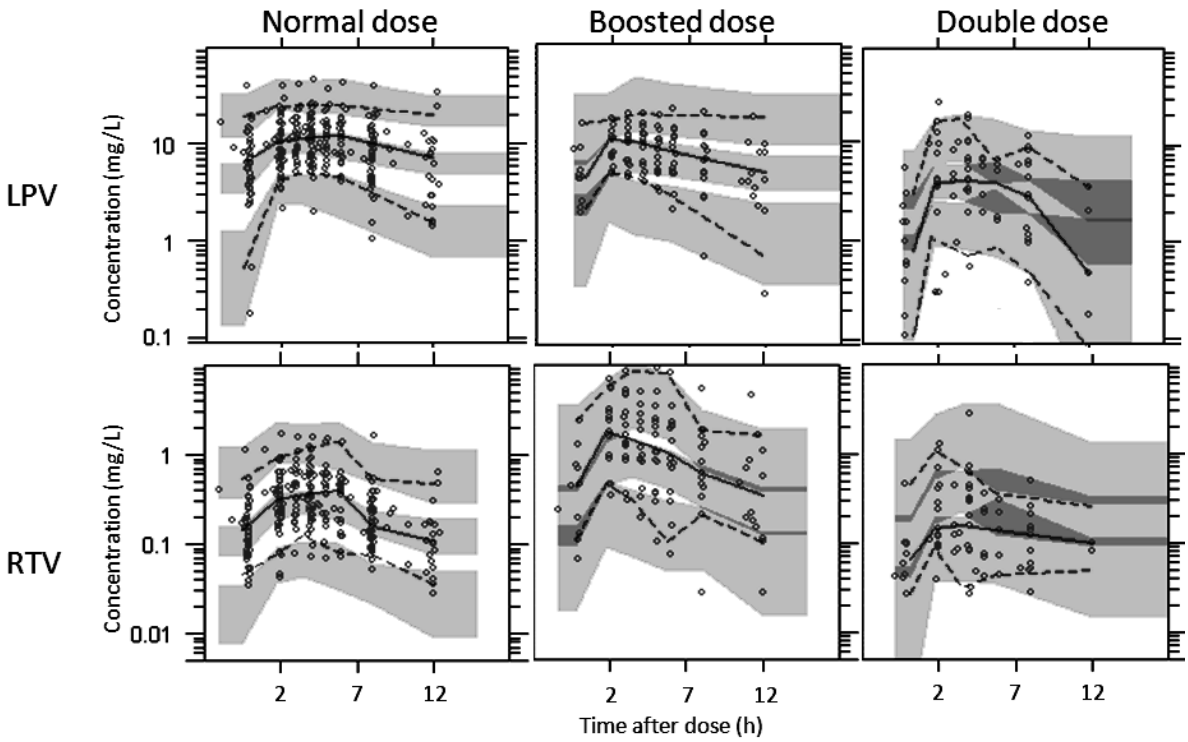

Figure 3.1.20. Visual predictive check (VPC) of the final integrated model for lopinavir (LPV; upper panel) and ritonavir (RTV; lower panel) stratified for regimens (from left to right; standard, 'super-boosted', and 'double dose' approach). The solid line is the median of the observed data and the dotted lines are the 5th and 95th percentiles of the observed data. The grey shaded areas are the 95% confidence intervals for the median, 5th percentile and the 95th percentiles of the simulated data (n=1000). Observed concentrations are displayed as circles.

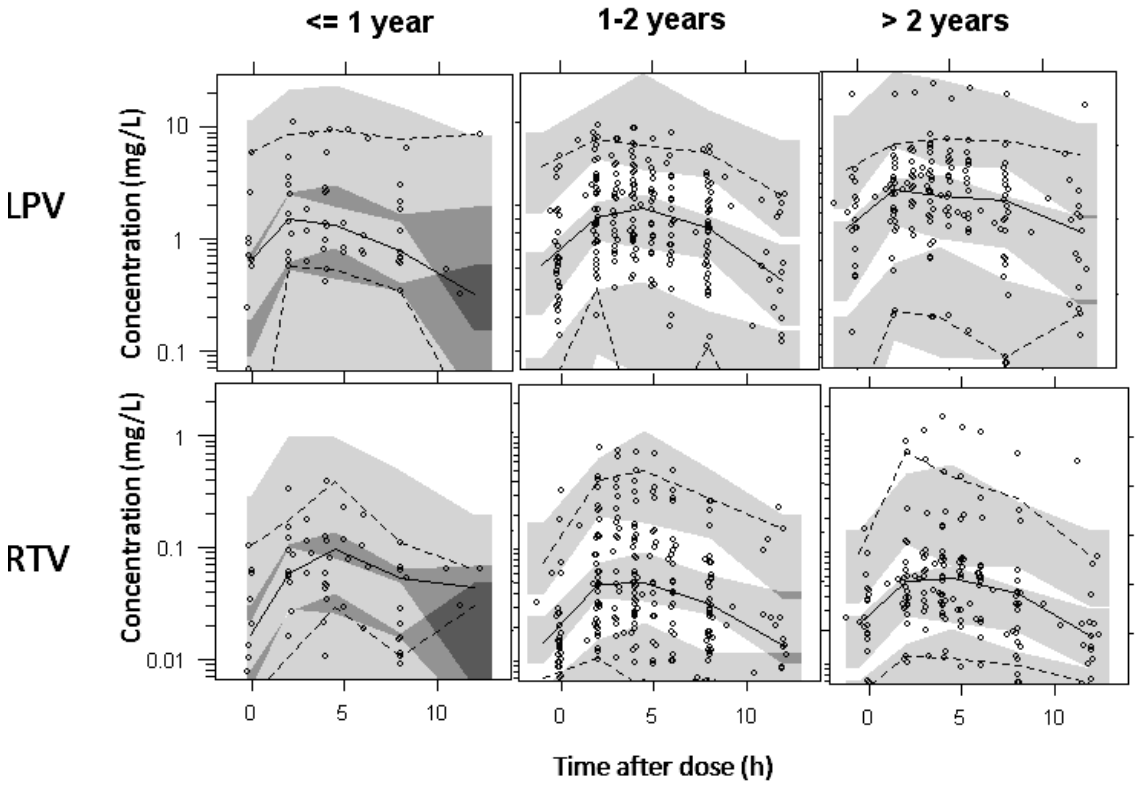

Figure 3.1.21. Visual predictive check (VPC) of the final integrated model for lopinavir (LPV; upper panel) and ritonavir (RTV; lower panel) stratified by age. The solid line is the median of the observed data and the dotted lines are the 5th and 95th percentiles of the observed data. The grey shaded areas are the 95% confidence intervals for the median, 5th percentile and the 95th percentiles of the simulated data (n=1000). Observed concentrations are displayed as circles.

1.4. Simulation

Optimal lopinavir/ritonavir dose recommendations during rifampicin co-administration are presented in Table 3.1.6. Simulations predicted that children weighing 3-5.9, 6-9.9, 10-13.9 and 14-19.9 kg need respective doses of 52, 40, 35 and 30 mg/kg LPV/r in 4:1 ratio 12 hourly in order to maintain lopinavir concentrations > 1 mg/L in at least 95% of children. An 8 hourly dosing strategy would require lower doses of 27, 21, 20 and 18 mg/kg for the respective weight bands. When giving lopinavir/ritonavir in 'super-boosted' ratio (1:1), the model predicted that lopinavir doses of 22, 16, 14 and 12 mg/kg twice daily are needed in children weighing 3.0-5.9, 6.0-9.9, 10.0-13.9 and 14.0-19.9 kg, respectively. The 5th percentiles of simulated lopinavir concentrations using the original and the

proposed dosage regimens in a typical patient (the patient who has a median age and median body weight) when lopinavir/ritonavir was given as standard ratio 4:1 are presented in Figure 3.1.22.The prediction concentrations of lopinavir using our recommended dose strategies are shown in Figure 3.1.23, Figure 3.1.24 and Figure 3.1.25.

Table 3.1.6 Predicted optimal dosage regimens of lopinavir/ritonavir when rifampicin is co-administered based on simulations using the final combined model.

Body weight (kg)	**Lopinavir:ritonavir=4:1**		**Lopinavir:ritonavir=1:1**
	12 hourly LPV dose (mg/kg)	**8 hourly LPV dose (mg/kg)**	**12 hourly LPV dose (mg/kg)**
3.0-5.9	52	27	22
6.0-9.9	40	21	16
10.0-13.9	35	20	14
14.0-19.9	30	18	12

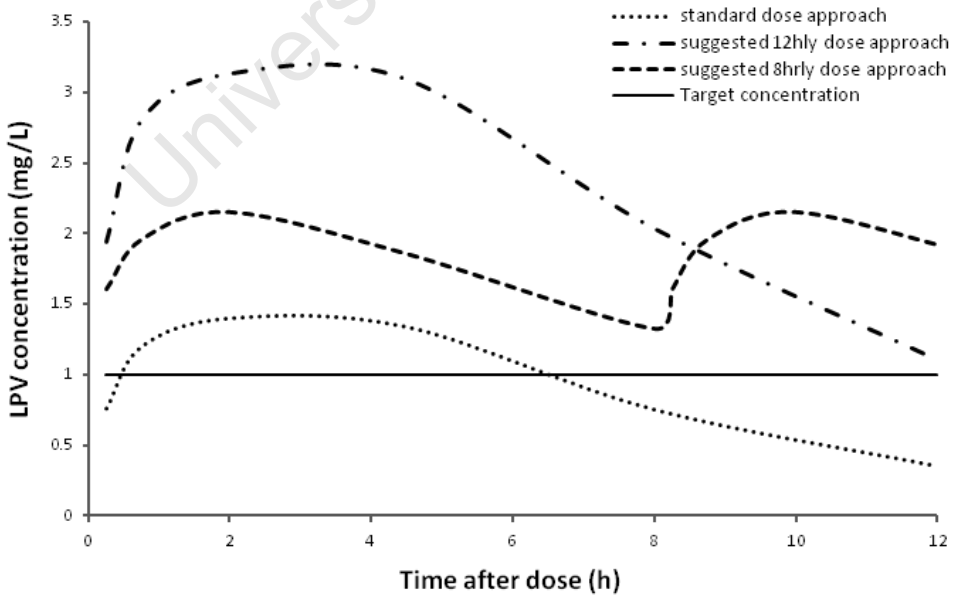

Figure 3.1.22.The 5th percentile of simulated lopinavir concentrations obtained for a typical patient using different dosage regimens. The dashed line is the target concentration of 1 mg/L.

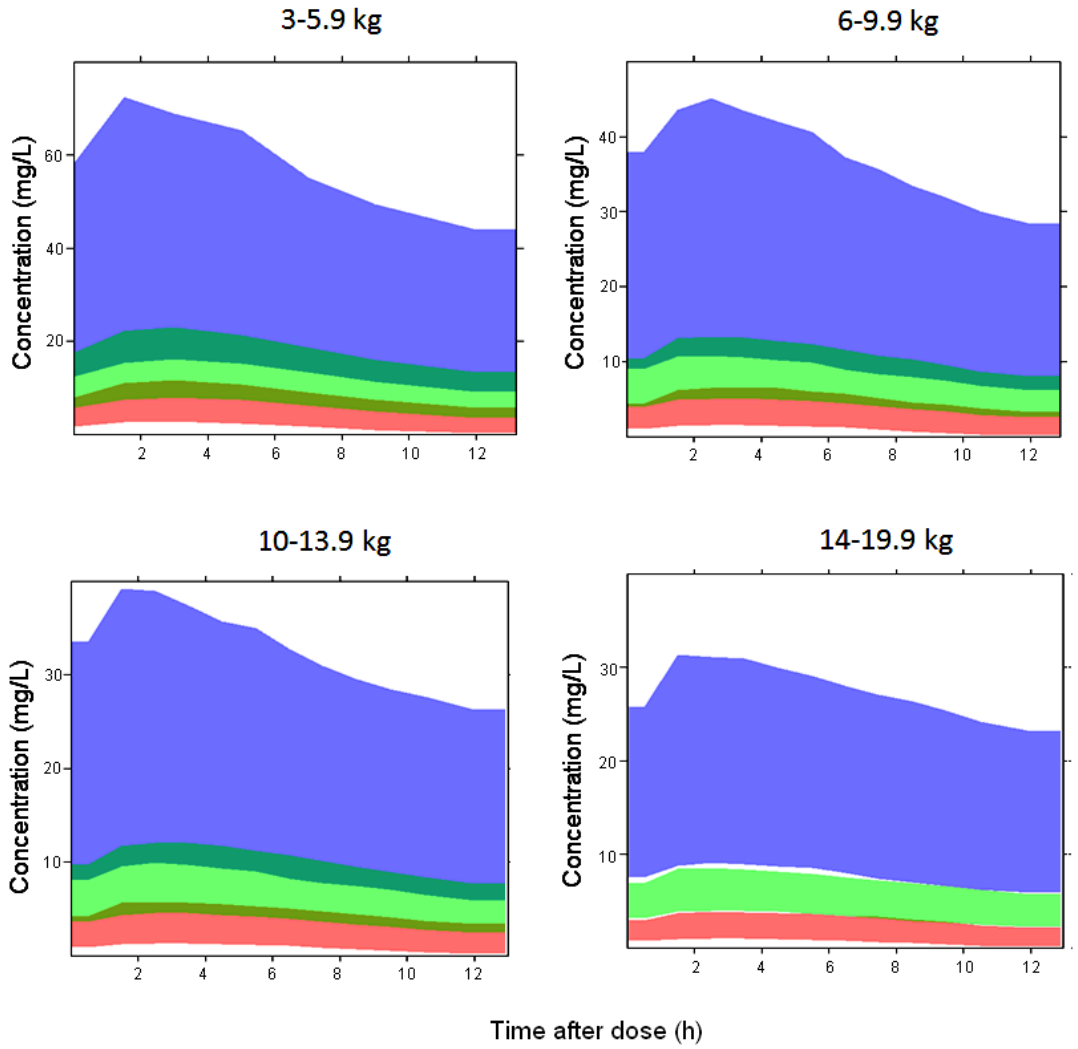

Figure 3.1.23. The predicted concentrations of lopinavir using recommended dose in Table 3.1.6 as lopinavir:ritonavir= 1:1, 12 hourly strategy stratified by WHO recommended body weight bands. The shaded areas, from bottom to top, are the 95% confidence intervals for the 5th percentile, median, and the 95th percentiles of the simulated data (n=1000).

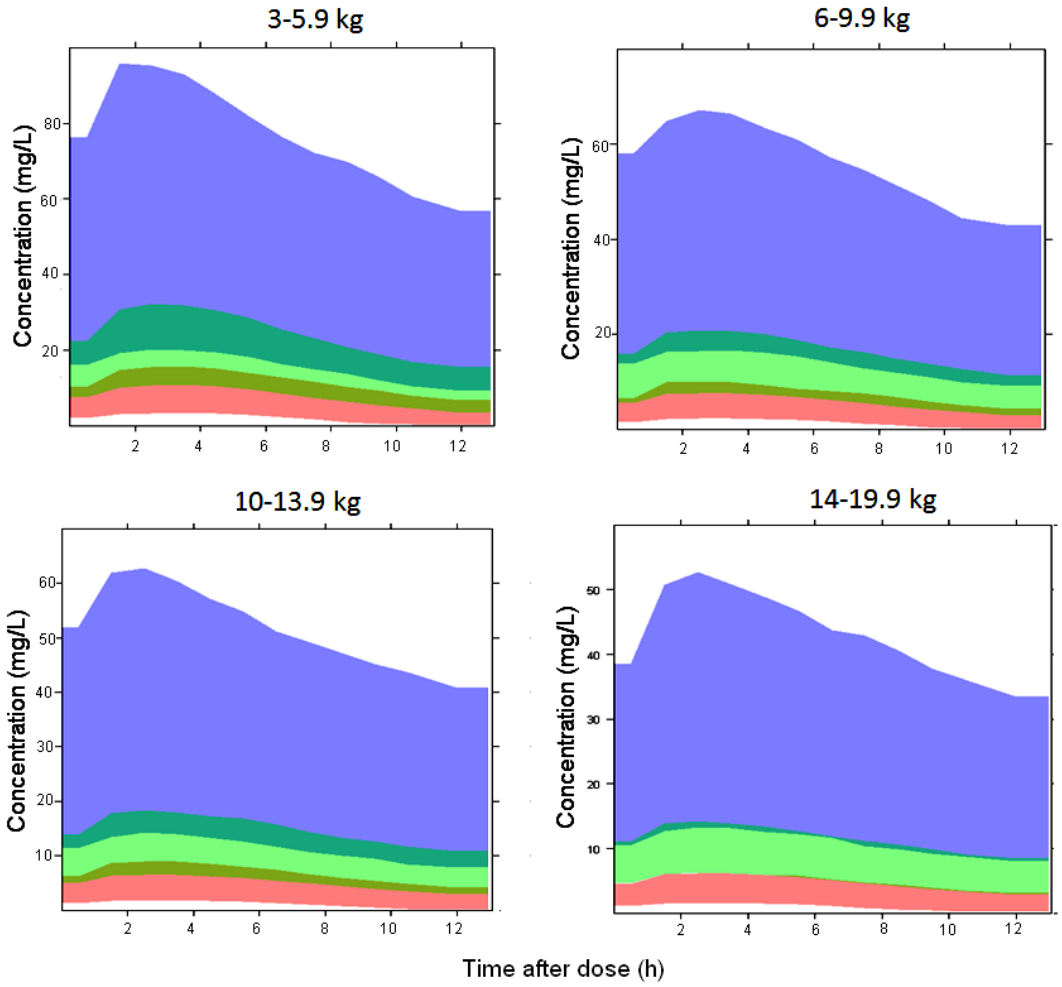

Figure 3.1.24. The predicted concentrations of lopinavir using recommended dose in Table 3.1.6 as lopinavir:ritonavir= 4:1, 12 hourly strategy stratified by WHO recommended body weight bands. The shaded areas, from bottom to top, are the 95% confidence intervals for the 5th percentile, median, and the 95th percentiles of the simulated data (n=1000).

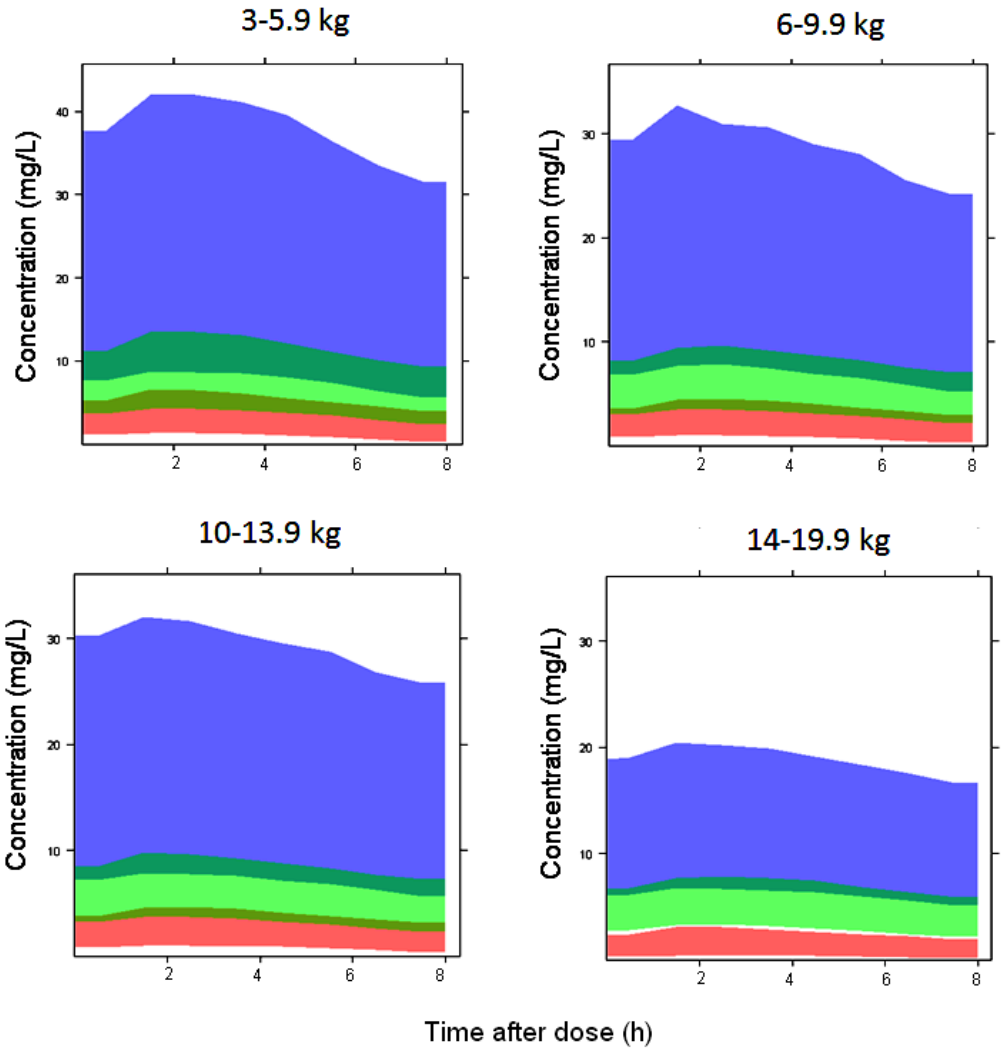

Figure 3.1.25. The predicted concentrations of lopinavir using recommended dose in Table 3.1.6 as lopinavir:ritonavir= 4:1, 8 hourly strategy stratified by WHO recommended body weight bands. The shaded areas, from bottom to top, are the 95% confidence intervals for the 5th percentile, median, and the 95th percentiles of the simulated data (n=1000).

2. Results (Paper II)

2.1. Patients and data description

The demographic characteristics of patients and trough concentrations observed (C_0 and C_{12}) are summarized in Table 3.2.1 and Figure 3.2.1 respectively. Twenty-one patients, of whom 18 were females, were enrolled in the study, but 3 patients experiencing adverse events were withdrawn before they completed the

study, so only partial data are available for them. Of these three patients, two developed grade 3/4 asymptomatic transaminitis (one on standard dose of LPV/r with rifampicin and the other on LPV/r 600/150 mg with rifampicin), while another patient withdrew consent after developing grade 2 nausea (on LPV/r 600/150 mg with rifampicin). Other adverse events were mild and resolved spontaneously. All participants had 100% adherence according to regular pill counts and questioning throughout the study period. Fat free mass was calculated using the approach proposed in Janmahasatian et al [170]. A total of 800 concentrations were collected for both lopinavir and ritonavir. Data description of this study is presented in Table 3.2.2. Figure 3.2.2 illustrates the distribution of relvant demographic and clinical variables in this study. Plots of concentrations of lopinavir and ritonavir against time after dose in patients are presented in Figure 3.2.3 and Figure 3.2.4.

Table 3.2.1. Demographic characteristics of patients (n=21).

Characteristic	**Median (range)**
Sex (F/M)	18/3
Age (year)	36 (26 -58)
Body weight (kg)	64.5 (43.0-110.0)
Height (cm)	160.5 (148.0 -186.5)
Body mass index (BMI, kg/m^2)	26.7 (17.4 -41.4)
Fat free mass (kg)	39.5 (30.6 -65.9)
Haemoglobin (g/dL)[1]	11.5 (8.4 -15.0)
Total bilirubin (umol/L)[2]	7.0 (2.0 -24.0)

[1] normal range: 11.5-15.0 g/dL
[2] normal range: 0-21 umol/L

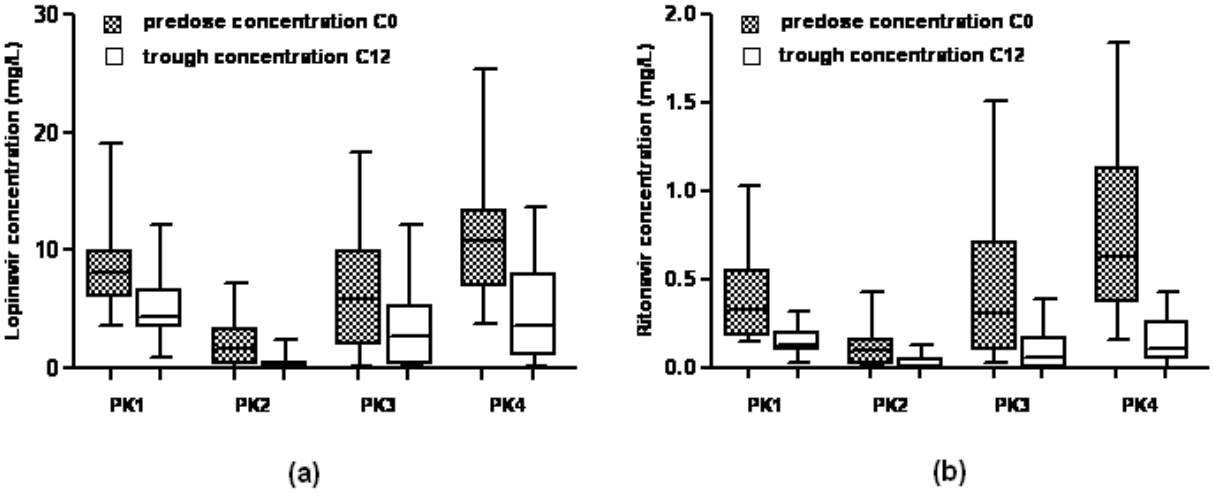

Figure 3.2.1.Observed morning and evening trough concentrations of lopinavir (a) and ritonavir (b) (PK1-PK4 indicates 4 sequential occasions of this study).

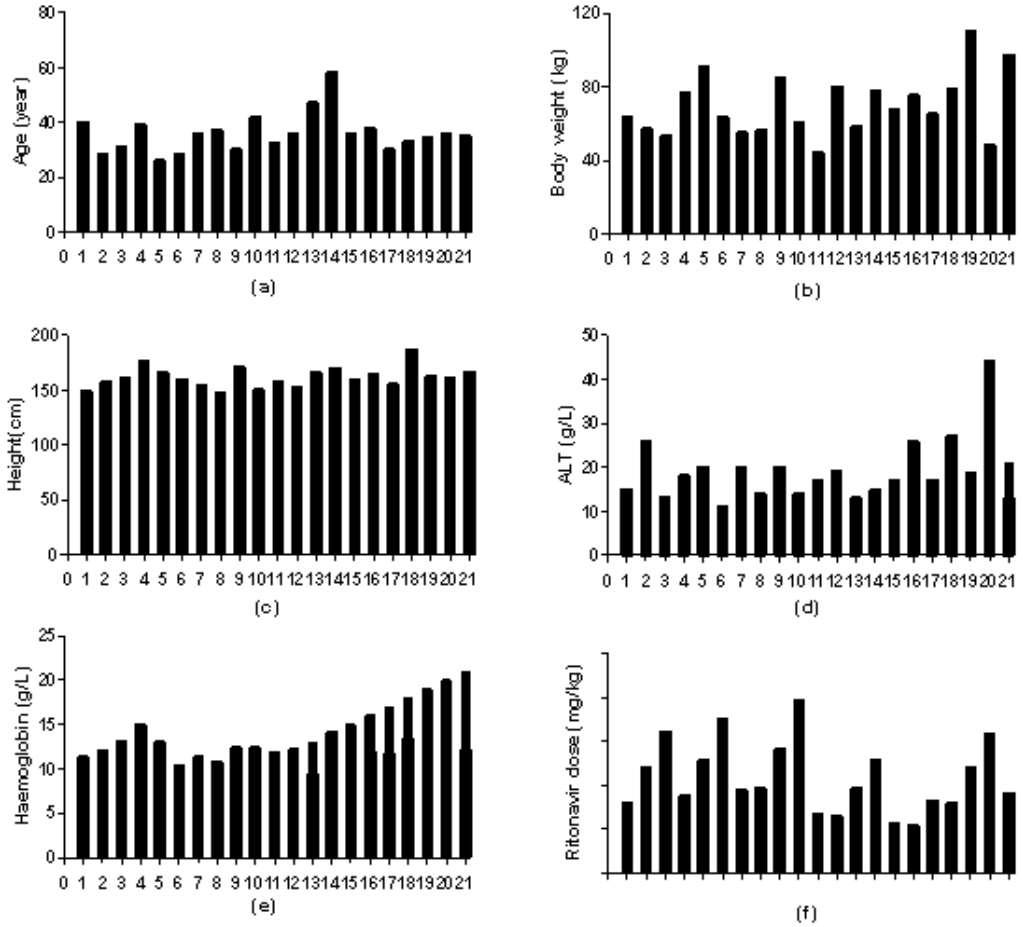

Figure 3.2.2. The distribution of relvant demographic and clinical variables in the study population,: age (a); body weight (b); height (c); ALT (d); haemoglobin (e); ritonavir dose per kg (f).

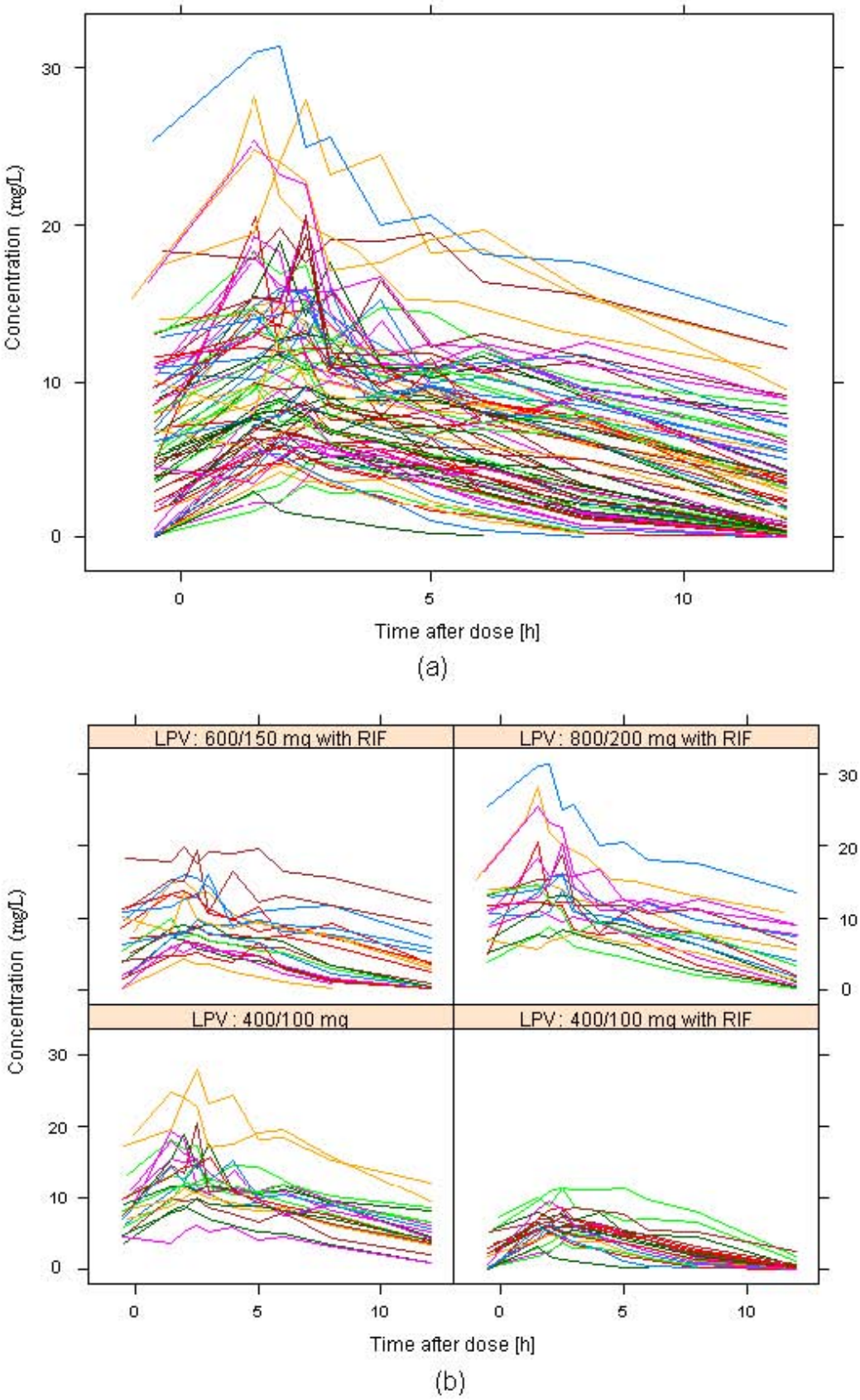

Figure 3.2.3. Plots of lopinavir concentrations vs. time after dose in total patients (a) and different occasions (b).

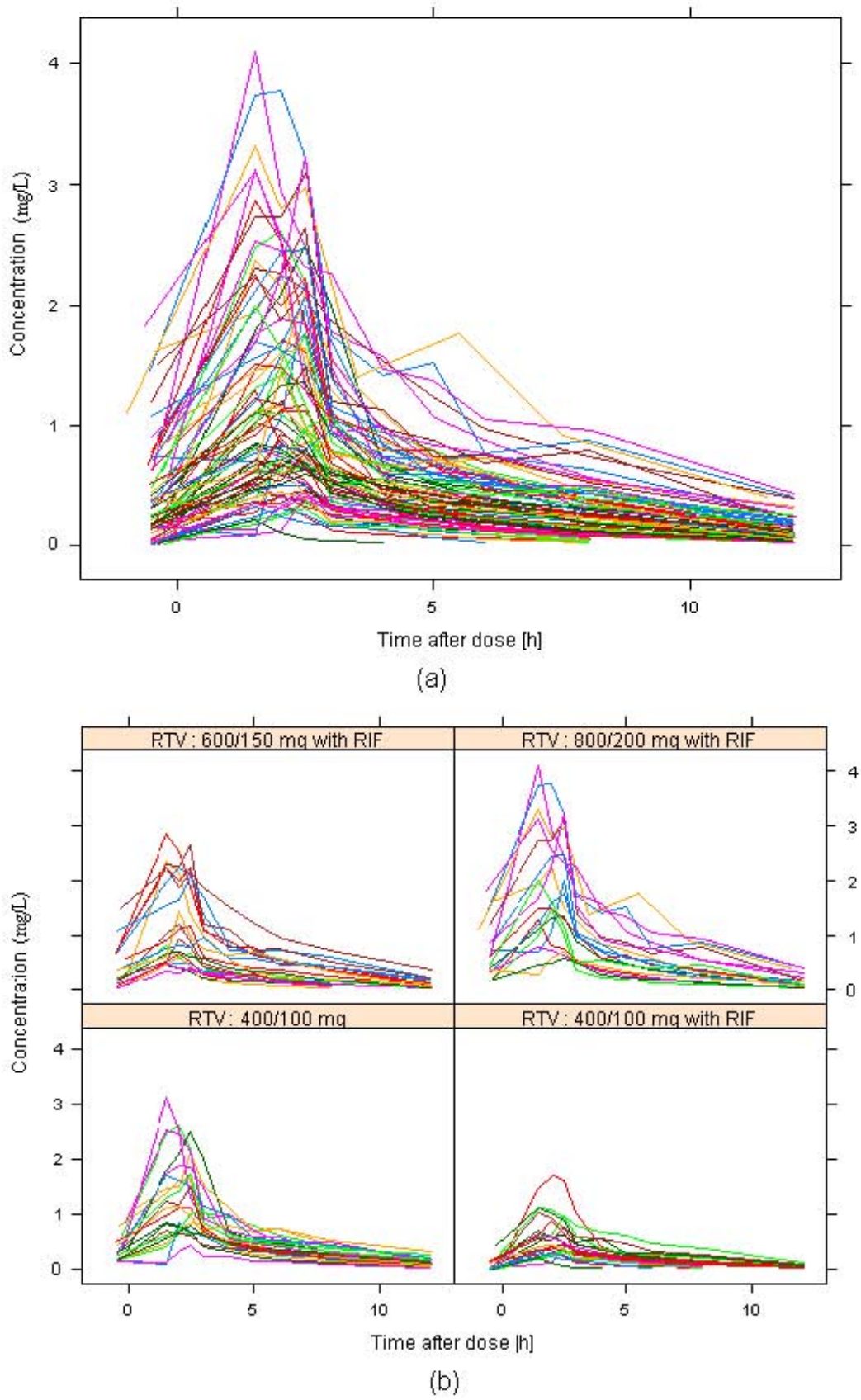

Figure 3.2.4. Plots of ritonavir concentrations vs. time after dose in total patients (a) and different occasions (b).

Table 3.2.2. Data descriptions of Paper II.

Data description	Characteristics
Patients status	HIV infected
Number of patients	21
Treatment	4 sequential treatments
Number of total samples	800
Dose strategy	PK1 (day 1 to 7): 400/100 mg lopinavir/ritonavir PK2 (day 8 to 14): 400/100 mg lopinavir/ritonavir + 600 mg rifampicin PK3 (day 15 to 21): 600/150 mg lopinavir/ritonavir + 600 mg rifampicin PK4 (day 22 to 28): 800/200 mg lopinavir/ritonavir + 600 mg rifampicin

2.2. Model description

2.2.1. Lopinavir separate model

A one-compartment model with first-order absorption and elimination best described the pharmacokinetics of lopinavir. Models with two-compartment disposition did not adequately improve the model fit, nor did zero-order absorption and the absorption with lag time fit the data. The absorption with transit compartments model also did not improve the model fit. The variability (IIV and IOV) in oral clearance, volume of distribution, bioavailability and k_a were tested in the model according to model development as described in the methods. The FOCE approach was used in the model building. IIV was found on clearance and volume, and IOV was found on ka and bioavailability. The residual error is implemented as a combined model: additive and proportional relationship. IIV was also found on the residual error in the separate lopinavir model.

Rifampicin effect was evaluated on the bioavailability and oral clearance of lopinavir as an on/off relationship since the rifampicin induction was assumed to achieve steady state. Compared to dosing without rifampicin treatment (assuming 100% as a reference), the relative bioavailability of lopinavir with rifampicin was estimated. Rifampicin was found to increase oral clearance of lopinavir by 61.4% and meanwhile, decrease bioavailability by 27.7%.

Table 3.2.3. Population pharmacokinetic parameter estimates of lopinavir separate model.

Parameter	Estimate (η shrinkage%)	RSE (%)
CL/F (L/h)	4.73	9.0
V/F (L)	45.7	8.9
RIF on CL	+ 61.4%	15.2
Relative bioavailability with RIF	72.3%	7.6
ka (h^{-1})	0.71	9.8
Additive error (mg/L)	0.685	8.4
Proportional error (%)	10.2	7.9
IIV on CL/F (%CV)	35.2 (28.4)	17.2
IIV on V/F (%CV)	31.5 (19.3)	21.2
IOV on F (%CV)	21.7 (10.1)	12.4
IOV on ka (%CV)	60.5 (37.7)	12.7
IIV on RUV (%CV)	23.4 (38.9)	23.8

CL: oral clearance; V: volume of distribution; F: bioavailability; RUV: residual unexplained variability; ka: oral absorption rate; RIF: rifampicin administration; IIV: interindividual variability; IOV: interoccasional variability.

Different covariates, including body weight, age, gender, haemoglobin, and ALT, were analyzed one by one according to the covariates model development

methodology as a continuous or discrete factor. Fat free mass was found having significant influence on the oral clearance, while total body weight on the volume of distribution of lopinavir with an allometric scaling relationship in the final model as in Equation 3.2.1 and Equation 3.2.2.

$$CL/F = CL/F_{STD} \cdot \left(\frac{FFM_i}{40}\right)^{0.75} \quad (3.2.1)$$

$$V/F = V/F_{STD} \cdot \left(\frac{WT_i}{65}\right)^{1} \quad (3.2.2)$$

where the *CL/F* is the apparent oral clearance, CL/F_{STD} is the apparent oral clearance of standard patient (with mean body weight or fat free mass), WT_i and FFM_i are each patient's body weight and fat free mass, respectively, and 65 kg and 40 kg are the median body weight and the median fat free mass in our population, respectively.

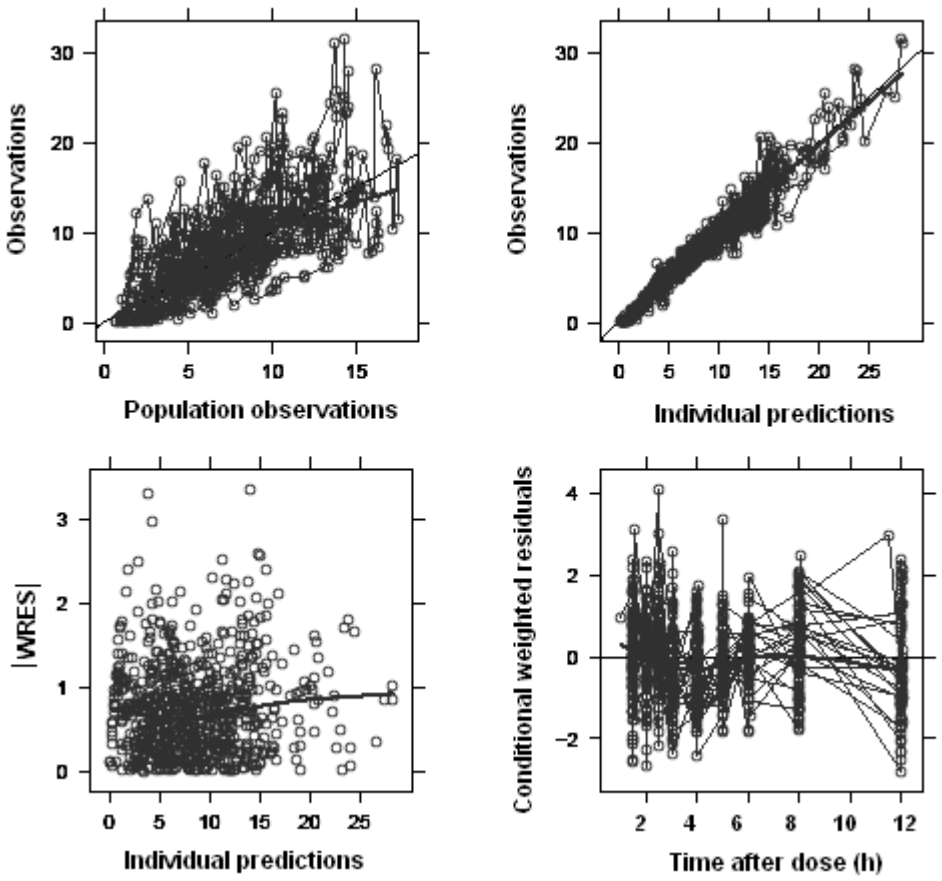

Figure 3.2.5. Goodness-fit-plots of final lopinavir separate model.

The oral clearance and volume of distribution were 4.73 L/h and 45.7 L, respectively. The IIV of clearance and volume were 35.2% and 31.5%, respectively. The IOV of relative bioavailability was 21.7%. The additive and proportional residual errors were 0.685 mg/L and 10.2%, respectively. The parameter estimates of lopinavir separate final model are shown in Table 3.2.3. The goodness-fit-plots are shown in Figure 3.2.5. VPC plots of lopinavir separate model are shown in Figure 3.2.6.

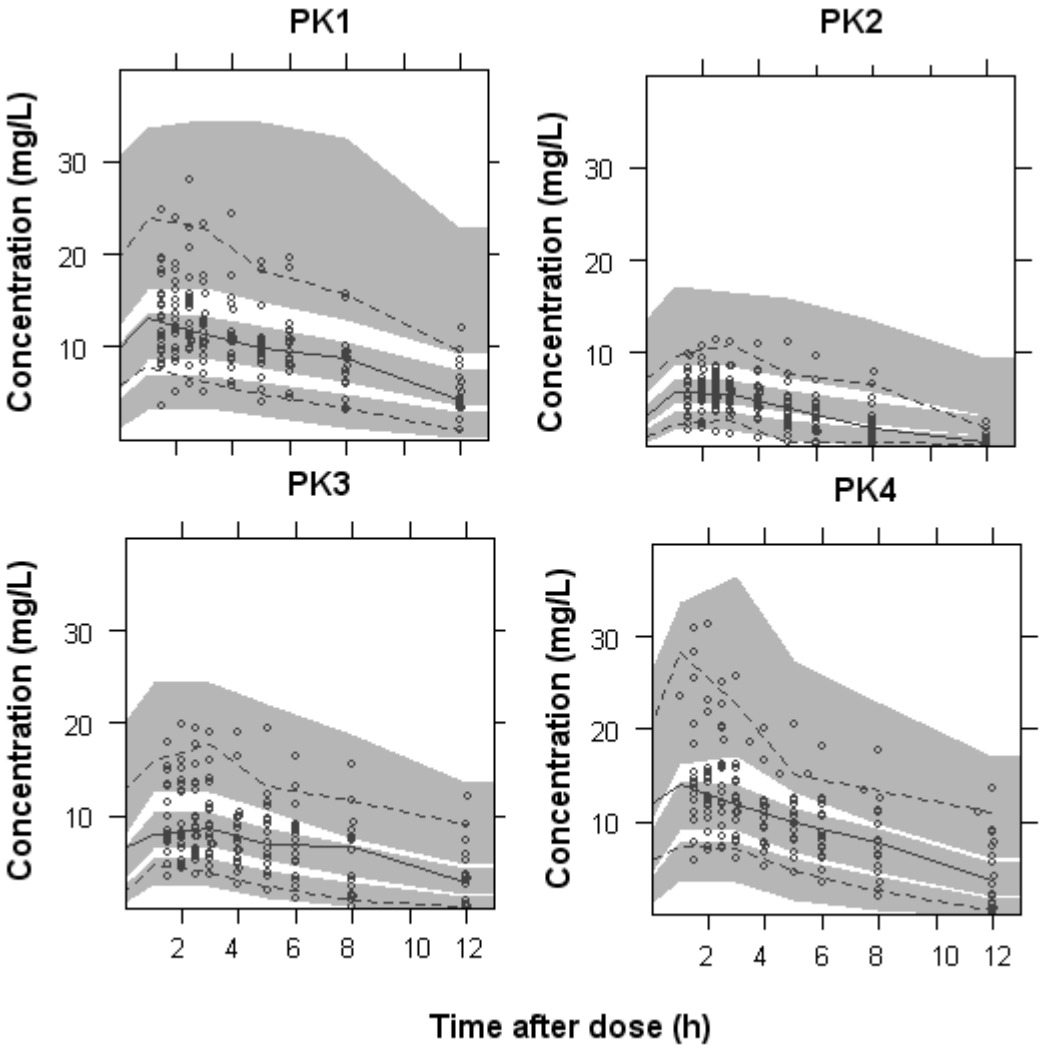

Figure 3.2.6. Visual predictive check (VPC) of the final lopinavir separate model stratified by different occasions. The solid line is the median of the observed data and the dotted lines are the 5th and 95th percentiles of the observed data. The shaded areas are the 95% confidence intervals for the median, 5th percentile and the 95th percentiles of the simulated data (n=1000). Observed concentrations are displayed as circles.

2.2.2. Ritonavir separate model

A two-compartment model with first-order elimination and a transit compartment absorption best described the pharmacokinetics of ritonavir. The structure of ritonavir separate model is shown in Figure 3.2.7. Model with zero-order absorption did not adequately fit the data. Transit compartment model was used to represent a more physiological delay in absorption onset and a gradual increase in absorption rate. The number of transit compartment was estimated 6.33 for the absorption model of ritonavir.

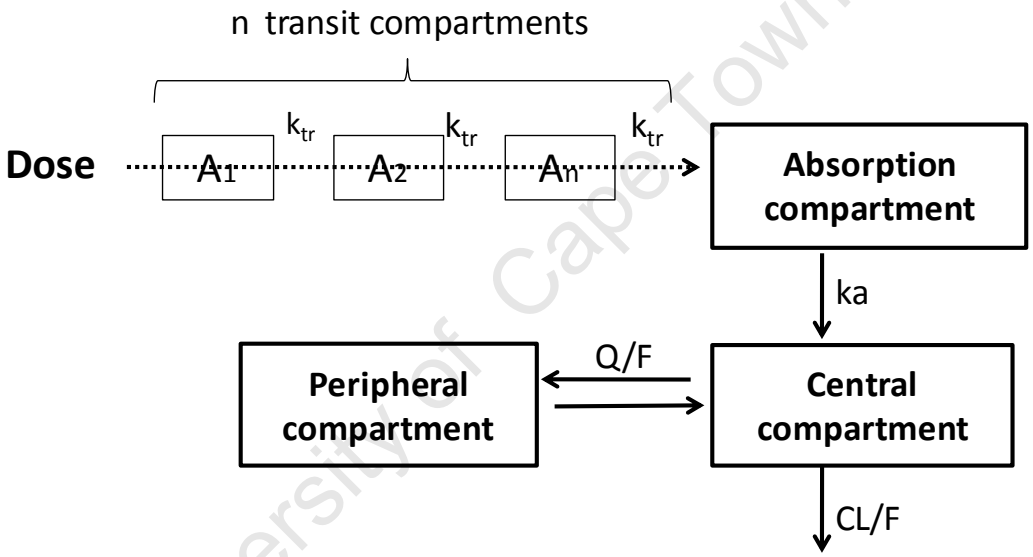

Figure 3.2.7 Structure of ritonavir separate model.

The variability (IIV and IOV) on oral clearance, volume of distribution, and k_a were tested according to model development methodology. FOCE approach was used in the model building. The residual error was implemented as a combined model: additive and proportional relationship. The additive residual error was estimated close to zero; therefore only proportional residual error was kept in the final model. IIV was found on the oral clearance and volume of distribution in the final model. IOV on bioavailability, MTT and clearance were found in the final model.

Rifampicin induction effect was evaluated on the bioavailability and oral clearance of ritonavir as an on/off relationship since the rifampicin induction was assumed to achieve steady state. Compared to dosing without rifampicin treatment (assuming 100% as a reference), the relative bioavailability of ritonavir with rifampicin was estimated. Rifampicin administration increased the clearance of ritonavir by about 22.7% and decreased the bioavailability of ritonavir by about 49.3%.

The bioavailability of ritonavir was found increased with increasing its dose. A linear relationship (Equation 3.2.4) was used to evaluate this kind of effect. The relative bioavailability of ritonavir was increased by 5.8% for each 10 mg increment of its dose.

$$F = F_{STD} \cdot (1 + SLP \cdot (DOSE_{RTV} - 100) \quad (3.2.3)$$

where F is bioavailability of ritonavir, F_{STD} is is the bioavailability of ritonavir when given 100 mg dose, SLP is the slope of linear relationship between bioavailability and dose, $DOSE_{RTV}$ is the dose of ritonavir would be given.

Different covariates, including body weight, age, gender, haemoglobin, and ALT, were analyzed one by one according to model covariates development steps as a continuous or discrete factor. Similar to lopinavir, allometric scaling of fat free mass on oral clearance and total body weight on volume of distribution were applied into the final separate model of ritonavir (Equation 3.2.2 and Equation 3.2.3). The OFV dropped about 22 points when this allometric scaling was introduced into the model.

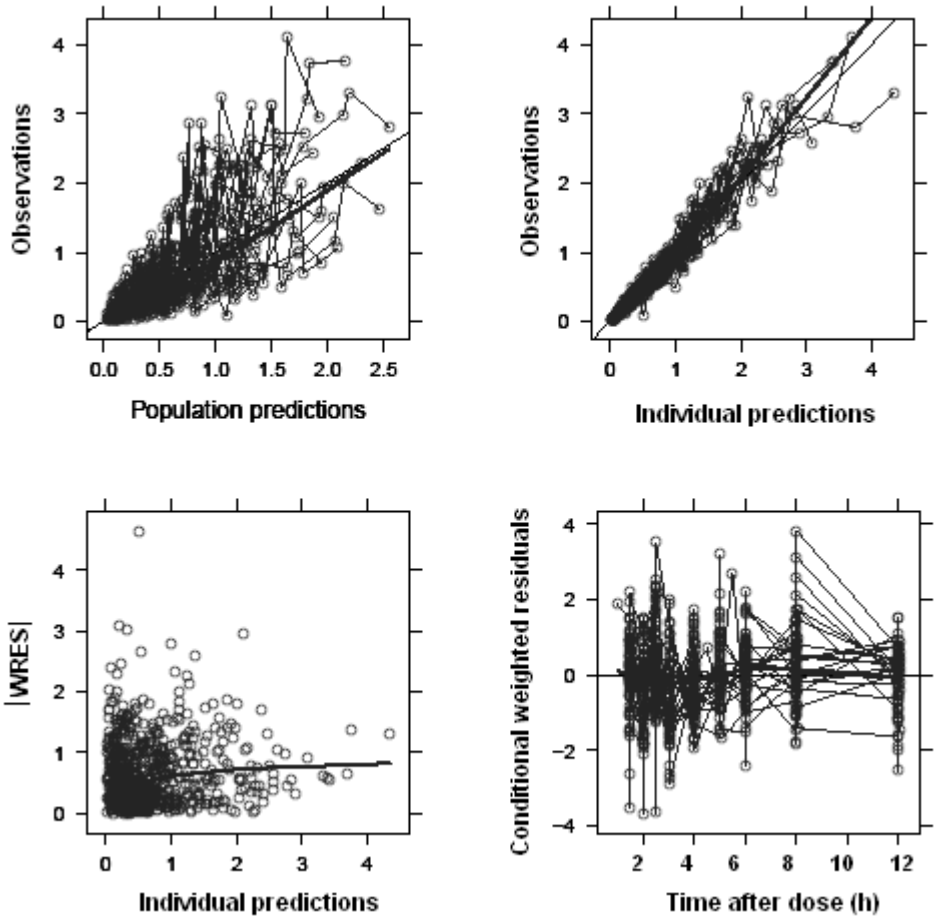

Figure 3.2.8. Goodness-fit-plots of final ritonavir separate model.

The central oral clearance of ritonavir without rifampicin effect was 18.6 L/h, whereas it was 22.9 L/h with rifampicin. The peripheral oral clearance was 33.3 L/h. The central and peripheral volume of distribution was 22.9 L and 48 L, respectively. The number of transit compartment was estimate as 6.33 and MTT was 1.43 h. The IIV of oral clearance and volume of distribution were 30.2% and 52.9%, respectively. The IOV of clearance and MTT were 16.1% and 16.9%, respectively. IOV of bioavailability was 37%. The proportional residual error was 18.1%. The parameter estimates of ritonavir separate final model are shown in Table 3.2.4. The goodness-fit-plots are shown in Figure 3.2.8. Visual prediction check of ritonavir separate model is shown in Figure 3.2.9.

Table 3.2.4. Population pharmacokinetic parameter estimates for ritonavir separate model (RSE% was not available).

Parameter	Estimate (ɳ shrinkage%)
CL/F (L/h)	18.6
Vc/F (L)	22.9
RIF on CL	+ 22.9%
Relative bioavailability with RIF	50.7%
Q/F (L/h)	33.3
Vp/F (L)	48
ka (h^{-1})	8.45
NN	6.33
MTT (h)	1.43
RTV dose on F	+ 5.8%/ 10 mg
Proportional error (%)	18.1
IIV on CL/F (%CV)	30.2 (12.8)
IIV on V/F (%CV)	52.9 (38.2)
IOV on F (%CV)	37 (25.1)
IOV on MTT (%CV)	16.9 (27.4)
IOV on CL (%CV)	16.1 (27.5)

CL: central oral clearance; Vc: central volume of distribution; Q: peripheral oral clearance; Vp: peripheral volume of distribution; F: bioavailability; ka: oral absorption rate; NN: number of transit compartment; MTT: mean transit time; RIF: rifampicin administration; IIV: interindividual variability; IOV: interoccasional variability.

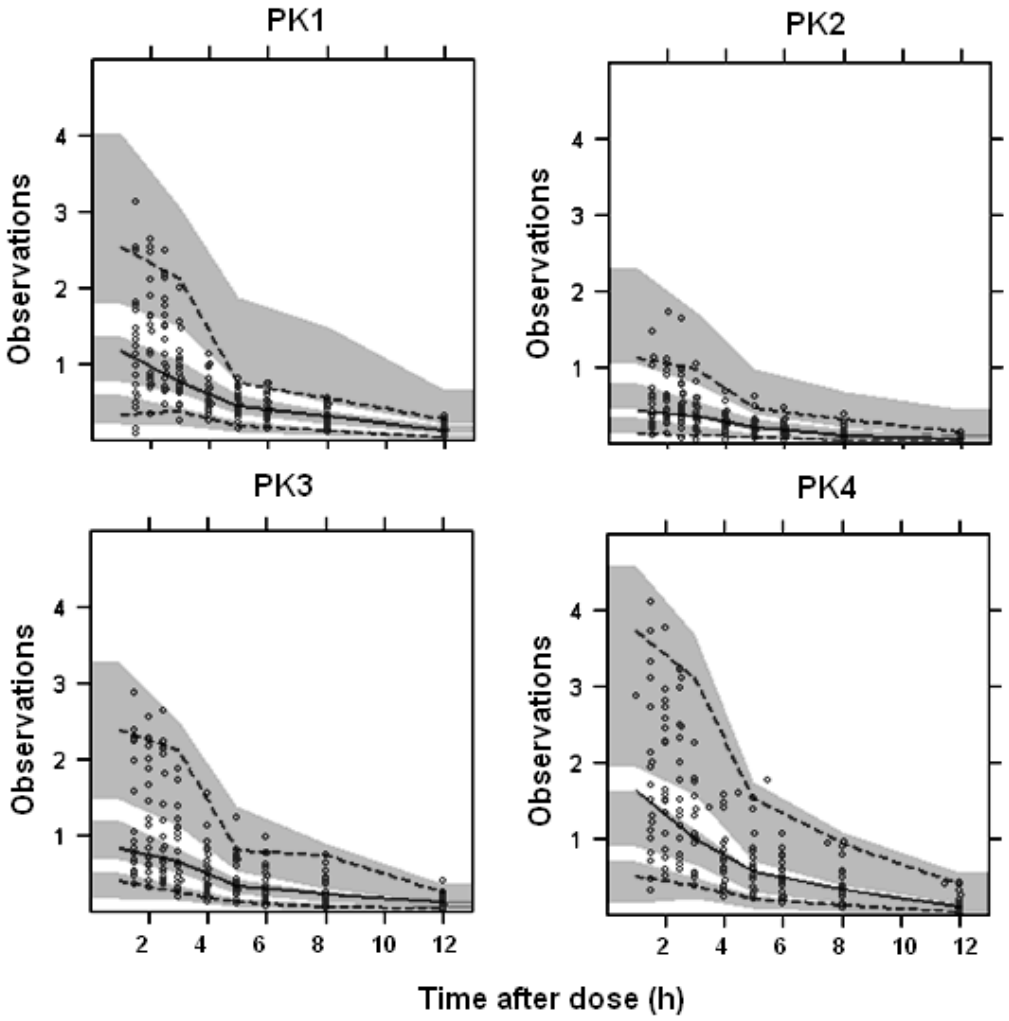

Figure 3.2.9. Visual predictive check (VPC) of the final ritonavir separate model stratified by different occasions. The solid line is the median of the observed data and the dotted lines are the 5th and 95th percentiles of the observed data. The shaded areas are the 95% confidence intervals for the median, 5th percentile and the 95th percentiles of the simulated data (n=1000). Observed concentrations are displayed as circles.

2.2.3. Integrated lopinavir-ritonavir model

The structure of the final integrated pharmacokinetic model is illustrated in Figure 3.2.10. A one-compartment model with first-order absorption and elimination best described the pharmacokinetics of lopinavir. For ritonavir, a two-compartment model was appropriate and a series of transit compartments was used to describe the complex kinetics in the absorption phase. IIV was supported in CL/F and V/F of both drugs, while IOV was characterized in absorption parameters (absorption

rate and absorption mean transit time), bioavailability, and to a lesser extent in CL/F.

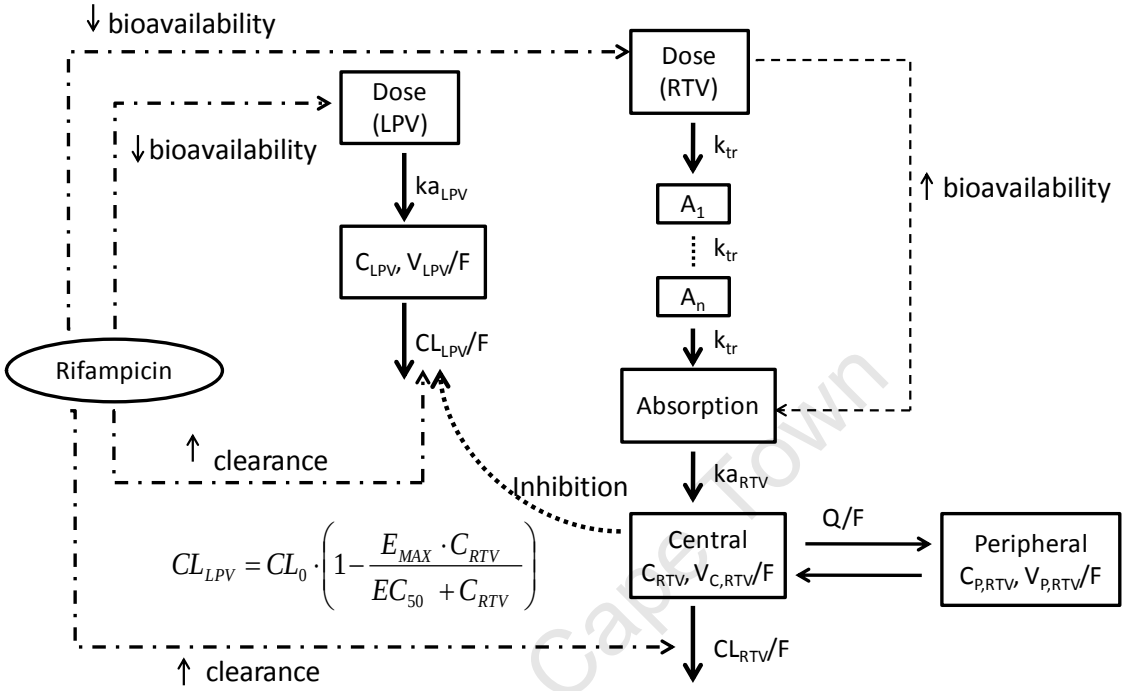

Figure 3.2.10. Structure of the final integrated lopinavir-ritonavir pharmacokinetic model. (LPV: lopinavir; RTV: ritonavir; MTT: mean transit time; CL/F: apparent oral clearance; V/F: apparent volume of distribution; k_a: absorption rate constant; k_{TR}: transit absorption rate constant; E_{max}: the maximum inhibition effect on lopinavir oral clearance by ritonavir; EC_{50}: the ritonavir concentration needed to reach half of E_{max}; *C*: concentration)

Rifampicin was found to increase the oral clearance of lopinavir and ritonavir by 71.0% and 36.0%, respectively. Rifampicin treatment also significantly reduced the bioavailability of both lopinavir and ritonavir, by 20.2% and 45.0%, respectively. The individual bioavailability, oral clearance and elimination rate of lopinavir and ritonavir influenced by rifampicin are shown in Figure 3.2.11 and Figure 3.2.12 respectively.

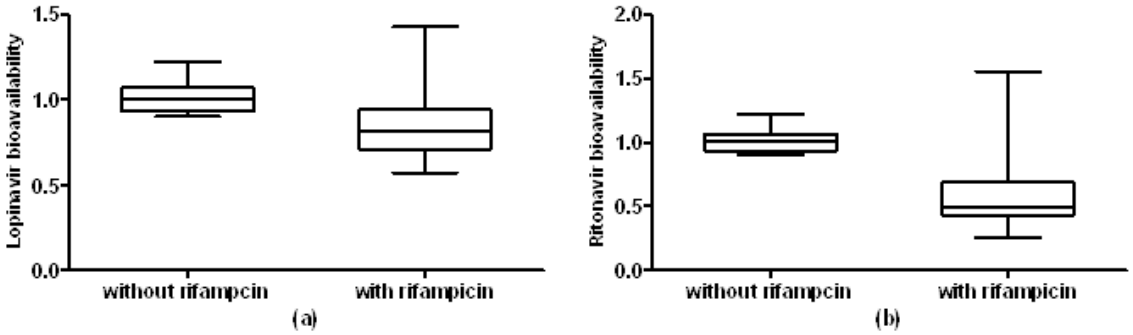

Figure 3.2.11. Individual bioavailability distributions of lopinavir (a) and ritonavir (b) influenced by rifampicin.

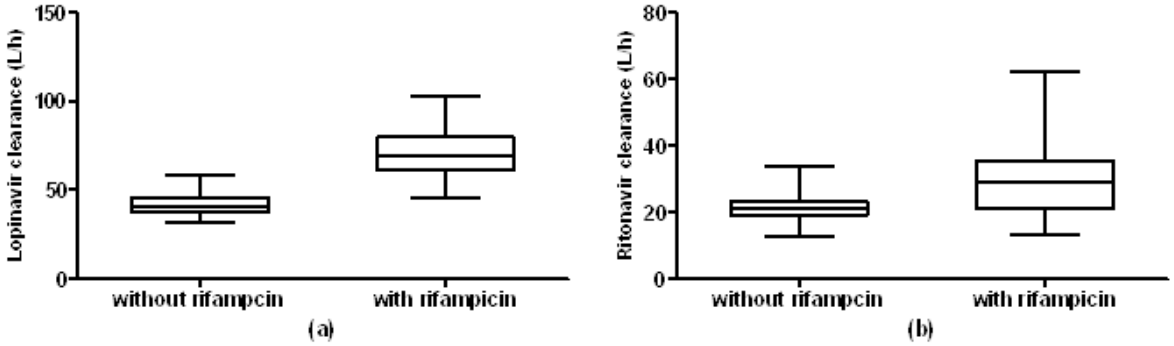

Figure 3.2.12. Individual oral clearance distributions of lopinavir (a) and ritonavir (b) influenced by rifampicin.

The bioavailability of ritonavir was found increased by its dose. A linear relationship (Equation 3.2.3) was used to evaluate this kind of effect. The relative bioavailability of ritonavir was increased by 5.8% for each 10 mg increment of its dose.

The bioavailability of ritonavir increased with increasing doses: when co-administered with rifampicin, the relative bioavailability of ritonavir increased by 8.1% for each 10 mg increment of dose. The individual bioavailability of ritonavir in different doses of lopinavir/ritonavir is shown in Figure 3.2.13.

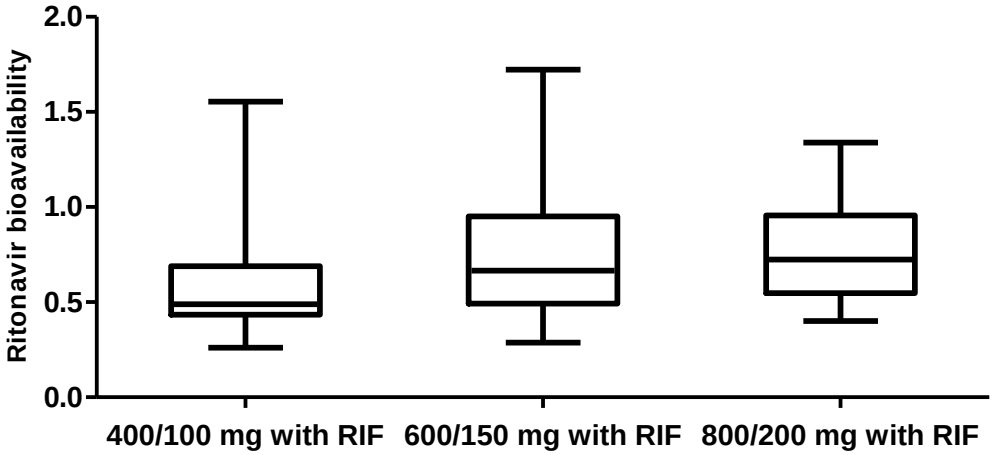

Figure 3.2.13. Individual bioavailability of ritonavir in different doses of lopinavir/ritonavir (RIF: rifampicin).

A different model was used to test the relationship between ritonavir concentrations and lopinavir clearance. Besides the direct interaction model, the presence of a delay in the onset of inhibition of lopinavir CL/F by ritonavir was tested using an indirect model. Finally, in the model, the oral clearance of lopinavir is influenced by ritonavir concentration, according to an E_{max} function (Equation 3.2.4). This dynamic interaction between ritonavir and lopinavir significantly improved the model fit (ΔOFV=-120, compared to the model no drug-drug interaction included). An indirect model describing delay of the interaction was not supported by the data. The maximum inhibition effect of ritonavir on lopinavir CL/F was 95%, and EC_{50} was estimated 0.04 mg/L. The model estimated oral clearance of lopinavir was 37.9 L/h when no ritonavir is present and the oral clearance of ritonavir was estimated 19.2 L/h.

$$CL_{LPV} = CL_0 \cdot \left(1 - \frac{E_{max} \cdot C_{RTV}}{EC_{50} + C_{RTV}}\right) \qquad (3.2.4)$$

where CL_0 is the CL/F of lopinavir when no ritonavir is present, E_{max} is the maximum inhibition effect of ritonavir by lopinavir, EC_{50} is the ritonavir concentration required to reach half of E_{max}, and C_{RTV} is the concentration of ritonavir.

The BQL data were few in the dataset, 1% of total data for lopinavir and 2% for ritonavir, and these data were set to LLOQ/2 (0.025 mg/L for lopinavir and 0.0125 mg/L for ritonavir) values in model building. In order to evaluate the accuracy of the prediction of BQL data, the bias between predicted and LLOQ values were calculated, in which LLOQ values 0.05 mg/L for lopinavir and 0.025 mg/L for ritonavir were used. The following equation was applied to evaluate the prediction accuracy of BQL data:

$$BQLA\ (\%) = \frac{\mathrm{BQLE} - \mathrm{LLOQ}}{\mathrm{LLOQ}} \qquad (3.2.5)$$

where BQLA is the accuracy of prediction for BQL data, BQLE is the individual estimate of BQL data by the final model, and LLOQ is the lowest limit of quantification. Figure 3.2.14 describes the accuracy of prediction for BQL data of lopinavir and ritonavir. The low BQLA indicates prediction of BQL data by our model are close to LLOQ value, which further proves minor bias related to exclusion BQL data during modeling building.

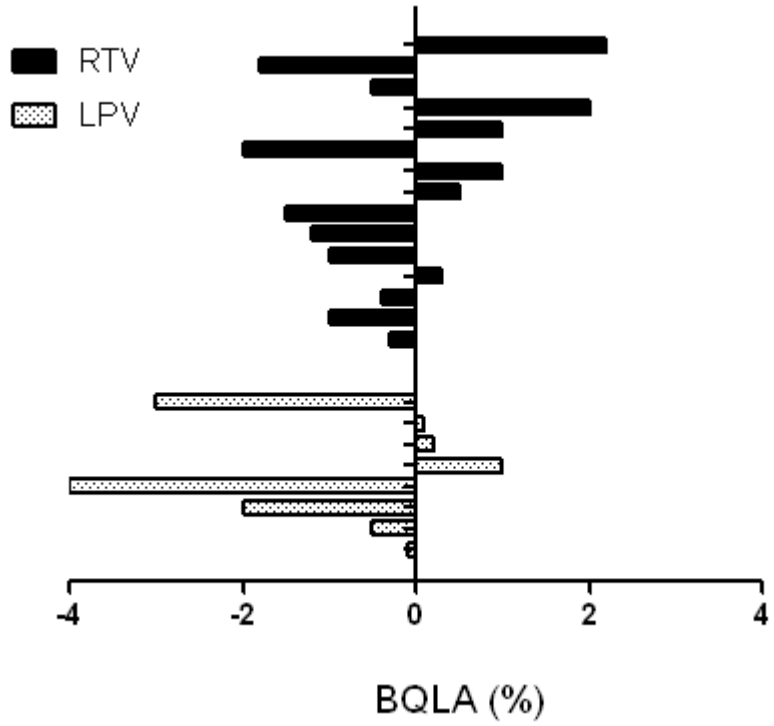

Figure 3.2.14 The prediction precisions of BQL data for lopinavir and ritonavir by the final model.

The typical clearance of lopinavir without ritonavir was 37.9 L/h, while it should be kept in mind that this value is an extrapolation, since lopinavir was never given without ritonavir. The number of transit compartment of ritonavir was estimate 2.03 in the integrated model. The maximum effect (E_{max}) of ritonavir concentration on lopinavir clearance was 95.3%, while EC_{50} was estimated 0.0351 mg/L. The population pharmacokinetic parameter estimates for the final combined model are shown in Table 3.2.5. All the parameters were estimated simultaneously. The diurnal variation distribution of individual bioavailability and oral clearance for lopinavir and ritonavir are presented in Figure 3.2.15 and Figure 3.2.16 respectively. The representative individual plots of lopinavir and ritonavir are presented in Figure 3.2.17.

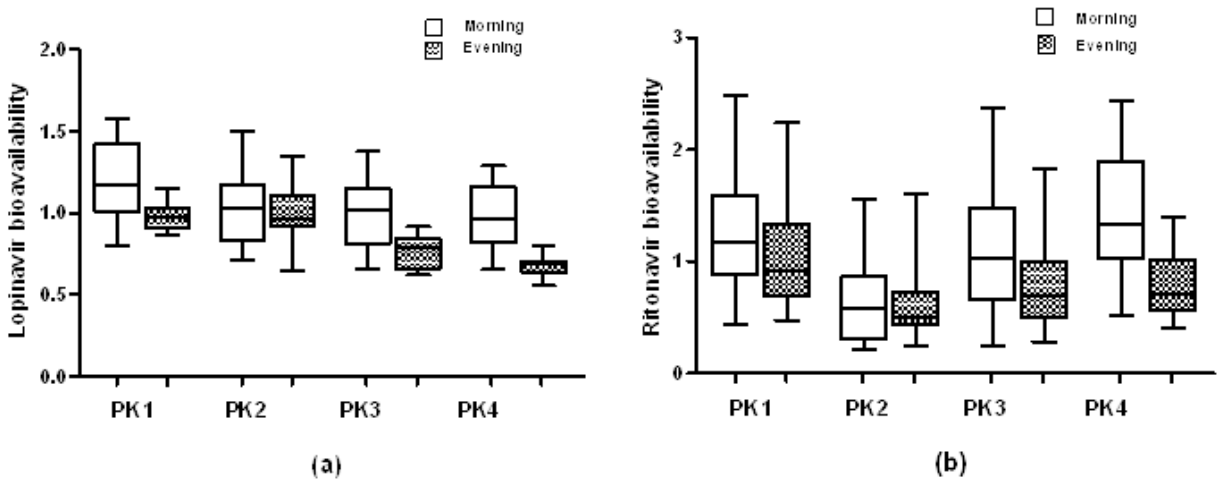

Figure 3.2.15. The diurnal variation distribution in individual bioavailability of lopinavir (a) and ritonavir (b).

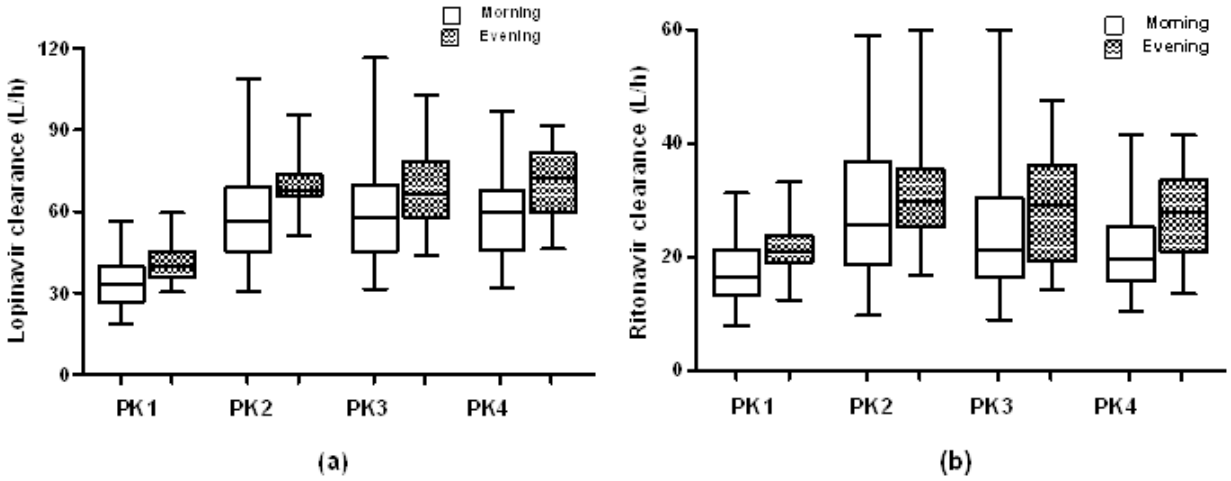

Figure 3.2.16. The diurnal variation distribution in individual oral clearance of lopinavir (a) and ritonavir (b).

Table 3.2.5. Population pharmacokinetic parameter estimates based on the final model of both lopinavir and ritonavir.

Parameters	Lopinavir		Ritonavir	
	Estimates (η shrinkage%)	**95% CI***	**Estimates** (η shrinkage%)	**95% CI***
CL/F (L/h)	37.9	28.5-52.1	19.2	18.4 - 22.2
RIF on CL/F (+)[#]	71.0%	65.7%-75.4%	36.0%	35.2% -40.0%
V_c/F (L)[1]	54.7	50.5 - 64.7	22.6	21.9 - 24.6
ka (h^{-1})	0.991	0.63 - 1.43	3.28	2.90 - 3.38
Relative bioavailability given with RIF	79.8%	75.7 - 84.7	55.0%	53.8% - 58.7%
Proportional error (%)	12.7	11.6 - 13.6	18.8	17.1 - 20.3
Evening effect on bioavailability (+)[#]	42.0%	38.0% - 48.2%	45.0%	41.4% - 53.6%
Evening effect on CL/F (-)[#]	32.7%	29.6% - 38.4%	32.7%	29.6% - 38.4%
Bioavailability/10 mg ritonavir(+)[##]			8.1%	5.7% - 11.2%
Intercompartmental clearance (Q/F) (L/h)			31.0	25.7 - 34.7
V_p/F (L)[2]			56.6	50.8 - 66.0
NN			2.03	1.83 - 2.37
MTT (h)			1.44	1.39 - 1.53
IIV CL/F (%CV)	20.2 (28.4)	12.7 - 25.1	21.5 (10.6)	11.5 - 31.7
IIV V/F (%CV)	27.2 (5.5)	10.3 - 41.4	10.2 (28.7)	9.85 - 10.5
IOV F (%CV)	21.9 (25.1)	17.1 - 24.0	30.3 (21.8)	24.1 - 40.7
IOV ka (%CV)	94.2 (41.7)	46.5 - 150.1		
IOV CL/F (%CV)	11.8 (36.4)	4.55 - 16.1	20.4 (27.5)	15.5 - 25.1
IOV RUV (%CV)	17.1 (38.3)	9.63 - 25.2		
IIV F (%CV)			30.3 (7.3)	17.4 - 49.6
IOV MTT (%CV)			27.9 (27.4)	19.6 - 38.2
Lopinavir-ritonavir interaction	**Estimates**	**95% CI***		
E_{max}	95.3%	94.5% - 96.3%		
EC_{50} (mg/L)	0.0351	0.0194-0.0438		

CL: central oral clearance; V_c: central volume of distribution; V_p: peripheral volume of distribution; F: bioavailability; RUV: residual unexplained variability; MTT: mean transit time; ka: oral absorption rate; IIV: interindividual variability; IOV: interoccasional variability; RIF: rifampicin; NN: number of transit compartment. [1] central volume of distribution; [2] peripheral volume of distribution;

[##] increase in bioavailability per every 10 mg ritonavir dose; [#](+)the effect is increased, (-) the effect is decreased; *CI: confidence intervals based on mean and SD from 10 bootstrap

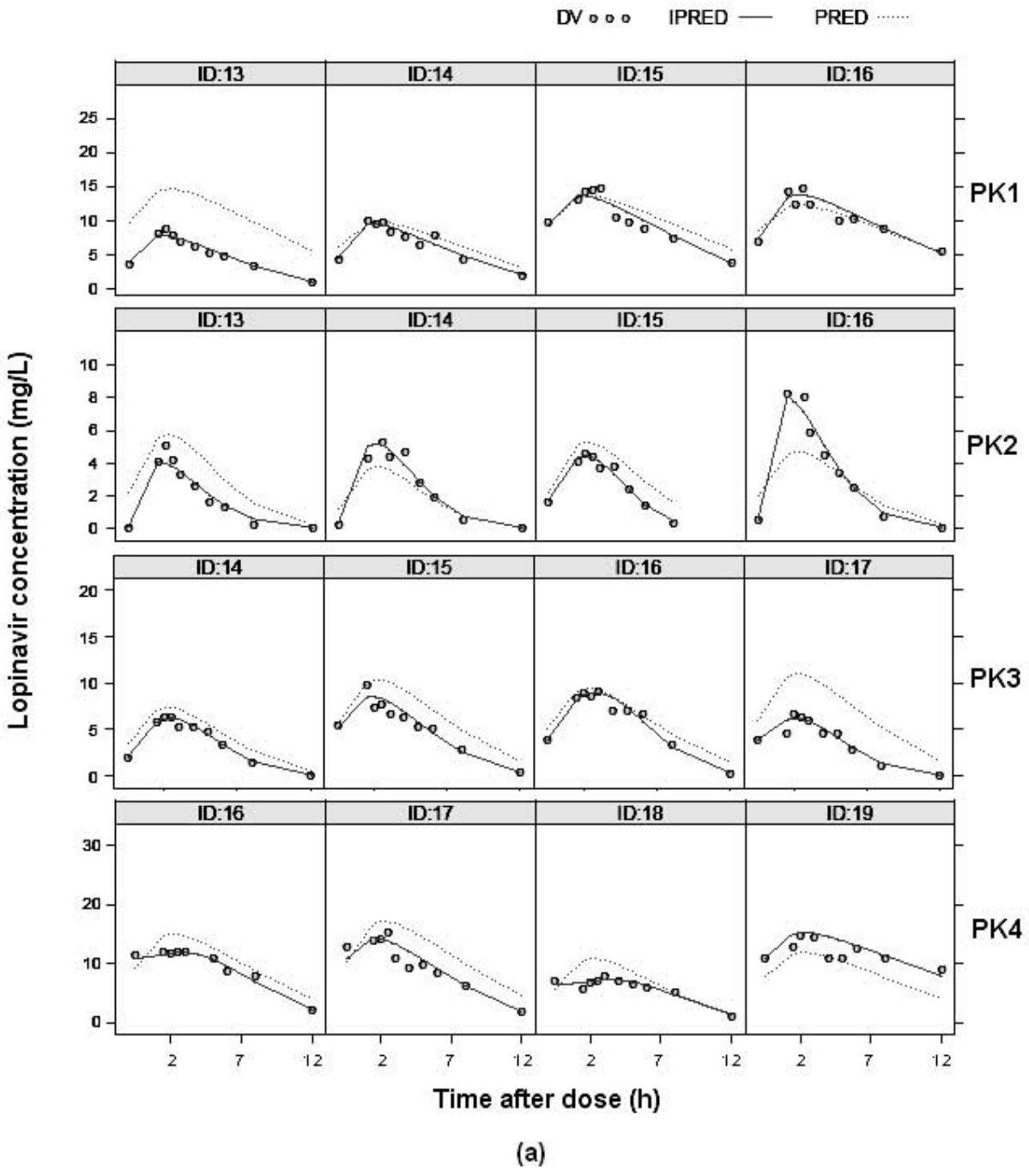

(a)

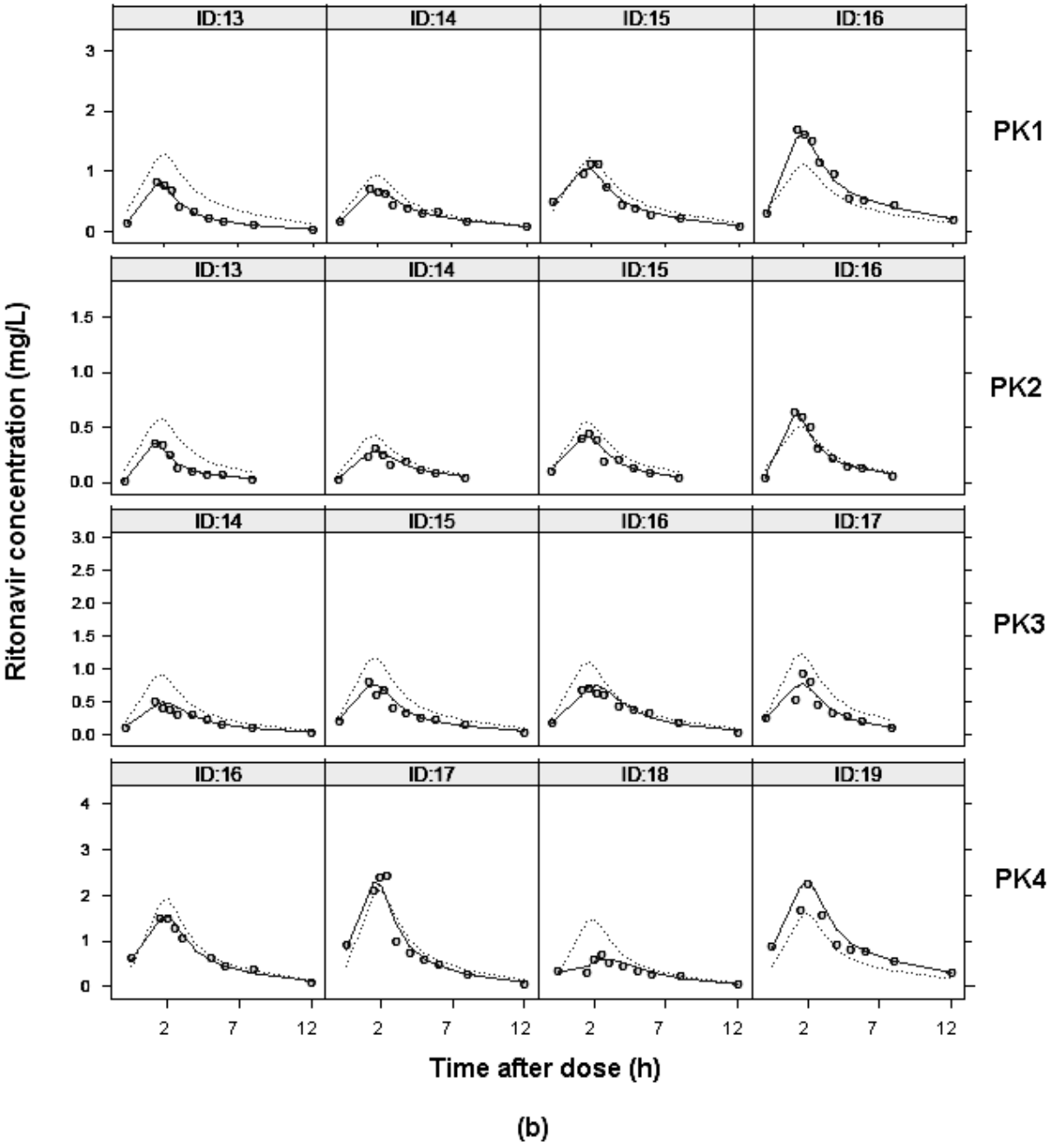

Figure 3.2.17. The representative individual plots of lopinavir (a) and ritonavir (b) (the solid line is the individual predictive data and the dotted line is the population predictive data and observed concentrations are displayed as circles).

2.3. Final model evaluation

Goodness of fit plots of final integrated model for lopinavir and ritonavir are shown in Figure 3.2.18. Figure 3.2.19 show VPC plots stratified by different occasions. The results of 1000 simulations from the final model demonstrated the

adequacy of the model and indicated that the model had good properties to investigate alternative dosing strategies using simulation. The bootstrap results (Table 3.2.5) confirmed the robustness of the final model.

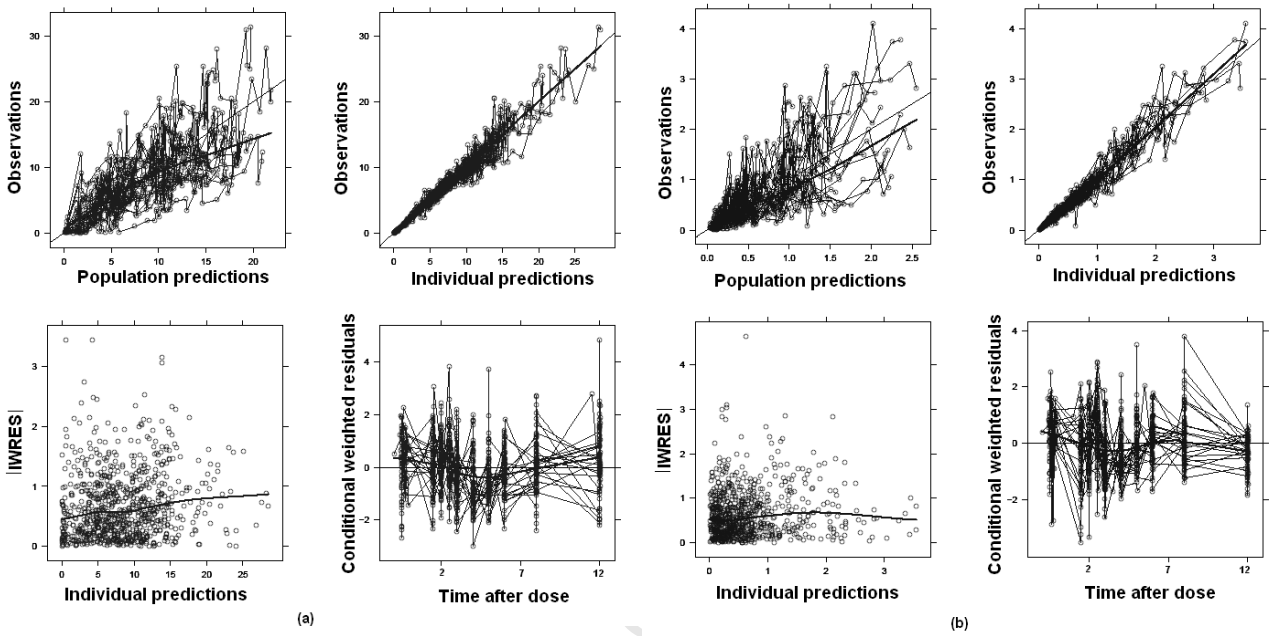

Figure 3.2.18. Goodness fit plots of final integrated model for lopinavir (a) and ritonavir (b) (the solid line is the individual predictive data and the dotted line is the population predictive data and observed concentrations are displayed as circles).

2.4. Simulation

The simulation predicted that 99.5% of the subjects given 800/200 mg LPV/r during rifampicin co-administration can achieve the lopinavir target concentrations ($\geq$1 mg/L) for C_0 (predose concentration), but only 77.9% of subjects for C_{12} (12 h concentration after dose). For patients with body weight <50kg, simulation indicated that 600/150 mg doses of LPV/r can achieve target C_0 in 95% of patients during rifampicin co-administration. An 800/200 mg dose of LPV/r was sufficient for patients weighing > 110 kg (95% achieve $C_0 \geq 1$ mg/L during rifampicin co-administration).

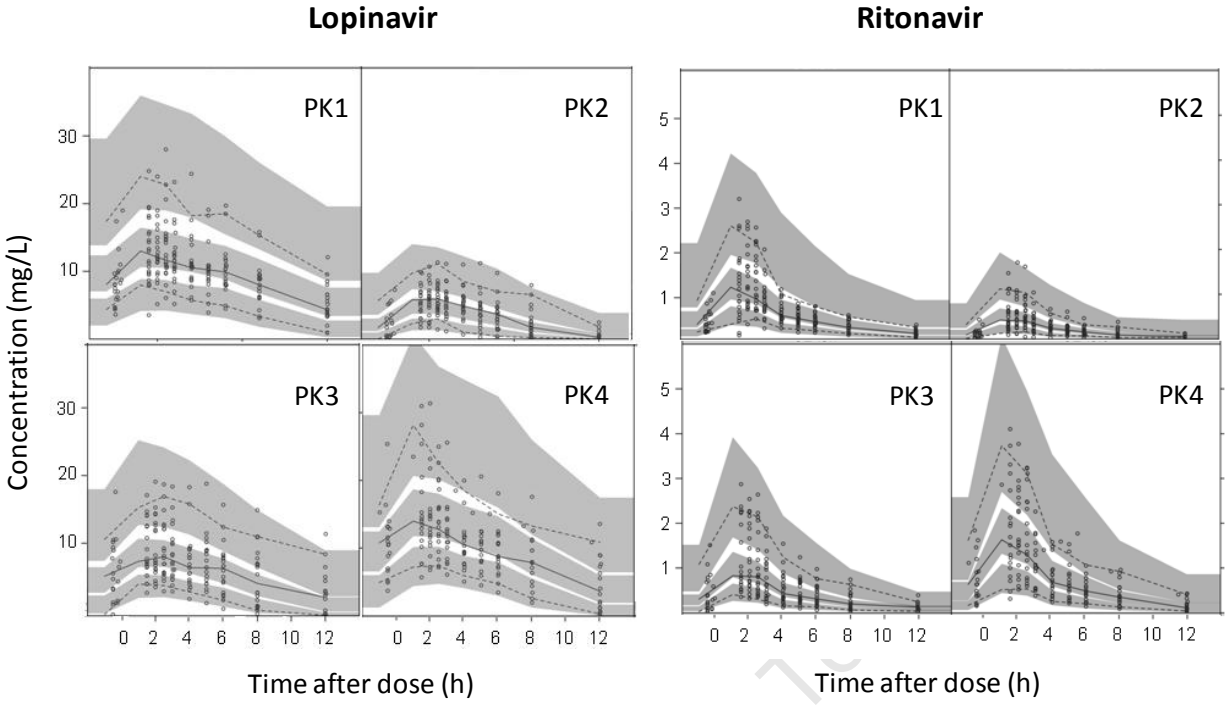

Figure 3.2.19. Visual predictive check (VPC) of the final combined model for lopinavir (left panel) and ritonavir (right panel) stratified by occasion (PK1-PK4). The solid line is the median of the observed data and the dotted lines are the 5th and 95th percentiles of the observed data. The grey shaded areas are the 95% confidence intervals for the median, 5th percentile and the 95th percentiles of the simulated data (n=1000). Observed concentrations are displayed as circles.

3. Results (Paper III)

3.1. Patients and data description

Ninety-five patients were involved in this pooled study. A total of 1226 steady-state concentrations of lopinavir and ritonavir were available in this study. As mentioned before, the intensive sampling approach was conducted in the adult study, but for children, both intensive and sparse sampling approaches were used. The data descriptions are summarized in Table 3.3.1. BQL data were set to LLOQ/2 values (0.025 mg/L for lopinavir and 0.0125 mg/L for ritonavir). The standard dose of lopinavir and ritonavir without rifampicin for children and adults is presented in Figure 3.3.1. The doses of lopinavir and ritonavir actually received by children in different dose strategies are presented in Figure 3.3.2.

Table 3.3.1. Data descriptions of the combined dataset in this study.

	Children	Adults
Patients status	HIV or HIV/TB	HIV
Number of patients	74	21
Number of samples	426	800
Gender (male/female)	34/40	3/18
Age (range)	6 months – 4.5 years	26 – 58 years
Body weight (median, kg)	10.2 (5.0 -17.0)	64.5 (43.0 -110.0)
Lopinavir median dose no RIF (mg/kg)	12.0 (9.2 -16.0)	6.0 (3.6 -9.0)
Ritonavir median dose no RIF (mg/kg)	2.9 (2.3 - 4.0)	1.5 (0.9 – 2.5)

TB: tuberculosis; RIF: rifampicin-based antituberculosis treatment.

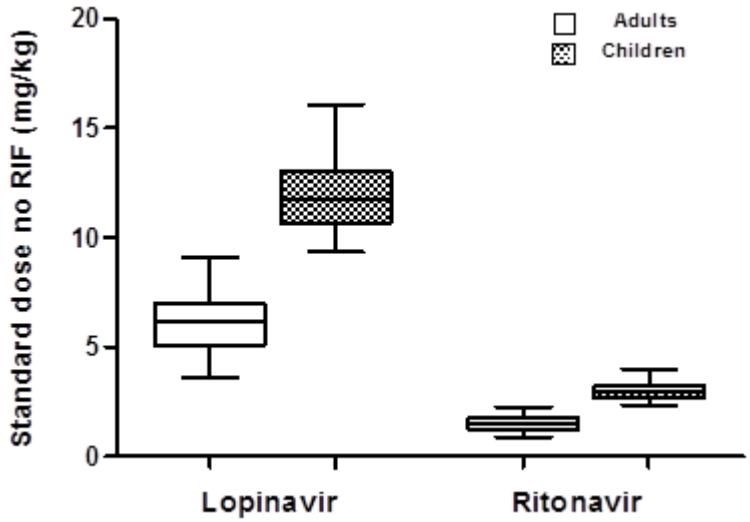

Figure 3.3.1. The standard doses of lopinavir and ritonavir without rifampicin-based ATT for children and adults.

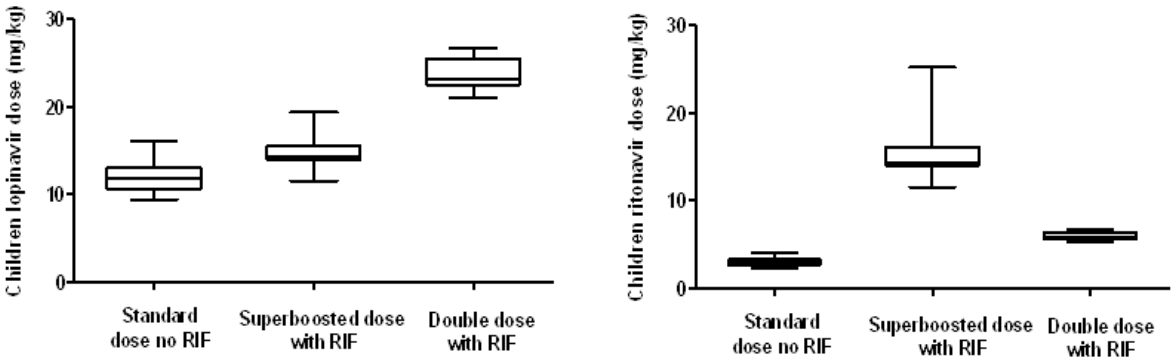

Figure 3.3.2. The doses of lopinavir and ritonavir actually received by children in different dose strategies (RIF: rifampicin-based antituberculosis treatment).

3.2. Model development

3.2.1. Summary of model characteristics of children and adults

The structure model of lopinavir is a one-compartment with the first-order elimination for both children and adults. For ritonavir, a one-compartment model was used for children, but a two-compartment model fitted the adult data, and a transit absorption model was used for both children and adults to describe the delay characteristics of the drug absorption. Allometric scaling of body size was applied on the oral clearance and volume of distribution for both children and adults. The dose strategy of lopinavir and ritonavir in children included different ratios: 1:1 and 4:1. For adults, lopinavir and ritonavir was given as the same ratio of 4:1, but with sequential increased doses. With increase of concentration of ritonavir, the oral clearance of lopinavir decreased in a sigmoid relationship for both children and adults. In children, rifampicin induction effect was found a significant reduction in the bioavailability of lopinavir, and meanwhile it increased the oral clearance of ritonavir. While in adults, this effect was found significant on the bioavailability and oral clearance for both lopinavir and ritonavir. When ritonavir dose increased, the bioavailability was found significant increased for lopinavir in children and for ritonavir in adults. The comparisons of population

pharmacokinetic differences between the built model of children and adults are summarized in Table 3.3.2.

Table 3.3.2. Comparisons of built population pharmacokinetic model between children and adults.

Items	Adult model	Children model
Model structure	One-compartment model for lopinavir; two-compartment model for ritonavir	One-compartment for lopinavir; one-compartment model for ritonavir
Rifampicin induction effect	Lopinavir F and CL; Ritonavir F and CL	Lopinavir F; Ritonavir CL
Ritonavir dose effect	Ritonavir F	Lopinavir F
Allometric scaling	FFM for CL and WT for V	WT for CL and V
Sampling approach	Intensive	Some intensive, some sparse
Doses for lopinavir:ritonavir	4:1; 6:1.5; 8:2	4:1; 4:4; 8:2

F: bioavailability; CL: clearance; V: volume of distribution; FFM: fat free mass; WT: body weight.

3.2.2. Integrated lopinavir-ritonavir model using combined dataset for children and adults

The lopinavir and ritonavir model was integrated as the final model using combined dataset of children and adults. All pharmacokinetic parameters of children and adults were estimated simultaneously. As described before, a sigmoid model was used to capture the dynamic effect of ritonavir concentration on the oral clearance of lopinavir. The model structure is shown in Figure 3.3.3. A one-compartment with the first-order elimination model was used for lopinavir and a two-compartment with transit absorption model was used for ritonavir. IIV and IOV were kept the same as the separate model of lopinavir and ritonavir using the combined dataset of children and adults.

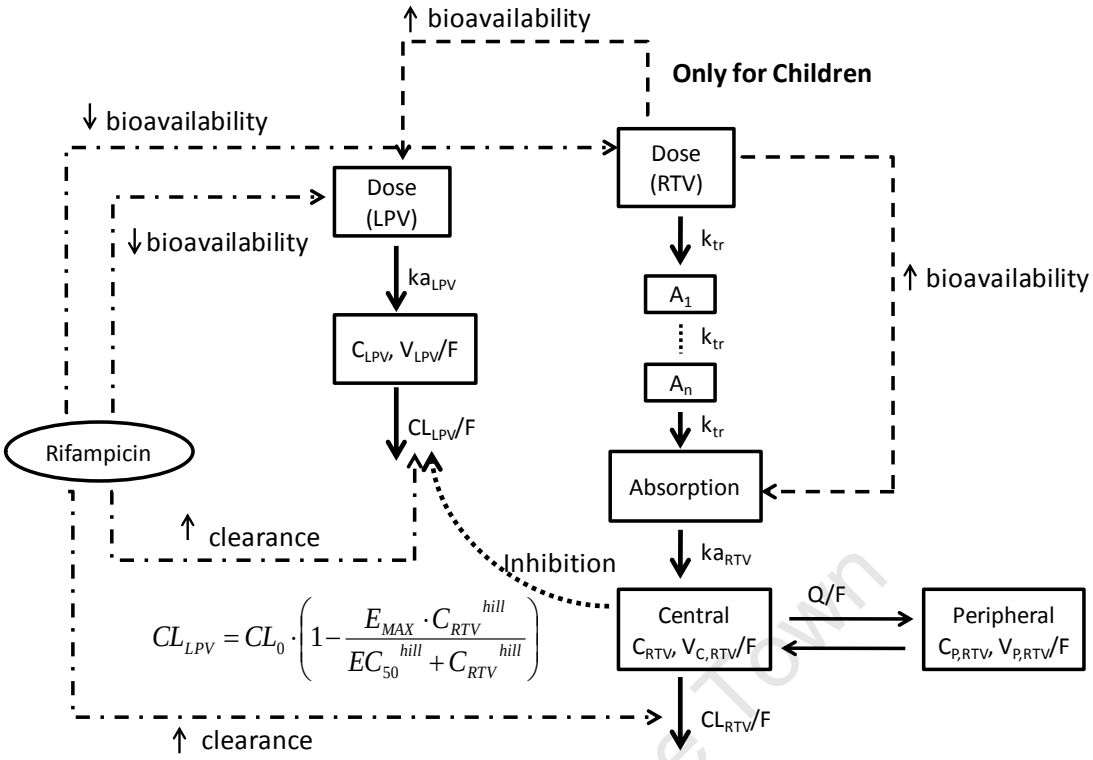

Figure 3.3.3. Structure of the final integrated lopinavir-ritonavir pharmacokinetic model. (LPV: lopinavir; RTV: ritonavir; MTT: mean transit time; CL/F: apparent oral clearance; V/F: apparent volume of distribution; k_a: absorption rate constant; k_{TR}: transit absorption rate constant; E_{max}: the maximum inhibition effect on lopinavir oral clearance by ritonavir; EC_{50}: the ritonavir concentration needed to reach half of E_{max}; *C*: concentration; *hill*: shape factor)

Allometric scaling of body weight on the oral clearance and volume of distribution in both central and peripheral compartments were applied for lopinavir and ritonavir. The follow equations were used in the combined dataset of this study:

$$CL/F \quad = CL/F_{STD} \cdot \left(\frac{WT_i}{65}\right)^{0.75} \qquad (3.3.1)$$

$$V/F \quad = V/F_{STD} \cdot \left(\frac{WT_i}{65}\right)^{1} \qquad (3.3.2)$$

where the *CL/F* and *V/F* are the apparent oral clearance and the apparent volume of distribution respectively; CL/F_{STD} and V/F_{STD} are the apparent oral clearance of standard patient (with median body weight), respectively; WT_i is each patient's body weight, and 65 kg is the median body weight of adult population.

Since no intra-venous dosing data were available, estimating absolute bioavailability was not possible. Thus, the relative bioavailability of lopinavir and ritonavir was fixed to the reference value of 1 for adults without rifampicin co-treatment, and the other values are reported as compared to this reference. In children given the median 2.9 mg/kg dose of ritonavir without rifampicin, the relative bioavailability of lopinavir was estimated to be 0.787 of that in the adults and the relative bioavailability of ritonavir 0.245. Rifampicin decreased the bioavailability of lopinavir and ritonavir: for adults and children respectively, the bioavailability of lopinavir was reduced to 0.753 and 0.325 of the bioavailability in adults without concomitant rifampicin; and the bioavailability of ritonavir was reduced to 0.482 in adults and 0.021 in children. Meanwhile, rifampicin increased CL/F of lopinavir by 57.7% in adults and 47.6% in children, and the CL/F of ritonavir by 33.7% and 22.0% for adults and children respectively. The rifampicin effect was also tested to be altered according to body size, but it was not supported by our data. Addition of a maturation model was also not supported by the data. Diurnal variation was included into the model on the oral clearance and bioavailability with a linear relationship to indicate how much diruanal effect to decrease oral clearance and increase bioavailability for both children and adults.

In the final integrated model, the relative bioavailability of lopinavir in children increased by 0.019 for every 1 mg/kg increment in the dose of ritonavir. However, in adults the dose of ritonavir was not found to affect lopinavir's bioavailability. The bioavailability of ritonavir increased by 0.464 and 0.026 in adults and children respectively, for every 1 mg/kg increment in the dose of ritonavir. The following equations were used for lopinavir and ritonavir:

$$F_{LPV} = BIO_{LPV} + SLP_{LPV} \cdot (\mathrm{Dose}_{RTV} - Dose_{RTV-STD}) \quad (3.3.3)$$

$$F_{RTV} = BIOP_{RTV} + SLP_{RTV} \cdot (\mathrm{Dose}_{RTV} - Dose_{RTV-STD}) \quad (3.3.4)$$

where F_{LPV} and F_{RTV} are the typical value of the bioavailability of lopinavir and

ritonavir respectively; BIO_{LPV} and BIO_{RTV} are the typical value of bioavailability for the standard dose of ritonavir (which changes in children and adults); $Dose_{RTV}$ and $Dose_{RTV\text{-}STD}$ denote the individual dose of ritonavir (mg/kg) and the median ritonavir dose given without rifampicin co-administration (1.5 mg/kg for adult and 2.9 mg/kg for children), respectively. BIO_{LPV} and BIO_{RTV} have been fixed to 1 for adults without rifampicin co-treatment, while the values for adults with rifampicin and for children with and without rifampicin are estimated. The linear relationship between F and ritonavir dose is described by the parameter SLP_{LPV} and SLP_{RTV} for lopinavir and ritonavir respectively.

Allometric scaling was used to account for size differences, and the typical value of the CL and V parameters was thus estimated for an individual of 65 kg, the median weight in our adult population. After adjusting for body weight with allometric scaling, the typical value for CL/F/ of lopinavir in children was 33.8% lower than that in adults. This value refers to lopinavir CL in absence of ritonavir and is as such extrapolated from the model. It does not include the inhibitory effect of ritonavir, which is captured separately. For ritonavir, the typical value for CL/F was about 39% lower in children (13.3 L/h) than in adults (21.7 L/h). Rifampicin therapy in administered doses increased CL/F of lopinavir by 57.7% in adults and 47.6% in children, and the CL/F of ritonavir by 33.7% and 22.0% for adults and children respectively. The addition of a maturation model to account for CL changes with age was not supported by the data. The correlations between lopinavir and ritonavir in IOV of bioavailability and clearance were 87.3% and 100% respectively the IIV correlation between bioavailabilities for the two drugs was 82.4%.

The absorption parameters also differed in children and adults: absorption half-life was 0.6 h and 1.8 h in adults and children respectively; and MTT for ritonavir was shorter in adults (1.09 h) than in children (2.23 h). Simulation indicated that the

maximal concentration occurs much later in children than in adults, of which 3.9 h after dosing for children compared to 2.5 h after dosing for adults. All parameters were estimated simultaneously. The parameter estimates are presented in Table 3.3.3. The relative bioavailability of lopinavir and ritonavir predicted by our model for children on the different dosing strategies (standard, super-boosted, and double dose) with the median doses actually received is shown in Table 3.3.4. The AUC of lopinavir and ritonavir predicted by our model for adults and children are shown in Figure 3.3.4. In children, compared to adults, the relative bioavailability of ritonavir was estimated 0.245 when the standard dose was given without rifampicin. Meanwhile, the clearance of ritonavir of children was estimated about 39% of that of adults. The median of ritonavir concentrations for children and adults when standard dose was given without rifampicin were 0.237 mg/L and 0.527 mg/L respectively. The ritonavir concentrations when standard dose was given without rifampicin for adults and children are shown in Figure 3.3.5.

Table 3.3.3. Parameter estimates of final integrated lopinavir-ritonavir model using combined dataset of children and adults. (The values in parentheses are RSE% obtained from 50 samples of bootstrap results; the values in square bracket are η shrinkage)

Parameters	Lopinavir		Ritonavir	
	Adults	**Children**	**Adults**	**Children**
CL/F (L/h)	23.1(14.5)	15.3 (25.2)	21.7 (6.0)	13.3 (12.3)
V/F (L)	56.8 (7.0)		38.8 (18.2)	
ka (1/h)	1.12 (14.1)	0.376 (21.4)	2.34 (16.8)	
Bioavailability no RIF #	1 fix	0.787 (15.9)	1 fix	0.245 (16.3)
Bioavailability with RIF #	0.753 (6.5)	0.325 (27.2)	0.482 (11.1)	0.021 (25.7)
RIF on CL/F (+)*	57.7% (17.9)	47.6% (14.8)	33.7% (19.1)	22.0% (24.3)
Slope of RTV dose effect on bioavailability**	0	0.0188 (30.6)	0.464 (12.7)	0.0259 (25.6)
Additive error (mg/L)	0.0535 (14.3)			
Proportional error (%)	13.2 (5.9)		21.1 (7.2)	
Evening effect on clearance (-)	51.4% (5.4)	27.3% (6.4)	51.4% (5.4)	27.3% (6.4)
Evening effect on bioavailability (+)	19% (3.6)			
MTT (h)			1.09 (14.5)	2.23 (12.9)
Q/F (L/h)			29.6 (13.3)	
V_p/F (L)			52.7 (11.1)	
IIV CL/F (%CV)	22.2 (39.8) [36]		26.1 (19.9) [25.7]	
IIV V/F (%CV)	22.2 (45.4) [44.4]			
IOV CL/F (%CV)	18.2 (24.8) [24.3]		18.2 (24.8) [25.3]	
IOV ka (%CV)	68.4 (28.2) [47.2]			
IIV F (%CV)	26.3 (27.3) [25.9]		64.5 (15.4) [13.3]	
IOV F (%CV)	28.0 (21.9) [28.8]		42.5 (14.8) [28.9]	
IOV MTT (%CV)			39.0 (16.4) [19.3]	
Lopinavir-ritonavir interaction				
E_{max}	0.821 (3.7)			
EC_{50} (mg/L)	0.0983 (17.4)			
Hill	2.76 (19.6)			
Correlation between lopinavir and ritonavir				
IOV F 87.3% (16.7)	IOV CL/F 100% fix		IIV F 82.4% (28.1)	

CL/F: apparent central oral clearance; V_c/F: apparent central volume of distribution; Q/F: apparent peripheral oral clearance of ritonavir; V_p/F: apparent peripheral volume of distribution; MTT: mean transit time; RIF: rifampicin; IIV: interindividual variability; IOV: interoccasion variability; E_{max}: maximum of ritonavir concentration effect on clearance of lopinavir; EC_{50}: the concentration of

ritonavir when half E_{max} is achieved; Hill: shape factor. [#] the median dose of 1.5 mg/kg and 2.9 mg/kg of ritonavir for adults and children respectively was considered to report these values; [*]rifampicin increases the apparent clearance of ritonavir. [**]$F = 1 + SLP \cdot (Dose_{RTV} - Dose_{RTV-STD})$; clearance and volume are estimated using allometric scaling for an individual of 65 kg.

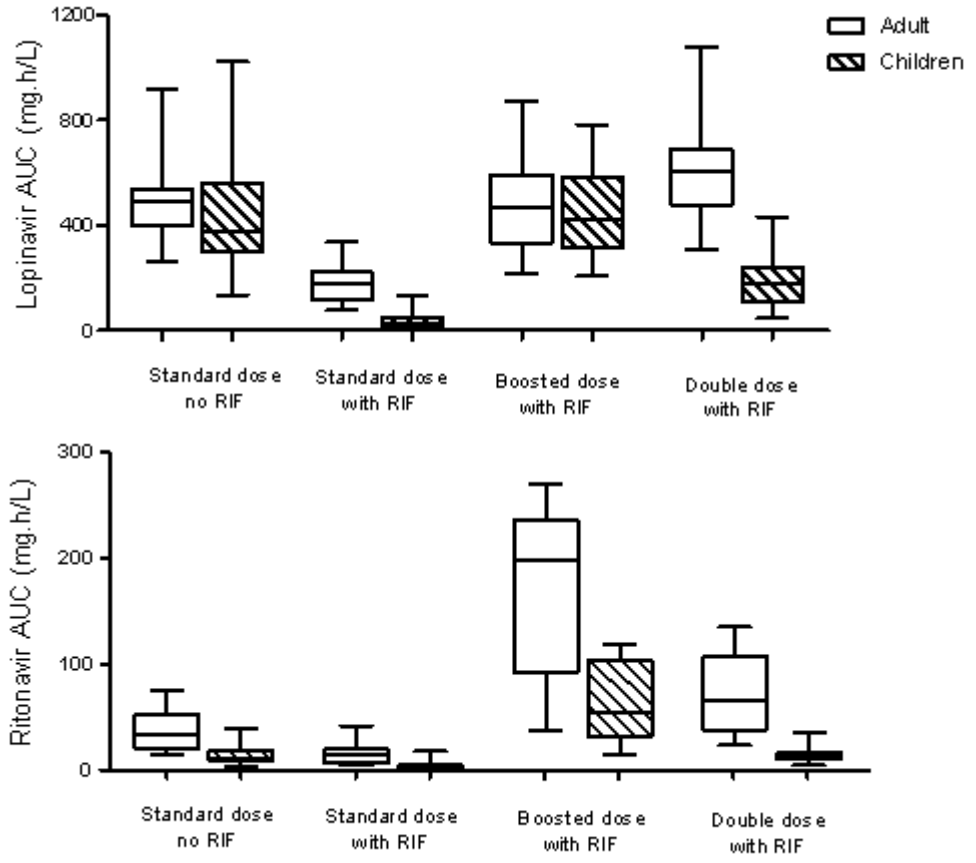

Figure 3.3.4. The exposure of lopinavir (upper) and ritonavir (lower) in adults and children stratified by dose strategies in integrated lopinavir-ritonavir model using combined dataset.

Table 3.3.4. The relative bioavailability of lopinavir and ritonavir adjusted to the median doses actually received by children. (The bioavailability without rifampicin of adults is assumed as 100% as reference).

LPV/r dose strategy	**Median dose of ritonavir**	**Relative bioavailability**	
		Lopinavir	**Ritonavir**
Standard dose without rifampicin	2.9 mg/kg	0.787	0.245
Super-boosted dose with rifampicin	14 mg/kg	0.534	0.308
Double dose with rifampicin	6 mg/kg	0.383	0.101

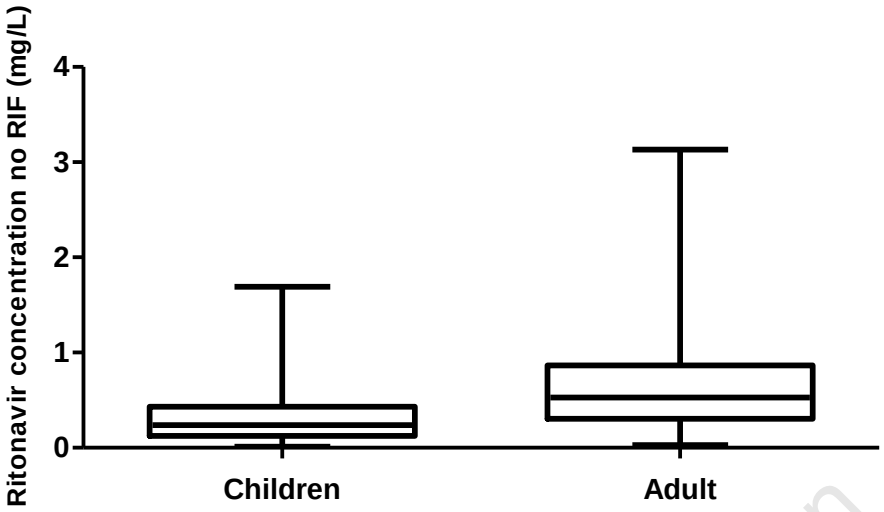

Figure 3.3.5. Ritonavir concentrations in children and adults when standard dose of LPV/r was given without rifampicin.

3.3. Final model evaluation

Goodness fit plots of lopinavir and ritonavir in the final integrated model for adults and children are shown in Figure 3.3.6 and Figure 3.3.7, respectively. The visual predictive check plots of final integrated model for lopinavir and ritonavir are shown in Figure 3.3.8. The visual predictive check plots for lopinavir and ritonavir in children stratified by different dose strategies are shown in Figure 3.3.9. All validation results demonstrated the adequacy and robust of the model. Since the model we built was quite complicate, including huge number of parameters, it was extreme time consuming. Ten bootstraps were performed and results are presented in Table 3.3.3.

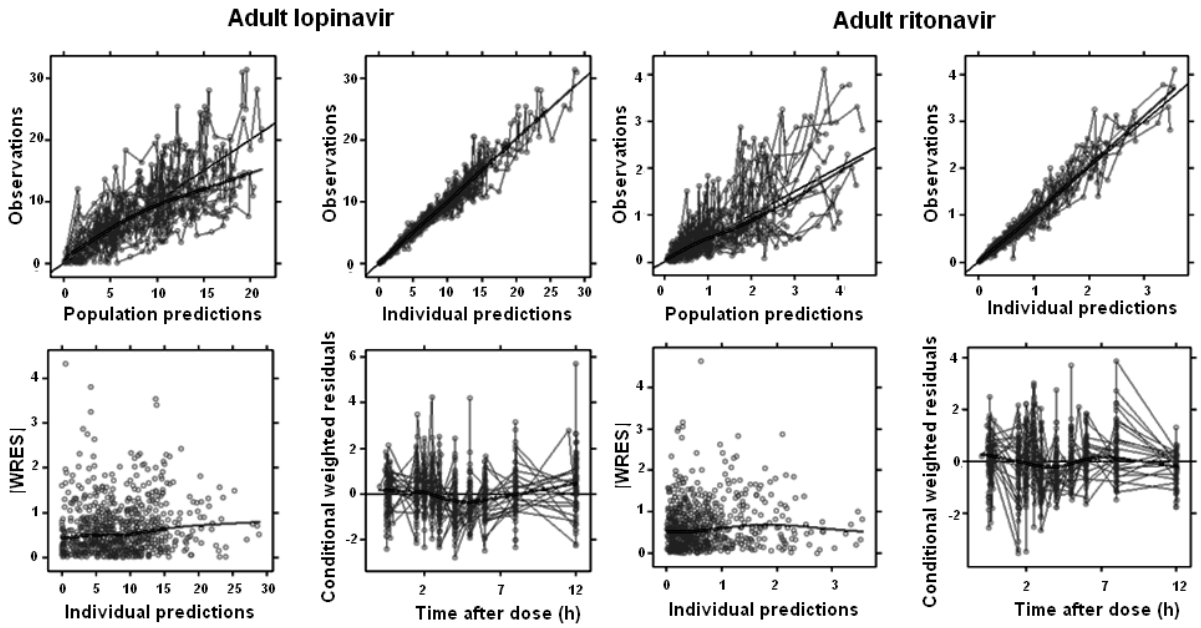

Figure 3.3.6. Goodness fit plots of lopinavir (left) and ritonavir (right) of final integrated model for adults.

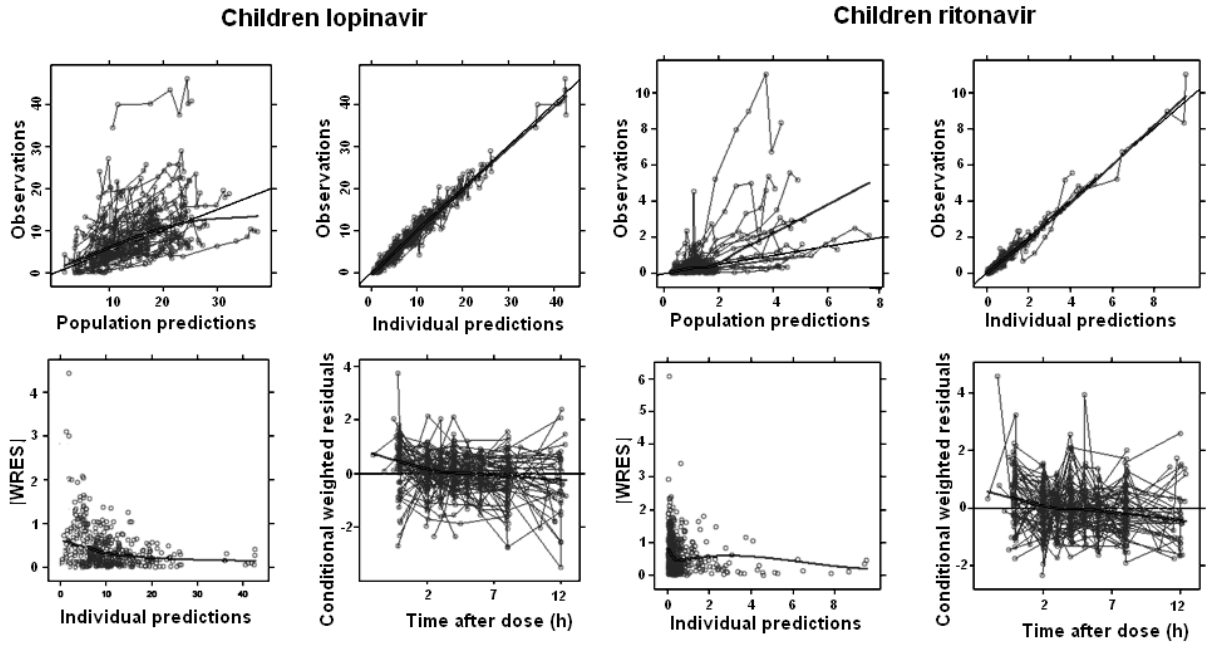

Figure 3.3.7. Goodness fit plots of lopinavir (left) and ritonavir (right) of final integrated model for children.

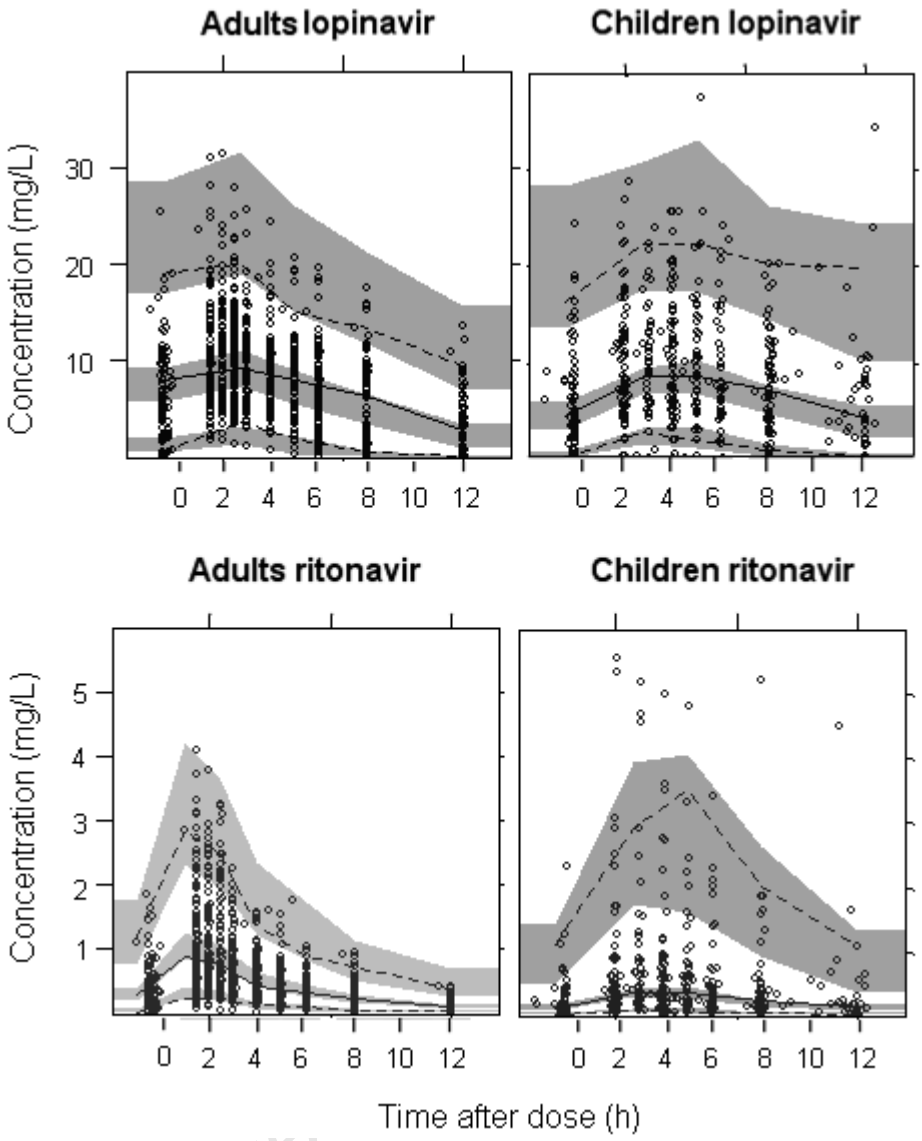

Figure 3.3.8. Visual predictive check (VPC) of lopinavir and ritonavir of the final integrated model for adults (left panel) and children (right panel). The solid line is the median of the observed data and the dotted lines are the 5th and 95th percentiles of the observed data. The grey shaded areas are the 95% confidence intervals for the median, 5th percentile and the 95th percentiles of the simulated data (n=1000). Observed concentrations are displayed as circles.

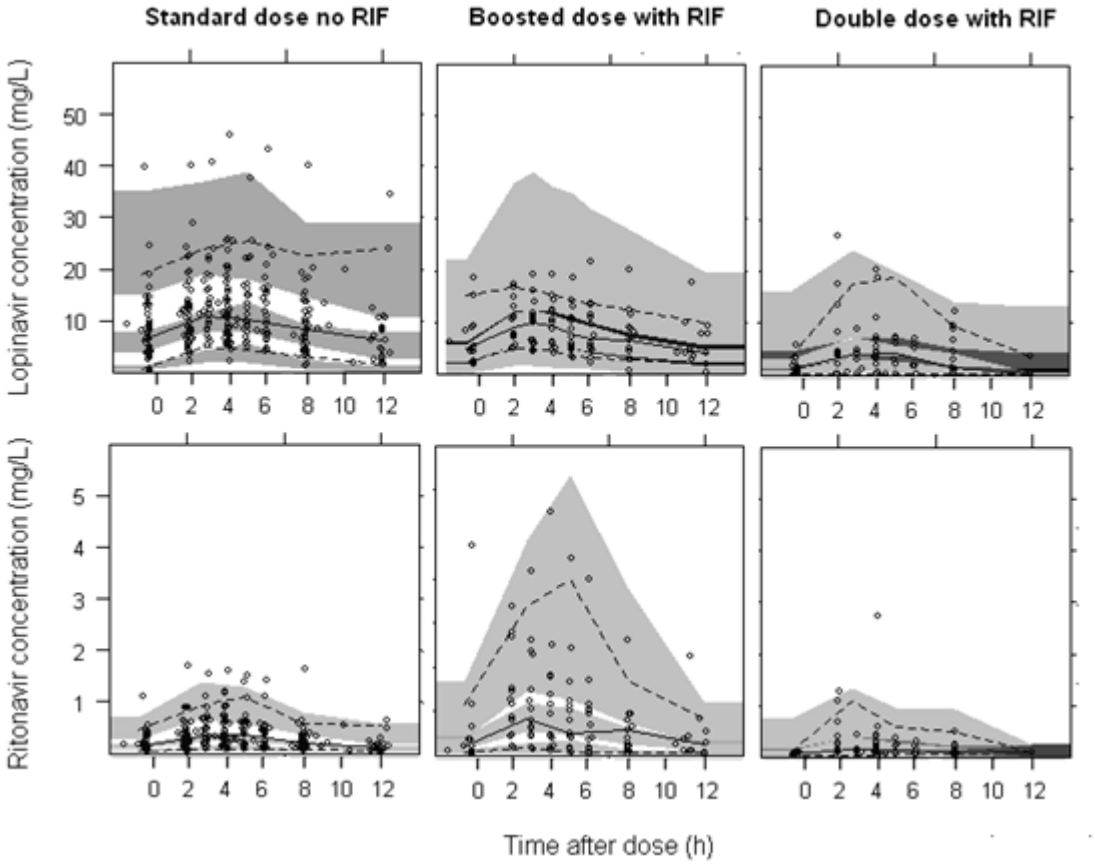

Figure 3.3.9. Visual predictive check (VPC) of lopinavir and ritonavir of the final integrated model for children stratified by different dose strategies. The solid line is the median of the observed data and the dotted lines are the 5th and 95th percentiles of the observed data. The grey shaded areas are the 95% confidence intervals for the median, 5th percentile and the 95th percentiles of the simulated data (n=1000). Observed concentrations are displayed as circles.

4. Results (Paper IV)

4.1. Patients and data description

The patients and data description were presented before. The lamivudine are pooled data from Study I and Study II. Briefly, 68 young HIV infected children aged 6 months to 4.5 years, of whom 36 were female, were recruited at three antiretroviral clinics in South Africa. All children were on antiretroviral treatment comprising lamivudine, stavudine or zidovudine and lopinavir/ritonavir and 33 children with tuberculosis received rifampicin-based ATT. A total of 493

concentrations of lamivudine were available from this study. Demographic characteristics of study patients are summarized in Table 3.4.1. Figure 3.4.1 illustrates the distribution of relvant demographic and clinical variables in the study population, including age, body weight, BSA, haemoglobin, and ALT. Plots of concentration of lamivudine against time after dose in patients are shown in Figure 3.4.2 and Figure 3.4.3. The boxplots of pre-dose (C_0) and trough concentrations (C_{12}) were illustrated in Figure 3.4.4. Only 5 samples were BQL data and set to LLOQ/2 value (10 ng/mL) during analysis.

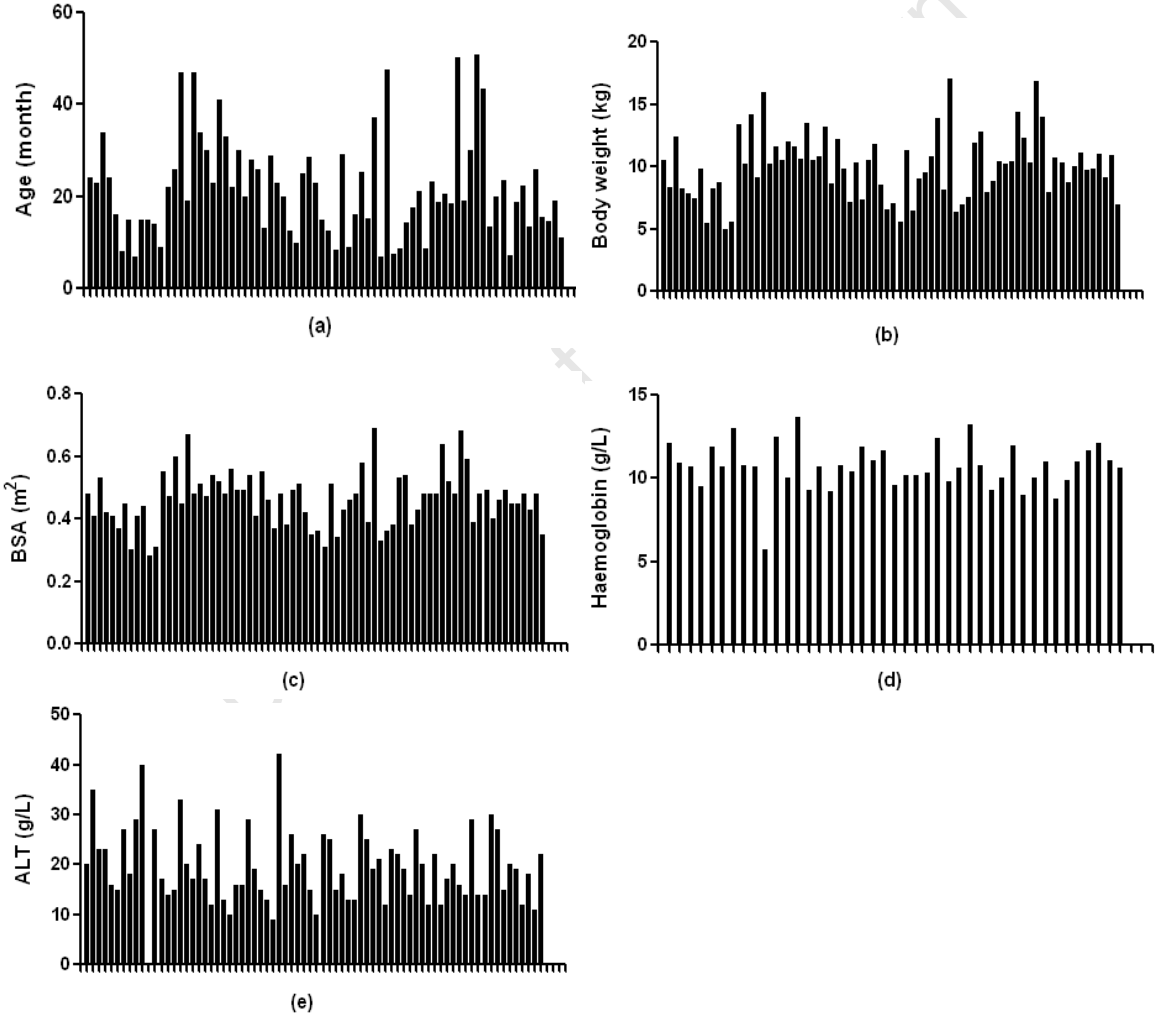

Figure 3.4.1. The distribution of relvant demographic and clinical variables of this study: age (a); body weight (b); BSA (c); haemoglobin (d); ALT (e).

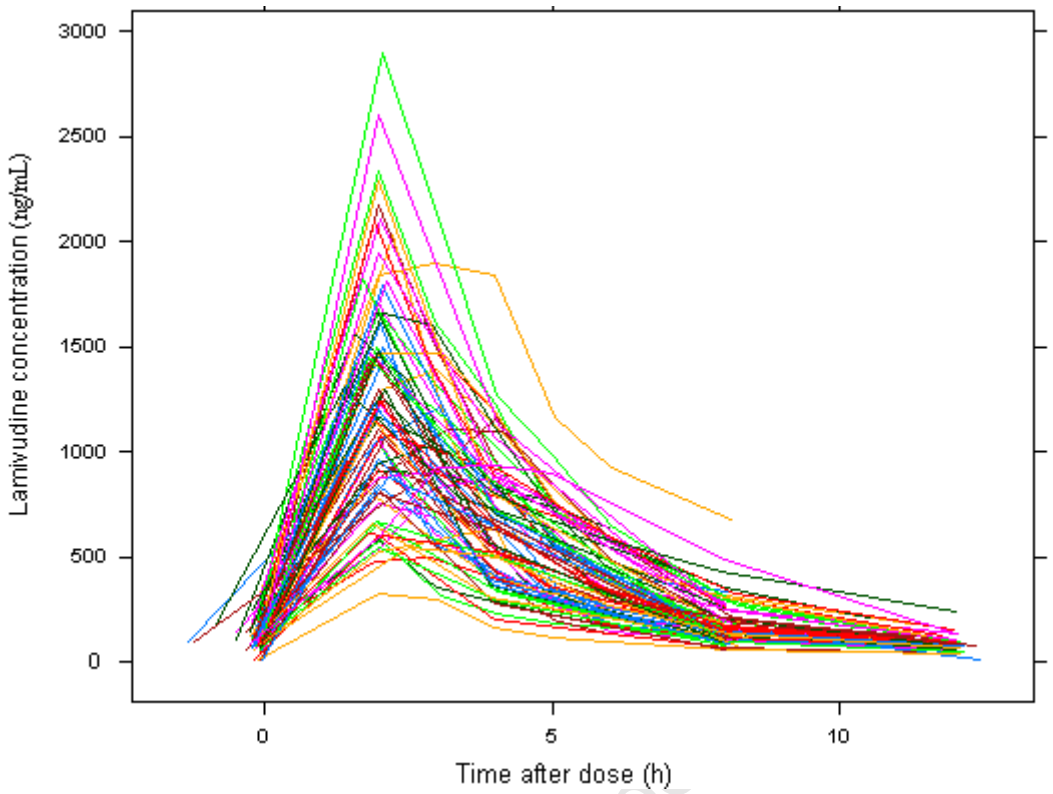

Figure 3.4.2. Plots of lamivudine concentration vs time after dose of total patients

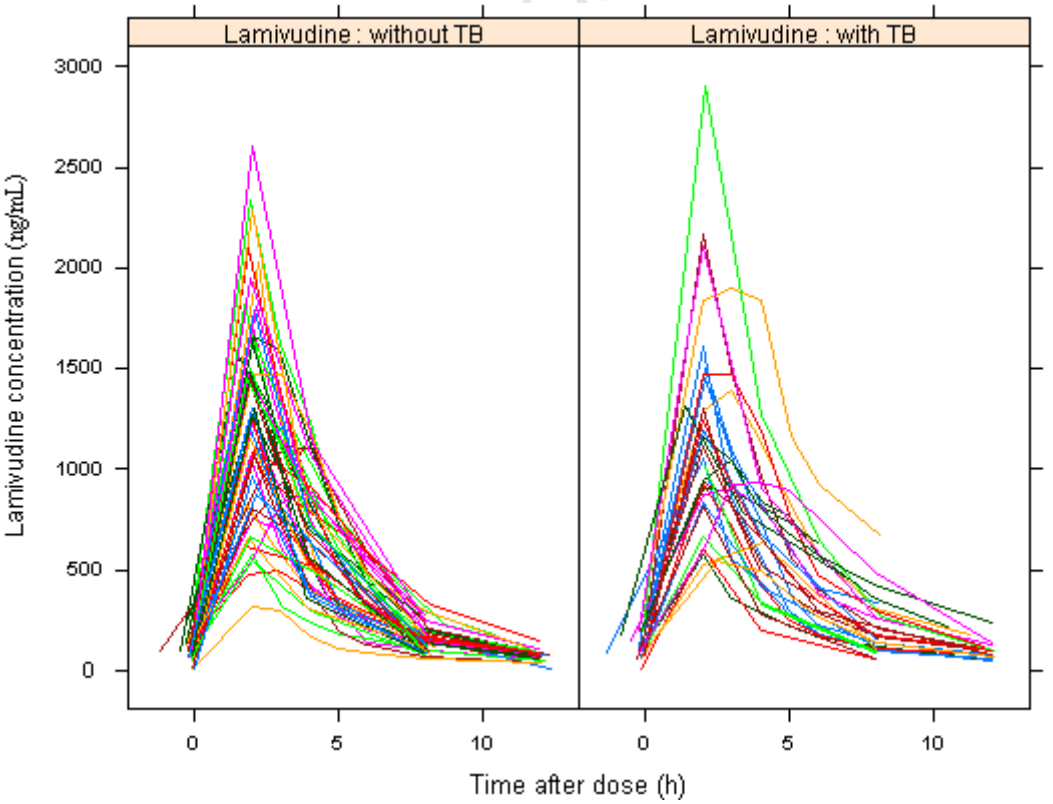

Figure 3.4.3. Plots of lamivudine concentration vs time after dose stratified by patients with or without antituberculosis.

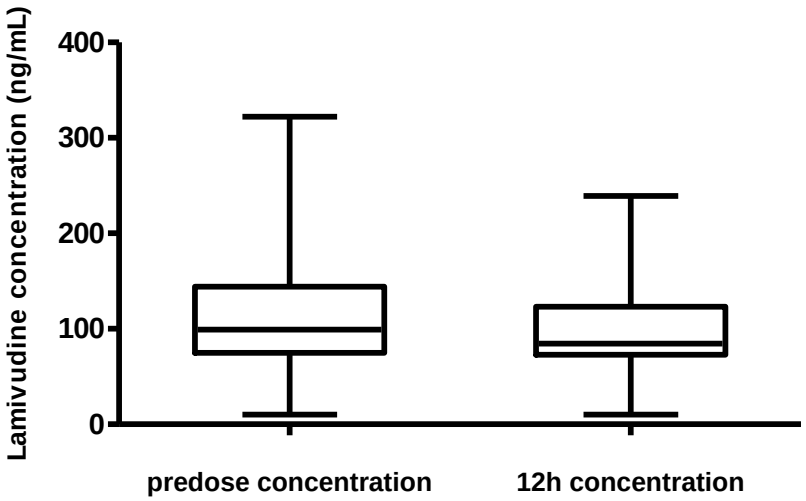

Figure 3.4.4. Boxplots of pre-dose and trough concentrations of this study.

Table 3.4.1. Demographic characteristics of patients.

Characteristic	**Median**	**Range**
Age (month)	22	6 months - 4.5 years
Body weight (kg)	10.0	5 - 17
Gender (M/F)	32/36	
Height (cm)	79	58 - 103
BSA (m^2)	0.48	0.28 - 0.69
Haemoglobin (g/L)	10.7	5.7 - 29.7
Albumin (g/L)	38	29 - 47
Weight-for-age z-score (WFA)	-0.88	-4.6 – 1.73
Weight-for-height z-score (WFH)	0.1	-4.8 – 3.75
Proportion of children with diagnosis of TB	48.5%	

TB: tuberculosis; WFA and WFH are calculated from each child's weight compared to that a normal child (50^{th} percentile) of the same age or height according to the WHO maturation chart.

4.2. Model development

Compared to a one-compartment model, a two-compartment model significantly improved the fit of data (Δ OFV=-20). Finally, a two-compartment model with first-order elimination best described the pharmacokinetics of lamivudine. The structure of the final model of lamivudine is illustrated in Figure 3.4.5. Model with zero-order absorption did not adequately fit the data. Transit compartment model was used to represent a more physiological delay in absorption onset and a gradual increase in absorption rate. The number of transit compartment was estimated 2.3 for the absorption model of lamivudine. Mean transit time was used to describe the delay of absorption. Drug transferred from the final transit compartment to the central compartment occurred through an absorption compartment with first-order absorption rate ka. The k_{tr} was used to describe the transit absorption rate between different transit compartments. This model significantly improved model fit by about 15 points in OFV value.

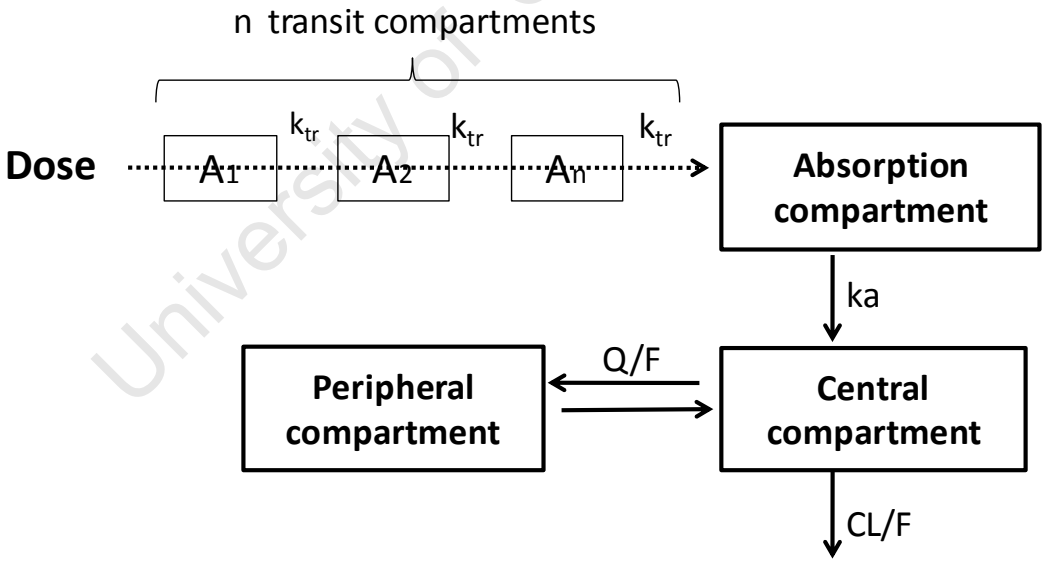

Figure 3.4.5. Structure of lamivudine final pharmacokinetic model. (ka: absorption rate; CL: central oral clearance; Q: peripheral oral clearance; F: bioavailability; k_{tr}: transit absorption rate)

The variability (IIV and IOV) in oral clearance (central and peripheral), volume of

distribution (central and peripheral), and k_a were tested in the model according to model development described in method. FOCE approach was used in the model building. IIV was supported in the clearance, volume of distribution and bioavailability in the final model. IOV was characterized in absorption parameters (absorption rate and absorption mean transit time), and bioavailability. A proportional structure was suitable for the residual error.

Different covariates, including body weight, age, gender, haemoglobin, albumin and ALT, were analyzed one by one according to model covariates development steps as a continuous or discrete factor. Body weight was found having significant influence on both the central and peripheral oral clearance and volume of distribution of lamivudine with an allometric scaling relationship in the final model (Equation 3.4.1 and Equation 3.4.2). The inclusion of allometric scaling of body weight on apparent clearance and volume of distribution had a significant impact on the goodness of fit, improving the OFV by approximately 7 points and explaining about 2% of IIV in both clearance and volume of distribution.

$$CL/F = CL/F_{STD} \cdot \left(\frac{WT_i}{10}\right)^{0.75} \quad (3.4.1)$$

$$V/F = V/F_{STD} \cdot \left(\frac{WT_i}{10}\right)^{1} \quad (3.4.2)$$

where the *CL/F* is the apparent oral clearance, CL/F_{STD} is the apparent oral clearance of standard patient (with mean body weight), WT_i is each patient's body weight, respectively, and 10 kg is the median body weight in our population.

Moreover, age was found have significant influence on oral clearance. Different maturation models were compared in our model: linear, exponential and sigmoidal relationship. The different maturation equations are shown as follows:

$$CL/F = TVCL/F \cdot (1 + (PMA_i - 31) \cdot \theta_{AGE}) \quad (3.4.3)$$

$$CL/F = TVCL/F \cdot (PMA_i/31))^{\theta_{AGE}} \quad (3.4.4)$$

$$CL/F = TVCL/F \cdot \frac{PMA_i{}^{Hill}}{PMA_i{}^{Hill} + PMA50^{Hill}} \quad (3.4.5)$$

where *CL/F* is the apparent oral clearance, *TVCL/F* is the typical value for a subject with the median postmenstrual age of 31 months, PMA_i is postmenstrual age of each patient, $\theta_{AGE}$is the coefficient of PMA on *TVCL/F, PMA50* is the PMA at which half of the maturation is reached, and *Hill* is a shape parameter that controls steepness of the sigmoidal maturation function.

Figure 3.4.6 illustrates the different maturation functions on the clearance. No significant differences were found between three maturation relationships. It might due to the age range in our dataset was from 6 months to 54 months, and within this age range the clearances were almost overlapped in different models (Figure 3.4.6). However, sigmoidal maturation function indicates more physiological meaning than other two relationships. Therefore, sigmoidal maturation was used in the final model. The OFV dropped by about 20 points and IIV in CL/F decreased from 10.1% to 8.2% when age was introduced into the model with a sigmoidal maturation model. The hill coefficient in the sigmoidal model was initially estimated to be 0.96, and fixed to 1 in the final model. The effect of maturation on CL/F reached 50% by 4 months after birth (Figure 3.4.7). Weight for age or weight for height z-score was used to investigate whether wasting patients had the different oral clearance or volume of distribution, but neither weight-for-age nor weight-for-height z-score improved the model fit. Oral clearance and bioavailability were similar in patients with and without tuberculosis. Antituberculosis treatment did not influence the pharmacokinetics of lamivudine.

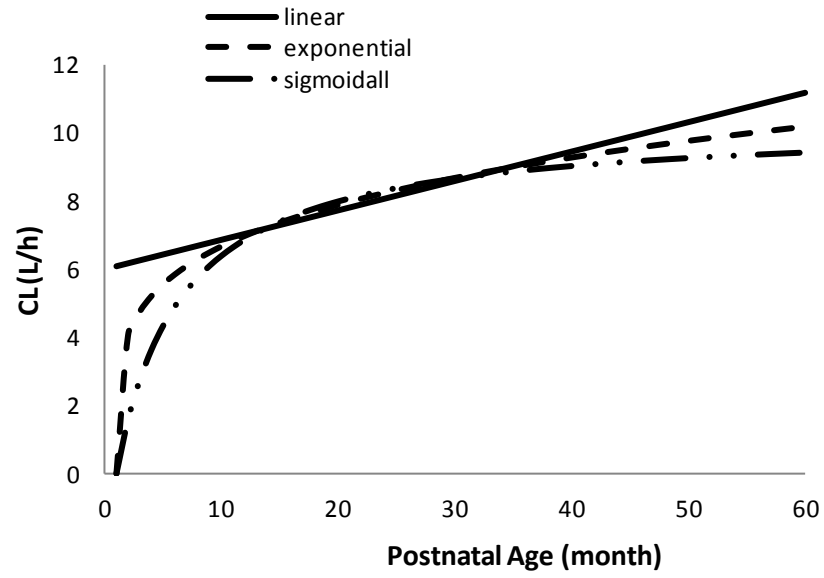

Figure 3.4.6. Different maturation function tested using our dataset.

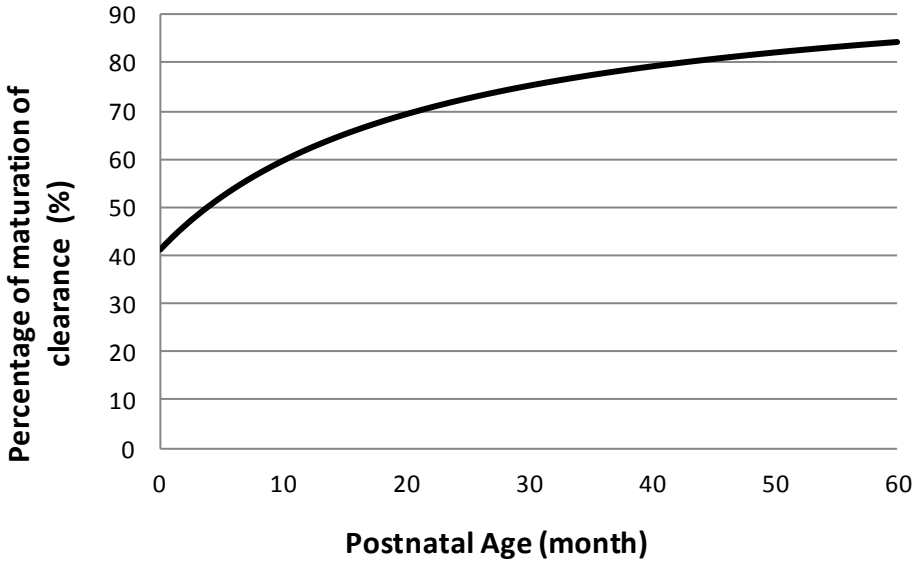

Figure 3.4.7. The maturation of lamivudine clearance with age. These values account only for the effect of age.

Trough concentrations were on average slightly higher in the morning (C_0) than in the evening (C_{12}) (Figure 3.4.4). To account for this, diurnal variations were tested on both bioavailability and clearance in our model, with the latter being found

significant. The OFV dropped 26 points when diurnal variations were included in the model. The oral clearance was estimated to be 16.7% slower overnight. The individual oral clearances of lamivudine during morning and evening are shown in Figure 3.4.8. Furthermore, to account for the uncertainty about the time of the evening dose, the RUV for the pre-dose concentrations was allowed a larger level of error. The proportional error was 12.6% for pre-dose concentrations compared to 8.3% for concentrations at later time points. The OFV improved about 17 points when different residual errors of pre-dose concentrations were investigated.

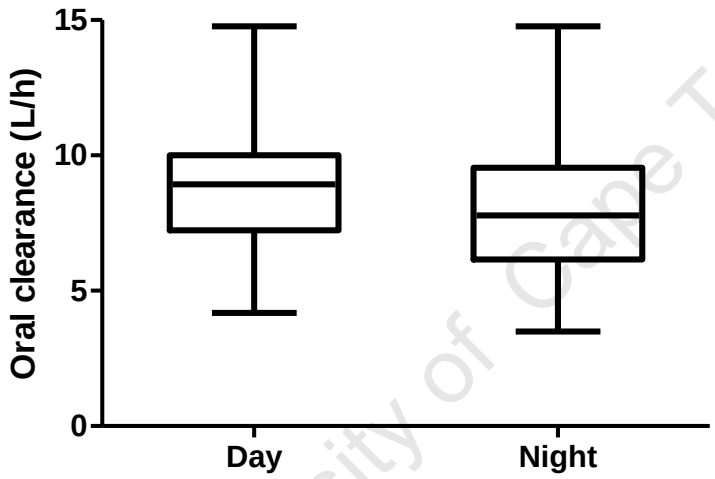

Figure 3.4.8. Diurnal variation in individual oral clearances.

The population pharmacokinetic parameter estimates are shown in Table 3.4.2. The clearance at full maturation was 12.2 L/h/10 kg. The typical value of clearance of patients who have median body weight of 10 kg and median age of 22 months for our dataset is calculated as 8.6 L/h. The variability on bioavailability was found to be 28.5% for IIV and 27.0% for IOV with good estimation precision. Large variability of absorption parameters, ka and MTT, was found, 71.9% for IOV in ka and 70.9% for IOV in MTT. However, variability of clearance was limited to 8.2%. The representative individual plots of lamivudine are presented in Figure 3.4.9.

Table 3.4.2. Population pharmacokinetic parameter estimates of final model for lamivudine

Parameter	**Estimate (η shrinkage%)**	**RSE (%)**
CL/F (L/h)*	12.2	16.6
V_c/F (L)*	20.7	8.4
Q/F (L/h)*	1.67	12.9
V_p/F (L)*	37.2	78.8
ka (h^{-1})	1.65	18.7
NN	2.3	40.2
MTT (h)	0.547	24.3
PMA50 (month)	12.9	37.1
Proportional error for PRE (%)	12.6	70.6
Proportional error (%)	8.3	8.3
Evening effect on CL/F (- %)	16.7	5
IIV on CL/F (%CV)	8.2 (18.9)	34.2
IIV on V/F (%CV)	25.2 (16.8)	15.8
IIV on F (%CV)	28.5 (22.2)	17.9
IOV on F (%CV)	27.0 (23)	16.4
IOV on ka (%CV)	71.9 (39.2)	20.8
IOV on MTT (%CV)	70.9 (41.8)	35.3

CL: central oral clearance; V_c: central volume of distribution; Q: peripheral oral clearance; V_p: peripheral volume of distribution; F: bioavailability; ka: oral absorption rate; NN: number of transit compartment; MTT: mean transit time; PMA50: half life of maturation for postmenstrual age; IIV: interindividual variability; IOV: interoccasional variability; PRE: pre-dose concentrations; *For a child of 10 kg (the median weight of the studied cohort).

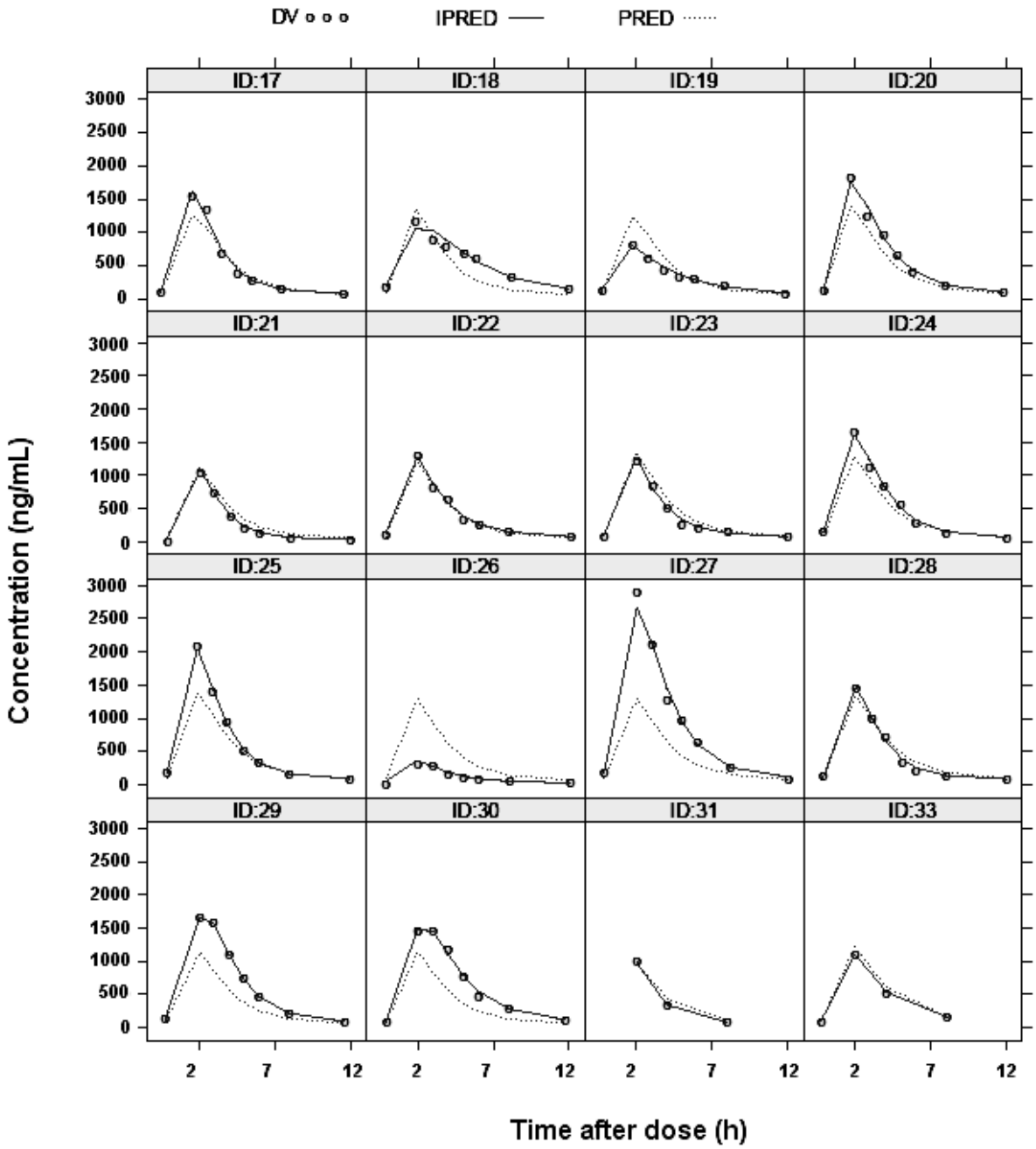

Figure 3.4.9. The representative individual plots of lamivudine (the solid line is the individual predictive data and the dotted line is the population predictive data and observed concentrations are displayed as circles).

4.3. Model validation

Goodness fit plots of model are shown in Figure 3.4.10. VPC plots are shown in Figure 3.4.11 and Figure 3.4.12. The results of 1000 simulations from the final model demonstrated the adequacy of the model and indicated that the model had

good properties to predict concentration reference using simulation. The bootstrap results (Table 3.4.3) confirmed the robustness of the final model.

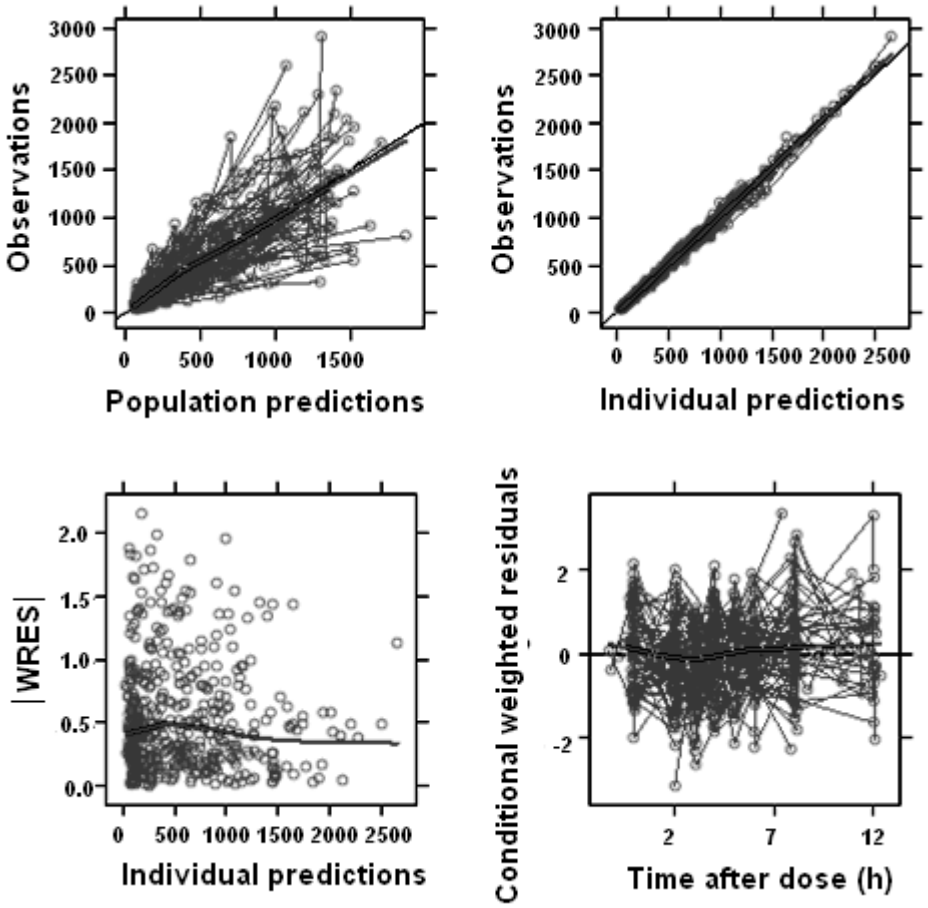

Figure 3.4.10 Goodness fit plots of the final model.

Table 3.4.3. Bootstrap results from 1000 samples using final model for lamivudine

Parameter	Median*	95% CI*
CL/F (L/h)**	12.5	10.6 – 14.4
V_c/F (L)**	20.5	16.4– 24.6
Q/F (L/h)**	1.85	1.48 – 2.22
V_p/F (L)**	38.4	12.1 – 64.7
ka (h^{-1})	1.67	1.07 – 2.26
NN	2.31	1.46 – 3.17
MTT (h)	0.53	0.35 – 0.71
PMA50 (month)	13.0	9.7 – 16.2
Proportional error for PRE (%)	10.4	3.5 - 17.4
Proportional error (%)	8.2	7.0 - 9.4
Evening effect on CL/F (- %)	16.4	13.9 - 18.9
IIV on CL/F (%CV)	10.7	3.6 – 14.7
IIV on V/F (%CV)	24.7	19.8 – 25.3
IIV on F (%CV)	28.7	20.9 – 36.5
IOV on F (%CV)	26.9	21.5– 32.4
IOV on ka (%CV)	73.7	53.1 – 93.3
IOV on MTT (%CV)	73.4	58.7 – 88.1

CL: central oral clearance; V_c: central volume of distribution; Q: peripheral oral clearance; V_p: peripheral volume of distribution; F: bioavailability; ka: oral absorption rate; NN: number of transit compartments; MTT: absorption mean transit time; PMA50: postmenstrual age at which half of maturation is reached; PRE: pre-dose concentrations; IIV: inter-individual variability; IOV: inter-occasional variability. *median and 95% confidence interval from 1000 bootstraps. **For a child of 10 kg (the median weight of the studied cohort).

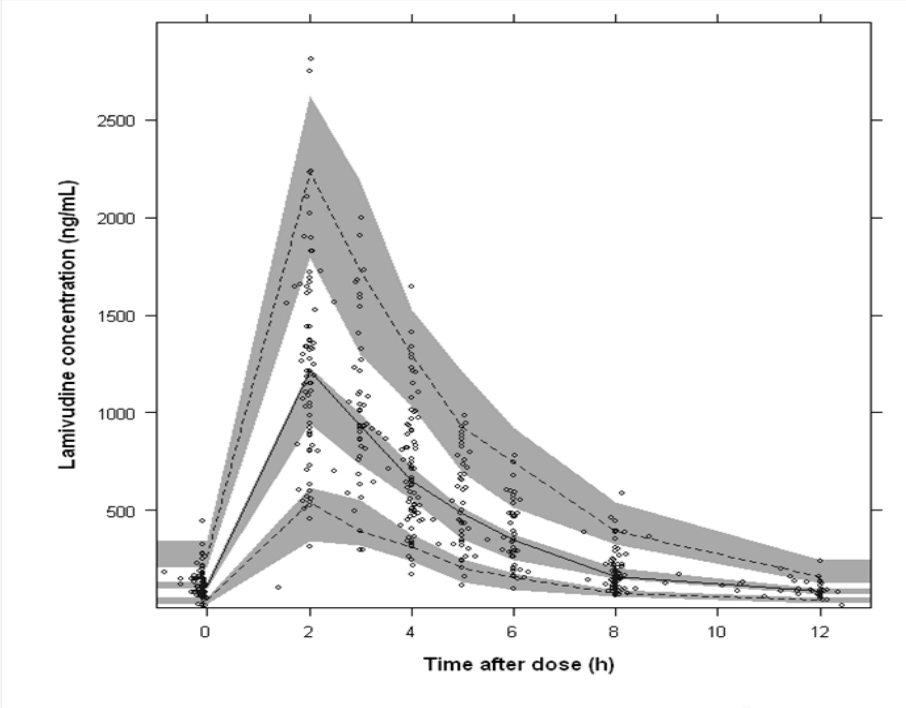

Figure 3.4.11. Visual predictive check (VPC) of the final model for lamivudine. The solid line is the median of the observed data and the dotted lines are the 5th and 95th percentiles of the observed data. The shaded areas are the 95% confidence intervals for the median, 5th percentile and the 95th percentiles of the simulated data (n=1000). Observed concentrations are displayed as circles.

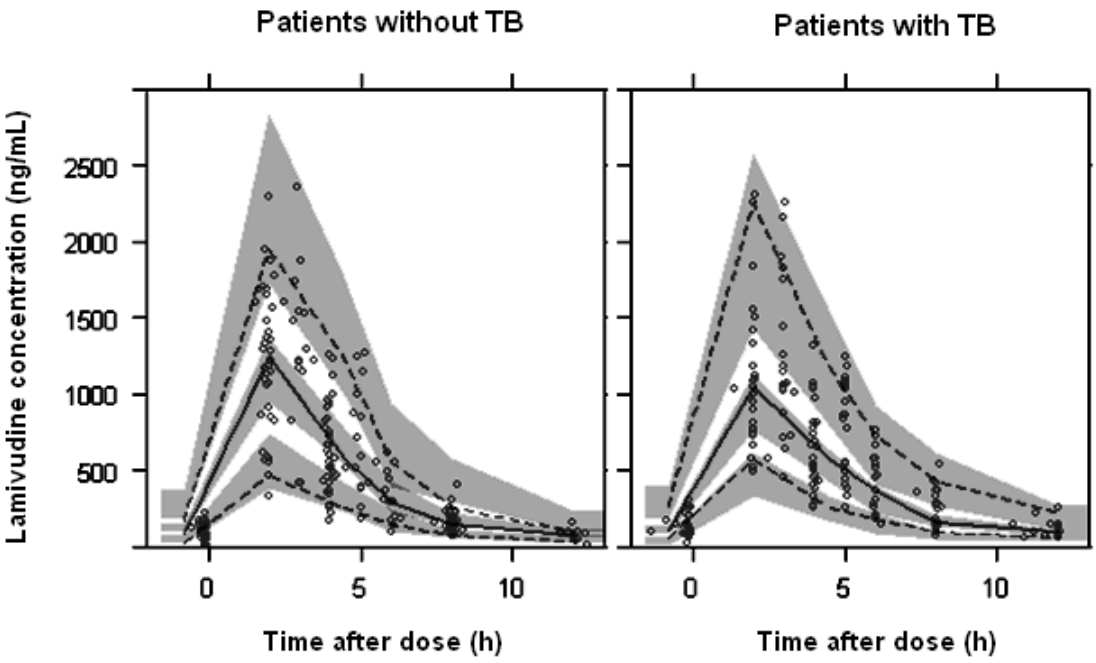

Figure 3.4.12. Visual predictive check (VPC) of the final model for lamivudine stratified by patients with or without antituberculosis. The solid line is the median of the observed data and

the dotted lines are the 5th and 95th percentiles of the observed data. The shaded areas are the 95% confidence intervals for the median, 5th percentile and the 95th percentiles of the simulated data (n=1000). Observed concentrations are displayed as circles.

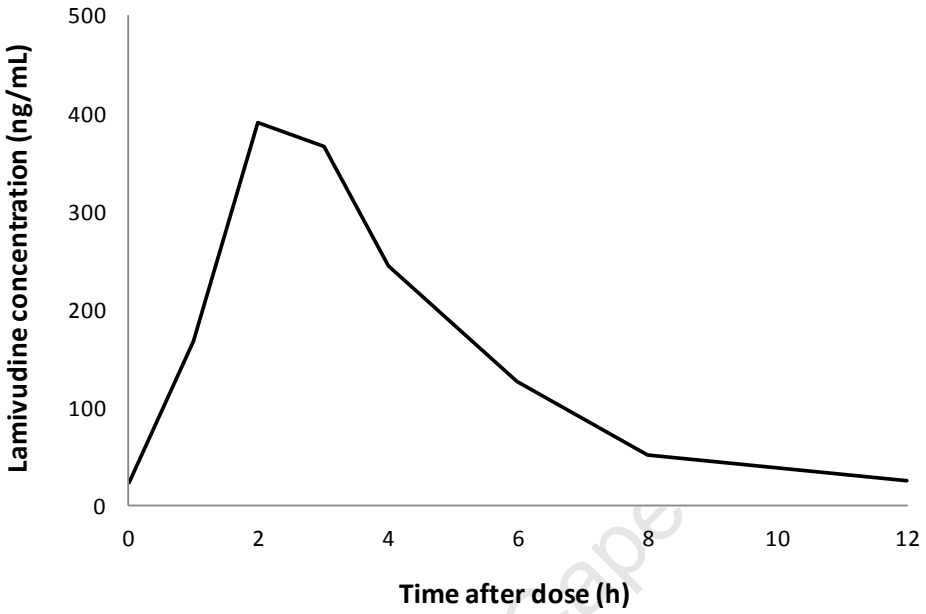

Figure 3.4.12. The 5th percentile of lamivudine concentrations in typical patients by 2000 simulations.

4.4. Simulation

2000 simulations were used to predict reference concentration of lamivudine. Therapeutic drug monitoring results can be used to compare with these reference concentrations. The patients whose concentrations are below the cutoff values are high likely to have poor adherence. The 5th percentile of lamivudine concentrations in typical patients is shown in Figure 3.4.12. Plots of the 5th percentile for lamivudine concentrations in children of different ages are shown in Figure 3.4.13. The cutoff values of 1st, 2.5th and 5th concentration percentiles at 4 and 12 h after the dose were estimated using 2000 simulations. The results are shown in Table 3.4.4. For patients who missed the previous one or two doses, the simulations indicated that 99% of concentrations at 4 h after dosing were below the cutoff values of 1st, 2.5th and 5th percentiles. But if patients missed only the second last dose, 94% and 87% concentrations at 4 h and 12 h after dosing are

above the 5th percentile of reference cut-offs. If we use concentrations at 12 h after dosing as an indicator, only about 40% and 85% of concentrations were found to be below the 5th percentile of cutoff values for patients who skipped last one dose and two doses, respectively.

Table 3.4.4. The cutoff concentration values of lamivudine calculated from 2000 simulations.

Age	Cutoff value (ng/mL)					
	1st percentile		2.5th percentile		5th percentile	
	4 h	12 h	4 h	12 h	4 h	12 h
6 months	297.0	44.7	328.9	52.1	372.5	62.0
1 year	230.1	28.4	262.8	33.5	293.0	39.5
2 year	200.7	22.4	236.7	26.5	263.6	31.0
5 year	202.7	20.7	239.1	24.5	265.8	28.6

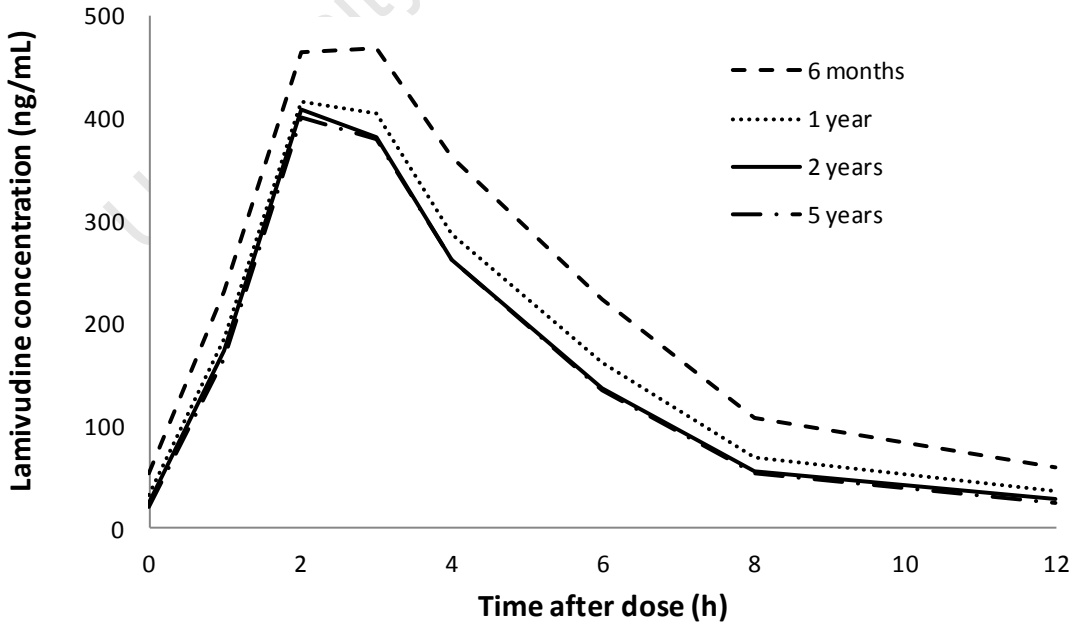

Figure 3.4.13. The 5th percentile of concentrations of lamivudine stratified by different age by 2000 simulations.

Discussion

1. Pharmacokinetics of lopinavir and ritonavir co-administation with rifampicin in children

Despite the complexity of combined antituberculosis and antiretroviral therapies, survival of patients presenting with HIV-associated tuberculosis is significantly improved when antiretroviral treatment is introduced during anti-tubercular therapy[171–173]. However, combined treatment options are limited for young children, especially children who have been exposed to nevirapine for prevention of mother to child HIV transmission, and those younger than 3 years, in whom efavirenz cannot be used. In young children, there is very little data about the pharmacokinetics of lopinavir and ritonavir when co-administered with rifampicin-based ATT. In Paper I, the pharmacokinetics of lopinavir using an integrated population model was described based on two studies evaluating lopinavir and ritonavir concentrations in children with and without tuberculosis in order to predict the optimal dose of LPV/r (in a 4:1 ratio) in young children treated with a rifampicin-based regimen.

Lopinavir target trough concentrations (>1 mg/L) were achieved in the control group who received standard doses of LPV/r without rifampicin). In children concurrently administered rifampicin-based ATT, 'super-boosted' lopinavir almost always achieved adequate trough concentrations of lopinavir, but the strategy using doubled doses of LPV/r failed. Simulations from this model indicated that, using LPV/r oral solution twice daily, lopinavir doses would need to be increased dramatically during ATT, especially in children with lower body weights. For children weighing 3.0-5.9 kg, the lopinavir dose needed to attain the target would be 52 mg/kg 12 hourly, which considerably exceeds the doses used in clinical practice and could lead to the appearance of adverse events. High dose of ritonavir

is link to toxicity and consequently, an 8 hourly dosage regimen was investigated to reduce doses, and indeed this thrice-daily approach would require, in children weighing 3.0-5.9 kg, only 27 mg/kg (daily total of 81 mg/kg compared to 104 mg/kg for twice daily dosing). The total daily doses required to maintain therapeutic lopinavir concentrations were lower using the 8 hourly doses. The 5th percentiles of simulated lopinavir concentrations using the original and the proposed dosage regimens in a typical patient (the patient who has a median age and median body weight) when lopinavir/ritonavir was given as standard ratio 4:1 are presented in Figure 4.1. The predicted 95th percentile of lopinavir trough concentrations for the 8 hourly approach is 15.8 (5.61-31.5), 12.4 (5.2-24.2), 12.6 (5.7-25.8), 9.5 (5.1-16.6) mg/L for children weighing 3.0-5.9, 6.0-9.9, 10.0-13.9, 14.0-19.9 kg respectively. These values are lower than those predicted trough concentrations for 12 hourly doses of super-boosted lopinavir: 22.2 (8.3-41.7), 14.6 (6.2-28.3), 13.3 (5.9-26.3), 10.9 (5.9-23.2) respectively.

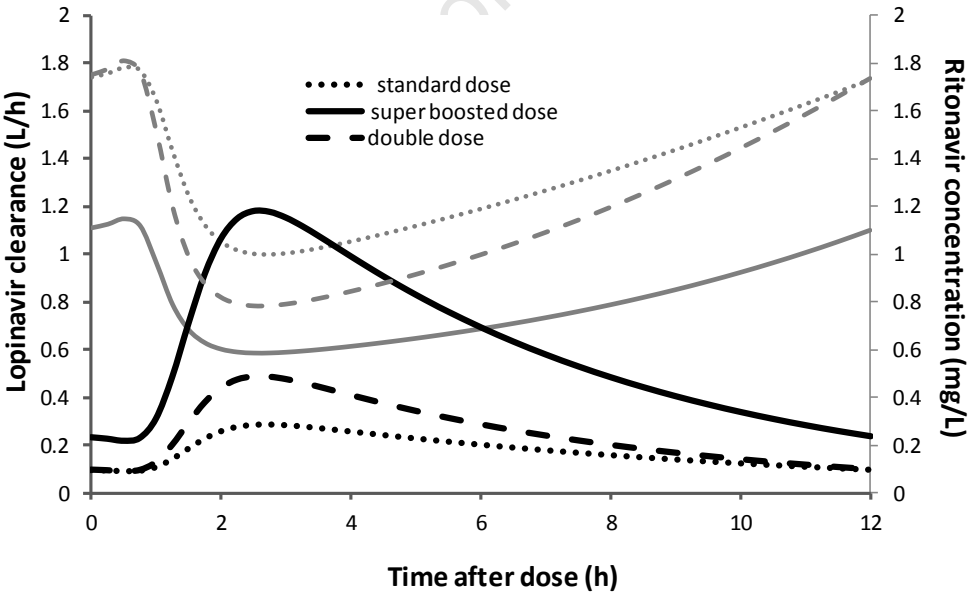

Figure 4.1 The influence of ritonavir concentrations on the oral clearance of lopinavir (The x axis is time after dose, the left y axis is lopinavir clearance, and the right y axis is ritonavir concentration).

The bioavailability of lopinavir was estimated considering the effects of both rifampicin and ritonavir. This model predicts that AUC to lopinavir would drop by 83.2% if ATT was concomitantly given without any further dose adjustments. On the other hand, it increased by 2.1% for each mg/kg of ritonavir added to the dose. Even though the relationship between ritonavir dose and bioavailability is probably quite complicated, in this model it was described using a linear proportionality. This choice was compelled by the limited range of ritonavir doses available in the dataset, and should not be used too far outside the tested range. It is expected that it to provide reasonable predictions for our purposes. During ATT, the relative bioavailability of lopinavir was reduced to 22.6% of the reference in children receiving twice the usual dose of LPV/r, while for children given 'super-boosted' lopinavir this value almost doubled reaching 40.5%. IOV in k_a of lopinavir was significant in the model whereas IIV in lopinavir k_a was not supported by the data, pointing towards a greater relevance of occasion- rather than subject-specific changes during the absorption phase.

The typical oral clearance of ritonavir when concurrently administered with rifampicin was 19.1 L/h, an increase of about 50% compared to the value estimated without ATT. This model is the first to describe the dynamic effect of ritonavir concentrations on the clearance of lopinavir in children using an integrated model. The EC_{50} was estimated to be 0.0519 mg/L, which is a low value when compared to normally achieved ritonavir concentrations which supports the potency of ritonavir as an inhibitor. In Figure 4.1, the change of lopinavir oral clearance due to ritonavir concentrations can be seen for each dosing strategy.

Body weight was introduced as allometric scaling for oral clearance and volume of distribution of both lopinavir and ritonavir which is in agreement with previous studies in children [16,138]. Jullien et al [161] observed a 39% increase in oral clearance

of lopinavir after the age of 12 years for boys. The age range in this dataset (6 months to 4.5 years) is narrow and could not detect the influence from age and gender. This narrow age might explain why age and gender were not significant covariates in this model. Development of expression of CYP450 enzymes is profoundly affected by age. Distinct patterns of development of isoform-specific CYP expression have been found after birth. CYP3A7 is the predominant CYP isoform enzyme expressed in fetal hepatocytes and its expression attains a peak shortly after birth and then diminishes rapidly to levels that are undetectable in most adults. The clearance of carbamzaepine, which is largely dependent on CYP3A4, is greater in children than in adults [84]. Phenytoin metabolism is not attatining saturation until approximately 10 days of postnatal age, demonstrating the developmental attainment of CYP2C9 activity. A maturation model was not supported by this dataset, probably due to lack of data in children below 1 year of age [174] since most data of this study is above 1 year though the youngest is 6 mohths. This model could not be used to confidently predict the doses of LPV/r achieving the target concentrations beyond the range of the available data. Moreover, the pharmacokinetics, efficacy, safety and feasibility of the 8 hourly dosing approach needs to be evaluated prospectively in children.

2. Pharmacokinetics of lopinavir and ritonavir when co-administered rifampicin in adults

In Paper II, an integrated population pharmacokinetic model is reported, which includes covariate effects and describes the complicated induction and inhibition interactions between lopinavir, ritonavir, and rifampicin. The diurnal variation of lopinavir and ritonavir concentrations that were observed is explained. Finally, previous reported findings have been extended that double dose LPV/r counteracts the inducing effect of rifampicin to predict alternative dose regimens of LPV/r for low and high weight patients.

As shown by La Porte et al. [12], either doubling the dose of the capsule form of LPV/r or boosting LPV/r with additional ritonavir (such that the ratio of lopinavir/ritonavir=1) can sufficiently counteract the effect of rifampicin induction. Doubling the dose of LPV/r is more practical to implement, and may be associated with less hepatotoxicity than ritonavir boosting. However increased doses of LPV/r appear to be poorly tolerated in healthy volunteers given rifampicin [12, 125]. As noncompartment analysis reported by Decloedt et al. [124], doubling the dose of the tablet form of LPV/r achieved adequate trough concentrations of lopinavir during rifampicin coadministraton was found and was better tolerated in HIV infected individuals established on a LPV/r antiretroviral regimen.

Previous studies have reported single compartmental elimination kinetics for ritonavir [162,175–177]. However, possibly because of the rich sampling schedule used in this study, a two-compartment model was more appropriate to describe the kinetics in data of this study. The OFV drop of about 100 points and the improvement in the fit of the individual plots supported the inclusion of a peripheral compartment. A transit compartment absorption model described the delay in absorption better than a model using a lag-time. Dickinson et al. [178] recently reported a sequential population pharmacokinetic model for lopinavir and ritonavir in healthy volunteers. Their model did not involve rifampicin-based antituberculosis treatment.

Full induction of drug-metabolising enzymes by rifampicin has been thought to be reached about one week after starting daily doses of rifampicin [67]. Hence in this study blood samples were taken one week after each dose adjustment. A recent report amongst tuberculosis patients started on a rifampicin-containing regimen suggests that autoinduction of rifampicin metabolism may be incomplete after 7 days (the half-life of the induction process was estimated to 6-8 days) [168,179].

However, as autoinduction approached maximal levels (~85% of total) after 2 weeks, near full induction should have been achieved when patients in this study underwent pharmacokinetic evaluation on 1.5 and 2 times the standard dose of LPV/r with rifampicin. Besides the effect of rifampicin, the relative bioavailability of ritonavir was found to be influenced by its own dose. When standard doses of ritonavir (100 mg) were given with rifampicin, the relative bioavailability of ritonavir was 55.0%. This increased to 77.3% and 99.6% when 1.5 times, and doubled doses, respectively, were given. Therefore the dose escalation results in a more than proportional increase in ritonavir plasma concentrations, which may also lead to a stronger inhibition effect. This effect of ritonavir dose on its bioavailability might be explained by saturation of first pass metabolism. Moreover, as ritonavir is an inhibitor and a substrate of P-gp [175], it could inhibit its own efflux from enterocytes and hepatocytes. .

The model estimated a value of 37.9 L/h for lopinavir CL/F when no ritonavir effect is present, but it should be kept in mind that this value is only an extrapolation, since lopinavir was never given without ritonavir. Figure 4.2 depicts the dynamic effect between ritonavir concentrations and lopinavir CL/F in a typical patient given different dose regimens, and can be used to provide real-life values of lopinavir CL/F when the two drugs are administered concomitantly, as is always the case during treatment. The sigmoidal inhibition model which was finally selected estimates both a very high value of E_{max} (95%) and a low EC_{50} (0.04 mg/L). This points towards the high inhibitory potency of ritonavir at a low concentration. Ritonavir is thought to be an irreversible inhibitor [180], but Ernest et al. reported that reversible mechanisms are also involved [21]. Like a previous model, this model did not support irreversible inhibition [162,178].

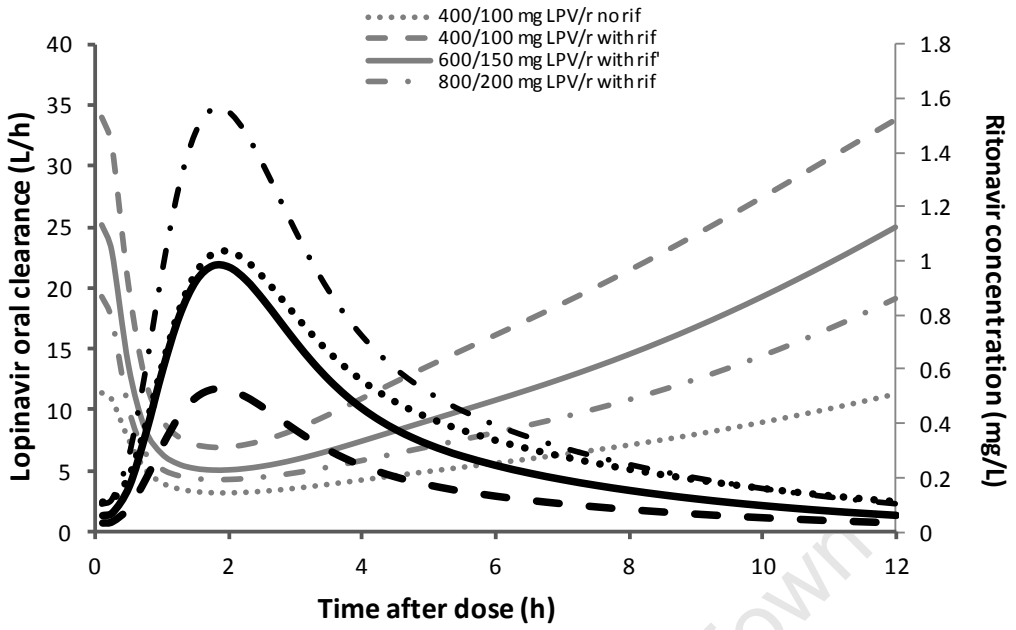

Figure 4.2. The influence of ritonavir concentrations (indicated in black) on the oral clearance of lopinavir (grey) in a typical patient. (LPV/r: lopinavir/ritonavir; rif: rifampicin)

Body size was the only covariate found to have a significant effect in this model, and it was implemented through allometric scaling. For both lopinavir and ritonavir, fat free mass was used to scale CL/F, while total body weight was better suited for V/F. Since fat tissue normally contributes little to metabolism (fat weight fraction estimated 0.001), fat free mass is expected to be a better predictor for CL/F when there are wide variations in body composition [169]. This was the case for the cohort of subjects of this study, in which the BMI ranged from 17.4 to 41.4 kg/m^2. On the other hand, fat contributes to V/F for lipophilic drugs like lopinavir and ritonavir. Jullien et al.[161] found CL/F of lopinavir to be related to age, sex, body weight, while V/F was related to body weight in children younger than 18 years-old. In this study, sex did not explain variability after inclusion of fat free mass. However, as few patients were male (3/21), it cannot exclude an independent effect of sex.

In this study, median C_0 concentrations were higher than C_{12}. Similarly,

Heeswijket al. [181] reported that some C_0 concentrations were higher than C_{12} trough concentrations of lopinavir in HIV infected patients, but the effect did not reach statistical significance. Robbin et al. [123] also found diurnal variation in lopinavir pharmacokinetics, with higher concentrations in the morning than in the evening. They attributed this phenomenon to reduced hepatic blood flow during sleep or to change in plasma lipid concentrations during the overnight fast, which may alter the rate of drug absorption or clearance. This pattern of diurnal variation has been identified by other investigators for ritonavir and other protease inhibitors [74,176,182,183]. Since in this study patients received a meal before the evening dose was taken, while the morning dose was taken after a 10 hour fast, food could be a possible explanation for this kind of variation. It was found in this study that lopinavir bioavailability was increased by 42.0% after the evening dose, which is in agreement with a study by Awnlet al. [184], who found that moderate fat content food increased the AUC of lopinavir from 76.5 to 97.1 μg.h/mL (a 26.9% increase).The difference between morning and evening trough concentrations in subjects of this study was more pronounced than that reported by Awnl et al., which indicates the higher C_0 concentrations are unlikely to be entirely explained by a food effect. Besides the difference detected in lopinavir and ritonavir bioavailability, lopinavir and ritonavir oral clearance was found to be slower overnight compared to that following the morning dose (a decreased of 32.7% for lopinavir). Moreover, one may speculate that other effects play a role, e.g. in this study it cannot exclude an absorption interaction between rifampicin (which was given with the morning dose) and LPV/r.

Guidelines for therapeutic drug monitoring recommend a lopinavir trough concentration $\geq$1 mg/L for patients who are naïve to protease inhibitors [185]. For practical reasons, morning trough concentrations are usually used for therapeutic drug monitoring studies linking antiviral effect to antiretroviral concentrations [12124,182,183]. In this study, all patients given 800/200 mg LPV/r with rifampicin

co-administration achieved this target. Therefore, 800/200 mg LPV/r is sufficient for most patients during rifampicin-based ATT, including patients weighing >110 kg. For patients with body weight below 50 kg, 600/150 mg LPV/r is sufficient to maintain lopinavir C_0 concentrations above the target in 95% of subjects during rifampicin treatment. In contrast, it has previously been reported that doubling the dose of LPV/r oral solution in young children failed to achieve target concentrations [186]. Therefore, further research is necessary to elucidate the reasons underlying this difference in the pharmacokinetics between children and adults.

3. Comparison of pharmacokinetics of lopinavir and ritonavir co-administration with rifampicin-based antituberculosis treatment between children and adults

A population model was developed to describe the pharmacokinetics of lopinavir and ritonavir and the drug-drug interactions between lopinavir, ritonavir and rifampicin in children and adults. The model demonstrated important differences in the effects of rifampicin, or rifampicin-based antituberculosis treatment, between adults and children and provides evidence that drug-drug interaction studies in adults should not be used to predict the magnitude of drug-drug interactions in children unless there is good mechanistic understanding of the processes involved.

The application of allometric scaling for body weight on oral clearance and volume of distribution accounted for the different body size of the study populations, thus allowing comparison of the pharmacokinetic parameters between children and adults. The volume of distribution of lopinavir and ritonavir were similar in children and adults after the implementation of allometric scaling. However, for both lopinavir and ritonavir, oral clearance was lower in children than in adults when size differences have been taken into account. This finding

could be explained by incomplete maturation of clearance in the children. The number of children aged below 1 year was 12 (16%) and 35 children (52%) were between 1 and 2 years old. Holford reported that maturation of hepatic and renal clearance of drugs is virtually complete within 2 years of birth, of which the half value is nearly achieved during the first year [187]. Hence, although the maturation model was not supported by data of this study, probably due to insufficient data in children under 1 year, full maturation of enzymes and transporters may not have been achieved in some young children. Moreover, lopinavir and ritonavir are metabolized mainly by CYP3A4, which is profoundly induced by postnatal environmental factors [188]; age-related changes in the composition and amount of circulating plasma proteins may influence the plasma free drug fractions, thus affecting clearance, of highly bound drugs like lopinavir and ritonavir [83]; and, in adults, blood pressure tends to be higher, which may lead to increased hepatic blood flow [189] and then may result in higher clearance than in children.

The model predicted lower bioavailability of lopinavir and markedly reduced bioavailability of ritonavir in children compared to adults. In children, given standard doses of LPV/r without rifampicin co-administration, the bioavailability of ritonavir was calculated to be 24.5% of that in adults on a 400/100 mg dose of LPV/r (Table 3.3.). Meanwhile, the clearance of ritonavir of children was estimated about 61% of that of adults after considering size differences. Therefore, this model predicted concentrations of ritonavir in children much lower than those in adults, which is consistent with the observed concentrations of ritonavir (Figure 3.3). Slower gastric emptying and reduced intestinal motility in children [84], may result in reduced bioavailability. Furthermore, differences in the enzymes and transporters expressed in enterocytes and hepatocytes resulting in altered affinity for the drug substrates may contribute to different bioavailability between adults and children. Differences in the disease status between the adult and paediatric study cohorts could also play a role: The children had recently been diagnosed

with tuberculosis, and tuberculosis could reduce drug absorption [190], whereas the adults were volunteers established on antiretroviral treatment and generally in a good state of health.

Differences in the formulation of LPV/r used in adults and children respectively are likely to have contributed to altered bioavailability. In this study, oral solution was administered to children and tablet to adults. The mean AUC of lopinavir was 22% lower for the LPV/r oral solution relative to the capsule formulation under fasting conditions [22]. Compared to capsule, following a single dose of LPV/r 400/100 mg, the tablet provides similar lopinavir AUC [184]. Moreover, the LPV/r oral solution has poor palatability, and if the children spat out part of their dose, lower model predictions of bioavailability would result. However, the morning dose of LPV/r on the day of pharmacokinetic evaluation was observed by study personnel and no failure to ingest the complete dose was reported. Also, bioavailability of ritonavir seems to have been disproportionately affected, suggesting that other factors play a role. Compared to adults, smaller ka of lopinavir and longer MTT of ritonavir in children were found in this study, which is consistent with the possible reasons that described above, such as slower gastric emptying and motility in children, as well as formulation factors.

The induction of oral clearance of lopinavir and ritonavir by rifampicin was greater in adults than in children (OFV decreased about 10 points). In contrast, the effect of antituberculosis treatment on the bioavailability of lopinavir and ritonavir was greater in children than was the effect of rifampicin in adults (OFV decreased about 30 points). Rifampicin potently induces the expression of CYP3A4 and P-gp both in the liver and in the intestine [67 191]. Whether CYP3A4 and p-glycoprotein in the intestine and liver, respectively, have altered susceptibility in children to induction by PXR-activators such as rifampicin is unknown. The children in this study may not have attained full maturation of hepatic CYP3A4 and P-gp and this

might account for a smaller effect of rifampicin on clearance than that found in adults. Moreover, receptor expression may be different in tuberculosis patients [192], and therefore autoinduction of rifampicin may display diverse between children and adults. However, the potential role of isoniazid which was part of the antituberculosis treatment given to the children and is an inhibitor of CYP3A4 and CYP2D6 [29,105], should be considered. It would counteract the rifampicin induction effect in some degree.

Higher ritonavir doses were associated with increased bioavailability of ritonavir. As ritonavir is an inhibitor and a substrate of Pgp [175], it could inhibit its own efflux from enterocytes and hepatocytes, thus increasing its bioavailability. Increased doses of ritonavir improved the bioavailability of lopinavir in children, but this effect was not supported by data in adults in this study.

Potential weaknesses in this study design include bias in the distribution of certain characteristics. Different dose strategies were given in adults and children in this study and rifampicin was given as part of antituberculosis treatment in children and therefore the rifampicin induction effect may be influenced by other comedications. Most of the adult patients were females (86%). Sex may affect the pharmacokinetics of lopinavir and ritonavir [193], and body composition, which accounts for sex as well, may be important for adults, especially for some obese ones since fat can only contribute to volume but clearance. Food considerably affects the bioavailability of lopinavir and ritonavir [49], and differences in study design with regard to control of food intake could have affected this findings. Lastly, although the treatment doses immediately before pharmacokinetic evaluation were carefully observed, differences in adherence to prior doses of antiretroviral treatment could contribute to the divergent findings between children and adults.

In conclusion, the lower bioavailability of lopinavir and ritonavir, as well as the more potent effect of rifampicin-based antituberculosis treatment on bioavailability in children were the main findings of this study, which sought to explain the failure of double dose LPV/r to achieve adequate concentrations in children on antituberculosis treatment. Ritonavir dose had an important influence on the bioavailability of lopinavir and ritonavir. Prospective studies are needed to confirm the role formulation factors as well as age and sex related changes in enzyme and transporter activity and susceptibility to induction, food and disease effects, different dose regimens and the role of concomitant drugs on the pharmacokinetics of lopinavir and ritonavir when co-administrated with rifampicin in children and adults.

4. Adherence evaluation using lamivudine therapeutic monitoring concentrations

In Paper IV, a population pharmacokinetic model was reported, which includes covariate effects and describes the pharmacokinetic variability of lamivudine in young children. The diurnal variation of observed lamivudine concentrations was explained. Finally, cutoff values for evaluation of adherence to prior doses were proposed using lamivudine concentration drug monitoring.

A two-compartment model best described the pharmacokinetics of lamivudine in this study. One- or two- or three-compartment pharmacokinetic structure models were reported by previous studies. [59–64, 197] Most of these studies reported a half life of 1-3 hours for lamivudine, while some of studies which measured lamivudine concentrations to 48 hours after dosing observed a half life of approximately 12 hours. The longer half life may reflect capture of redistribution from a slowly equilibrating tissue when an extended sampling period was used. [56] The typical value of the half life in this study was 1.7 h, which approximates that

reported from most studies. The delayed onset of absorption was modeled using a series of transit compartments, which was also reported by Van der Walt et al. [196]

Both body weight and age were found to have a significant effect in this model. Body weight was accounted for through allometric scaling for both clearance and volume. Bouazza et al. [131] also used allometric scaling of body weight for clearance and volume in 2-14 year old children, but they did not find any additional effect of age on clearance. Moote et al. [57] reported that body weight and glomerular filtration rate (GFR) influence clearance, but not volume, in adults. Tremoulet et al. [195] found only age as significant covariate in infants without accounting for body weight. In this study, different maturation models were tested but there was no statistically significant difference among them. Therefore, a sigmoidal model was opted, of which results in physiologically plausible predictions when extrapolated outside the observed age range. The age at which half of the maturation of clearance process is reached was about 4 months of postnatal age, compared to around 2 months described by data of Tremoulet et al [195]. Both studies indicate that half of the full maturation of lamivudine clearance is achieved at a very young age, which may explain why Bouazza et al. [131], analyzing slightly older children, did not detect such effect. Burger et al. [133] reported higher CL/F/kg and V/F/kg children under 7 years than in older children. This result was not disagreement to the finding because in this model the CL/F was adjusted for body weight using allometric scaling, which in part accounted for the effect of heavier children having reduced CL/F/kg, hence CL/F/kg decreased with increasing size. L'homme et al. [197] investigated the pharmacokinetics of lamivudine in African children. They reported mean AUC_{12h} values similar to that in the children mean (AUC_{12h} = 5.60 mg.h/L) in children weighing 3-20 kg.

Diurnal variations of lamivudine were investigated in this model, which is the first time to be reported. From Figure 1, median C_0 concentrations were slightly higher

than C_{12}. The clearance of lamivudine was found 16.7% lower overnight. This diurnal variation could not be explained by absorption difference because bioavailability was not found to change significantly after an evening dose compared to a morning dose. Hansen et al. [198] reported lower blood pressure during evening. Skotnicka et al. [199] reviewed diurnal variations of renal activity in livestock and indicated most renal activity had maximum values during the day and minimum values at night. The slower clearance may be related to decreased blood pressure and GFR overnight; but more evidence is needed to support this conjecture.

In order to compare this model to others, simulations were performed to compare this model to Bouazza et al [131] and Tremoulet et al [195]. This model could describe the concentrations in the typical individual for the model reported by Bouazza et al, but does not fit for the data used by Tremoulet et al. This may be due to different populations or study designs or due to ritonavir inhibition effect on transporters [200].

The model built in this thesis has very good prediction property and can be used to investigate drug concentrations or exposure for different dose regimens. However, there is not enough information to support the lower exposure or concentration is related to a reduced virological activity of lamivudine-containing HAART regimen in children. Furthermore, lamivudine plasma concentrations can only be considered as a limited marker of drug exposure as it is the intracellular lamivudine triphosphate metabolite that becomes pharmacologically active [201]. Therefore, it is difficult to investigate optimal dose regimens using plasma pharmacokinetic models. On the other hand, adherence has been shown to be directly related to clinical and virological outcomes of antiretroviral therapy. Higher levels of treatment adherence are associated with improved virological and clinical responses. As low variability of lamivudine clearance (only 8.2%) was

found, the proposed model has good predictive properties and can be used to evaluate adherence to the morning dose prior to a clinic visit. Furthermore, since companion antiretroviral drugs are usually administered at the same time, lamivudine concentrations can be helpful for interpretation of therapeutic drug monitoring results for other drugs in the regimen, like protease inhibitors and nonnucleoside reverse transcriptase inhibitors, which have greater pharmacokinetic variability.

Lamivudine concentration ranges for children with different ages were predicted using this model. As shown in Figure 3.4.13, 6 month-old children are expected to have higher concentrations compared to older children. During clinic-based therapeutic drug monitoring, pre-dose samples (represented by this 12 h concentration), or samples taken at a routine clinic visit (represented by this concentration 4 h after the morning dose) are commonly used. The visual predictive check plots (Figure 3.4.10), 4 h and 12 h after dosing show narrow variability, which is rather predictable. Therefore different percentile of cutoff values 4 h and 12 h after dosing of lamivudine are proposed as indicators of adherence. For patients ranging 6 months to 5 years, 5^{th} percentile of cutoff values for 4 h and 12 h after dosing of 263.6-372.5 and 28.6-62.0 ng/mL respectively. The simulations in this study demonstrate that almost all children who skip the morning dose on the day of their clinic visit, or the morning dose and the dose of the previous evening will have lamivudine concentrations below the proposed 5^{th} percentile cutoff value at 4 h after the morning dose time. Hence, lamivudine concentrations measured in a clinic visit sample can be compared to predicted 5^{th} percentile reference values, and when lower, they are likely to be related to poor adherence to the last dose. This marker of short term adherence is potentially useful for interpretation of therapeutic drug monitoring results of PIs and NNRTIs and further studies are needed to evaluate how it relates to virological outcome.

Ideas about prospective work and limitations

The primary important aim of this thesis was to investigate pharmacokinetics of PI-based antiretrovirals (lopinavir, ritonavir and lamivudine), including the complicated drug-drug interactions with rifampicin. The secondary important aim was to optimize the dose regimens of PI-based antiretrovirals in combination with rifampicin. In this thesis, the population pharmacokinetic models of lopinavir, ritonavir and lamivudine have been built to describe thoroughly the pharmacokinetics of these drugs, as well as the drug-drug interactions between rifampicin-based ATT in different populations. The models also investigated the effect of patient and treatment factors on the pharmacokinetics of these drugs. Different variability, including interindividual, interoccasion and residual variability, has been evaluated. The models can be used as a prior to predict drug concentrations or exposures and therefore to provide a strong reference for dose regimen rationale when PI-based antiretrovirals in combination with rifampicin are given. But due to the model being developed based on specific population and study design, it need to be cautious when apply the models to other populations. A study can be designed in future to investigate whether this models can be expanded to other populations. External validation was not applied for the models in this thesis due to limit data source. It would be a more powerful evidence to confirm the models built in this thesis.

Given this studies were based on a limited number of patients, more prospective studies are needed to verify the pharmacokinetic charactercteristics, safety and efficacy of antiretroviral treatment in a large number of patients. In silico predictions, such as thrice daily dosing approach with LPV/r for children during TB treatment, need to be confirmed in clinical studies. Wide age range of children can be chosen in futher study to investigate pharmacokinetics and drug-drug interactions.

Another important aim of this thesis was to compare pharmacokinetic differences between children and adults. The first comparison between pharmacokinetics of lopinavir and ritonavir with rifampicin-based ATT coadministration in children and adults was investigated in this thesis. A further meticulous study can be designed to exclude other factors might influence the conclusion, such as dose, formulations, companion TB drugs, disease status. Disease progress in patients may influence pharmacokinetics of lopinavir and ritonavir, and might affect rifampicin induction as well. In future, if possible, the disease progress could be considered together with pharmacokinetic model, in which new findings might be found.

The last important aim of this thesis was to investigate reference drug concentrations for adherence evaluation. Reference lamivudine concentrations were investigated for adherence evaluation based on the population pharmacokinetic model built in this thesis. However, besides poor adherence, low concentrations of patients can be related to other factors, such as give food concurrently with drugs. Therefore, in the future, a study can be developed to further confirm the reference values proposed by this thesis.

Conclusions

In this thesis, pharmacometric models with improved prediction of antiretroviral agents with co-administration of rifampicin-based ATT were developed. A population pharmacokinetic model was built to simultaneously describe the pharmacokinetics of lopinavir and ritonavir, capturing the complicated drug-drug interactions between lopinavir, ritonavir and rifampicin in young children and adults respectively. The models describe clearly the influence on the lopinavir concentrations of induction by rifampicin and inhibition by ritonavir. Considering the major concern of administration of ART and ATT concurrently is sub-therapeutic drug concentrations due to drug-drug interaction, the model has good prediction properties and can be used to investigate optimal dose regimens when lopinavir/ritonavir is co-administered with rifampicin-based ATT.

Allometric scaling of body size, including body weight and fat free mass, was used to scale oral clearance and volume of distribution of both lopinavir and ritonavir in young children and adults. Hence, children or adults with low body weight receiving rifampicin-based ATT require higher mg/kg doses of lopinavir/ritonavir (no matter in 4:1 or 1:1 ratio) than heavy patients. Oral clearance of lopinavir was inhibited dynamically by ritonavir concentrations in a sigmoid relationship. The model was used to predict the doses of LPV/r needed to maintain therapeutic concentrations of lopinavir during ATT and suggests that an 8 hourly dosing regimen should be evaluated in young children. In adults, doubling the dose of LPV/r is required for most patients during rifampicin-based ATT, but for patients weighing less than 50 kg, 600/150 mg LPV/r can maintain lopinavir trough concentrations above the recommended minimum concentration. The higher concentrations detected in the morning trough concentrations compared with the evening troughs, are explained by both higher bioavailability due to a food effect (the evening dose was taken with a meal and the morning dose when fasting) and

lower clearance overnight.

Double dose strategy can attain target lopinavir concentration in adults, but it failed in most of young children when co-administration of rifampicin-based ATT. A more comprehensive population pharmacokinetic model was developed to compare the difference of pharmacokinetics of lopinavir and ritonavir in children and adults. For both lopinavir and ritonavir, a lower bioavailability of children was found compare to adults, and a stronger induction effect of rifampicin on the bioavailability was detected in children. The low bioavailability in children might be the main reason to explain the different behaviors of double dose strategy in children and adults. Ritonavir dose will increase the bioavailability of lopinavir or ritonavir, but this effect was also found different in children and adults. The model elucidates thoroughly, in children and adults, the pharmacokinetics of lopinavir and ritonavir, and accounts for drug-drug interaction with rifampicin. This model has extended the available knowledge and would helpful to improve the clinical outcome.

Lamivudine was used to develop a population model to predict reference concentrations for adherence evaluation. The model has very good prediction properties and can also be used to simulate an alternative dose regimen. Compared to lopinavir, lamivudine is more predictable due to low variability and less drug-drug interactions occurs. The patient whose concentrations are lower than the reference values investigated in this theis is high likely to behave poor adherence. The model has provided an optional approach to evaluate adherence of patients in order to enhance antiretroviral treatment effect and help for interpretation of therapeutic drug monitoring results of PIs and NNRTIs.

In conclusion, population pharmacokinetic models for antiretroviral agents (lopinavir, ritonavir and lamivudine) co-administration with rifampicin-based ATT

were developed. Those models are strong basis for the dose regimen rationale when concomitant with ART and ATT in subpopulations or individual, as well as in adherence evaluation. The developed models and methods may also demonstrate principles in study of treatment improvement in HIV/TB patients and could be useful for pharmacometric community.

Acknowledgement

The work presented in this thesis was carried out at the Division of Clinical Pharmacology, Department of Medicine, University of Cape Town.

I would like to thank my funding first to support my PhD study, which is Wellcome Trust Programme Grant (083851/Z/07/Z). Thanks Professor Gerry Davies for kindly manage and provide this financial support for my PhD study.

I would like to express my sincere gratitude and appreciation to the following persons who have all contributed to this thesis and have been very important to me throughout my time of study.

My supervisor, Professor Helen McIlleron, for giving me the opportunity to study my PhD degree and for sharing your vast knowledge and enthusiasm about research. I appreciate all the care and consideration you have always shown for me and rewarding discussion during these years. Thanks for all your support, especially when I first came to Cape Town and started my work, for being positive and encouraging.

My co-supervisor Dr. Paolo Denti for your help on NONMEM software and modeling building. Thanks for all your helpful ideas, rewarding discussion, critical thinking and supports.

My co-supervisor Professor Mats O Karlsson for your vast scientific knowledge that you generously share, for your amazing ideas on modeling and for your kindly help.

My co-supervisor Professor Ulrika SH Simonsson for your encouragement,

thoughtfulness and critical thinking. Thanks for all your input in my work and your valuable ideas on my modeling. I would also thank you for your care and concern besides study.

Professor Gary Maartens for all scientific discussions and valuable knowledge you contributed to this work, and for your support and creating a great working atmosphere at the division.

Professor Peter Smith for all your kindly support and scientific discussion for my study, and also for managing my funding.

Dr. Jan-Stefan van der Walt for scientific discussion and all modeling help, especially at the beginning of my work with NONMEM.

Professor Nick Horford for your scientific discussion and valuable knowledge you contribute to my study, thanks for your time sharing with me to answer my questions patiently and your unique angle for research questions.

Wynand Smythe, Emmanuel Chigutsa, Simbarashe Peter Zvada, for discussion and all helps from you. I am very happy to be one member of our great group and I want to thank all lot of wonderful time with you all together.

My friend Ludvig Heiberg, for your care and concern for my life, for your encouragement and consolation when I was in difficulties. I really want to say thanks to you for your help on my language review in this thesis.

My friend Rory Leisegang for your friendship to make me cheer up to overcome a lot of difficulties and thanks for your company to make a lot of fun.

Acknowledgement

The Laboratory of Department of Clinical Pharmacology of University of Cape Town for drug assay.

Thanks all present and former colleagues at the division, for your friendly and kindly smile and support, thanks for indelible birthday cakes I had before, thanks for all suggestions from department seminars.

Thanks all colleagues at the Department of Pharmaceutical Biosciences, Faculty of Pharmacy, Uppsala University, for friendly atmosphere. I would like to especially thank Kajsa Harling for your support and help on cluster and PsN. Thanks Elin Svensson, for your friendship, encouragement and many helps when I was in Sweden.

My previous colleagues at Peking University Third Hospital, for your active support and kind encouragement for my study. I would like to especially thank Professor Suodi Zhai for invaluable advices and care for myself and my families. Professor Rongsheng Zhao, Professor Xiaole Zhang and Professor Jingli Duan for your active support. Professor Yiheng Yang for your concerns on my work and daily life.

Thanks all my friends around me no matter where you are, for all your cherish friendship, for joy and happiness you have brought to me, which is the most treasure in my life.

Finally, I want to give my special appreciate to my husband and my daughter. Thanks for your love and support, giving me courage to overcome all kind of difficulties, for believing in me and encouraging me, simply, without you I would not have come that far, and you are the key to all of my achievement. Lots of thanks to my parents and my mother in law, for always support me and help me to

look after my daughter.

Reference

1. World Health Organization *Global HIV/AIDS response: epidemic update and health sector progress towards universal access.Progress report 2011*. at < http://www.who.int/hiv/pub/progress_report2011/en/>

2. World Health Organization *Global HIV/AIDS response: epidemic update and health sector progress towards universal access.Progress report 2011*.

3. World Health Organization *Global Tuberculosis Control*. *Control* (2010).

4. Small, P. M. *et al.* Exogenous reinfection with multidrug-resistant Mycobacterium tuberculosis in patients with advanced HIV infection. *The New England journal of medicine* 328, 1137–44 (1993).

5. Daley, C. L. *et al.* An outbreak of tuberculosis with accelerated progression among persons infected with the human immunodeficiency virus. An analysis using restriction-fragment-length polymorphisms. *The New England journal of medicine* 326, 231–5 (1992).

6. World Health Organization *Antiretroviral therapy for HIV infection in adults and adolescents - recommendations for a public health approach*. *World Health* (2010).

7. Noor, M. A. *et al.* The effects of HIV protease inhibitors atazanavir and lopinavir/ritonavir on insulin sensitivity in HIV-seronegative healthy adults. *AIDS (London, England)* 18, 2137–44 (2004).

8. Noor, M. A. *et al.* The effects of HIV protease inhibitors atazanavir and lopinavir/ritonavir on insulin sensitivity in HIV-seronegative healthy adults. *AIDS (London, England)* 18, 2137–44 (2004).

9. Frohoff, C. *et al.* Antiretroviral therapy outcomes in HIV-infected children after adjusting protease inhibitor dosing during tuberculosis treatment. *PloS one* 6, e17273 (2011).

10. Huisman, M. T., Smit, J. W. & Schinkel, A. H. Significance of P-glycoprotein for the pharmacology and clinical use of HIV protease inhibitors. *AIDS (London, England)* 14, 237–42 (2000).

11. Mcilleron, H. & Khoo, S. H. Interactions between Antituberculosis and Antiretroviral Agents. *Prog Respir Res* 40, 1–12 (2011).

12. Porte, C. L. J. L. *et al.* Pharmacokinetics of adjusted-dose lopinavir-ritonavir combined with rifampin in healthy volunteers. *Antimicrobial agents and chemotherapy* 48, 1553–1560 (2004).

13. Department of Health and Human Services, C. for D. C. *Managing Drug Interactions in the Treatment of HIV-Related Tuberculosis*. *The international journal of tuberculosis and lung disease: the official journal of the International Union against Tuberculosis and Lung Disease* 9, (2010).

14. Apor, M. I. J. Z. & Ozza, K. E. L. C. Med-Psych Drug-Drug Interactions Update Antiretrovirals, Part II: Focus on Non-Protease Inhibitor Antiretrovirals (NRTIs, NNRTIs, and Fusion Inhibitors). *Psychosomatics* (2004).

15. Balzarini, J. Current status of the non-nucleoside reverse transcriptase inhibitors of human immunodeficiency virus type 1. *Current topics in medicinal chemistry* 4, 921–44 (2004).

16. Boffito, M. *et al.* Protein binding in antiretroviral therapies. *AIDS research and human retroviruses* 19, 825–35 (2003).

17. Bonfanti, P. *et al.* Incidence of adverse reactions in HIV patients treated with protease inhibitors: a cohort study. Coordinamento Italiano Studio Allergia e Infezione da HIV (CISAI) Group. *Journal of acquired immune deficiency syndromes (1999)* 23, 236–45 (2000).

18. Flentge, C. A. *et al.* Synthesis and evaluation of inhibitors of cytochrome P450 3A (CYP3A) for pharmacokinetic enhancement of drugs. *Bioorganic & medicinal chemistry letters* 19, 5444–8 (2009).

19. Jetter, A. *et al.* Do activities of cytochrome P450 (CYP) 3A , CYP2D6 and P-glycoprotein differ between healthy volunteers and HIV-infected patients□? *Antiviral Therapy* 983, 975–983 (2010).

20. Washington, C. Effect of simultaneous versus staggered dosing on pharmacokinetic interactions of protease inhibitors. *Clinical Pharmacology & Therapeutics* 73, 406–416 (2003).

21. Ii, C. S. E., Hall, S. D. & Jones, D. R. Mechanism-Based Inactivation of CYP3A by HIV Protease Inhibitors. *Pharmacology* 312, 583–591 (2005).

22. Porche, D. J. & Care, A. Lopinavir/Ritonavir. *Journal of the Association of Nurses in AIDS care* 12, 101–104 (2001).

23. Wyen, C. *et al.* Effect of an antiretroviral regimen containing ritonavir boosted lopinavir on intestinal and hepatic CYP3A, CYP2D6 and P-glycoprotein in HIV-infected patients. *Clinical pharmacology and therapeutics* 84, 75–82 (2008).

24. Jayakanthan, M., Chandrasekar, S., Muthukumaran, J. & Mathur, P. P. Analysis of CYP3A4-HIV-1 protease drugs interactions by computational methods for Highly Active Antiretroviral Therapy in HIV/AIDS. *Journal of molecular graphics & modelling* 28, 455–63 (2010).

25. Lee, G. A. *et al.* Effects of ritonavir and amprenavir on insulin sensitivity in healthy volunteers. *AIDS (London, England)* 21, 2183–90 (2007).

26. World Health Organization *Treatment of Tuberculosis - Guidelines*. (2009).

27. World Health Organization *Guidelines for intensified tuberculosis case-finding and isoniazid preventive therapy for people living with HIV in resource- constrained settings*. *World Health*

28. Leucuta, S. E. & Vlase, L. Pharmacokinetics and metabolic drug interactions. *Current clinical pharmacology* 1, 5–20 (2006).

29. Desta, Z., Soukhova, N. V & Flockhart, D. A. Inhibition of cytochrome P450 (CYP450) isoforms by isoniazid: potent inhibition of CYP2C19 and CYP3A. *Antimicrobial agents and chemotherapy* 45, 382–92 (2001).

30. Cvetkovic, R. S. & Goa, K. L. Lopinavir/ritonavir: a review of its use in the management of HIV infection. *Drugs* 63, 769–802 (2003).

31. World Health Organization *Antiretroval therapy for HIV infection in infants and children: towards universal access recommendations for a public health approach*. *World Health* (2010).

32. South Africa, D. H. *THE SOUTH AFRICAN ANTIRETROVIRAL TREATMENT GUIDELINES*. (2010).

33. Paul Palumbo, A Violari, J Lindsey, M Hughes, P Jean-Philippe, L Mofenson, M Bwakura-Dangarembizi, P Kamthunzi, S Eshleman, L Purdue, and I. P. T. NVP- vs LPV/r-based ART among HIV+ Infants in Resource-limited Settings: The IMPAACT P1060 Trial. *18th Conference on Retroviruses and Opportunistic Infections (CROI).February 27-March 3, 2011. Oral abstract:129LB*

34. Hurst, M. & Faulds, D. Lopinavir. *Drugs* 60, 1371–9; discussion 1380–1 (2000).

35. Oldfield, V. & Plosker, G. L. Lopinavir/ritonavir: a review of its use in the management of HIV infection. *Drugs* 66, 1275–99 (2006).

36. Lucia, M. B. *et al.* Exposure to HIV-protease inhibitors selects for increased expression of P-glycoprotein (ABCB1) in Kaposi's sarcoma cells. *British journal of cancer* 105, 513–22 (2011).

37. Gorny, M., Röhm, S., Läer, S., Morali, N. & Niehues, T. Pharmacogenomic adaptation of antiretroviral therapy: overcoming the failure of lopinavir in an African infant with CYP2D6 ultrarapid metabolism. *European journal of clinical pharmacology* 66, 107–8 (2010).

38. Rakhmanina, N. *et al.* Population pharmacokinetics of lopinavir predict suboptimal therapeutic concentrations in treatment-experienced human immunodeficiency virus-infected children. *Antimicrobial agents and chemotherapy* 53, 2532–8 (2009).

39. Sulkowski, M. S., Mehta, S. H., Chaisson, R. E., Thomas, D. L. & Moore, R. D. Hepatotoxicity associated with protease inhibitor-based antiretroviral regimens with or without concurrent ritonavir. *Aids* 18, 2277 (2004).

40. Sham, H. L. *et al.* ABT-378, a highly potent inhibitor of the human immunodeficiency virus protease. *Antimicrobial agents and chemotherapy* 42, 3218–24 (1998).

41. Olson, D. P., Scadden, D. T., D'Aquila, R. T. & De Pasquale, M. P. The protease inhibitor ritonavir inhibits the functional activity of the multidrug resistance related-protein 1 (MRP-1). *AIDS (London, England)* 16, 1743–7 (2002).

42. van Heeswijk, R. P. *et al.* Combination of protease inhibitors for the treatment of HIV-1-infected patients: a review of pharmacokinetics and clinical experience. *Antiviral therapy* 6, 201–29 (2001).

43. Cypc, C. P. E. *et al.* Lopinavir/ritonavir induces the hepatic activity of cytochrome P450 enzymes CYP2C9, CYP2C19, and CYP1A2 but inhibits the hepatic and intestinal activity of CYP3A as measured by a phenotyping drug cocktail in healthy volunteers. *Journal of acquired immune deficiency syndromes (1999)* 42, 52–60 (2006).

44. Crommentuyn, K. M. L. *et al.* The plasma and intracellular steady-state pharmacokinetics of lopinavir/ritonavir in HIV-1-infected patients. *Antiviral therapy* 9, 779–85 (2004).

45. Murphy, R. L. *et al.* ABT-378/ritonavir plus stavudine and lamivudine for the treatment of antiretroviral-naive adults with HIV-1 infection: 48-week results. *AIDS (London, England)* 15, F1–9 (2001).

46. World Health Organization *ic health approachANTIRETROVIRAL THERAPY FOR HIV INFECTION IN ADULTS AND ADOLESCENTS - Recommendations for a publ. World Health* (2010).

47. Eron, J. J. *et al.* Once-daily versus twice-daily lopinavir/ritonavir in antiretroviral-naive HIV-positive patients: a 48-week randomized clinical trial. *The Journal of infectious diseases* 189, 265–72 (2004).

48. L. GUSTAVSON, W. LAM, R. BERTZ, A.HSU, K. RYNKIEWICZ, J. QI, S. GHOSH, I FACEY, B. BERNSTEIN, E. S. Assessment of the Bioequivalence and Food Effects for Liquid and Soft Elastic Capsule Co-formulations of ABT-378/ritonavir (ABT-378/r) in Healthy Subjects.

40th Interscience Conference on Antimicrobial Agents and Chemotherapy (ICAAC)

49. W Awni1,Y-L Chiu1,T Zhu1, N Braun1, C Klein1, R Heuser1, J Breitenbach2, J Morris1,T Doan1, S. B. and G. H. Significantly Reduced Food Effect and Pharmacokinetic Variability with a Novel Lopinavir/ritonavir Tablet Formulation. *Third IAS Conference on HIV Pathogenesis and Treatment*

50. Abbott Laboratories *Kaletra® (lopinavir/ritonavir) tablets and oral solution. Prescribing information. [online]*. (Available from URL: http://www.kaletra.com [Accessed 2005 Nov 15],).

51. Barth, R. E., van der Loeff, M. F. S., Schuurman, R., Hoepelman, A. I. M. & Wensing, A. M. J. Virological follow-up of adult patients in antiretroviral treatment programmes in sub-Saharan Africa: a systematic review. *The Lancet infectious diseases* 10, 155–66 (2010).

52. Achenbach, C. J., Scarsi, K. K. & Murphy, R. L. Abacavir/lamivudine fixed-dose combination antiretroviral therapy for the treatment of HIV. *Advances in therapy* 27, 1–16 (2010).

53. Lewis, L. L. *et al.* Lamivudine in children with human immunodeficiency virus infection: a phase I/II study. The National Cancer Institute Pediatric Branch-Human Immunodeficiency Virus Working Group. *The Journal of infectious diseases* 174, 16–25 (1996).

54. Ormseth, E. J. *et al.* Hepatic decompensation associated with lamivudine: a case report and review of lamivudine-induced hepatotoxicity. *The American journal of gastroenterology* 96, 1619–22 (2001).

55. Rodriguez, A. E. *et al.* Efficacy and Safety of Abacavir / Lamivudine / Zidovudine Plus Tenofovir in HBV / HIV-1 Coinfected Adults: 48-Week Data. *Aids* 167–170 (2010).

56. Johnson, M. A., Moore, K. H., Yuen, G. J., Bye, A. & Pakes, G. E. Clinical pharmacokinetics of lamivudine. *Clinical pharmacokinetics* 36, 41–66 (1999).

57. Moore, K. H. P. *et al.* Population Pharmacokinetics of Lamivudine in Adult Human Immunodeficiency Virus-Infected Patients Enrolled in Two Phase III Clinical Trials. *Society* 43, 3025–3029 (1999).

58. Panhard, X. *et al.* Population pharmacokinetic analysis of lamivudine, stavudine and zidovudine in controlled HIV-infected patients on HAART. *European journal of clinical pharmacology* 63, 1019–29 (2007).

59. Sabo, J. P., Lamson, M. J., Leitz, G., Yong, C. L. & MacGregor, T. R. Pharmacokinetics of nevirapine and lamivudine in patients with HIV-1 infection. *AAPS pharmSci* 2, E1 (2000).

60. Marier, J. F. *et al.* Pharmacokinetics of lamivudine, zidovudine, and nevirapine administered as a fixed-dose combination formulation versus coadministration of the individual products. *Journal of clinical pharmacology* 47, 1381–9 (2007).

61. Moore, K. H. P. *et al.* Population Pharmacokinetics of Lamivudine in Adult Human Immunodeficiency Virus-Infected Patients Enrolled in Two Phase III Clinical Trials. *Society* 43, 3025–3029 (1999).

62. Tuon, F. F., Guastini, C. M. de F. & Boulos, M. I. C. Acute pancreatitis associated with lamivudine therapy for chronic B hepatitis. *The Brazilian journal of infectious diseases: an official publication of the Brazilian Society of Infectious Diseases* 12, 263 (2008).

63. Van Dyke, R. B., Wang, L. & Williams, P. L. Toxicities associated with dual nucleoside reverse-transcriptase inhibitor regimens in HIV-infected children. *The Journal of infectious diseases* 198, 1599–608 (2008).

64. Manfredi, R. & Calza, L. HIV infection and the pancreas: risk factors and potential management guidelines. *International journal of STD & AIDS* 19, 99–105 (2008).

65. sanofi-aventis U.S. LLC *Rifampicin package insert. RIFADIN®(rifampin capsules).*

66. Zhang, B., Xie, W. & Krasowski, M. D. PXR: a xenobiotic receptor of diverse function implicated in pharmacogenetics. *Pharmacogenomics* 9, 1695–709 (2008).

67. Niemi, M., Backman, J. T., Fromm, M. F., Neuvonen, P. J. & Kivist, K. T. Pharmacokinetic Interactions with Rifampicin. *Clinical Pharmacokinetics* 42, 819–850 (2003).

68. Gurumurthy, P. *et al.* Decreased Bioavailability of Rifampin and Other Antituberculosis Drugs in Patients with Advanced Human Immunodeficiency Virus Disease. *Society* 48, 4473–4475 (2004).

69. Sahai, J. *et al.* Reduced plasma concentrations of antituberculosis drugs in patients with HIV infection. *Annals of internal medicine* 127, 289–93 (1997).

70. Gurumurthy, P. *et al.* Malabsorption of rifampin and isoniazid in HIV-infected patients with and without tuberculosis. *Clinical infectious diseases: an official publication of the Infectious Diseases Society of America* 38, 280–3 (2004).

71. Wilkins, J. J. *et al.* Population pharmacokinetics of rifampin in pulmonary tuberculosis patients, including a semimechanistic model to describe variable absorption. *Antimicrobial agents and chemotherapy* 52, 2138–48 (2008).

72. Ndanusa, B. U., Mustapha, A. & Abdu-Aguye, I. The effect of single does of rifampicin on the pharmacokinetics of oral nifedipine. *Journal of pharmaceutical and biomedical analysis* 15, 1571–5 (1997).

73. Herman, R. J., Nakamura, K., Wilkinson, G. R. & Wood, A. J. J. INDUCTION OF PROPRANOLOL METABOLISM BY RIFAMPICIN. *Blood* 565–569 (1983).

74. Fabbiani, M. *et al.* Pharmacokinetic variability of antiretroviral drugs and correlation with virological outcome: 2 years of experience in routine clinical practice. *The Journal of antimicrobial chemotherapy* 64, 109–17 (2009).

75. Kwara, A. *et al.* Interindividual variability in pharmacokinetics of generic nucleoside reverse transcriptase inhibitors in TB/HIV-coinfected Ghanaian patients: UGT2B7*1c is associated with faster zidovudine clearance and glucuronidation. *Journal of clinical pharmacology* 49, 1079–90 (2009).

76. Stöhr, W. *et al.* Factors influencing efavirenz and nevirapine plasma concentration: effect of ethnicity, weight and co-medication. *Antiviral therapy* 13, 675–85 (2008).

77. Arab-Alameddine, M. *et al.* Pharmacogenetics-based population pharmacokinetic analysis of efavirenz in HIV-1-infected individuals. *Clinical pharmacology and therapeutics* 85, 485–94 (2009).

78. Mukonzo, J. K. *et al.* A novel polymorphism in ABCB1 gene, CYP2B6*6 and sex predict single-dose efavirenz population pharmacokinetics in Ugandans. *British journal of clinical pharmacology* 68, 690–9 (2009).

79. Burger, D. *et al.* Interpatient variability in the pharmacokinetics of the HIV non-nucleoside reverse transcriptase inhibitor efavirenz: the effect of gender, race, and CYP2B6 polymorphism. *British journal of clinical pharmacology* 61, 148–54 (2006).

80. Ren, Y. *et al.* Effect of rifampicin on efavirenz pharmacokinetics in HIV-infected children with tuberculosis. *Journal of acquired immune deficiency syndromes (1999)* 50, 439–43 (2009).

81. Friedland, G., Khoo, S., Jack, C. & Lalloo, U. Administration of efavirenz (600 mg/day) with rifampicin results in highly variable levels but excellent clinical outcomes in patients treated for tuberculosis and HIV. *The Journal of antimicrobial chemotherapy* 58, 1299–302 (2006).

82. Mahmood, I. Prediction of drug clearance in children from adults: a comparison of several allometric methods. *British journal of clinical pharmacology* 61, 545–57 (2006).

83. Pelkonen, O. Metabolism and pharmacokinetics in children and the elderly. *Expert opinion on drug metabolism & toxicology* 3, 147–8 (2007).

84. Hattis, D. *et al.* Differences in pharmacokinetics between children and adults--II. Children's variability in drug elimination half-lives and in some parameters needed for physiologically-based pharmacokinetic modeling. *Risk analysis: an official publication of the Society for Risk Analysis* 23, 117–42 (2003).

85. Hoefnagel, J. G. M. *et al.* The genotypic inhibitory quotient and the (cumulative) number of mutations predict the response to lopinavir therapy. *AIDS (London, England)* 20, 1069–71 (2006).

86. la Port, C. J. L. *et al.* Updated guideline to perform therapeutic drug monitoring for antiretroviral agents Fosamprenavir. *Antiviral Therapy* 3, (2006).

87. Obach, R. S. Drug-drug interactions: an important negative attribute in drugs. *Drugs of today (Barcelona, Spain□: 1998)* 39, 301–38 (2003).

88. Fish, D. N. Fluoroquinolone Adverse Effects and Drug Interactions. *Pharmacotherapy* 21, 253S–272S (2001).

89. Guengerich, F. P. Cytochrome P-450 3A4: regulation and role in drug metabolism. *Annual review of pharmacology and toxicology* 39, 1–17 (1999).

90. Kenworthy, K. E., Bloomer, J. C., Clarke, S. E. & Houston, J. B. CYP3A4 drug interactions: correlation of 10 in vitro probe substrates. *British journal of clinical pharmacology* 48, 716–27 (1999).

91. Shen, D., Kunze, K. & Thummel, K. Enzyme-catalyzed processes of first-pass hepatic and intestinal drug extraction. *Advanced drug delivery reviews* 27, 99–127 (1997).

92. Watkins, P. The barrier function of CYP3A4 and P-glycoprotein in the small bowel. *Advanced drug delivery reviews* 27, 161–170 (1997).

93. Ogu, C. C. & Maxa, J. L. Drug interactions due to cytochrome P450. *Proceedings (Baylor University. Medical Center)* 13, 421–3 (2000).

94. Venkatakrishnan, K., Obach, R. S. & Rostami-Hodjegan, a Mechanism-based inactivation of human cytochrome P450 enzymes: strategies for diagnosis and drug-drug interaction risk assessment.

Xenobiotica; the fate of foreign compounds in biological systems 37, 1225–56

95. Zhang, L., Zhang, Y. & Huang, S. reviews Scientific and Regulatory Perspectives on Metabolizing Enzyme-Transporter Interplay and Its Role in Drug Interactions□: Challenges in Predicting Drug Interactions †. *Molecular Pharmaceutics* 6, 1766–1774 (2009).

96. Chien, J. Y., Thummel, K. E. & Slattery, J. T. Pharmacokinetic consequences of induction of CYP2E1 by ligand stabilization. *Drug metabolism and disposition: the biological fate of chemicals* 25, 1165–75 (1997).

97. Galetin, A., Burt, H., Gibbons, L. & Houston, J. B. Prediction of time-dependent CYP3A4 drug-drug interactions: impact of enzyme degradation, parallel elimination pathways, and intestinal inhibition. *Drug metabolism and disposition: the biological fate of chemicals* 34, 166–75 (2006).

98. Lin, J. H. CYP induction-mediated drug interactions: in vitro assessment and clinical implications. *Pharmaceutical research* 23, 1089–116 (2006).

99. Grime, K. H., Bird, J., Ferguson, D. & Riley, R. J. Mechanism-based inhibition of cytochrome P450 enzymes: an evaluation of early decision making in vitro approaches and drug-drug interaction prediction methods. *European journal of pharmaceutical sciences: official journal of the European Federation for Pharmaceutical Sciences* 36, 175–91 (2009).

100. Hassan, M. *et al.* A mechanism-based pharmacokinetic-enzyme model for cyclophosphamide autoinduction in breast cancer patients. *British journal of clinical pharmacology* 48, 669–77 (1999).

101. Bjornsson, T. D. *et al.* The conduct of in vitro and in vivo drug-drug interaction studies: a Pharmaceutical Research and Manufacturers of America (PhRMA) perspective. *Drug metabolism and disposition: the biological fate of chemicals* 31, 815–32 (2003).

102. Ito, K. *et al.* Prediction of in vivo drug-drug interactions based on mechanism-based inhibition from in vito data: inhibition of 5-fluorouracil metabolism by (E)-5-(2-bromovinyl)uracil. *Pharmacology* 28, 2–9 (2000).

103. Kumar, G. N. *et al.* Potent inhibition of the cytochrome P-450 3A-mediated human liver microsomal metabolism of a novel HIV protease inhibitor by ritonavir: a positive drug-drug interaction. *Pharmacology* 27, 902–908 (1999).

104. Rodrigues, A. D., Winchell, G. A. & Pharmacol, C. The Journal of Clinical Use of In Vitro Drug Metabolism Data to Evaluate Metabolic Drug-Drug Interactions in Man□: The Need. *The Journal of Clinical Pharmacology* (2001).

105. Wen, X., Wang, J.-S., Neuvonen, P. & Backman, J. Isoniazid is a mechanism-based inhibitor of cytochrome P 450 1A2, 2A6, 2C19 and 3A4 isoforms in human liver microsomes. *European Journal of Clinical Pharmacology* 57, 799–804 (2002).

106. Faber, K. N., Müller, M., Jansen, P. L. M., Nico, K. & Muller, M. Drug transport proteins in the liver. *Advanced drug delivery reviews* 55, 107–24 (2003).

107. Kalliokoski, A. & Niemi, M. Impact of OATP transporters on pharmacokinetics. *British Journal of Pharmacology* 1, 693–705 (2009).

108. Niemi, M. Role of OATP transporters in the disposition of drugs. 8, 787–802 (2007).

109. Tsuji, A. Impact of transporter-mediated drug absorption, distribution, elimination and drug interactions in antimicrobial chemotherapy. *Journal of infection and chemotherapy□: official journal of the Japan Society of Chemotherapy* 12, 241–50 (2006).

110. Hagenbuch, B. & Meier, P. J. Organic anion transporting polypeptides of the OATP/ SLC21 family: phylogenetic classification as OATP/ SLCO superfamily, new nomenclature and molecular/functional properties. *Pflügers Archiv□: European journal of physiology* 447, 653–65 (2004).

111. Shugarts, S. & Benet, L. Z. The role of transporters in the pharmacokinetics of orally administered drugs. *Pharmaceutical research* 26, 2039–54 (2009).

112. Reitman, M. L. *et al.* Rifampin's acute inhibitory and chronic inductive drug interactions: experimental and model-based approaches to drug-drug interaction trial design. *Clinical pharmacology and therapeutics* 89, 234–42 (2011).

113. Lin, J. H. Drug-drug interaction mediated by inhibition and induction of P-glycoprotein. *Advanced drug delivery reviews* 55, 53–81 (2003).

114. Jung, N. & Taubert, D. Organic cation transporters and their roles in antiretroviral drug disposition. *Expert opinion on drug metabolism & toxicology* 5, 773–87 (2009).

115. Negishi*, Y. E. T. and M. CAR and PXR: The Xenobiotic-Sensing Receptors. *Steroids.* 72, 231–246 (2007).

116. Itsuya, H. M., Anoue, N. T., Amada, A. H. & Aito, H. S. P-Glycoprotein Mediates Efflux Transport of Darunavir in Human Intestinal Caco-2 and ABCB1 Gene-Transfected Renal LLC-PK1 Cell Lines. *Transport* 32, 1588–1593 (2009).

117. Grover, A. & Benet, L. Z. Effects of drug transporters on volume of distribution. *The AAPS journal* 11, 250–61 (2009).

118. Chen, J. & Raymond, K. Roles of rifampicin in drug-drug interactions: underlying molecular mechanisms involving the nuclear pregnane X receptor. *Annals of clinical microbiology and antimicrobials* 5, 3 (2006).

119. Goodwin, B., Hodgson, E., D'Costa, D. J., Robertson, G. R. & Liddle, C. Transcriptional regulation of the human CYP3A4 gene by the constitutive androstane receptor. *Molecular pharmacology* 62, 359–65 (2002).

120. Boulanger, C. *et al.* Pharmacokinetic Evaluation of Rifabutin in Combination with Lopinavir-Ritonavir in Patients with HIV Infection and Active Tuberculosis. *Clinical Infectious Diseases* 0486, 1305–1311 (2009).

121. Merry, C. *et al.* Saquinavir pharmacokinetics alone and in combination with ritonavir in HIV-infected patients Drug analysis. *Aids* 29–33 (1997).

122. Winston, A. *et al.* Effect of omeprazole on the pharmacokinetics of saquinavir-500 mg formulation with ritonavir in healthy male and female volunteers. *Aids* 1401–1406 (2006).

123. Robbins, B. L. *et al.* Pharmacokinetics of high-dose lopinavir-ritonavir with and without saquinavir or nonnucleoside reverse transcriptase inhibitors in human immunodeficiency virus-infected pediatric and adolescent patients previously treated with protease inhibitors. *Antimicrobial agents and chemotherapy* 52, 3276–83 (2008).

124. Decloedt, E. H. *et al.* Pharmacokinetics of lopinavir in HIV-infected adults receiving rifampin with adjusted doses of lopinavir-ritonavir tablets. *Antimicrobial agents and chemotherapy* 55, 3195–200 (2011).

125. L, F. A. *et al.* High incidence of adverse events in healthy volunteers receiving rifampicin and adjusted doses of lopinavir/ritonavir tablets. *AIDS (London, England)* 22, 931–5 (2008).

126. Frohoff, C. *et al.* Antiretroviral therapy outcomes in HIV-infected children after adjusting protease inhibitor dosing during tuberculosis treatment. *PloS one* 6, e17273 (2011).

127. Ren, Y. *et al.* Effect of rifampicin on lopinavir pharmacokinetics in HIV-infected children with tuberculosis. *Journal of acquired immune deficiency syndromes (1999)* 47, 566–9 (2008).

128. Bangsberg, D. R. *et al.* Adherence to protease inhibitors, HIV-1 viral load, and development of drug resistance in an indigent population. *AIDS (London, England)* 14, 357–66 (2000).

129. USAID *Adult adherence to treatment and retention care*. *Development* 1–43at <http://www.aidstar-one.com/focus_areas/treatment/resources/technical_briefs/adult_adherence_treatment_and_retention_care>

130. Rosenblum, M., Deeks, S. G., van der Laan, M. & Bangsberg, D. R. The risk of virologic failure decreases with duration of HIV suppression, at greater than 50% adherence to antiretroviral therapy. *PloS one* 4, e7196 (2009).

131. Bouazza, N. *et al.* Is the recommended once-daily dose of lamivudine optimal in West African HIV-infected children? *Antimicrobial agents and chemotherapy* 54, 3280–6 (2010).

132. van Leeuwen, R. *et al.* The safety and pharmacokinetics of a reverse transcriptase inhibitor, 3TC, in patients with HIV infection: a phase I study. *AIDS (London, England)* 6, 1471–5 (1992).

133. Burger, D. M. *et al.* Age-dependent pharmacokinetics of lamivudine in HIV-infected children. *Clinical pharmacology and therapeutics* 81, 517–20 (2007).

134. E.I.Ette and P.J.William *Pharmacometrics: The science of quantitative of pharmacology*. (John Wiley & Sons, Ltd: 2007).

135. Holford, N. H. & Sheiner, L. B. Kinetics of pharmacologic response. *Pharmacology & therapeutics* 16, 143–66 (1982).

136. Gisleskog, P. O., Karlsson, M. O. & Beal, S. L. Use of prior information to stabilize a population data analysis. *Journal of pharmacokinetics and pharmacodynamics* 29, 473–505 (2002).

137. Nyberg, J., Karlsson, M. O. & Hooker, A. C. Simultaneous optimal experimental design on dose and sample times. *Journal of pharmacokinetics and pharmacodynamics* 36, 125–45 (2009).

138. N Holford, S. C. M. and B. A. P. Clinical Trial Simulation: A Review. *Clinical Pharmacology & Therapeutics* 88, 166–182 (2010).

139. Wallin Johan *Dose adaptation based on pharmacometric models*. (Uppsala University: 2009).

140. Sheiner, L. B. The population approach to pharmacokinetic data analysis: rationale and standard data analysis methods. *Drug metabolism reviews* 15, 153–71 (1984).

141. Steimer, J. L., Mallet, A., Golmard, J. L. & Boisvieux, J. F. Alternative approaches to estimation of population pharmacokinetic parameters: comparison with the nonlinear mixed-effect model. *Drug metabolism reviews* 15, 265–92 (1984).

142. Sheiner, B. L. & Beal, S. L. Evaluation of methods for estimating population pharmacokinetic parameters. II. Biexponential model and experimental pharmacokinetic data. *Journal of pharmacokinetics and biopharmaceutics* 9, 635–51 (1981).

143. Sheiner, L. B. & Beal, S. L. Evaluation of methods for estimating population pharmacokinetics parameters. I. Michaelis-Menten model: routine clinical pharmacokinetic data. *Journal of pharmacokinetics and biopharmaceutics* 8, 553–71 (1980).

144. Sheiner, L. B. & Beal, S. L. Evaluation of methods for estimating population pharmacokinetic parameters. III. Monoexponential model: routine clinical pharmacokinetic data. *Journal of pharmacokinetics and biopharmaceutics* 11, 303–19 (1983).

145. Sheiner, L. B. & Ludden, T. M. Population pharmacokinetics/dynamics. *Annual review of pharmacology and toxicology* 32, 185–209 (1992).

146. Burtin, P., Mentre, F., van Bree, J. & Steimer, J. L. Sparse sampling for assessment of drug exposure in toxicological studies. *European journal of drug metabolism and pharmacokinetics* 21, 105–11

147. Karlsson, M. O. & Sheiner, L. B. The importance of modeling interoccasion variability in population pharmacokinetic analyses. *Journal of pharmacokinetics and biopharmaceutics* 21, 735–50 (1993).

148. Beal, S. L. L. B. S. and A. J. B. *NONMEM User's Guides*. ICON Development Solutions,Ellicott City, MD.

149. Wählby, U., Matolcsi, K., Karlsson, M. O. & Jonsson, E. N. Evaluation of type I error rates when modeling ordered categorical data in NONMEM. *Journal of pharmacokinetics and pharmacodynamics* 31, 61–74 (2004).

150. Wählby, U., Jonsson, E. N. & Karlsson, M. O. Assessment of actual significance levels for covariate effects in NONMEM. *Journal of pharmacokinetics and pharmacodynamics* 28, 231–52 (2001).

151. Wählby, U., Bouw, M. R., Jonsson, E. N. & Karlsson, M. O. Assessment of type I error rates for the statistical sub-model in NONMEM. *Journal of pharmacokinetics and pharmacodynamics* 29, 251–69 (2002).

152. Ene I.Ette and Thomas M.Ludden Population Pharmacokinetic Modeling: The Importance of Informative Graphics. *Pharmaceutical research* 12, 1845–1855 (1995).

153. Karlsson, M. O. & Savic, R. M. Diagnosing model diagnostics. *Clinical pharmacology and therapeutics* 82, 17–20 (2007).

154. Nyberg, J., Bauer, R. J. & Hooker, A. C. Investigations of the weighted residuals in NONMEM 7. *PAGE 2010, Berline [www.page-meeting.org/abstract=1883]*

155. Brendel, K., Comets, E., Laffont, C. & Mentré, F. Evaluation of different tests based on observations for external model evaluation of population analyses. *Journal of pharmacokinetics and pharmacodynamics* 37, 49–65 (2010).

156. Comets, E., Brendel, K. & Mentré, F. Computing normalised prediction distribution errors to evaluate nonlinear mixed-effect models: the npde add-on package for R. *Computer methods and programs in biomedicine* 90, 154–66 (2008).

157. Ette, E. I. Stability and performance of a population pharmacokinetic model. *Journal of clinical pharmacology* 37, 486–95 (1997).

158. Kenney, K. B., Wring, S. A., Carr, R. M., Wells, G. N. & Dunn, J. A. Simultaneous determination of zidovudine and lamivudine in human serum using HPLC with tandem mass spectrometry. *Journal of pharmaceutical and biomedical analysis* 22, 967–83 (2000).

159. Lindbom, L., Ribbing, J. & Jonsson, E. N. Perl-speaks-NONMEM (PsN)--a Perl module for NONMEM related programming. *Computer methods and programs in biomedicine* 75, 85–94 (2004).

160. Jonsson, E. N. & Karlsson, M. O. Xpose--an S-PLUS based population pharmacokinetic/pharmacodynamic model building aid for NONMEM. *Computer methods and programs in biomedicine* 58, 51–64 (1999).

161. Jullien, V. *et al.* Population analysis of weight-, age-, and sex-related differences in the pharmacokinetics of lopinavir in children from birth to 18 years. *Antimicrobial agents and chemotherapy* 50, 3548–55 (2006).

162. Jos, M. *et al.* Simultaneous population pharmacokinetic model for lopinavir and ritonavir in HIV-infected adults. *Clinical pharmacokinetics* 47, 681–92 (2008).

163. Crommentuyn, K. M. L. *et al.* Population pharmacokinetics of lopinavir in combination with ritonavir in HIV-1-infected patients. *British journal of clinical pharmacology* 60, 378–89 (2005).

164. Kerbusch, T., Karlsson, M. O., Savic, R. M. & Jonker, D. M. Implementation of a transit compartment model for describing drug absorption in pharmacokinetic studies. *Journal of pharmacokinetics and pharmacodynamics* 34, 711–26 (2007).

165. Wählby, U., Jonsson, E. N. & Karlsson, M. O. Comparison of stepwise covariate model building strategies in population pharmacokinetic-pharmacodynamic analysis. *AAPS pharmSci* 4, E27 (2002).

166. Ron J. Keizer, Akash Khandelwal, Andrew C. Hooker, M. O. K. The bootstrap of Stepwise Covariate Modeling using linear approximations. *PAGE 2011, Athen*

167. Barrett, J. S. *et al.* Population pharmacokinetic meta-analysis with efavirenz. *International journal of clinical pharmacology and therapeutics* 40, 507–19 (2002).

168. Smythe, W. *et al.* A semimechanistic pharmacokinetic-enzyme turnover model for rifampin autoinduction in adult tuberculosis patients. *Antimicrobial agents and chemotherapy* 56, 2091–8 (2012).

169. Anderson, B. J. & Holford, N. H. G. Mechanism-based concepts of size and maturity in pharmacokinetics. *Annual review of pharmacology and toxicology* 48, 303–32 (2008).

170. Janmahasatian, S. *et al.* Quantification of lean bodyweight. *Clinical pharmacokinetics* 44, 1051–65 (2005).

171. Martinson, N. A. *et al.* HAART and risk of tuberculosis in HIV-infected South African children: a multi-site retrospective cohort. *The international journal of tuberculosis and lung disease: the official journal of the International Union against Tuberculosis and Lung Disease* 13, 862–7 (2009).

172. Walters, E. *et al.* Clinical presentation and outcome of tuberculosis in human immunodeficiency virus infected children on anti-retroviral therapy. *BMC pediatrics* 8, 1 (2008).

173. Abdool Karim, S. S., Churchyard, G. J., Abdool Karim, Q. & Lawn, S. D. HIV infection and tuberculosis in South Africa: an urgent need to escalate the public health response. *Lancet* 374, 921–33 (2009).

174. Allegaert, K., van den Anker, J. N., Naulaers, G. & de Hoon, J. Determinants of drug metabolism in early neonatal life. *Current clinical pharmacology* 2, 23–9 (2007).

175. Kappelhoff, B. S. *et al.* Development and validation of a population pharmacokinetic model for ritonavir used as a booster or as an antiviral agent in HIV-1-infected patients. *British journal of clinical pharmacology* 59, 174–82 (2005).

176. Hsu, A. *et al.* Multiple-dose pharmacokinetics of ritonavir in human immunodeficiency virus-infected subjects. *Antimicrobial agents and chemotherapy* 41, 898–905 (1997).

177. W Awni, Y-L Chiu, T Zhu, N Braun, C Klein, R Heuser, J Breitenbach, J Morris1, T Doan, S. B. and G. H. Significantly Reduced Food Effect and Pharmacokinetic Variability with a Novel Lopinavir/ritonavir Tablet Formulation. *Third IAS Conference on HIV Pathogenesis and Treatment 24–27 July 2005, Rio de Janeiro, Brazil*

178. Dickinson, L. *et al.* Sequential population pharmacokinetic modeling of lopinavir and ritonavir in healthy volunteers and assessment of different dosing strategies. *Antimicrobial agents and chemotherapy* 55, 2775–82 (2011).

179. Denti, P. *et al.* A population pharmacokinetic model for rifampicin auto-induction. *3rd International workshop on clinical pharmacology of TB drugs.2010 Boston, USA. Abstract*

180. Levy, R. H., Hachad, H., Yao, C. & Ragueneau-Majlessi, I. Relationship between extent of inhibition and inhibitor dose: literature evaluation based on the metabolism and transport drug interaction database. *Current drug metabolism* 4, 371–80 (2003).

181. van Heeswijk, R. P. G. *et al.* Absence of circadian variation in the pharmacokinetics of lopinavir/ritonavir given as a once daily dosing regimen in HIV-1-infected patients. *British journal of clinical pharmacology* 59, 398–404 (2005).

182. Hsu, A. *et al.* Pharmacokinetic-pharmacodynamic analysis of lopinavir-ritonavir in combination with efavirenz and two nucleoside reverse transcriptase inhibitors in extensively pretreated human immunodeficiency virus-infected patients. *Antimicrobial agents and chemotherapy* 47, 350–9 (2003).

183. Justesen, U. S. & Pedersen, C. Diurnal variation of plasma protease inhibitor concentrations. *AIDS (London, England)* 16, 2487–9 (2002).

184. Awnl W, Chlu YL, Zhu T, Braun N, Klein C, Heuser R, Breitenbach J, Morris J, Doan T, Brun S, H. G. Significantly reduced food effect and pharmacokinetic variability with a novel lopinavir/ritonavir tablet formulation. *Third IAS conference on HIV pathogenesis and treatment.Abstract no. WeOa0206* (2012).

185. Panel, D., Guidelines, A., Group, W. & Council, A. Guidelines for the Use of Antiretroviral Agents in HIV-1-Infected Adults and Adolescents. *Review Literature And Arts Of The Americas* (2011).

186. McIlleron, H. *et al.* Lopinavir exposure is insufficient in children given double doses of lopinavir/ritonavir during rifampicin-based treatment for tuberculosis. *Antiviral therapy* 16, 417–21 (2011).

187. Holford, N. Dosing in children. *Clinical pharmacology and therapeutics* 87, 367–70 (2010).

188. Mukherjee, A., Dombi, T., Wittke, B. & Lalonde, R. Population pharmacokinetics of sildenafil in term neonates: evidence of rapid maturation of metabolic clearance in the early postnatal period. *Clinical pharmacology and therapeutics* 85, 56–63 (2009).

189. Olufsen, M. S. *et al.* Blood pressure and blood flow variation during postural change from sitting to standing: model development and validation. *Journal of applied physiology (Bethesda, Md.: 1985)* 99, 1523–37 (2005).

190. Gurumurthy, P. *et al.* Malabsorption of rifampin and isoniazid in HIV-infected patients with and without tuberculosis. *Clinical infectious diseases: an official publication of the Infectious Diseases Society of America* 38, 280–3 (2004).

191. Westphal, K. *et al.* Induction of P-glycoprotein by rifampin increases intestinal secretion of talinolol in human beings: a new type of drug/drug interaction. *Clinical pharmacology and therapeutics* 68, 345–55 (2000).

192. G.Rosas-Taraco, A., Y.Arce-Mendoza, A., Cabaliero-Olin, G. & C.Salinas-Carmona, M. Mycobacterium tuberculosis upregulates coreceptors CCR5 and CXCR4 while HIV modulates CD14 favoring concurrent infection. *AIDS research and human retroviruses* 22, 45–51 (2006).

193. Umeh, O. C. *et al.* Sex Differences in Lopinavir and Ritonavir Pharmacokinetics Among HIV-Infected Women and Men. *Journal of clinical pharmacology* (2011).doi:10.1177/0091270010388650

194. Hemanth Kumar, a K. *et al.* Pharmacokinetics of lamivudine & stavudine in generic fixed-dose combinations in HIV-1 infected adults in India. *The Indian journal of medical research* 130, 451–7 (2009).

195. Tremoulet, A. H. *et al.* Population pharmacokinetics of lamivudine in human immunodeficiency virus-exposed and -infected infants. *Antimicrobial agents and chemotherapy* 51, 4297–302 (2007).

196. Walt, J.-S. van der, Savic, R. M., Cohen, K., Smith, P. J. & Karlsson, M. O. *A nonlinear mixed effects model to characterise lamivudine absorption and distribution*. *Newcastle 2009 11th Annual Scientific Meeting*

197. L'homme, R. F. A. *et al.* Nevirapine , stavudine and lamivudine pharmacokinetics in African children on paediatric fixed-dose combination tablets. *Aids* (2008).doi:QAD.0b013e3282f4a208

198. Hansen, P. M. *et al.* Diurnal variation in glomerular charge selectivity, urinary albumin excretion and blood pressure in insulin-dependent diabetic patients. *Kidney international* 48, 1559–62 (1995).

199. Skotnicka, E., Muszczyñski, Z., Dudzinska, W. & Suska, M. A review of the renal system and diurnal variations of renal activity in livestock. *Irish veterinary journal* 60, 161–8 (2007).

200. Jung, N. *et al.* Relevance of the Organic Cation Transporters 1 and 2 for Antiretroviral Drug Therapy in Human Immunodeficiency Virus Infection ABSTRACT: *Pharmacology* 36, 1616–1623 (2008).

201. Anderson, P. L. & Rower, J. E. Zidovudine and Lamivudine for HIV Infection. *Clinical Medicine* (2010).

I. Final model control file (Paper I)

```
$PROBLEM    final children model,update    ;no problem data|no BQL
$INPUT ID SDID=DROP DMID=DROP TB RATI STUD=DROP GROU=DROP
OCC REP=DROP DAT1=DROP TIME AMT DVID ORDV=DROP DV BQL
MDV EVID CMT SEX=DROP AGE=DROP WT HT=DROP BSA=DROP
HB=DROP ALB=DROP ALT=DROP SS=DROP II=DROP PROB WRON RDS
RDSW
$DATA Dataset_fulldose_RDOSE.csv IGNORE=#
IGNORE(DVID.EQ.3,PROB.EQ.1,BQL.EQ.1,WRON.EQ.1)    ;no problem
data,no spurious predose
$SUBROUTINE ADVAN6 TRANS1 TOL=4
$MODEL
COMP(LPVDOSE)     ;1 LPV DOSE
COMP(LPVOBS)      ;2 LPV CENTRAL
COMP(RTVDOSE)     ;3 RTV DOSE
COMP(RTVOBS)      ;4 RTV CENTRAL
COMP(TRANS)       ;5
COMP(TRANS)       ;6
COMP(TRANS)       ;7
COMP(TRANS)       ;8
COMP(TRANS)       ;9
COMP(TRANS)       ;10
COMP(TRANS)       ;11
COMP(TRANS)       ;12
COMP(TRANS)       ;13
COMP(ABS)         ;14

$PK
; ------------LPV MODEL------------------
      TVCLL= THETA(1)*(WT/10)**0.75
        TVVL    = THETA(2)*(WT/10)
        TVKAL = THETA(3)
     TVKL = TVCLL/TVVL
     SLP = THETA(4)
     RIF = 0
     IF (RATI.NE.0) RIF=THETA(5)
       TVF1=1+(RDSW-3)*SLP-RIF
     ;IF (RATI.EQ.1) TVF1=THETA(4)
     ;IF (RATI.EQ.2) TVF1=THETA(5)

     CLL       = TVCLL*EXP(ETA(1))
     VL        = TVVL*EXP(ETA(3))
     KAL1=0
```

```
      KAL2=0
      IF (OCC.EQ.1) KAL1=1
      IF (OCC.EQ.2) KAL2=1
     BOVM = KAL1*ETA(4)+ KAL2*ETA(5)
      KAL       = TVKAL*EXP(BOVM)

      OC1L=0
      OC2L=0
      IF (OCC.EQ.1) OC1L=1
      IF (OCC.EQ.2) OC2L=1
     BOVL = OC1L*ETA(6)+ OC2L*ETA(7)
     F1 = TVF1*EXP(BOVL)
     K12 = KAL
     K20 = CLL/VL
     S2 = VL
;----------RTV MODEL-------------------
     IF (TB.EQ.1) THEN
     TVCLR = THETA(6)*(WT/10)**0.75
     ELSE
     TVCLR = THETA(7)*(WT/10)**0.75
      ENDIF

       TVVR    = THETA(8)*(WT/10)
       TVKAR = THETA(9)
      TVK = TVCLR/TVVR
      TVMTT = THETA(10)

      OC1R=0
      OC2R=0
      IF (OCC.EQ.1) OC1R=1
      IF (OCC.EQ.2) OC2R=1
      BOVR = OC1R*ETA(8)+ OC2R*ETA(9)
      CLR       = TVCLR*EXP(ETA(2))*EXP(BOVR)
      VR        = TVVR*EXP(THETA(11)*ETA(2))
      KAR       = (TVK+TVKAR)*EXP(THETA(14)*BOVM)
     MTTR1=0
     MTTR2=0
      IF (OCC.EQ.1) MTTR1=1
      IF (OCC.EQ.2) MTTR2=1
      BOVT = MTTR1*ETA(10)+ MTTR2*ETA(11)
    MTT = TVMTT*EXP(BOVT)
    KTR=10/MTT
    K35=KTR
```

```
      K56=KTR
      K67=KTR
      K78=KTR
    K89=KTR
    K910=KTR
    K1011=KTR
    K1112=KTR
    K1213=KTR
    K1314=KTR
    K14T4=KAR
    K40 = CLR/VR
    S4 = VR

;-----------EFFECT MODEL-----------------
      EMAX = THETA(15)
      EC50 =THETA(16)*EXP(ETA(12))

$DES
C4 = A(4)/VR
EFF = EMAX*C4/(EC50 + C4)
DADT(1) = -KAL*A(1)
DADT(2) = KAL*A(1)-K20*(1-EFF)*A(2)
DADT(3) = -KTR*A(3)
DADT(4) = KAR*A(14)-K40*A(4)
DADT(5) = KTR*A(3)-KTR*A(5)
DADT(6) = KTR*A(5)-KTR*A(6)
DADT(7) = KTR*A(6)-KTR*A(7)
DADT(8) = KTR*A(7)-KTR*A(8)
DADT(9) = KTR*A(8)-KTR*A(9)
DADT(10) = KTR*A(9)-KTR*A(10)
DADT(11) = KTR*A(10)-KTR*A(11)
DADT(12) = KTR*A(11)-KTR*A(12)
DADT(13) = KTR*A(12)-KTR*A(13)
DADT(14) = KTR*A(13)-KAR*A(14)
$ERROR ;(OBSERVATIONS ONLY)
    CP2 = A(2)/VL
    CP4 = A(4)/VR
    DEL=1E-6
    PREDL = (A(2)/VL+DEL)
    PREDR = (A(4)/VR+DEL)
    IF(DVID.EQ.1)IPRED = LOG(PREDL)
    IF(DVID.EQ.2)IPRED = LOG(PREDR)
    IRES    = DV - IPRED
```

```
IF (DVID.EQ.1)    W =THETA(12)      ;LPV proportional error
IF (DVID.EQ.2)    W =THETA(13)      ;RTV proportional error
     IF (W.EQ.0) W = 1
     IWRES = IRES/W
IF (DVID.EQ.1) Y = IPRED + W*EPS(1)
IF (DVID.EQ.2) Y = IPRED + W*EPS(2)
AA1=A(1)
AA3=A(3)
AA15=A(15)
ACL = K20*(1-EMAX*A(4)/VR/(EC50 + A(4)/VR))
$THETA
  (0,4.18194) ; 1      LPV CL
  (0,11.6494) ; 2      LPV V
  (0,0.742656) ; 3      LPV KA
  0.0209982    ; 4      SLOPE
  (0,0.832441) ; 5      LPV F1 3.5 RTV
  (0,19.0592) ; 6      RTV CL ON WITH TB
  (0,12.7679) ; 7      RTV CL ON CONTROL AND AFTER TB
  (0,105.047) ; 8      RTV V
  (0,2.30321) ; 9      RTV KA
  (0,1.2786) ; 10    RTV MTT
  (0,1.36432) ; 11    RTV Scale parameter of IIV CL-V
  (0,0.303897) ; 12    LPV Proportional error
  (0,0.33894) ; 13    RTV Proportional error
  (0,1.65796) ; 14    Scale parameter of IOV RTVKA-LPVKA
  0.9 FIX ; 15      EMAX
  (0,0.0519067) ; 16      EC50
$OMEGA    BLOCK(1) FIX
  0    ; 1    IIV on LPV CL
$OMEGA    BLOCK(1)
  0.530957    ; 2    IIV on RTV CL
$OMEGA    BLOCK(1)
  0.321054    ; 3    IIV on LPV V
$OMEGA    BLOCK(1)
  0.579458    ; 4    IOV on LPV KA
$OMEGA    BLOCK(1) SAME
$OMEGA    BLOCK(1)
  0.288538    ; 6    IOV on LPV F1
$OMEGA    BLOCK(1) SAME
$OMEGA    BLOCK(1)
  0.172492    ; 8    IOV on RTV CL
$OMEGA    BLOCK(1) SAME
$OMEGA    BLOCK(1)
```

```
 0.0951473    ; 10 IOV on RTV MTT
$OMEGA    BLOCK(1) SAME
$OMEGA    BLOCK(1) FIX
 0    ; 12    IIV on EC50
$SIGMA    1.000000    FIX
$SIGMA    1.000000    FIX
$ESTIMATION PRINT=1 MAXEVALS=9999 MSFO=run11.msf
METHOD=1 NOABORT
$COVARIANCE PRINT=E    MATRIX=S
$TABLE ID DVID TIME IPRED RES WRES IWRES DV CMT NOPRINT
ONEHEADER                              FILE=sdtab11
$TABLE ID TB RATI    OCC NOPRINT ONEHEADER
FILE=catab11
$TABLE ID WT NOPRINT ONEHEADER
FILE=cotab11
$TABLE ID DVID CLL VL KAL F1 CLR VR KAR MTT EMAX EC50 ACL
ETA1 ETA2 ETA3 ETA4 ETA5 ETA6 ETA7 ETA8 ETA9 ETA10 ETA11 ETA12
NOPRINT    ONEHEADER FILE=patab11
```

II. Final model control file (Paper II)

```
$PROBLEM run5,evening effect on F
$INPUT ID SDID=DROP TERM WHAT=DROP ODAT=DROP OTIM=DROP
TIME AMT DVID DV LNDV=DROP MDV EVID CMT SEX AGE WT HT ALT
HB BQL RDW RTVTOT TB=DROP RATI=DROP RIF EVEN
$DATA APK_PREDOSE_2.csv       IGNORE=#    ;     ;LPV-RTV data; no bql
$SUBROUTINES ADVAN13 TRANS1 TOL=8
$MODEL
COMP(LPVDOSE)     ;1 LPV DOSE
COMP(LPVOBS)      ;2 LPV CENTRAL
COMP(RTVDOSE)     ;3 RTV DOSE
COMP(RTVOBS)      ;4 RTV CENTRAL
COMP(LPVPER)      ;5 RTV PERIPHIRAL
$ABBREVIATED DERIV2=NO
$PK
"FIRST
"         USE PRCOM_INT, ONLY: IMAX
" IMAX=10000000
;---TAD variatle; define only for plot
TAD = TIME - 48     ;dose given at TAD=0
TADD = TAD+1              ; dose given at TAD=1

;---Code from Anderson & Holford 2009, page 33 [Drug Metab. Pharmacokinet.
24 (1): 25?6 (2009)]
IF (SEX.EQ.1) THEN    ; females
WHSMAX=37.99
WHS50=35.98
ELSE              ;males
WHSMAX=42.92
WHS50=30.93
ENDIF

HTM2 = (HT/100)**2
FFM = (WHSMAX*HTM2*WT)/(WHS50*HTM2+WT)

;----Clearance
CLFFAT    = THETA(17)
NFMCL     = FFM + CLFFAT*(WT-FFM)    ;Total weight
SCL         = (NFMCL/40)**(0.75)         ;CL scaled
;----volume
VFFAT    = THETA(18)
NFMV      = FFM+VFFAT*(WT-FFM)    ;Total weight,
```

```
SV        = NFMV/65                    ;V scaled

 ;-------IOV CODE--------------------
IF (TERM.EQ.1) THEN
     IOVFL = ETA(5)
     IOVFR = ETA(13)
     IOVKAL = ETA(21)
     IOVCLR = ETA(29)
     IOVCLL = ETA(37)
     IOVRUV = ETA(45)
     IOVMTT = ETA(53)
ENDIF
IF (TERM.EQ.2) THEN
     IOVFL = ETA(6)
     IOVFR = ETA(14)
     IOVKAL = ETA(22)
     IOVCLR = ETA(30)
     IOVCLL = ETA(38)
     IOVRUV = ETA(46)
     IOVMTT = ETA(54)
ENDIF
IF (TERM.EQ.3) THEN
     IOVFL = ETA(7)
     IOVFR = ETA(15)
     IOVKAL = ETA(23)
     IOVCLR = ETA(31)
     IOVCLL = ETA(39)
     IOVRUV = ETA(47)
     IOVMTT = ETA(55)
ENDIF
IF (TERM.EQ.4) THEN
     IOVFL = ETA(8)
     IOVFR = ETA(16)
     IOVKAL = ETA(24)
     IOVCLR = ETA(32)
     IOVCLL = ETA(40)
     IOVRUV = ETA(48)
     IOVMTT = ETA(56)
ENDIF
IF (TERM.EQ.5) THEN
     IOVFL = ETA(9)
     IOVFR = ETA(17)
     IOVKAL = ETA(25)
```

```
      IOVCLR = ETA(33)
      IOVCLL = ETA(41)
      IOVRUV = ETA(49)
      IOVMTT = ETA(57)
ENDIF
IF (TERM.EQ.6) THEN
      IOVFL = ETA(10)
      IOVFR = ETA(18)
      IOVKAL = ETA(26)
      IOVCLR = ETA(34)
      IOVCLL = ETA(42)
      IOVRUV = ETA(50)
      IOVMTT = ETA(58)
ENDIF
IF (TERM.EQ.7) THEN
      IOVFL = ETA(11)
      IOVFR = ETA(19)
      IOVKAL = ETA(27)
      IOVCLR = ETA(35)
      IOVCLL = ETA(43)
      IOVRUV = ETA(51)
      IOVMTT = ETA(59)
ENDIF
IF (TERM.EQ.8) THEN
      IOVFL = ETA(12)
      IOVFR = ETA(20)
      IOVKAL = ETA(28)
      IOVCLR = ETA(36)
      IOVCLL = ETA(44)
      IOVRUV = ETA(52)
      IOVMTT = ETA(60)
ENDIF

; INITIALIZATION
A_0(1) = 0.0001
A_0(2) = 0.0001
A_0(3) = 0.0001
A_0(4) = 0.0001
A_0(5) = 0.0001
; ------------LPV MODEL------------------
RIFCLL=1
RIFBIOL=1
EVECLL=1
```

```
EVEBIOL=1
EVEKAL=1

; Evening effect: FOOD + diunrnal variation
IF (EVEN.EQ.1) THEN
     EVECLL=THETA(24)
     EVEBIOL=THETA(25)
     EVEKAL=THETA(29)
ENDIF
; Rifampicin effect
IF (RIF.EQ.1) THEN
     RIFCLL=THETA(2)
     RIFBIOL=THETA(5)
ENDIF

; The first theta is the values of morning fasted parameters
TVCLL = THETA(1)*SCL*RIFCLL*EVECLL
TVVL    = THETA(3)*SV
TVKAL = THETA(4)*EVEKAL
TVF1 = 1*RIFBIOL*EVEBIOL

; BSV
IIVCLL = ETA(1)
IIVVL= ETA(2)
IIVFL = ETA(62)

CLL     = TVCLL*EXP(IIVCLL+IOVCLL)
VL       = TVVL*EXP(IIVVL)
KAL     = TVKAL*EXP(IOVKAL)
F1       = TVF1*EXP(IOVFL+IIVFL)

K20 = CLL/VL
S2 = VL

;----------RTV MODEL-------------------
RIFCLR=1
RIFBIOR=1
EVECLR=1
EVEBIOR=1
EVEMTTR=1

; Evening effect: FOOD + diunrnal variation
IF (EVEN.EQ.1) THEN
```

```
      EVECLR=THETA(26)
      EVEBIOR=THETA(27)
      EVEMTTR=THETA(28)
ENDIF

; Rifampicin effect
IF (RIF.EQ.1) THEN
      RIFCLR=THETA(7)
      RIFBIOR=THETA(10)
ENDIF

; RTV dose on RTV BIO
SLP = THETA(23)
RDBIOR=(1+SLP*(RTVTOT-100)/100)

TVCLR = THETA(6)*SCL*EVECLR*RIFCLR
TVVR    = THETA(8)*SV
TVKAR = THETA(9)
TVF3    = 1*RDBIOR*RIFBIOR*EVEBIOR
TVMTT = THETA(11)*EVEMTTR
TVQ      = THETA(12)*SCL
TVV5    = THETA(13)*SV
TVNN    = THETA(22)

; BSV
IIVCLR=ETA(3)
IIVVR=ETA(4)
IIVBIOR=ETA(61)

; Parameters
CLR    = TVCLR*EXP(IIVCLR+IOVCLR)
VR      = TVVR*EXP(IIVVR)
KAR    = TVKAR
MTT = TVMTT*EXP(IOVMTT)
Q      = TVQ
V5    = TVV5
NN    = TVNN

BIO    = TVF3*EXP(IOVFR+IIVBIOR) ; This is the actual bioavailability

K40 = CLR/VR
K45 = Q/VR
K54 = Q/V5
```

```
S4 = VR

;-----------EFFECT MODEL-----------------
EMAXR = THETA(19)
EC50 =THETA(20)
HILL = THETA(21)

; Transit
KTR = (NN+1)/MTT
F3=0

IF (NEWIND.NE.2.OR.EVID.GE.3.AND.DVID.EQ.2) THEN ; new individual, or reset event
      ; The values read here will be stored in TDOS and PD in this very PK call.
      TNXD=TIME ; Time of the dose
      PNXD=AMT ; Amount. If it's zero, the DE is deactivated.
ENDIF

TDOS=TNXD ; This will either save here the temporary values if it's a new individual...
PD=PNXD ; ...or the values which were read one record ahead during the execution of the previous record.

IF(AMT.GT.0.AND.DVID.EQ.2) THEN ; This reads one record ahead and stores the data to be used when running the following record
; IF(AMT.GT.0.AND.ALAG1.EQ.0) THEN ; ; Use this instead if there is ALAG, as it will also checks if the ALAG is not 0
      TNXD=TIME
      PNXD=AMT
ENDIF

; Uncomment this if you have ALAG or if you use ADDL
;IF (DOSTIM.GT.0) THEN ; This will account for the ADDL or lagged doses. It will overwrite the time, if it a non-event record
;      TNXD=DOSTIM
;      PNXD=AMT
;ENDIF

LNGAM =
NN*LOG(NN)-NN+LOG(NN*(1+4*NN*(1+2*NN)))/6+0.572364942 ; approximation of log of gamma(n), 0.572364942 is LOG(PI)/2
BPK=BIO*PD*KTR
IF (BPK.LE.0.0001) BPK=0.0001
```

```
PIZZA=LOG(BPK)-LNGAM
$DES
C4 = A(4)/VR
IF (C4.LE.0.0001) C4 = 0.0001
EFF = EMAXR*C4**HILL/(EC50**HILL + C4**HILL)

DADT(1) = -KAL*A(1)
DADT(2) = KAL*A(1)-K20*A(2)*(1-EFF)

TEMPO=T-TDOS ; this is time after dose, it should always be >= 0
IF(PD.GT.0.AND.TEMPO.GT.0) THEN
     KTT=KTR*TEMPO
     DADT(3)=EXP(PIZZA+NN*LOG(KTT)-KTT)-KAR*A(3)
ENDIF

DADT(4) = KAR*A(3)-K40*A(4)-K45*A(4)+K54*A(5)
DADT(5) = K45*A(4)-K54*A(5)

$ERROR ;(ONLY OBSERVATIONS)
IPREDL = A(2)/VL
IPREDR = A(4)/VR
IF(DVID.EQ.1)THEN
     IPRED = IPREDL
     W = SQRT(THETA(14)**2 +
(THETA(15)*IPRED)**2)*EXP(IOVRUV)      ;LPV additive and proportional
error
ENDIF
IF(DVID.EQ.2) THEN
     IPRED = IPREDR
     W =THETA(16)*IPRED      ;RTV proportional error
ENDIF

IRES    = DV - IPRED
IF (W.EQ.0) W = 1
IWRES = IRES/W
Y = IPRED + W*EPS(1)

$THETA    (0,37.4702) ; 1    LPV CL
  (0,1.59703) ; 2    RIF ON LPV CL
  (0,54.8) ; 3    LPV V
  (0,0.968) ; 4    LPV KA
  (0,0.779,1) ; 5    RIF on LPV BIO
  (0,19.2) ; 6    RTV CL WITHOUT RIF
```

```
 (0,1.29) ; 7    RIF on RTV CL
 (0,21.8) ; 8    RTV V1
 (0,3.3) ; 9    RTV KA
 (0,0.559,1) ; 10 RIF on BIO RTV
 (0,1.44) ; 11    RTV MTT
 (0,29.3) ; 12 RTV Q
 (0,53.1) ; 13 RTV V5
 0 FIX ; 14    LPV Additive error
 (0,0.13) ; 15    LPV Proportional error
 (0,0.188) ; 16    RTV Proportional error
 0 FIX ; 17    CLFFAT
 1 FIX ; 18    VFFAT
 (0,0.952,1) ; 19    EMAX ON RTV INHIBITION
 (0,0.0378) ; 20    EC50 OF RTV
 1 FIX ; 21    HILL
 2 FIX ; 22 NN
 (0,0.599) ; 23 RTV DOSE ON F3
 (1 FIX)       ; 24 evening LPV CL
 (0,1.98) ; 25 evening LPV F
 (1 FIX)       ; 26 evening RTV CL
 (0,3.65) ; 27 evening RTV F
 1 FIX ; 28 evening RTV MTT
 1 FIX ; 29 evening LPV KA
$OMEGA    DIAGONAL(1)
 0.0421    ; 1      IIV on LPV CL
$OMEGA    DIAGONAL(1)
 0.0791    ; 2      IIV on LPV V
$OMEGA    DIAGONAL(1)
 0.0487    ; 3      IIV on RTV CL
$OMEGA    DIAGONAL(1)
 0.0103    ; 4      IIV on RTV V
$OMEGA    BLOCK(1)
 0.0527    ; 5      IOV on LPV F1
$OMEGA    BLOCK(1) SAME
$OMEGA    BLOCK(1) SAME
$OMEGA    BLOCK(1) SAME
$OMEGA    BLOCK(1) SAME
$OMEGA    BLOCK(1) SAME
$OMEGA    BLOCK(1) SAME
$OMEGA    BLOCK(1) SAME

$OMEGA    BLOCK(1)
 0.105    ; 13      IOV on RTV F1
```

```
$OMEGA   BLOCK(1) SAME
$OMEGA   BLOCK(1) SAME
$OMEGA   BLOCK(1) SAME
$OMEGA   BLOCK(1) SAME
$OMEGA   BLOCK(1) SAME
$OMEGA   BLOCK(1) SAME
$OMEGA   BLOCK(1) SAME

$OMEGA   BLOCK(1)
 0.713   ; 21     IOV on LPV KA
$OMEGA   BLOCK(1) SAME
$OMEGA   BLOCK(1) SAME
$OMEGA   BLOCK(1) SAME
$OMEGA   BLOCK(1) SAME
$OMEGA   BLOCK(1) SAME
$OMEGA   BLOCK(1) SAME
$OMEGA   BLOCK(1) SAME

$OMEGA   BLOCK(1)
 0.0434   ; 29     IOV on RTV CL
$OMEGA   BLOCK(1) SAME
$OMEGA   BLOCK(1) SAME
$OMEGA   BLOCK(1) SAME
$OMEGA   BLOCK(1) SAME
$OMEGA   BLOCK(1) SAME
$OMEGA   BLOCK(1) SAME
$OMEGA   BLOCK(1) SAME

$OMEGA   BLOCK(1)
 0.0159   ; 37     IOV on LPV CL
$OMEGA   BLOCK(1) SAME
$OMEGA   BLOCK(1) SAME
$OMEGA   BLOCK(1) SAME
$OMEGA   BLOCK(1) SAME
$OMEGA   BLOCK(1) SAME
$OMEGA   BLOCK(1) SAME
$OMEGA   BLOCK(1) SAME

$OMEGA   BLOCK(1)
 0 FIX   ; 45     IOV on LPV RUV
$OMEGA   BLOCK(1) SAME
$OMEGA   BLOCK(1) SAME
$OMEGA   BLOCK(1) SAME
```

```
$OMEGA    BLOCK(1) SAME
$OMEGA    BLOCK(1) SAME
$OMEGA    BLOCK(1) SAME
$OMEGA    BLOCK(1) SAME

$OMEGA    BLOCK(1)
 0.0863    ; 53      IOV on RTV MTT
$OMEGA    BLOCK(1) SAME
$OMEGA    BLOCK(1) SAME
$OMEGA    BLOCK(1) SAME
$OMEGA    BLOCK(1) SAME
$OMEGA    BLOCK(1) SAME
$OMEGA    BLOCK(1) SAME
$OMEGA    BLOCK(1) SAME

$OMEGA    DIAGONAL(1)
 0.118    ; 61 IIV on RTV F
$OMEGA    DIAGONAL(1)
 0.03    ; 62 IIV on LPV F
$SIGMA    1.    FIX
$ESTIMATION PRINT=1 MAXEVALS=9999 SIGL=10 NSIG=2 METHOD
CONDITIONAL INTERACTION MSFO=run504e.msf
$COVARIANCE PRINT=E MATRIX=S
$TABLE ID TIME PRED IPRED RES WRES IWRES DV NPDE CWRES TAD
TADD NOPRINT    NOAPPEND ONEHEADER FILE=sdtab504e
$TABLE ID SEX DVID TERM NOPRINT NOAPPEND ONEHEADER
FILE=catab504e
$TABLE ID AGE WT FFM HB HT ALT NOPRINT    NOAPPEND
ONEHEADER FILE=cotab504e
$TABLE ID CLL CLR VL VR KAL KAR K20 K40 Q V5 F1 BIO MTT IIVCLL
IIVCLR IIVVL IIVVR IIVBIOR IOVCLL IOVFL IOVFR IOVKAL IOVCLR
IOVRUV IOVMTT NOPRINT    NOAPPEND ONEHEADER FILE=patab504e
$TABLE ID TERM TAD TADD CLL CLR VL VR KAL KAR K20 K40 Q V5 F1
BIO MTT IIVCLL IIVCLR IIVVL IIVVR IIVBIOR IOVCLL IOVFL IOVFR
IOVKAL IOVCLR IOVRUV IOVMTT AGE SEX WT HT FFM ALT HB RIF
EVEN RDW DVID NOPRINT    NOAPPEND ONEHEADER
FILE=mytab504e.tab
```

III. Final model control file (Paper III)

```
$SIZES LVR=64 MAXFCN=10000000 LTH=50
$PROBLEM **run390, no FIX for EMAX
$INPUT ID SDID=DROP STUDY TERM WHAT=DROP ODAT=DROP
OTIM=DROP TIME AMT DVID DV LNDV=DROP MDV EVID CMT
SEX AGE WT HT ALT HB BQL RDW TB RATI RIF WRON EVEN RTVTOT
$DATA combined_dataset0502_cheve_RDTOT.csv IGNORE=#
IGNORE(BQL.EQ.1) IGNORE(WRON.EQ.1);      ; no bql
$SUBROUTINES ADVAN6 TRANS1 TOL=6
$MODEL
COMP(LPVDOSE)     ; 1 LPV DOSE
COMP(LPVOBS)      ; 2 LPV CENTRAL
COMP(RTVDOSE)     ; 3 RTV DOSE
COMP(RTVOBS)      ; 4 RTV CENTRAL
COMP(RTVOBS)      ; 5 RTV PREPHRAL
COMP(RTVTR1)     ; 6 RTV TRANSIT 1
COMP(RTVTR2)     ; 7 RTV TRANSIT 2
COMP(RTVTR3)     ; 8 RTV TRANSIT 3
$ABBREVIATED DERIV2=NO
$PK
;allometric scaling
SCLW = (WT/65)**0.75
SVW = WT/65
 ;-------IOV CODE-------------------
    IF (TERM.EQ.1) THEN
    IOVFL = ETA(3)
    IOVFR = ETA(4)
    IOVKAL = ETA(19)
    IOVRUV = ETA(27)
    IOVCLL = ETA(35)
    IOVCLR = ETA(35)*THETA(39)
    IOVMTT = ETA(43)
    ENDIF
    IF (TERM.EQ.2) THEN
    IOVFL = ETA(5)
    IOVFR = ETA(6)
    IOVKAL = ETA(20)
    IOVRUV = ETA(28)
    IOVCLL = ETA(36)
    IOVCLR = ETA(36)*THETA(39)
    IOVMTT = ETA(44)
    ENDIF
    IF (TERM.EQ.3) THEN
```

```
IOVFL = ETA(7)
IOVFR = ETA(8)
IOVKAL = ETA(21)
IOVRUV = ETA(29)
IOVCLL = ETA(37)
IOVCLR = ETA(37)*THETA(39)
IOVMTT = ETA(45)
ENDIF
IF (TERM.EQ.4) THEN
IOVFL = ETA(9)
IOVFR = ETA(10)
IOVKAL = ETA(22)
IOVRUV = ETA(30)
IOVCLL = ETA(38)
IOVCLR = ETA(38)*THETA(39)
IOVMTT = ETA(46)
ENDIF
 IF (TERM.EQ.5) THEN
IOVFL = ETA(11)
IOVFR = ETA(12)
IOVKAL = ETA(23)
IOVRUV = ETA(31)
IOVCLL = ETA(39)
IOVCLR = ETA(39)*THETA(39)
IOVMTT = ETA(47)
ENDIF
IF (TERM.EQ.6) THEN
IOVFL = ETA(13)
IOVFR = ETA(14)
IOVKAL = ETA(24)
IOVRUV = ETA(32)
IOVCLL = ETA(40)
IOVCLR = ETA(40)*THETA(39)
IOVMTT = ETA(48)
ENDIF
IF (TERM.EQ.7) THEN
IOVFL = ETA(15)
IOVFR = ETA(16)
IOVKAL = ETA(25)
IOVRUV = ETA(33)
IOVCLL = ETA(41)
IOVCLR = ETA(41)*THETA(39)
IOVMTT = ETA(49)
```

```
      ENDIF
      IF (TERM.EQ.8) THEN
      IOVFL = ETA(17)
      IOVFR = ETA(18)
      IOVKAL = ETA(26)
      IOVRUV = ETA(34)
      IOVCLL = ETA(42)
      IOVCLR = ETA(42)*THETA(39)
      IOVMTT = ETA(50)
      ENDIF
;Initialization
A_0(1)=0.000001
A_0(2)=0.000001
A_0(3)=0.000001
A_0(4)=0.000001
A_0(5)=0.000001

; ------------LPV MODEL------------------
 RIFCLL=0
 EVEBIOL=1
 EVECL =1
 ; Rifampicin effect

IF (RIF.EQ.1.AND.STUDY.EQ.1) THEN
     RIFCLL=THETA(6)
ENDIF
IF (RIF.EQ.1.AND.STUDY.EQ.2) THEN
      RIFCLL=THETA(37)
ENDIF
IF (EVEN.EQ.1.AND.STUDY.EQ.1) THEN
     EVEBIOL= THETA(9)
     EVECL    = THETA(35)
ENDIF
IF (EVEN.EQ.1.AND.STUDY.EQ.2) THEN
     EVEBIOL= THETA(10)
     EVECL    = THETA(36)
ENDIF

TVCLL = THETA(1)*(1+RIFCLL)*SCLW
TVVL    = THETA(2)*SVW
TVKAL = THETA(3)
SLPLF = THETA(4) ; it is fixed to 0
IF (STUDY.EQ.2) THEN
```

```
      TVCLL= THETA(34)*(1+RIFCLL)*SCLW
       TVKAL = THETA(11)
       SLPLF = THETA(12)
ENDIF

BIOL = 1 ; BIO for adults NO RIF
IF (STUDY.EQ.1.AND.RIF.EQ.1) BIOL=THETA(7) ; BIO for adults WITH RIF
IF (STUDY.EQ.2.AND.RIF.EQ.0) BIOL=THETA(5) ; BIO for chilren NO RIF
IF (STUDY.EQ.2.AND.RIF.EQ.1) BIOL=THETA(8) ; BIO for children WITH
RIF

TVF1 = (BIOL+SLPLF*(RDW-3))*EVEBIOL

; IIV
IIVCLL = ETA(1)
IIVVL = ETA(2)
IIVFL = ETA(51)

       CLL       = TVCLL*EXP(IIVCLL+IOVCLL)*EVECL
       VL        = TVVL*EXP(IIVVL)
       KAL       = TVKAL*EXP(IOVKAL)
      F1       = TVF1*EXP(IOVFL+IIVFL)

       K20 = CLL/VL
       S2 = VL

;----------RTV MODEL----------
RIFCLR=0
EVEBIOR=1
;Rifampicin effect
;IF (RIF.EQ.1) THEN

;ENDIF
IF (RIF.EQ.1.AND.STUDY.EQ.1) THEN
     RIFCLR = THETA(23)
ENDIF
IF (RIF.EQ.1.AND.STUDY.EQ.2) THEN
       RIFCLR = THETA(38)
ENDIF
IF (EVEN.EQ.1.AND.STUDY.EQ.1) THEN
       EVEBIOR= THETA(28)
ENDIF
IF (EVEN.EQ.1.AND.STUDY.EQ.2) THEN
```

```
    EVEBIOR= THETA(29)
ENDIF

BIOR =1 ; BIO for adults NO RIF
IF (STUDY.EQ.1.AND.RIF.EQ.1) BIOR=THETA(24) ; BIO for adults WITH RIF
IF (STUDY.EQ.2.AND.RIF.EQ.0) BIOR=THETA(19) ; BIO for chilren NO RIF
IF (STUDY.EQ.2.AND.RIF.EQ.1) BIOR=THETA(25) ; BIO for children WITH
RIF

TVCLR = THETA(15)*(1+RIFCLR)*SCLW
TVVR   = THETA(16)*SVW
TVKAR = THETA(17)
TVMTT =THETA(18)
SLPRFR = THETA(20)
IF (STUDY.EQ.2) THEN
     TVCLR = THETA(26)*(1+RIFCLR)*SCLW
      TVMTT = THETA(27)
      SLPRFR = THETA(40)
ENDIF

TVQ = THETA(21)*SCLW
TVV5 = THETA(22)*SVW

IF (STUDY.EQ.1) THEN
TVF3 = (BIOR+SLPRFR*(RTVTOT-100)/100)*EVEBIOR
ENDIF
IF (STUDY.EQ.2) THEN
TVF3 = (BIOR+SLPRFR*(RDW-3))*EVEBIOR
ENDIF

; IIV
IIVFR = ETA(52)
IIVCLR= ETA(53)
IIVVR = ETA(54)

CLR   = TVCLR*EXP(IIVCLR+IOVCLR)*EVECL
VR     = TVVR*EXP(IIVVR)
KAR   = TVKAR
MTT = TVMTT*EXP(IOVMTT)
F3   = TVF3*EXP(IOVFR+IIVFR)
Q     = TVQ
V5   = TVV5
```

```
      KTR=3/MTT
      K36=KTR
      K67=KTR
      K78=KTR
      K8T4=KAR
      K40 = CLR/VR
     K45 = Q/VR
     K54 = Q/V5
      S4 = VR

;----------EFFECT MODEL----------------
EMAXR = THETA(32)
EC50 =THETA(33)
HILL=THETA(41)

$DES
C4 = A(4)/VR
IF (C4.LE.0.000001) THEN
     EFF=0
ELSE
     EFF = EMAXR*(C4**HILL)/(EC50**HILL + C4**HILL)
ENDIF

DADT(1) = -KAL*A(1)
DADT(2) = KAL*A(1)-K20*A(2)*(1-EFF)
DADT(3)= -KTR*A(3)
DADT(4) = KAR*A(8)-K40*A(4)+K54*A(5)-K45*A(4)
DADT(5) = K45*A(4)-K54*A(5)
DADT(6)= KTR*A(3)-KTR*A(6)
DADT(7)= KTR*A(6)-KTR*A(7)
DADT(8)= KTR*A(7)-KAR*A(8)

$ERROR ;(ONLY OBSERVATIONS)
    PREDL = A(2)/VL
    PREDR = A(4)/VR
    IF(DVID.EQ.1)IPRED = PREDL
    IF(DVID.EQ.2)IPRED = PREDR
    IRES   = DV - IPRED
     IF (DVID.EQ.1)
W = SQRT(THETA(13)**2 +
(THETA(14)*IPRED)**2)*EXP(IOVRUV)      ;LPV additive and proportional
error
```

```
      IF (DVID.EQ.2)
W = SQRT(THETA(30)**2 + (THETA(31)*IPRED)**2)      ;RTV additive and
proportional error
      IF (W.EQ.0) W = 1
      IWRES = IRES/W
 Y = IPRED + W*EPS(1)

$THETA   (0,50)   ; 1 LPV CL for adult
 (0,60.8) ; 2 LPV V
 (0,1.13) ; 3 LPV KA for adult
 0 FIX ; 4 RTV dose on LPV F for adult
 (0,0.849) ; 5 BIO LPV for children NO RIF
 (0,0.567) ; 6 RIF ON LPV CL for both
 (0,0.76,1) ; 7 BIO LPV for adults WITH RIF
 (0,0.373,1) ; 8 BIO LPV for children WITH RIF
 (0,1.24) ; 9 EVENING effect on LPV F for adult
 1 FIX ; 10 EVENING effect on LPV F for children
 (0,0.386) ; 11    LPV KA for children
 (0,0.0138) ; 12 RTV dose on LPV F for children
 (0,0.0729) ; 13    LPV Additive error
 (0,0.132) ; 14    LPV Proportional error
 (0,23.6) ; 15    RTV CL for adult
 (0,42.3) ; 16    RTV V
 (0,2.34) ; 17    RTV KA
 (0,1.08) ; 18    RTV MTT for adult
 (0,0.264,1) ; 19    BIO RTV for children no rif
 (0,0.742) ; 20 RTV DOSE ON F for adult
 (0,30.9) ; 21 RTV Q
 (0,55.9) ; 22 RTV V5
 (0,0.301) ; 23 RIF ON RTV CL for both
 (0,0.433,1) ; 24 BIO RTV for adult WITH RIF
 (0,0.0259,1) ; 25 BIO RTV for children WITH RIF
 (0,14.3) ; 26    RTV CL for children
 (0,2.23) ; 27    RTV MTT for children
 (0,1.05) ; 28 EVEN effect on RTV F for adult
 1 FIX ; 29 EVEN effect on RTV F for children
 0 FIX ; 30 RTV additive error
 (0,0.211) ; 31 RTV proportional error
 (0,0.918,1) ; 32 EMAX
 (0,0.0463) ; 33 EC50
 (0,31.8) ; 34 LPV CL for children
 (0,0.491) ; 35 EVEN effect on CL adults
 (0,0.722) ; 36 EVEN effect on CL children
```

```
  (0,0.444) ; 37 RIF effect on LPV CL for children
  (0,0.217) ; 38 RIF effect on RTV CL for children
  (0,0.972) ; 39 IOVCLL-LOVCLR
  (0,0.0275) ; 40 RTV DOSE ON F for children
  (0,1.74,30) ; 41 Hill
$OMEGA   BLOCK(1)
  0.0426   ; 1     IIV on LPV CL
$OMEGA   BLOCK(1)
  0.057   ; 2     IIV on LPV V
$OMEGA   BLOCK(2)
  0.0741   ; 3     IOV on LPV F1
  0.0996 0.185   ; 4     IOV on RTV F1
$OMEGA   BLOCK(2) SAME
$OMEGA   BLOCK(2) SAME
$OMEGA   BLOCK(2) SAME
$OMEGA   BLOCK(2) SAME
$OMEGA   BLOCK(2) SAME
$OMEGA   BLOCK(2) SAME
$OMEGA   BLOCK(2) SAME
$OMEGA   BLOCK(1)
  0.483   ; 19     IOV on LPV KA
$OMEGA   BLOCK(1) SAME
$OMEGA   BLOCK(1) SAME
$OMEGA   BLOCK(1) SAME
$OMEGA   BLOCK(1) SAME
$OMEGA   BLOCK(1) SAME
$OMEGA   BLOCK(1) SAME
$OMEGA   BLOCK(1) SAME
$OMEGA   BLOCK(1) FIX
  0   ; 27     IOV on LPV RUV
$OMEGA   BLOCK(1) SAME
$OMEGA   BLOCK(1) SAME
$OMEGA   BLOCK(1) SAME
$OMEGA   BLOCK(1) SAME
$OMEGA   BLOCK(1) SAME
$OMEGA   BLOCK(1) SAME
$OMEGA   BLOCK(1) SAME
$OMEGA   BLOCK(1)
  0.0293   ; 35     IOV on LPV CL
$OMEGA   BLOCK(1) SAME

$OMEGA   BLOCK(1) SAME
$OMEGA   BLOCK(1) SAME
```

```
$OMEGA    BLOCK(1) SAME
$OMEGA    BLOCK(1) SAME
$OMEGA    BLOCK(1) SAME
$OMEGA    BLOCK(1) SAME
$OMEGA    BLOCK(1)
 0.154    ; 43      IOV on RTV MTT
$OMEGA    BLOCK(1) SAME
$OMEGA    BLOCK(1) SAME
$OMEGA    BLOCK(1) SAME
$OMEGA    BLOCK(1) SAME
$OMEGA    BLOCK(1) SAME
$OMEGA    BLOCK(1) SAME
$OMEGA    BLOCK(1) SAME
$OMEGA    BLOCK(2)
 0.0642    ; 51      IIV on LPV F
 0.107 0.385    ; 52    IIV on RTV F
$OMEGA    BLOCK(1)
 0.0689    ; 53      IIV on RTV CL
$OMEGA    BLOCK(1) FIX
 0    ; 54      IIV on RTV V
$SIGMA    1.    FIX
$ESTIMATION MSFO=msf393 PRINT=1 MAXEVALS=9999    METHOD
CONDITIONAL INTERACTION
$COVARIANCE MATRIX=S PRINT=E
$TABLE FILE=sdtab393 ID TIME PRED IPRED RES WRES CWRES IWRES
DV NPDE NOPRINT ONEHEADER
$TABLE FILE=catab393 ID SEX    DVID TERM NOPRINT ONEHEADER
$TABLE FILE=cotab393 ID AGE WT NOPRINT ONEHEADER
$TABLE FILE=patab393 ID CLL VL KAL F1 CLR VR F3 Q V5 MTT IIVCLL
IIVVL IOVCLL IOVKAL IOVRUV IOVFL IIVCLR IIVVR IIVFR IOVFR
IOVMTT NOPRINT    ONEHEADER
$TABLE FILE=mytab393 ID STUDY SEX RIF TERM DVID CLL VL KAL F1
CLR VR Q V5 F3 MTT KAR IIVCLL IIVVL IOVCLL IOVKAL IOVRUV
IOVFL IIVFL IIVCLR IIVVR IIVFR IOVFR IOVCLR IOVMTT WT RDW
NOPRINT    ONEHEADER
```

IV. Final model control file (Paper IV)

```
$PROBLEM    **run14,maturation,PMA    ;lamivudine pediatric data (pilot+ddk
study)
$INPUT ID SDID=DROP OCC TERM ODAT=DROP OTIM=DROP TIME AMT
DVID DV MDV EVID SEX AGE WT HT ALT HB BQL TB RATI RIF EVEN
FLAG PRE
$DATA lamidata_full_halfblq2_pre.csv    IGNORE=#    IGNORE(FLAG.EQ.1) ;
missing data compared to lpv/rtv; half value for blq
$SUBROUTINE ADVAN6 TOL=4
$MODEL
NCOMP=3
COMP(DEPOT, DEFDOSE)
COMP(CENTRAL, DEFOBS)
COMP(PERI)
$PK
TAD = TIME-48
;allometric scaling
SCL = (WT/10)**0.75
SV    = WT/10
;maturation
PNA         = AGE+9
TM50        = THETA(10)
HILL        = 1
MFCL        = 1/(1+(PNA/TM50)**(-HILL)) ;maturation
 ;variability
    IIVCL = ETA(1)
    IIVV    = ETA(2)
    IIVKA = ETA(3)
    IIVMTT = ETA(4)
    IIVBIO = ETA(5)

    IF (TERM.EQ.1) THEN
    IOVBIO = ETA(6)
    IOVCL= ETA(10)
    IOVKA= ETA(14)
    IOVMTT=ETA(18)
    ENDIF
    IF (TERM.EQ.2) THEN
    IOVBIO = ETA(7)
    IOVCL= ETA(11)
    IOVKA= ETA(15)
    IOVMTT=ETA(19)
    ENDIF
```

```
    IF (TERM.EQ.3) THEN
    IOVBIO = ETA(8)
    IOVCL= ETA(12)
    IOVKA= ETA(16)
    IOVMTT=ETA(20)
    ENDIF
    IF (TERM.EQ.4) THEN
    IOVBIO = ETA(9)
    IOVCL= ETA(13)
    IOVKA= ETA(17)
    IOVMTT=ETA(21)
    ENDIF
;evening effect
EVECL=1
EVEBIO=1
IF (EVEN.EQ.1) THEN
    EVECL=THETA(11)
    EVEBIO=THETA(12)
ENDIF
;typical parameter
    TVCL = THETA(1)*MFCL
     TVV    = THETA(2)
     TVKA = THETA(3)
    TVMTT= THETA(4)
    TVQ    = THETA(5)
    TVV3 = THETA(6)
    TVNN = THETA(7)

     CL       = TVCL*EXP(IIVCL+IOVCL)*SCL*EVECL
     V2       = TVV*EXP(IIVV)*SV
      Q       = TVQ*SCL
    V3       = TVV3*SV
     KA       = TVKA*EXP(IIVKA+IOVKA)
    MTT      = TVMTT*EXP(IIVMTT+IOVMTT)
    NN       = TVNN

   K = CL/V2
   K23 = Q/V2
   K32 = Q/V3
   S2 = V2/1000

IF (NEWIND.NE.2) THEN ; beginning of dataset, or new individual
```

```
      TDOS=TIME ; TIME will be the time of the first record of that subject even if
it's not a dose, but...
      PD=AMT ; ...the amount will be 0 if the first record is not a dose, so no
problem.
  ENDIF

  F1=0 ; I need to set bioavailability in compartment 1 to 0
  BIO=1*EXP(IIVBIO+IOVBIO)*EVEBIO ; This is the actual bioavailability

KTR = (NN+1)/MTT
L = .9189385+(NN+.5)*LOG(NN)-NN+LOG(1+1/(12*NN)) ; log of gamma
function approximation. .9189385 is ln(sqrt(2*PI))

; To speed up the computation, I calculate here all the non-time-varying quantities
used in $DES
LBPD=LOG(BIO*PD)
LKTR=LOG(KTR)
PIZZA=LBPD+LKTR-L

$DES
TEMPO=T-TDOS ; this is time after dose, it should always be >= 0

IF(TEMPO.GT.0) THEN
      KTT=KTR*TEMPO
      DADT(1)=EXP(PIZZA+NN*LOG(KTT)-KTT)-KA*A(1)
ELSE
      DADT(1)=0 ; I believe this is executed only when TEMPO=0, or before the
first dose is given
ENDIF

DADT(2)=KA*A(1)-K*A(2)-K23*A(2)+K32*A(3)
DADT(3)=K23*A(2)-K32*A(3)

$ERROR ;(ONLY OBSERVATIONS)
       IPRED = F
       IRES    = DV - IPRED
       W = SQRT(THETA(8)**2 + (THETA(9)*F)**2)
      IF (PRE.EQ.1) THEN
       W = SQRT(THETA(13)**2 + (THETA(14)*F)**2)
      ENDIF
       IF (W.EQ.0) W = 1
       IWRES = IRES/W
       Y = IPRED + W*EPS(1)
```

```
IF(AMT.GT.0) THEN ; This reads one record ahead and stores the data to be used
when running the following record
TDOS=TIME
PD=AMT
ENDIF

$THETA    (0,12.2408) ; 1 CL
  (0,20.6749) ; 2 V2
  (0,1.65473) ; 3 KA
  (0,0.546805) ; 4 MTT
  (0,1.66709) ; 5 Q
  (0,37.216) ; 6 V3
  (0,2.29731) ; 7 NN
  10 FIX ; 8 Additive error
  (0,0.0833731) ; 9 Proportional error
  (0,12.9271) ; 10 maturation TM50
  (0,0.833404) ; 11 evening effect on CL
  1 FIX ; 12 evening effect on BIO
  (0,23.6968) ; 13 additive error for predose
  (0,0.126263) ; 14 preoportional error for predose
$OMEGA    BLOCK(1)
  0.00665976    ; 1 IIV on CL
$OMEGA    BLOCK(1)
  0.0636054    ; 2    IIV on V
$OMEGA    BLOCK(1) FIX
  0    ; 3    IIV on KA
$OMEGA    BLOCK(1) FIX
  0    ; 4 IIV on MTT
$OMEGA    BLOCK(1)
  0.0815093    ; 5    IIV on F
$OMEGA    BLOCK(1)
  0.0730012    ; 6    IOV on F
$OMEGA    BLOCK(1) SAME
$OMEGA    BLOCK(1) SAME
$OMEGA    BLOCK(1) SAME
$OMEGA    BLOCK(1) FIX
  0    ; 10    IOV on CL
$OMEGA    BLOCK(1) SAME
$OMEGA    BLOCK(1) SAME
$OMEGA    BLOCK(1) SAME
$OMEGA    BLOCK(1)
  0.517322    ; 14    IOV on KA
```

```
$OMEGA    BLOCK(1) SAME
$OMEGA    BLOCK(1) SAME
$OMEGA    BLOCK(1) SAME
$OMEGA    BLOCK(1)
 0.50193    ; 18    IOV on MTT
$OMEGA    BLOCK(1) SAME
$OMEGA    BLOCK(1) SAME
$OMEGA    BLOCK(1) SAME
$SIGMA    1.    FIX
$ESTIMATION PRINT=1 MAXEVALS=9999 MSFO=run17a.msf SIGL=6
NSIG=3 METHOD CONDITIONAL INTERACTION
$COVARIANCE MATRIX=S PRINT=E
$TABLE ID TIME PRED IPRED RES WRES IWRES CWRES NPDE DV
NOPRINT ONEHEADER FILE=sdtab17a
$TABLE ID SEX TERM OCC NOPRINT ONEHEADER FILE=catab17a
$TABLE ID AGE WT HT ALT HB NOPRINT ONEHEADER FILE=cotab17a
$TABLE ID CL V2 KA K V3 Q F1 MTT NN IIVCL IIVV IIVKA IOVBIO
IIVBIO IOVCL IIVMTT IOVMTT NOPRINT    ONEHEADER FILE=patab17a
$TABLE ID OCC TERM CL V2 KA K Q V3 F1 MTT NN SEX AGE WT HT
ALT HB RIF RATI IIVCL IIVV IIVKA IOVBIO IIVBIO IOVCL IIVMTT
IOVMTT NOPRINT ONEHEADER FILE=mytab17a.tab
```